


1-1-2014

# Role and Regulation of SnoN/SkiL and PLSCR1 Located at 3q26.2 and 3q23, Respectively, in Ovarian Cancer Pathophysiology

Madhav Karthik Kodigepalli

*University of South Florida*, [kkarthik@mail.usf.edu](mailto:kkarthik@mail.usf.edu)

Follow this and additional works at: <http://scholarcommons.usf.edu/etd>

 Part of the [Cell Biology Commons](#), [Microbiology Commons](#), and the [Molecular Biology Commons](#)

---

## Scholar Commons Citation

Kodigepalli, Madhav Karthik, "Role and Regulation of SnoN/SkiL and PLSCR1 Located at 3q26.2 and 3q23, Respectively, in Ovarian Cancer Pathophysiology" (2014). *Graduate Theses and Dissertations*.  
<http://scholarcommons.usf.edu/etd/5426>

This Dissertation is brought to you for free and open access by the Graduate School at Scholar Commons. It has been accepted for inclusion in Graduate Theses and Dissertations by an authorized administrator of Scholar Commons. For more information, please contact [scholarcommons@usf.edu](mailto:scholarcommons@usf.edu).

Role and Regulation of SnoN/SkiL and PLSCR1 Located at 3q26.2 and 3q23, Respectively, in Ovarian  
Cancer Pathophysiology

by

Madhav Karthik Kodigepalli

A dissertation submitted in partial fulfillment  
of the requirements for the degree of  
Doctor of Philosophy in Cell and Molecular Biology  
Department of Cell Biology, Microbiology and Molecular Biology  
College of Arts and Sciences  
University of South Florida

Major Professor: Meera Nanjundan, Ph.D.  
Richard Pollenz, Ph.D.  
Patrick Bradshaw, Ph.D.  
Sandy Westerheide, Ph.D.

Date of Approval:  
September 18, 2014

Keywords: Chemotherapeutics, phospholipid scramblase, toll-like receptor, interferon, dsDNA

Copyright © 2014, Madhav Karthik Kodigepalli

## **Dedication**

I dedicate this research at the lotus feet of Bhagwan Sri Sathya Sai Baba and all the Masters for I am what I am due to their divine grace. I also dedicate this work to my parents Prabhakar Kodigepalli and Subba Lakshmi Kodigepalli, to my brothers Deepak and Prashanth, and to my loving wife Punashi for their constant support and encouragement which has helped me throughout this journey.

## **Acknowledgments**

Firstly, I would like to thank my mentor Dr. Meera Nanjundan for all her support and guidance. I am deeply grateful to her for her contribution of time and ideas to make my Ph.D. experience both productive and motivating. I am thankful for all her advice and insightful suggestions without which this dissertation would not have been possible.

I wish to thank my committee members Dr. Richard Pollenz, Dr. Patrick Bradshaw and Dr. Sandy Westerheide for all their valuable time and constant support through my Ph.D. I also thank my current and former lab partners Punashi Dutta, Kyle Bauckman, and Dawn Smith for all the stimulating scientific discussions. Additionally, I would like to thank all the undergraduate students for their kind assistance in the laboratory.

I am also grateful to Dr. Lindsey Shaw who let me rotate in his lab when I first joined the department and has been very supportive and understanding of me. At last, I would like to thank my parents, all my family and friends for their encouragement and moral support.

## Table of Contents

List of Tables .....	iv
List of Figures .....	v
Abbreviations .....	vii
Abstract .....	viii
Chapter 1: Introduction .....	1
Ovarian Cancer .....	1
Current treatment strategies .....	2
Common genetic aberrations .....	2
Amplifications of chromosomal region 3q26 .....	3
TGF $\beta$ signaling .....	4
SnoN .....	4
Arsenic Trioxide (As <sub>2</sub> O <sub>3</sub> ) .....	6
Programmed Cell Death .....	7
Autophagy .....	7
Apoptosis .....	8
Necroptosis .....	9
Phospholipid Scramblase: PLSCR Family Members, TMEM16F and Xkr8 .....	10
Phospholipids, membrane asymmetry, scramblase activity, and blood coagulation .....	10
cDNA cloning of “phospholipid scramblases” .....	11
Gene location and protein structure of PLSCR1 isoforms .....	12
Scramblase activity of PLSCR family members .....	15
Defect in TMEM16/Ano6 is responsible for scramblase activity deficiency in Scott syndrome platelets .....	17
Regulation, Subcellular Localization, and Functions of PLSCR Family Members .....	18
Transcriptional regulation by growth factors, interferons, and Snail .....	18
Subcellular localization of PLSCR1 .....	19
Role of PLSCR1 in cell signaling/receptor trafficking events and protein-protein interactions .....	20
Role of PLSCR1 as a DNA-binding protein and transcription factor .....	22
Functions of PLSCR1: Innate Immune Recognition, Cell Death Pathways, and Cancer .....	23
Antiviral functions of PLSCR1 and viral entry .....	23
Role of PLSCR1 in autoimmune diseases (systemic lupus erythematosus) .....	25
PLSCR1 in innate immune responses: TLR signaling .....	25
Role of PLSCR1 in apoptosis and autophagy .....	26
Role of PLSCR1 in blood and solid cancers .....	27
Hypotheses and Objectives .....	28
Specific Aim 1 (presented in Chapter 3) .....	29
Aim 1.1 .....	29

Aim 1.2 .....	29
Specific Aim 2 (presented in Chapter 4).....	29
Aim 2.1 .....	29
Aim 2.2 .....	29
Aim 2.3 .....	29
Specific Aim 3 (presented in Chapter 5).....	29
Aim 3.1 .....	29
Aim 3.2 .....	29
Overall Impact and Significance.....	29
 Chapter 2: Materials and Methods .....	 31
Culture and Propagation of Cell Lines.....	31
Genomic DNA Isolation and STR profiling .....	32
Cellular Treatments with Growth Factors, Chemotherapeutic Agents, and Signaling pathway Inhibitors.....	33
Plasmids, microRNAs and Cloning of PLSCR1 into pBABE-puro .....	34
Generation and Cloning of PLSCR1 mutants .....	35
WT-PLSCR1-HA and C/A-PLSCR1-HA.....	35
$\Delta$ N-PLSCR1-HA .....	35
$\Delta$ TM-PLSCR1-HA .....	36
Plasmid and MicroRNA (miRNA) Transfection .....	37
siRNA-Mediated Knockdown .....	38
Establishment of Retroviral Stable Cell Lines.....	38
Protein Isolation, SDS-PAGE, and Western Blotting.....	39
Subcellular Fractionation.....	40
Immunoprecipitation.....	42
Total RNA Isolation and Real-Time PCR .....	42
Luciferase Promoter Activity Assays .....	43
Immunocytochemistry .....	43
Direct immunofluorescence.....	43
Indirect immunofluorescence.....	44
Annexin V/PI Assay .....	45
Caspase Activity Assay.....	45
Phosphatase Assay .....	46
ATP Viability Assays .....	46
Cell Growth Assays .....	46
Statistical Analyses.....	47
 Chapter 3: SnoN/SkiL Expression is Modulated via As <sub>2</sub> O <sub>3</sub> -Induced Activation of PI3K/AKT Pathway in Ovarian Cancer Cells.....	 48
Introduction.....	48
Results.....	50
As <sub>2</sub> O <sub>3</sub> activates EGFR and promotes its interaction with downstream adaptor protein Grb2 .....	50
Inhibition of Src family kinase activity alters As <sub>2</sub> O <sub>3</sub> -mediated EGFR activation and SnoN induction .....	54
Inhibition of PI3K signaling modulates the As <sub>2</sub> O <sub>3</sub> -induced SnoN expression and cellular sensitivity .....	58
Reduction of EGFR, pp60 c-Src, and MAPK1 alters As <sub>2</sub> O <sub>3</sub> -induced cellular responses.....	62
Discussion.....	65

Acknowledgements.....	69
Chapter 4: Phospholipid Scramblase 1, an IFN-Regulated Gene Located at 3q23, is Regulated by SnoN/SkiL in Ovarian Cancer Cells.....	70
Introduction.....	70
Results.....	73
Elevated PLSCR1 DNA copy number and mRNA expression in ovarian cancer.....	73
Altered PLSCR1 DNA copy number and mRNA expression correlate with SnoN in ovarian cancers.....	76
SnoN and TGF $\beta$ transcriptionally regulate the expression of PLSCR1.....	76
SnoN regulates the IFN-mediated induction of PLSCR1.....	79
PLSCR1 knockdown modulates the ovarian cancer cell responses to As <sub>2</sub> O <sub>3</sub> .....	82
Discussion.....	85
Acknowledgements.....	89
Chapter 5: Regulation of PLSCR1 by IRF3 Following Vector Transfection in Normal and Malignant Epithelial Cells.....	90
Introduction.....	90
Results.....	93
dsDNA plasmid transfection induces PLSCR1 mRNA/protein in T80 ovarian epithelial cells and HMEC mammary epithelial cells.....	93
Inhibition of MAP kinase activity and reduction of STAT3 expression does not modulate the dsDNA-induced PLSCR1 mRNA levels.....	98
Reduction of IRF3 modulates the dsDNA-mediated PLSCR1 induction.....	99
Plasmid transfection does not lead to PLSCR1 induction in ovarian cancer cells.....	102
Discussion.....	105
Acknowledgements.....	108
Chapter 6: Significance of PLSCR1 in Ovarian Cancer and Immunotherapy.....	109
Overview.....	109
Regulation of SnoN Expression Upon Chemotherapeutic Treatment.....	110
Phospholipid Scramblase Family Members and their Impact in Cancer Development.....	111
Scrambling Activity of PLSCR1.....	122
Role of PLSCR1 in Modulating Autophagic Flux.....	123
PLSCR1 and Cancer Immunotherapy.....	125
Prospective Studies.....	127
Specific aim 1.....	127
Specific aim 2.....	128
Specific aim 3.....	128
References.....	129
Appendices.....	141
Appendix A: Overexpression and Validation of HA-tagged PLSCR1 Mutants in T80 Cells.....	141
Appendix B.....	142
Appendix C.....	144

## List of Tables

Table 1: cDNA identity matrix of PLSCR family members.....	14
Table 2: Protein identity matrix of PLSCR family members.....	14
Table 3: Upregulation of PLSCR1 in response to various stimuli .....	18
Table 4: List of protein interaction partners of PLSCR1 .....	21
Table 5: List of all cell lines utilized for dissertation.....	31
Table 6: List of developed retroviral stable cell lines.....	38
Table 7: List of primary antibodies utilized for western analyses .....	41
Table 8: List of primary antibodies utilized for indirect immunofluorescence.....	44
Table 9: Altered DNA copy number and mRNA expression of PLSCR family members in ovarian cancers (cBioPortal Analysis) .....	114
Table 10: List of (A) assessed and (B) commercially available antibodies for PLSCR family members .....	115
Table 11: Altered DNA copy number, mRNA expression, and mutations of PLSCR1 in cancers (cBioPortal Analysis) .....	116
Table 12: Mutations identified in PLSCR1 in cancers (COSMIC Analysis).....	117



## List of Figures

Figure 1: Human chromosomal 3q region .....	3
Figure 2: Structural organization of SnoN protein.....	5
Figure 3: Schematic representation of autophagy pathway .....	7
Figure 4: Structural organization of PLSCR1 gene and protein .....	12
Figure 5: Amino acid sequence alignment of PLSCR family members .....	13
Figure 6: Role of PLSCR1 in viral/bacterial responses and in cancer development .....	24
Figure 7: Model of proposed hypotheses for Aims 1 and 2 .....	28
Figure 8: As <sub>2</sub> O <sub>3</sub> leads to activation of EGFR, Src, and AKT and modulates EGFR interaction with Grb2.....	51
Figure 9: Inhibition of Src family kinase activity modulates the As <sub>2</sub> O <sub>3</sub> -mediated EGFR activation and SnoN induction .....	55
Figure 10: Inhibition of PI3K-AKT signaling modulates the As <sub>2</sub> O <sub>3</sub> -mediated SnoN induction and cell responses .....	58
Figure 11: siRNA mediated reduction of EGFR, pp60 c-Src, and MAPK1 modulates the As <sub>2</sub> O <sub>3</sub> -induced cellular responses.....	63
Figure 12: Schematic representation of the mechanism of SnoN modulation by As <sub>2</sub> O <sub>3</sub> .....	66
Figure 13: Correlation between DNA copy number and mRNA alterations of PLSCR1 and SnoN in ovarian cancers .....	73
Figure 14: SnoN and TGFβ transcriptionally regulate PLSCR1 .....	77
Figure 15: Interferon-induced PLSCR1 mRNA expression is regulated by SnoN.....	80
Figure 16: PLSCR1 knockdown alters the sensitivity of ovarian cancer cells to As <sub>2</sub> O <sub>3</sub> .....	83
Figure 17: Model of the regulation of PLSCR1 by SnoN and modulation of As <sub>2</sub> O <sub>3</sub> -induced cell death response by PLSCR1 .....	86
Figure 18: IFN and empty plasmid transfection induce PLSCR1 mRNA and protein .....	93

Figure 19: Subcellular localization of PLSCR1 following IFN treatment and dsDNA transfection .....	96
Figure 20: Inhibition of MAPK activity does not antagonize PLSCR1 induction upon dsDNA transfection .....	98
Figure 21: IRF3 knockdown antagonizes dsDNA-induced PLSCR1 expression .....	100
Figure 22: Lack of PLSCR1 induction upon plasmid transfection in ovarian cancer cells .....	102
Figure 23: Induction of TLR9 and IFN- $\alpha$ mRNA with lack of PLSCR1 or TLR4 transcript induction in ovarian cancer cells .....	103
Figure 24: dsDNA transfection in normal epithelial cells induces PLSCR1 expression mediated by IRF3 activation .....	106
Figure 25: Altered DNA copy number levels and mRNA expression of PLSCR family members in ovarian cancers .....	112
Figure 26: Mutual exclusivity/co-occurrence of alterations of PLSCR family members in ovarian cancers .....	113
Figure 27: miRNAs with putative binding sites in the 3'UTR of PLSCR1 .....	120
Figure 28: miR-494 reduces PLSCR1 protein .....	121
Figure 29: IRF3 knockdown reduces the dsDNA transfection-induced increase in LC3-II levels in normal epithelial cells .....	124
Figure 30: Schematic of the proposed role of PLSCR1 and IRF3 in autophagic regulation .....	126
Figure A1: Overexpression and validation of HA-tagged PLSCR1 mutants.....	141

## Abbreviations

APL: Acute promyelocytic leukemia  
As<sub>2</sub>O<sub>3</sub>: Arsenic trioxide  
ATRA: All-trans retinoic acid  
BSA: Bovine serum albumin  
DMEM: Dulbecco's modified eagle's medium  
EGF: Epidermal growth factor  
EGFR: Epidermal growth factor receptor  
EMEM: Eagle's minimum essential medium  
EOC: Epithelial ovarian cancer  
FBS: Fetal bovine serum  
G-CSF: Granulocyte colony stimulating factor  
GFP: Green fluorescent protein  
HMEC: Human primary mammary epithelial cells  
HGSC: High grade serous epithelial ovarian carcinoma  
IFN: Interferon  
JNK: c-Jun N terminal kinase  
MAPK: Mitogen-activated protein kinase  
MECOM: MDS1-EVI1 complex  
NAC: N-acetyl-L- cysteine  
PARP: Poly ADP ribose polymerase  
PI: Propidium iodide  
PI3K: Phosphoinositide 3-kinase  
PIK3CA: Phosphoinositide 3-kinase catalytic subunit alpha  
PKC: Protein kinase C  
PLSCR: Phospholipid scramblase  
PS: Phosphatidylserine  
ROS: Reactive oxygen species  
RPMI: Roswell Park Memorial Institute  
RPPA: Reverse phase protein array  
RT-PCR: Real time quantitative PCR  
SCF: Stem cell factor  
STAT: Signal transducer and activator of transcription  
TGFβ: Transforming growth factor β  
TBST: Tris-buffered saline with Tween-20  
TMEM16F: Transmembrane protein 16F  
Xkr8: Kell blood group complex subunit-related family, member 8

## Abstract

Ovarian cancer is one of the most common causes of gynecological cancer related deaths in women. In 2014, the estimated number of deaths due to ovarian cancer is 14,270 with occurrence of over 22, 240 new cases (National Cancer Institute, <http://seer.cancer.gov/statfacts/html/ovary.html>). Despite improvement in treatment strategies, the 5-year survival rate is still below 50% mainly due to chemoresistance and relapse. Amplification of chromosomal region 3q26 is a common characteristic in various epithelial cancers including ovarian cancer [9-12, 28-30]. This region harbors various oncogenes including the TGF $\beta$  signaling mediators EVI1 [10] and SnoN/SkiL [9], PKC $\iota$  [31], and PIK3CA [11] amplified at 3q26.2 and 3q26.3, respectively, in ovarian cancers. Previous studies indicate that these genes can exhibit cooperative oncogenicity by cross-regulating one another and facilitating cancer development [32, 33]. Our earlier studies demonstrated that treatment of ovarian cancer cells with arsenic trioxide (As<sub>2</sub>O<sub>3</sub>) promotes cytoprotective autophagy regulated by induction of SnoN to antagonize the cytotoxic effects of As<sub>2</sub>O<sub>3</sub> [1]. Since exact mechanisms underlying As<sub>2</sub>O<sub>3</sub>-induced SnoN expression and cytoprotective responses were unclear, we hypothesized that SnoN may be regulated by signaling pathways involving genes amplified at the 3q26 locus.

Phospholipid scramblase 1 (PLSCR1) is located at 3q23 proximal to the amplified 3q26 region. It had been implicated in disruption of plasma membrane asymmetry by mediating phospholipid scrambling, a process critical for cellular events such as blood coagulation and apoptosis [34, 35]. However, recent findings have led to more investigations on the role and regulation of PLSCR1 in cancer development and immune responses [4-8, 21, 22, 36]. PLSCR1 expression is regulated by various stimuli including growth factors (EGF, G-CSF, and SCF) [19, 37], cytokines (IFN) [38, 39], and differentiation-inducing agents (ATRA) [40]. Despite these studies, transcriptional regulation of PLSCR1 remains incompletely understood. Numerous studies have suggested a critical role for PLSCR1 in the

pathophysiology of various cancers including leukemia [16, 17, 41], ovarian cancer [15], colorectal cancer, and metastatic liver cancer [20-22, 36]. However, the precise contribution of PLSCR1 and its regulation in ovarian cancer development is unclear. Since PLSCR1 (at 3q23) is located in close proximity to SnoN/SkiL (at 3q26.2), we hypothesized that PLSCR1 expression in ovarian cancer cells could be regulated by SnoN. Herein, we present studies that primarily focus on understanding the role and regulation of SnoN/SkiL (a TGF $\beta$  pathway regulator) and PLSCR1 (an interferon-regulated gene), which are located at 3q26.2 and 3q23, respectively, in epithelial ovarian cancer.

In Chapter 3, we determined that activation of the PI3K signaling pathway mediates SnoN expression and cytoprotective responses upon stimulation of ovarian cancer cells with As<sub>2</sub>O<sub>3</sub>. We first identified that As<sub>2</sub>O<sub>3</sub> stimulation leads to activation of EGFR and its downstream signaling mediators as well as modulates its interaction with the adaptor proteins, ShcA and Grb2. Interestingly, while treatment with a general SFK inhibitor (PP2), reduced the As<sub>2</sub>O<sub>3</sub>-induced EGFR activation and SnoN induction, a more specific inhibitor SU6656 did not alter SnoN expression. Further, via studies utilizing specific inhibitors and siRNA targeting PI3K, we determined that inhibition of PI3K signaling pathway decreases SnoN induction and increases apoptosis in ovarian cancer cells in response to As<sub>2</sub>O<sub>3</sub>. This suggests that PI3K (PIK3CA) activity is required for the As<sub>2</sub>O<sub>3</sub>-mediated SnoN induction and the cell survival responses in ovarian cancer cells. Finally, we determined by siRNA-mediated knockdown that EGFR and MAPK1 alter As<sub>2</sub>O<sub>3</sub>-induced cell death response independently of SnoN induction.

In Chapter 4, via bioinformatic analyses, we identified that PLSCR1 DNA copy number and mRNA expression is elevated in ovarian cancer patients and cell lines relative to immortalized (Tag/hTERT) normal ovarian surface epithelial (OSE) cells. Interestingly, altered PLSCR1 DNA and mRNA levels were correlated with SnoN in ovarian cancers. We next identified that SnoN knockdown leads to a significant (~35%, P<0.05) reduction of PLSCR1 mRNA levels and promoter activity suggesting that SnoN may transcriptionally regulate PLSCR1 expression. More importantly, SnoN knockdown ablated IFN-induced PLSCR1 mRNA expression. Together, these studies indicate an important role of SnoN in regulation of PLSCR1 expression in ovarian cancer cells. We also determined

that As<sub>2</sub>O<sub>3</sub> transcriptionally downregulates PLSCR1 in a ROS-independent mechanism. Furthermore, PLSCR1 knockdown, similar to SnoN knockdown increases ovarian cancer cell sensitivity to As<sub>2</sub>O<sub>3</sub>. PLSCR1 knockdown increases cleaved PARP (marker of apoptosis) with a consequent reduction in LC3-II levels (marker of autophagosomes). Collectively, these studies implicate PLSCR1 in the pathophysiology of ovarian cancers and in altering the chemotherapeutic responses in ovarian cancer cells.

PLSCR1 is an IFN-regulated gene and mediates antiviral/immune responses [4-8]. More recent studies in plasmacytoid dendritic cells have implicated PLSCR1 in regulating TLR9 signaling upon stimulation with CpG ODN [42]. However, whether PLSCR1 could mediate the innate immune responses upon stimulation with dsDNA remained unclear. In Chapter 5, we identified that stimulation of normal ovarian and mammary epithelial cells with dsDNA (empty plasmid) markedly induces PLSCR1 consequent with activation of IRF3, a downstream mediator of TLR signaling that transcriptionally regulates the expression of type 1 IFNs [43-45]. Interestingly, IRF3 knockdown ablates the dsDNA-induced PLSCR1 expression suggesting that PLSCR1 induction in response to dsDNA could be mediated by IRF3. Additionally, we have determined that dsDNA stimulation induces nucleic acid sensing TLRs, TLR9 and TLR4 as well as IFN- $\alpha$  and IFN- $\beta$  mRNAs. Interestingly, dsDNA stimulation did not induce PLSCR1 or IRF3 activation in ovarian cancer cells suggesting that the mechanisms of IRF3 activation and PLSCR1 induction in response to dsDNA might be dysregulated in ovarian cancers.

Collectively, our studies demonstrate a possible synergistic role of SnoN and PLSCR1 in ovarian cancer pathophysiology and suggest a potentially dysregulated role of PLSCR1 in the dsDNA-induced immune responses of malignant epithelial cells relative to normal epithelial cells. These studies could potentially lead to development of a novel combinatorial therapeutic strategy that targets both these molecules for improving treatment of patients with ovarian carcinoma.

## Chapter 1

### Introduction

#### Ovarian Cancer

Ovarian cancer is one of leading causes of death from gynecological cancers among women with 14,270 deaths and 22,240 new cases estimated in 2014 in United States (National Cancer Institute, <http://seer.cancer.gov/statfacts/html/ovary.html>). Lack of effective early detection methods and resistance to chemotherapeutics make ovarian cancers deadly with a 5-year survival rate of less than 50% (National Cancer Institute, <http://seer.cancer.gov/statfacts/html/ovary.html>). The current treatment strategies for ovarian cancer include surgical debulking followed by chemotherapy and radiation therapy (NCI) [46]. Current FDA approved drugs in the treatment of ovarian cancer majorly include platinum-based drugs such as cisplatin, carboplatin, and paclitaxel [47].

Epithelial ovarian cancer (EOC), one of the major types of ovarian cancers (NCI), is a heterogeneous disease composed of specific subtypes with distinctive morphology, molecular characteristics, pathogenesis, and progression [48-51]. EOC can be further classified into the following subtypes: (1) mucinous invasive ovarian cancer, proposed origin of which is still unclear [52]; (2) endometrioid carcinoma, (3) clear cell carcinoma, proposed to be derived from endometriosis due to retrograde menstruation [53, 54], and (4) high-grade serous epithelial ovarian carcinoma (HGSC), proposed to be derived from the ovary surface epithelium and/or the distal fallopian tube [55, 56]. Of these subtypes, HGSC is the most commonly occurring, accounting for almost 70% of all the cases and most patients present with advanced stage disease [57]. Although HGSCs are sensitive to chemotherapy with platinum-based drugs and taxanes, disease recurrence often occurs leading to untreatable disease [57].

### Current treatment strategies:

Although there have been advances in the strategies of treatment of solid tumors in the last few decades, the survival rate of women with EOC has changed minimally [49]. Current treatment of EOC is based on the combination of surgery and chemotherapy. Over the past three decades, surgical tumor debulking and platinum/taxanes-based chemotherapy have been the standard treatments for advanced ovarian cancer [58, 59]. Platinum-based chemotherapeutics that were first introduced in late 1970s are still the major drugs used in the treatment of ovarian cancer [49, 59]. Pegylated liposomal doxorubicin is commonly used in association with carboplatin and paclitaxel and has been recently shown to improve the survival rate in platinum-sensitive EOC patients [60]. Another strategy used in treatment of ovarian cancer is the targeted therapies, which are aimed at inhibiting the activity of specific molecular factors involved in development of ovarian cancer. Although PARP (poly (ADP-ribose) polymerase) inhibitors [61, 62], angiogenesis inhibitors [63], and many such drugs targeting the specific molecular factors [62] appear effective, they have only yielded small increments in improving progression-free survival in ovarian cancers. Although the advances in surgery and chemotherapy have improved the 5-year survival rate to 50%, the cure rate of ovarian cancer has not improved concurrently. Hence, there is a need for the development of novel therapeutic strategies in the treatment of ovarian carcinoma.

### Common genetic aberrations:

HGSCs are most commonly characterized by mutations in *TP53* in almost 80% of the cases [51, 64] in addition to inactivating mutations in *BRCA* in up to 50% of cases either via genetic or epigenetic mutations [51]. Endometrioid and clear cell carcinomas are commonly associated with *PTEN* mutations [65] along with activating mutations in *PIK3CA* [66] and *KRAS* [67]; whereas *KRAS* mutation at codon 13 is reported to be an early occurrence in the pathogenesis of mucinous ovarian cancers [52, 68]. Alterations are also found in various mediators of important signaling pathways such as  $TGF\beta$  signaling (transforming growth factor- $\beta$ ) pathway [69], *EGFR*/*ErbB* receptor signaling [70], and *Ras*/*MAPK*/*Src*/*AKT* pathways [70].



### Amplification of chromosomal region 3q26:

In addition to the above genetic aberrations, amplification of chromosomal region 3q26 is a frequent occurrence in most epithelial cancers including ovarian cancers [9-12, 31]. Various studies

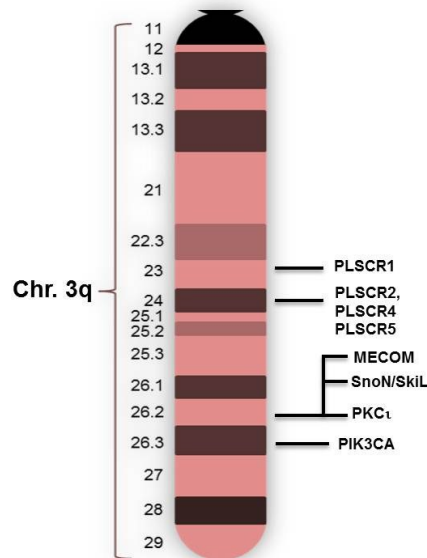


**Figure 1: Human chromosomal 3q region**

The chromosomal region 3q26 is highly amplified in various epithelial cancers including ovarian cancers. This region harbors many oncogenes including EVI1, SnoN/SkiL, PKC $\epsilon$  at the locus 3q26.2 and PIK3CA at 3q26.3 that are amplified in ovarian cancers [9-12]. Proximal to 3q26 region, PLSCR family members are clustered at loci 3q23 (PLSCR1) and 3q24 (PLSCR2, PLSCR4 and PLSCR5) (<https://genome.ucsc.edu/>, December 2013). (\*Figure created by Madhav Karthik Kodigepalli)

including our recent studies report that the chromosomal loci around 3q26 harboring various oncogenes such as MECOM (MDS1-EVI1 complex) [10], SnoN/SkiL, and PKC $\epsilon$  at 3q26.2 [9, 31] as well as PIK3CA [catalytic subunit of phosphoinositide-3-kinase (PI3K)] at 3q26.3 [11] (shown in Figure 1) are highly amplified in ovarian cancers. EVI1 (ecotropic viral integration site) and SnoN (Ski related novel protein N) are negative transcriptional regulators of the TGF $\beta$  pathway.

### TGF $\beta$ signaling:

TGF $\beta$  is an ubiquitous and essential regulator of cellular and physiological processes including proliferation, differentiation, migration, cell survival, angiogenesis, and immunosurveillance [71]. TGF $\beta$  exerts its activity by binding to a family of transmembrane serine/threonine kinase receptors [72]. TGF $\beta$  binds initially to TGF $\beta$  type-II receptor (TGF $\beta$ RII) and this ligand-receptor complex recruits and phosphorylates TGF $\beta$  type-I receptor (TGF $\beta$ RI) by homodimerization. Activated TGF $\beta$ RI initiates a signaling cascade by phosphorylating and activating the receptor SMAD proteins (SMAD2/3) [72] which form a complex with SMAD4 (Co-SMAD) and translocate into the nuclear compartment. This complex binds and activates/represses specific TGF $\beta$  responsive genes which play a prominent role in regulating various cellular responses including (1) differentiation, (2) proliferation, and (3) apoptosis [71, 73]. This pathway mediates both tumor promoting and tumor suppressing functions to repress transformation in normal cells while increasing aggressiveness of transformed cells by inducing epithelial-mesenchymal transition (EMT) [74]. Aberrations in the TGF $\beta$  signaling pathway, including mutations or loss of expression of mediators in the signaling pathway are noted in various human cancers [73, 74]. Specifically, in ovarian cancer, EVI1, SnoN/SkiL, TGF $\beta$ RII, and PI3K/AKT [75] are dysregulated and lead to resistance to the growth inhibitory effects of TGF $\beta$  [9, 10, 69]. TGF $\beta$  signaling is negatively regulated by various proteins including EVI1, SnoN, and inhibitory SMADs (SMAD7) [71].

### **SnoN**

SnoN (Ski related novel protein N) belongs to the Ski family of nuclear oncogenes; it is an important negative regulator of TGF $\beta$  signaling pathway. SnoN directly binds to SMAD2/3 as well as SMAD4 preventing them from binding to transcriptional co-activators; this leads to repression of TGF $\beta$  target genes and blockade of TGF $\beta$ -induced growth arrest [28, 76, 77]. SnoN, along with its closely related oncoprotein Ski, have been identified to induce cancer cell proliferation and transformation; this activity is dependent on their TGF $\beta$  signaling repressing function [78, 79]. In various cancers including ovarian [9], lung [80], breast [79], esophageal [28], and colorectal cancers [81], SnoN expression is

elevated due to gene amplification, altered transcription, and protein stability [9, 81]. SnoN also elicits tumor suppressor activity in various cancers including microsatellite unstable cancers which have a disrupted TGF $\beta$  signaling pathway due to reduced endogenous expression of SnoN [82, 83]. Interestingly, increased SnoN levels induces senescence via interaction with PML (promyelocytic leukemia) protein and stabilization of p53 leading to tumor suppression [84]. As shown in Figure 2, SnoN has various domains such as: (1) R-SMAD domain through which it binds to SMAD2/3; (2) Dachshund domain which binds to N-CoR, a transcriptional co-repressor; (3) SMAD domain which promotes interaction with SMAD4; and (4) oligomerization domain which is involved in heterodimeric formation with c-Ski (Figure 2). Additionally, SnoN contains sites for post-translational modifications such as phosphorylation, ubiquitination, and

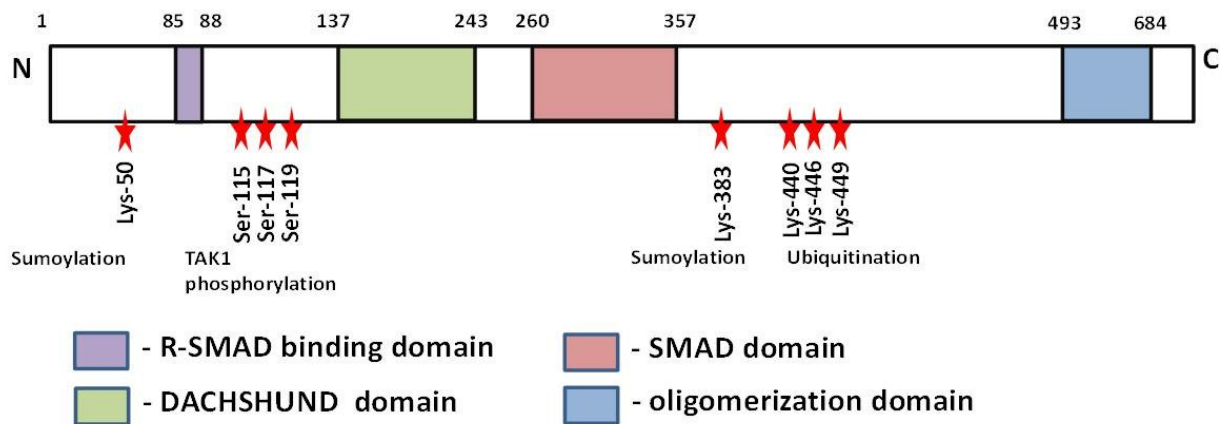


**Figure 2: Structural organization of SnoN protein**

SnoN/SkiL is a 684 aa protein composed of the following structural domains. (1) R-SMAD domain which binds to TGF $\beta$  signaling mediator SMAD2/3; (2) Dachshund domain binds to transcriptional co-repressor N-CoR; (3) SMAD domain that facilitates interaction with activator SMAD4; and (4) oligomerization domain which is involved in heterodimeric formation with c-Ski [14]. (\*Figure created by Madhav Karthik Kodigepalli)

SUMOylation [85-88]. SnoN can also be phosphorylated by TAK1, a MAPKK protein which is required for TGF $\beta$ -induced degradation of SnoN [86]. Additionally, SnoN protein stability is regulated via ubiquitination by specific E3 ubiquitin ligases. Anaphase promoting complex (APC), a ring finger

containing E3 ligase enzyme recruited to SnoN by SMAD3 results in ubiquitination and degradation of SnoN [88]. Other E3 ligases, including Arkadia and Smurf2, also mediate TGF $\beta$  dependent SnoN ubiquitination and degradation [85, 87]. Studies indicate that SnoN expression, located at 3q26.2 is highly amplified in EOC patients and promotes ovarian epithelial and cancer cell proliferation [9]. More recently, our group has implicated SnoN in inducing cytoprotective autophagy in ovarian carcinoma cells following treatment with arsenic trioxide (As<sub>2</sub>O<sub>3</sub>) [1].

### **Arsenic Trioxide (As<sub>2</sub>O<sub>3</sub>)**

Arsenic trioxide is a carcinogen of human skin, lung, liver, kidney, and urinary bladder cancers [89]. Paradoxically, it is also a clinically used chemotherapeutic agent in the treatment of acute promyelocytic leukemia (APL) [90]. APL is a subtype of acute myeloid leukemia (AML), characterized by a specific chromosomal translocation (t(15;17)) resulting in production of the leukemic PML-RAR fusion oncoprotein which drives APL cellular proliferation; As<sub>2</sub>O<sub>3</sub> is an FDA approved drug which is used for patients that become resistant to the primary treatment agent, ATRA (all-trans retinoic acid) [90]. Many studies report that As<sub>2</sub>O<sub>3</sub> exerts its therapeutic effect by promoting the degradation of the PML-RAR fusion protein. The drug binds directly to the cysteine residues in the zinc fingers of the PML and PML-RAR proteins thereby increasing its interaction with small ubiquitin-like molecules leading to SUMOylation-mediated degradation [91]. As<sub>2</sub>O<sub>3</sub> promotes cell death via apoptosis and beclin-1 dependent autophagy in leukemia cells [92]. As<sub>2</sub>O<sub>3</sub> can also decrease expression of TGF $\beta$  signaling pathway mediators including EVI1, TAK1, SMAD2/3, and TGF $\beta$ RII as well as increase the expression of SnoN/SkiL in ovarian cancer cells [1]. Furthermore, As<sub>2</sub>O<sub>3</sub> induces a beclin-1 independent autophagy pathway by modulating the expression of SnoN [1]. However, the exact mechanism by which SnoN is modulated by As<sub>2</sub>O<sub>3</sub> remains unclear.

## Programmed Cell Death

Programmed cell death can be classified into three subgroups based on the morphological characteristics: (1) apoptosis, (2) autophagy, and (3) necroptosis [93].

### Autophagy:

Autophagy is a tightly regulated and complex catabolic process leading to intracellular degradation of its own cellular components involving lysosomal-mediated degradation. Autophagic flux

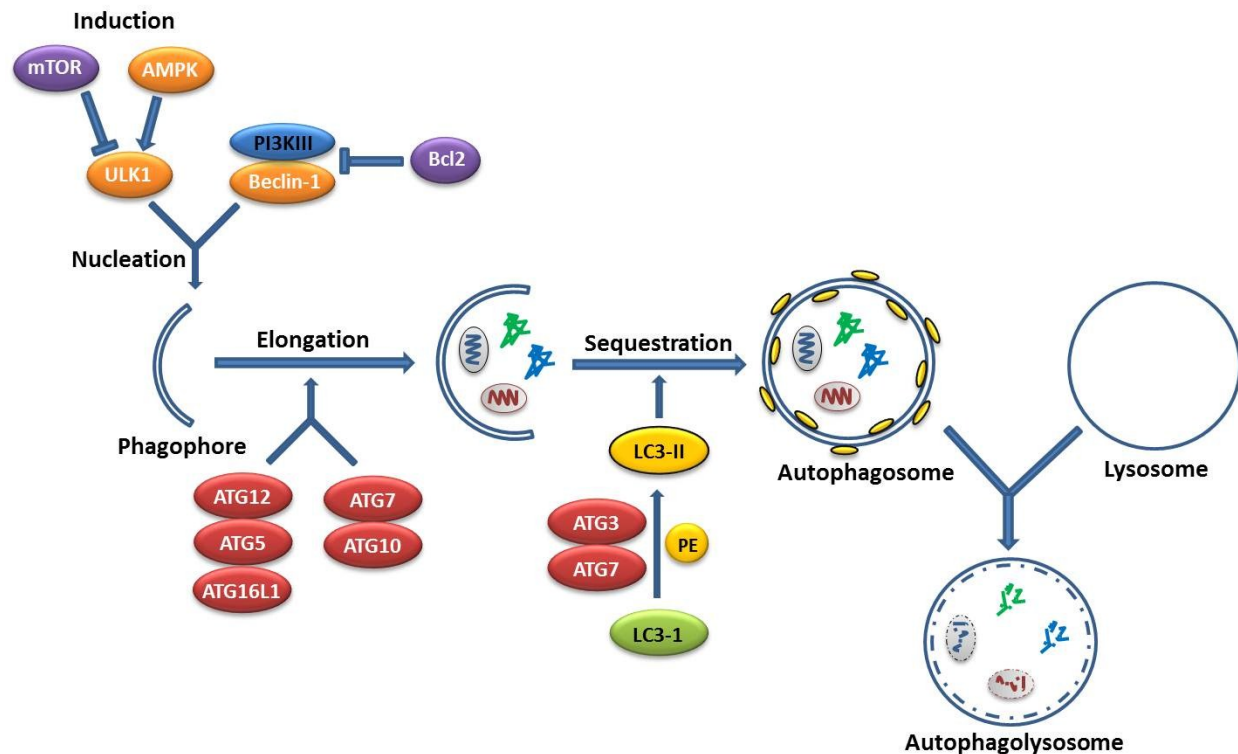


**Figure 3: Schematic representation of autophagy pathway**

Induction of autophagy is regulated by mTOR (mammalian target of rapamycin), AMPK ((5'-AMP-activated protein kinase) and class I and III members of PI3K family [2, 3]. ULK1 and Beclin-1 aid in the step of vesicle nucleation resulting in the formation of phagophore. The next step of vesicle elongation is facilitated by function of various ATG proteins (ATG12, ATG5, ATG7 and ATG10). Conversion of LC3-I to LC3-II via lipidation is facilitated by ATG7 and ATG3 resulting in formation of autophagosome that sequesters the damaged organelles and proteins. Finally, autophagosome fuses with the lysosomes to form autophagolysosome which results in degradation of damaged cargo [2, 3]. (\*Model created by Madhav Karthik Kodigepalli)

is an important physiological pathway which occurs constantly in all cells at basal levels aiding in clearance and degradation of damaged proteins and cell organelles; the flux can be increased under conditions of stress and starvation [3]. Figure 3 shows the important steps and molecules that are involved in the process of autophagy. These include (1) vesicle nucleation which involves formation of the initiating membrane, (2) vesicle elongation which involves expansion of the isolation membrane (referred to as phagophore), and (3) vesicle completion which leads to fusion of the membrane forming the double membrane autophagosomes which sequester the cellular cargo to be degraded [3]. In the next step, fusion of the autophagosome with a lysosome leads to formation of the autophagolysosome which results in the degradation of the encapsulated damaged organelles/proteins; increased autophagic flux can lead to cell death when reached beyond a threshold level [3]. One of the major regulators of autophagy is the mammalian target of rapamycin (mTOR), which inhibits autophagic activation under nutrient-rich conditions (i.e. in the presence of growth factors) [2]. Autophagy is also regulated by class I and class III PI3K family members and AMPK (5'-AMP-activated protein kinase) [2, 3]. AMPK responds to various stress factors such as nutrient starvation and endoplasmic reticulum (ER) stress which then phosphorylates ULK1 which initiates the autophagic cascade. ULK1 (or named ATG1) is one of the many evolutionarily conserved effector autophagy molecules known as the ATG proteins, which is essential for the execution of autophagy (Figure 3) [2, 94]. Although autophagy can be defined as a cell death mechanism, it elicits dual function in cancer development: tumor suppressor at the initial/early stages and then as an oncogene in the late stages of cancer progression [95, 96]. In addition, radiotherapy and certain cytotoxic drugs can elevate levels of autophagy which promote cancer cell survival [95, 97].

#### Apoptosis:

Apoptosis is a form of cell death characterized by chromatin condensation, nuclear fragmentation, plasma membrane blebbing that occurs in response to various stimuli such as DNA damage and treatment with cytokines [98]. It is an energy-dependent process involving proteases known as caspases. Apoptosis occurs via two different pathways: (1) extrinsic and (2) intrinsic. The extrinsic pathway is mediated by transmembrane death receptors located at the plasma membrane (i.e. tumor necrosis factor (TNF) family

of receptors [98]) which upon activation results in a cascade of events leading to activation of caspases. On the other hand, the intrinsic pathway is activated primarily by internal stimuli such as DNA damage; it is mediated by the mitochondrial release of cytochrome c that contributes to the formation of the apoptosome and thus activation of effector caspases. In both the pathways, caspases initiate a cascade of proteolytic events leading to consumption of the apoptotic cells by macrophages [97]. The apoptotic process is antagonized by various anti-apoptotic members of the Bcl-2 family of regulatory proteins [99] including Bcl-2, Bcl-xL, Bcl-w, Mcl-1, and A1 which bind to and suppress the function of the proapoptotic proteins Bax and Bak which are embedded in the mitochondrial outer membrane. Evasion of apoptosis is one of the hallmarks of cancer. Therefore, induction of apoptosis can be utilized as an efficient therapeutic strategy in the treatment of various cancers.

#### Necroptosis:

Necroptosis is another form cell death which was earlier considered as an accidental and non-programmed process referred to as necrosis. However, necroptosis is now defined to be a finely regulated process which is activated by various stimuli including tumor necrosis factor (TNF) family members [100], Fas ligand [101], lipopolysaccharides (LPS) (upon caspase inhibition) [102] in addition to physical and chemical stress conditions (i.e. treatment with chemotherapeutic drugs) [103]. For example, cellular stimulation with TNF- $\alpha$  leads to activation of TNF receptors (TNFR1 and TNFR2) which trigger a downstream signaling by forming a complex with death domain containing proteins including TNF- $\alpha$  receptor-associated death domain (TRADD), receptor interacting protein kinase 1 (RIP1), and other E3 ubiquitin ligases that lead to activation of RIP1 [104]. Activated RIP1 forms a complex with receptor interacting protein kinase 3 (RIP3) [105] leading to necroptosis characterized by features similar to necrosis including plasma membrane permeabilization, lysosomal permeabilization, and mitochondrial hyperpolarization [106]. The complete mechanism involved in execution of necroptosis requires further investigation.

## **Phospholipid Scramblase: PLSCR Family Members, TMEM16F and Xkr8**

### Phospholipids, membrane asymmetry, scramblase activity, and blood coagulation:

Phospholipids are essential components of mammalian cell membranes; specifically, these lipids are distributed asymmetrically on the inner and outer leaflets of the plasma membrane (PM). Phospholipids that are located in the cytosolic leaflet allow anchoring of signaling proteins that need to be membrane associated to elicit functionality [107]. For instance, phosphatidylserine (PS, ~15% of total), one of the four major phospholipids in the plasma membrane is located in the inner leaflet along with phosphatidylethanolamine (PE, ~25%) while sphingomyelin (SM, ~25%) and phosphatidylcholine (PC, ~25%) are localized in the outer leaflet. This asymmetrical distribution of phospholipids, which is maintained in the quiescent cells under normal conditions, collapses in response to two major cellular events, blood coagulation and apoptosis; these events involve “scrambling” of these phospholipids between the inner and outer leaflets of plasma membrane. Injuries leading to activation of the blood coagulation pathway involves PS externalization in platelets; this event promotes its interactions with various coagulation factors which stimulates the formation of thrombin and consequently, blood clotting [108-110]. In apoptotic cells, scramblase activity leads to altered phospholipid PM asymmetry resulting in PS externalization. This PS exposure provides a signal for recruitment of macrophages to bind to and engulf these apoptotic cells [111, 112]. Indeed, regulation of scramblase activity is essential in maintaining and altering the asymmetry of membrane phospholipids [110, 113, 114]. In addition to the blood coagulation and apoptosis, calcium dependent phospholipid scrambling has also been reported to regulate the activity of plasma membrane cholesterol [115]. Treatment of erythrocytes with calcium ionophore led to a marked increase in the chemical activity (escape potential) of cholesterol which was abolished by scramblase inhibitors [115]. Phospholipid scrambling leading to PS externalization has been attributed to various proteins. For example, several groups have reported that phospholipid scramblase (PLSCR) family members contribute to calcium dependent PS externalization in blood platelets aiding in the process of blood coagulation [34, 35]. However, later studies in PLSCR knockout mice have suggested that PLSCR members might only have a partial role in this process [37, 116]. TMEM16 family



of transmembrane proteins that function as chloride channels, especially were identified later to be involved in the calcium dependent phospholipid scrambling activity and PS externalization [117-122]. However, TMEM16F<sup>-/-</sup> knockout mice exhibit normal levels of PS externalization during apoptosis [122]; this indicates that different mechanisms may be responsible for PS externalization in apoptotic cells and upon calcium mobilization. Recently, a six transmembrane protein called XK related protein 8 (Xkr8, located at 1p35.3) has been shown to be involved in PS externalization induced by apoptotic mediators; this was demonstrated using Xkr8<sup>-/-</sup> knockout mice cells and human cancer cells treated with Xkr8 siRNA [123-125]. Xkr8 was directly activated by caspase 8, an important mediator in process of apoptosis. In support, the *C. elegans* homolog of Xkr8 (CED-8), also promoted PS externalization [123, 124]. However, the exact mechanism by which Xkr8 regulates the PS externalization in apoptotic cells remains unknown. Collectively, these findings implicate different proteins in PS externalization induced under different conditions (PS exposure in response to coagulation, calcium activation, and apoptosis).

#### cDNA Cloning of “phospholipid scramblases”:

Previous studies implicated increased calcium ions in the activation of scramblase activity thereby leading to PS externalization in multiple cell types including platelets and erythrocytes [126-129]. However, the molecules and mechanisms involved in this particular process remained unknown until 1996 when Basse and colleagues reported the purification of a type II transmembrane protein from erythrocytes, which upon reconstitution into liposomes, could mediate calcium-dependent redistribution of membrane phospholipids including PS and PC [34]. Its cDNA was isolated via a plaque hybridization technique [35] and was named PL scramblase (PLSCR1), a ~37 kDa protein. PLSCR1 was found to be expressed ubiquitously in multiple cell lines including erythrocytes, blood platelets, and others which were associated with phospholipid scramblase activity in the presence of Ca<sup>+2</sup> [130]. In 2000, Wiedmer and colleagues cloned the human PLSCR1 gene from a human genomic BAC library and estimated the size of its gene to be 29.7 Kb encompassing 9 exonic regions [131]. The first exon of PLSCR1 is untranslated and was identified to be its promoter region [131]. Additionally, three other cDNAs with

high homology to PLSCR1 were cloned by a PCR-based approach utilizing a cDNA library [131]. These newly identified proteins were named PLSCR2, PLSCR3, and PLSCR4 [131]. More recently, another gene with similarity to PLSCR1, named PLSCR5, has been identified as a fifth member of phospholipid scramblase family. PLSCR1 (318 aa), PLSCR2 (297 aa), PLSCR4 (329 aa), and PLSCR5 (271 aa) are all located at the 3q24 cluster whereas PLSCR3 (295 aa) is located at 17p13.

Gene Location and Protein Structure of PLSCR1 isoforms:

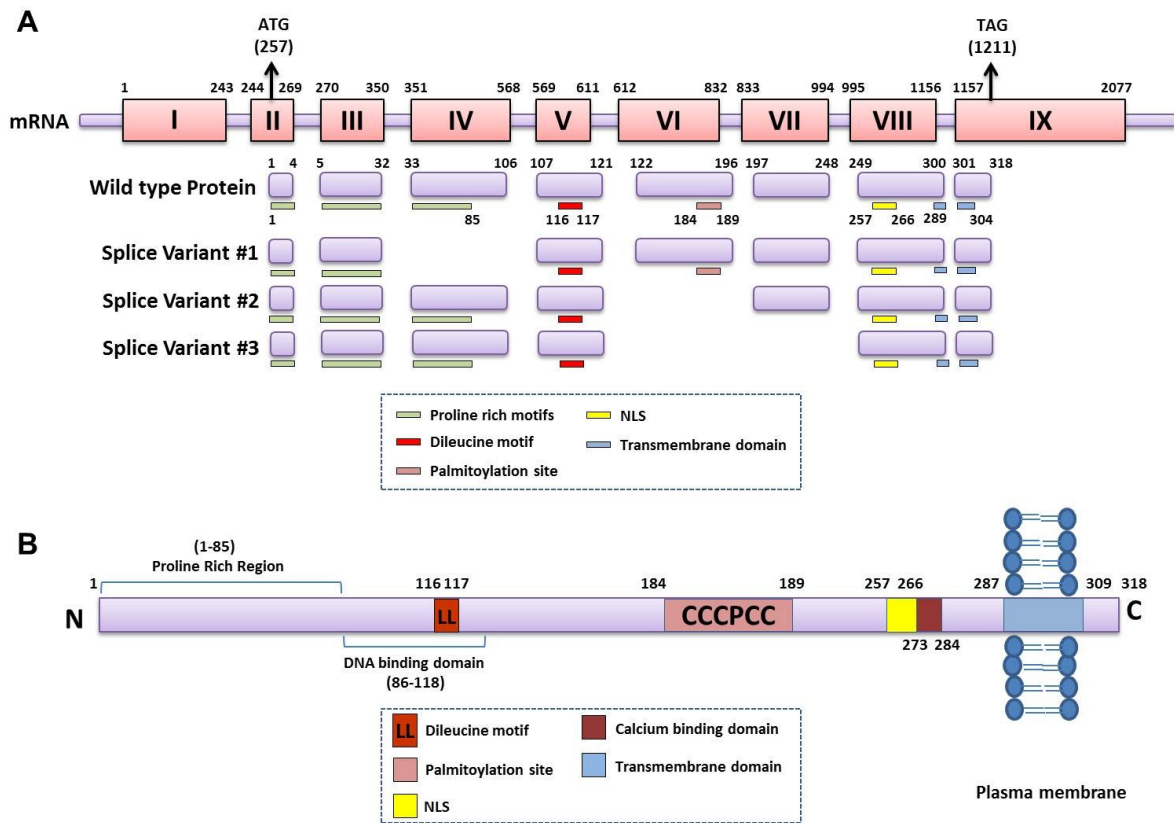


**Figure 4: Structural organization of PLSCR1 gene and protein**

(A) PLSCR1 gene, located at 3q23 is comprised of 9 exonic regions. The coding region lies between bases 257 (in exon II) and 1211 (exon IX). Four alternate variants of PLSCR1 are presented in the figure. Variant 1 lacks exon IV, variant II lacks exon VI and variant III lacks exons VI and VII. Alignment of exons with their corresponding amino acid regions and the deleted protein domains in each variant are presented. (B) PLSCR1 protein structure comprises of the following important structural domains. (1) Proline rich N terminal region (1-85 aa) [18, 19], (2) Dileucine motif (amino acids 116, 117), (3) DNA binding domain (86-118 aa) [23], (4) Palmitoylation site (184-189 aa) [24], (5) NLS (257-266 aa) [25], (6) Calcium binding domain (273-284 aa) [26] and (7) Transmembrane domain (287-309) [27]. (\*Figure created by Madhav Karthik Kodigepalli)

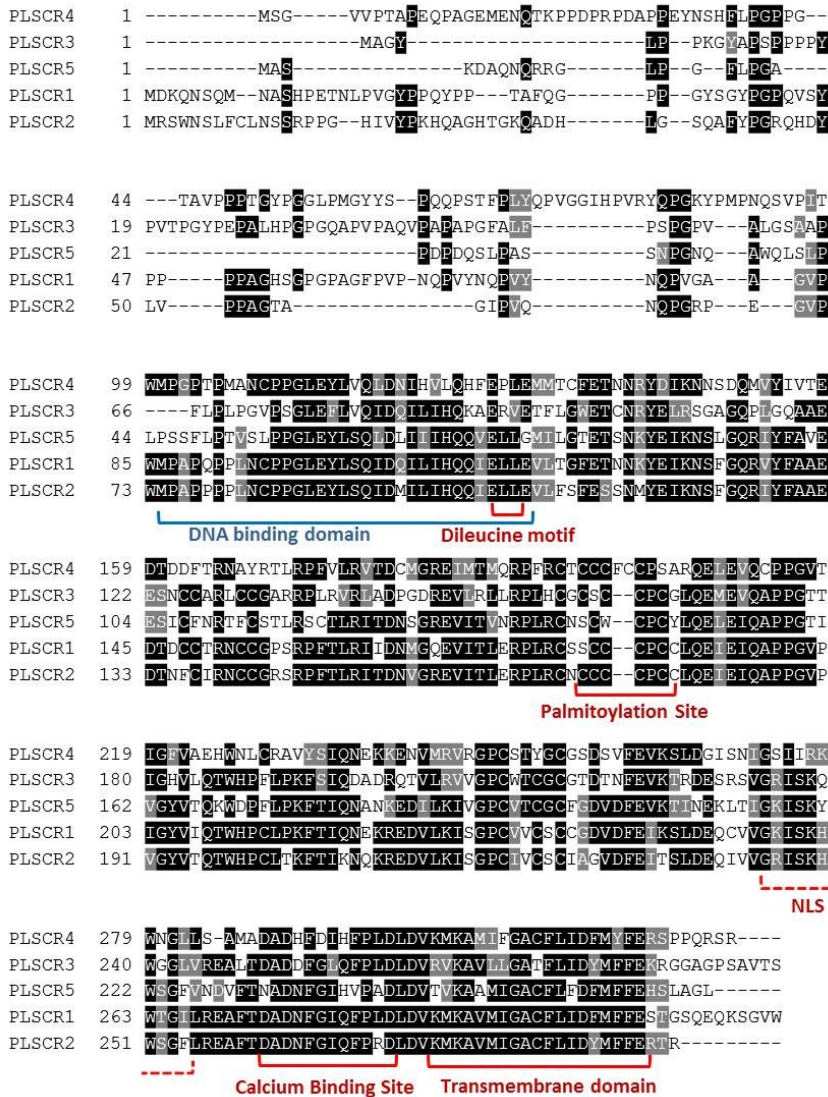


**Figure 5: Amino acid sequence alignment of PLSCR family members**

Amino acid sequences of PLSCR2 (NP\_001186907.1), PLSCR3 (NP\_001188505.1), PLSCR4 (NP\_001121777.1), and PLSCR5 (NP\_001078889.1) were aligned with that of PLSCR1 (AAH21100.1) via Clustal Omega bioinformatic program (<http://www.ebi.ac.uk/Tools/msa/clustalo/>). The alignment output was then analyzed via BoxShade program ([http://www.ch.embnet.org/software/BOX\\_form.html](http://www.ch.embnet.org/software/BOX_form.html)) to highlight the identical amino acids among the PLSCR family members.

With the exception of PLSCR3, all of the PLSCR family members are clustered on the q arm of chromosome 3, specifically at 3q23 and 3q24 loci (<https://genome.ucsc.edu/>, December 2013). In the

order from the centromere, PLSCR4 is located at chr3:146,192,336-146,251,179 (58.543 Kb), PLSCR2 is located at chr3:146,433,288-146,469,301 (36.013 Kb), PLSCR1 chr3:146,515,180-146,544,841 (~29.661 Kb), and PLSCR5 is located at chr3:146,576,608-146,606,216 (29.608 Kb) (Figure 1). On the other hand, PLSCR3 is located distantly from the other PLSCR family members on the p arm of chromosome 17 at

**Table 1: cDNA identity matrix of PLSCR family members**

cDNA sequences of PLSCR2 (NM\_001199978.1), PLSCR3 (NM\_001201576.1), PLSCR4 (NM\_001128305.1), and PLSCR5 (NM\_001085420.1) were aligned with that of PLSCR1 (BC021100) via Clustal Omega bioinformatic program (<http://www.ebi.ac.uk/Tools/msa/clustalo/>). Percent cDNA identities obtained are presented in the form of matrix.

	PLSCR1	PLSCR2	PLSCR3	PLSCR4	PLSCR5
PLSCR1	100	70.24	38.61	45.35	55.95
PLSCR2	70.24	100	35.55	43.12	52.81
PLSCR3	38.61	35.55	100	44.70	34.13
PLSCR4	45.35	43.12	44.70	100	41.88
PLSCR5	55.95	52.81	34.13	41.88	100

**Table 2: Protein identity matrix of PLSCR family members**

Amino acid sequences of PLSCR2 (NP\_001186907.1), PLSCR3 (NP\_001188505.1), PLSCR4 (NP\_001121777.1), and PLSCR5 (NP\_001078889.1) were aligned with that of PLSCR1 (AAH21100.1) via Clustal Omega bioinformatic program (<http://www.ebi.ac.uk/Tools/msa/clustalo/>). Percent protein identities obtained are presented in the form of matrix.

	PLSCR1	PLSCR2	PLSCR3	PLSCR4	PLSCR5
PLSCR1	100	73.63	50	48.14	57.36
PLSCR2	73.63	100	49.24	46.04	56.15
PLSCR3	50	49.24	100	37.81	47.45
PLSCR4	48.14	46.04	37.81	100	41.85
PLSCR5	57.36	56.15	47.45	41.85	100

chr17:7,389,728-7,394,843 (5.115 Kb) [131]. PLSCR1 gene is comprised of 9 exons with the coding region beginning at exon 2 and ending at exon 9. Figure 4 (Upper panel) illustrates the exon structures and the corresponding protein structural domains that they code. Although various alternate splice forms

of PLSCR1 are predicted, only three such forms have been identified experimentally [132]. As shown in Figure 4 (Upper panel), these three variants are 905 bp, 750 bp, and 551 bp which harbor deletions in exon IV, exon VI, exons VI and VII respectively; in contrast, the full length PLSCR is represented by 1122 bp [132]. Interestingly, exon IV codes for the proline-rich region important for mediating interactions with various signaling mediators [18, 19, 133] while exon VI codes for the region encompassing the palmitoylation site which regulates the localization of PLSCR1 [24]. Although these splice variants have been identified, it remains to be investigated whether they elicit altered localization and/or functionality. As shown in Table 1, the cDNA alignment of the PLSCR family members performed by Clustal Omega bioinformatic program (<http://www.ebi.ac.uk/Tools/msa/clustalo/>) shows that the mRNAs of PLSCR2 (NM\_001199978.1), PLSCR3 (NM\_001201576), PLSCR4 (NM\_001128305), and PLSCR5 (NM\_001085420) have a sequence identity of 70.24%, 38.61%, 45.35% and 55.95% with PLSCR1 (BC021100), respectively. The protein sequence alignment analyses of PLSCR family members using the same program indicates that the PLSCR2 (297 aa, NP\_001186907.1), PLSCR3 (295 aa, NP\_001188505.1), PLSCR4 (329 aa, NP\_001121777.1) and PLSCR5 (271 aa, NP\_001078889.1) proteins have 73.63%, 50.00%, 48.14% and 57.36% identity with PLSCR1 (318 aa, AAH21100.1), respectively (Table 2). As shown in Figure 5, all the PLSCR members with the exception of PLSCR2 possess a proline-rich N-terminal region containing PXXP and PPXY domains, a cysteine-rich region, a conserved calcium ion binding domain, and a putative transmembrane region rich in hydrophobic amino acids. In addition, PLSCR1 contains a nuclear localization signal (NLS) and a DNA binding domain (Figure 4, Lower panel) that is known to mediate direct binding to IP<sub>3</sub>R promoter [23] whereas PLSCR4 contains a minimal nuclear localization signal [134].

#### Scramblase activity of PLSCR family members:

PLSCR1, isolated from erythrocytes, was reconstituted into liposomes containing PS and PC in 9:1 ratio; this resulted in rapid bidirectional movement similar to that in plasma membranes following Ca<sup>+2</sup> mobilization [34]. Similar results were obtained upon reconstitution of recombinant MBP-tagged

PLSCR1 in the liposomal-based reconstitution assay or GFP-tagged PLSCR1 expressed in Burkitt's lymphoma Raji cells treated with A23187, a calcium ionophore [82][35]. The calcium binding site in PLSCR1 (amino acid 278–284) is critical in mediating calcium-induced phospholipid scrambling activity [26]. Interestingly, in *C. elegans*, PS externalization in apoptotic germ cells is mediated by Scrm1, an ortholog of human PLSCR1 [135]. These reports provide evidence for scramblase activity for PLSCR1 in calcium-dependent manner. With respect to other PLSCR family members, mutations in the calcium-binding site of PLSCR4 resulted in a marked reduction in its  $\text{Ca}^{+2}$  and  $\text{Mg}^{+2}$ -induced scramblase activity [136]. Interestingly, PLSCR3, which is localized to mitochondrial membranes, is capable of externalizing cardiolipin from the inner to the outer mitochondrial membrane [137]. In contrast, PLSCR2 was demonstrated to lack scramblase activity; this was attributed to the absence of a proline-rich N-terminal region which is present in other PLSCR family members [138]. Indeed, studies indicate that PLSCR2, when fused with the proline-rich domain of PLSCR1, leads to increased calcium-dependent scrambling activity [138]. Although the above studies implicate PLSCRs in the redistribution of phospholipids between membrane leaflets, studies by Fadeel and colleagues suggested that there may be other factors responsible for PS externalization induced by apoptotic stimuli [116]. Furthermore, the PLSCR1 expression was detected to be normal in patients with Scott syndrome, a disease characterized by defective phospholipid scrambling in platelets leading to a deficiency in blood coagulation [139]. Also, PLSCR1 knockout mice did not display any deficiency in scramblase activity suggesting that PLSCR1 is not essential for mediating PS exposure *in vivo* [37, 116]. Since PLSCR3 and PLSCR4 may also contribute to scrambling activity, they might overcome the loss of PLSCR1 by eliciting redundant function thus leading to PS externalization in PLSCR1<sup>-/-</sup> mice [136-138]. It would be interesting to determine whether combinatorial knockouts of specific PLSCR family members results in dysregulated scramblase activity. PLSCR3<sup>-/-</sup> knockout mice have been developed and utilized by Mutch et.al. in 2007 [140]. Strikingly, PLSCR1 and PLSCR3 double knock-out mice still retain scramblase activity [140]. The role of PLSCR2 and PLSCR4 in scrambling activity still remains unknown.

### Defect in TMEM16/Ano6 is Responsible for Scramblase Activity Deficiency in Scott Syndrome platelets:

Scott Syndrome is a severe bleeding disorder that is characterized by lack of PS exposure in platelets, red cells, and lymphocytes resulting in a defective blood coagulation process [141]. Platelets from Scott syndrome patients failed to expose PS to the outer leaflet of the plasma membrane following cellular activation by treatment with calcium ionophore [142]; although PLSCR1 was thought to be implicated in mediating scramblase activity, PLSCR1 expression was normal in these cells [139]. Recently, TMEM16F (Transmembrane protein 16F, Anoctamin), a calcium-dependent chloride channel, was identified to be involved in the  $\text{Ca}^{+2}$ -dependent PS externalization in Scott syndrome platelets via studies in mouse Ba/F3 B-cells and a calcium ionophore [117]. TMEM16F/Ano6, a gene located at chromosome 12q12, belongs to TMEM family of chloride channels and encodes for a protein containing 8 transmembrane domains [119]. Indeed, TMEM16F is mutated in patients with Scott syndrome and its reconstitution in liposome systems as well as in Scott Syndrome cells promoted PS externalization [117, 118, 120, 121, 143]. In support, TMEM16F knockout mice displayed excessive bleeding defects and defective lipid scrambling activity in platelets [121, 122]. Collectively, evidence has accumulated supporting TMEM16F in playing an essential role in phospholipid scrambling, in particular PS exposure, under conditions of increased calcium. However, immortalized fetal thymocyte cells isolated from the TMEM16F<sup>-/-</sup> knockout mice did not show any abnormalities in PS externalization following exposure to apoptotic stimuli [122]. This implicates another mechanism responsible for PS externalization during apoptosis. Nonetheless, the contribution of PLSCR family members, XKR8, and TMEM16F in mediating phospholipid scrambling and the extent to which they are required for this process needs further investigation.

## Regulation, Subcellular Localization, and Functions of PLSCR Family members

Transcriptional regulation by growth factors, interferons, and Snail:

**Table 3: Upregulation of PLSCR1 in response to various stimuli**

List of various stimuli including growth factors (i.e. EGF, G-CSF, and SCF) along with cytokines (i.e. IFN) and differentiation inducing agents (i.e. ATRA) in specific cell types leading to upregulation of PLSCR1 expression is presented. The corresponding citations are presented for each stimulus presented.

Stimulant	Cell type (with PLSCR1 induction)	Reference
Epidermal Growth Factor (EGF)	KB - HeLa contaminant epithelial carcinoma	[19]
Interferons (IFN)	HT1080 - human fibrosarcoma	[39]
	HeLa – cervical carcinoma	
	HUVEC – human umbilical vein endothelial cells	
	Jurkat – human T-lymphocytes	
	Daudi – B-lymphoblast cells	
	Raji – burkitt’s B-lymphoma cells	
	HEY – ovarian carcinoma cells	[177]
All trans retinoic acid (ATRA)	NB4 – promyelocytic leukemia	[40]
Stem cell factor (SCF)	Mouse cultured bone marrow progenitors	[37]
Granulocyte colony stimulating factor (G-CSF)	Mouse cultured bone marrow progenitors	[37]

PLSCR1 expression is upregulated in response to stimulation with growth factors and cytokines [19, 39]. In particular, long term treatment with epidermal growth factor (EGF) leads to increased expression of PLSCR1 whereas short-term treatment leads to PLSCR1 tyrosine phosphorylation (Y69/Y74) mediated by c-Src [19] [144]. In addition to EGF, activated c-Abl also leads to tyrosine phosphorylation of PLSCR1 upon stimulation with the DNA damaging agent cisplatin [18]. Other growth factors that lead to induction of PLSCR1 expression include stem cell factor (SCF) and granulocyte



colony stimulating factor (G-CSF) [37]. In acute promyelocytic leukemia (APL) NB4 cells, PLSCR1 expression is induced with all trans-retinoic acid (ATRA), a differentiation-inducing agent [40]. This ATRA-mediated induction of PLSCR1 is mediated by PKC $\delta$  activation [40]. PLSCR1 is transcriptionally activated by Type I interferons (i.e. IFN- $\alpha$ , IFN- $\beta$ , and IFN- $\gamma$ ) [39] and is one of the most potently induced interferon regulated genes [38]. It is presently unclear based on the microarray screen performed by Der and colleagues [38] whether other members of PLSCR family are transcriptionally induced by interferons. Treatment with IFN- $\alpha$  led to an 8-fold increase in PLSCR1 protein (in comparison to 10-fold and 3-fold induction in protein) with IFN- $\beta$  and IFN- $\gamma$ , respectively; genomic sequencing of PLSCR1 indicated that the IFN stimulated response element (ISRE) located in exon I was essential for its induction [39]. The transcriptional activation of PLSCR1 by IFN- $\alpha$  was mediated by activation of PKC $\delta$  (protein kinase C), JNK (c-Jun N terminal Kinase), and followed by STAT1 [145]. Collectively, these studies provide evidence for PLSCR1 regulation under different conditions (Table 3); however, the exact mechanism through which PLSCR1 is regulated at the transcriptional level in response to these stimulants is not well understood. Recent studies implicate Snail, a transcriptional regulator of epithelial-mesenchymal transition (EMT), as a direct regulator of PLSCR1 mRNA [146].

#### Subcellular localization of PLSCR1:

PLSCR1 (318 amino acids) is a type-II transmembrane protein that is tail-anchored to the plasma membrane at its C-terminal end [27]. PLSCR1 protein is comprised of important structural domains which regulate its function and subcellular localization as shown in Figure 4 (Lower panel): (1) proline-rich N-terminal region (1-98 aa region) containing PXXP and PPYP domains that aid in its interactions with various signaling molecules [18, 19], (2) a DNA binding domain (86-118 aa) [23], (3) cysteine-rich palmitoylation site (<sup>184</sup>CCCPC<sup>189</sup>) [24], (4) an atypical nuclear localization signal (NLS, 257-266 aa) [25], (5) a conserved calcium binding domain (273-284 aa) [26], and (6) a single membrane spanning transmembrane domain at the C-terminal end (288-306 aa) [27]. Although PLSCR1 predominantly localizes at the plasma membrane, it is also located in other subcellular compartments [19, 24, 42, 133].

Palmitoylation status at the cysteine rich palmitoylation site regulates the localization of PLSCR1 [24]. Studies indicate that C/A mutations (via site directed mutagenesis) in the palmitoylation site or treatment with 2-bromopalmitate (inhibitor of palmitoylation) promotes nuclear localization of PLSCR1 in specific cell types [24]. Stimulation with interferons can also promote nuclear localization of PLSCR1 in specific cell types including HEY and HEY1B ovarian cancer cells [24] and SVT2 fibroblast cells [24]. Nuclear import of PLSCR1 is dependent on the importin  $\alpha/\beta$  nuclear receptor pathway [25] in which the atypical NLS of PLSCR1 (257-266 aa) interacts and binds to importin  $\alpha/\beta$  [25, 147]. In the nuclear compartment, PLSCR1 regulates transcriptional activity of IP<sub>3</sub>R [23] and may also play a putative role in DNA replication due to its physical interaction with topoisomerase [148]. Interestingly, stimulation with EGF leads to plasma membrane PLSCR1 internalization into endocytic vesicles which recycles back to the plasma membrane in contrast to the EGF receptor [19]. Moreover, PLSCR1 is also located in the endoplasmic reticulum (ER), Golgi, and endosomal compartments [133]. PLSCR2 and PLSCR4 are also localized at the plasma membrane [131, 149] whereas PLSCR3 although primarily localized to the mitochondrial membrane [131, 150, 151], is also present in the nuclear compartments in the absence of palmitoylation in macrophages [152]; nuclear functions of this PLSCR isoform remain unknown.

#### Role of PLSCR1 in cell signaling/receptor trafficking events and protein-protein interactions:

Although initial studies implicated PLSCR family members primarily in mediating lipid scrambling activity, later studies reported PLSCR1 to participate in various signaling pathways. Stimulation of human A431 epidermoid carcinoma cells with EGF leads to tyrosine phosphorylation of PLSCR1 and promotes its interaction with EGFR and ShcA, an adaptor molecule [144]. Specifically, EGF-mediated activation of PLSCR1 occurs at tyrosines 69 and 74 and is mediated by c-Src kinase activity; PLSCR1 interaction with ShcA requires its PXXP and PPYP motifs in its N-terminal region [144]. Further, PLSCR1 and EGF receptor are co-internalized into endosomal pools upon EGF stimulation; while EGF receptor is trafficked to lysosomes for degradation, PLSCR1 recycles back to the plasma membrane [19]. Additionally, activation of the FCER1 (IgE receptor), an immune receptor

expressed in mast cells, with IgE immunoglobulins also leads to tyrosine phosphorylation of PLSCR1 [153] implicating PLSCR1 in IgE receptor signaling and degranulation in mast cells, a process that results in production of antimicrobial molecules [153]. Collectively, these results suggests a potential role of PLSCR1 in participating in EGF (and other growth factor) mediated signaling pathways and receptor

**Table 4: List of protein interaction partners of PLSCR1**

Various identified interaction partners of PLSCR1 are listed along with the subcellular localization of the interaction and specific techniques utilized to determine and validate them. The corresponding citations are presented for each of the PLSCR1 interaction partners.

Interaction Partner	Interaction localization	Identified by	Validated by	Reference
EGFR	Lipid Rafts	Co-IP	Immunofluorescence	[19]
ShcA	Lipid Rafts	Co-IP	Immunofluorescence	[19]
RELT	Plasma membrane & perinuclear regions of Cytoplasm.	Yeast-2-Hybrid	Co-localization, Co-IP	[228]
ECM1	Extracellular matrix	Yeast-2-Hybrid, IHC	Co-IP and pull down	[155]
c-Abl	cytoplasm	GST-SH3 domain binding assay	Co-IP	[18]
Topoisomerase – II	Nucleus	Yeast-2-Hybrid	Co-IP and pull down	[148]
BACE	Cytoplasm, Endosomes/Golgi	Yeast-2-Hybrid	Co-localization, Co-IP	[133]
Onzin	Cytoplasm	Yeast-2-Hybrid	Co-IP	[154]
TLR9	Endoplasmic Reticulum	Yeast-2-Hybrid	Co-IP and immunofluorescence	[42]
Proteinase 3	Cytoplasm and plasma membrane	Co-IP	Immunofluorescence	[156]

internalization. PLSCR1 can also regulate the toll like receptor (TLR9) signaling pathway upon cellular stimulation with pathogenic or foreign nucleic acids/proteins [42]. In plasmacytoid dendritic cells, PLSCR1 interacts with TLR9 in endosomal compartments to regulate TLR9-mediated production of IFN- $\alpha$  [42]. In addition to receptor-mediated pathways, the DNA damage inducing agent cisplatin leads to c-Abl tyrosine kinase-mediated activation of PLSCR1 [18] implicating a role for PLSCR1 in cellular

responses to chemotherapeutic agents. Since PLSCR3 and PLSCR4 also possess the proline-rich N-terminal domains (which mediates interaction with signaling mediators in PLSCR1 [18, 19, 133]), it would thus be interesting to determine whether these members of PLSCR family are involved in similar signaling pathways.

Additionally, PLSCR1 interacts directly with various other proteins of signaling importance. In SH-SY5Y human neuroblastoma cells, PLSCR1 interacts with  $\beta$ -secretase ( $\beta$ -secretase APP cleaving enzyme, BACE), a membrane proteinase enzyme that regulates the production of amyloid  $\beta$ -peptide molecules which is a characteristic feature of Alzheimer's disease [133]. PLSCR1 and BACE co-localize in the Golgi and endosomal compartments; this observation implicates a role for PLSCR1 in regulating the intracellular distribution of BACE and potentially a role for PLSCR1 in Alzheimer's disease pathophysiology. In myeloid cells, PLSCR1 also binds directly to Onzin, a negative transcriptional regulatory target of c-Myc which regulates cell proliferation [154]. These findings potentially implicate PLSCR1 in cancer cell survival and proliferation. Furthermore, PLSCR1 interacts with RELT (receptor expressed in lymphoid tissues). Interestingly, PLSCR1 interaction with RELT leads to phosphorylation of PLSCR1 by OSR1, an oxidative stress response kinase protein; this interaction may implicate PLSCR1 in oxidative stress response pathways. Additionally, PLSCR1 is secreted into the extracellular matrix via a lipid raft-dependent pathway leading to interaction with ECM1 (extracellular matrix protein 1) [155] suggesting a potential role in regulatory mechanisms in human skin tissue such as epidermal differentiation which is mediated by ECM1. PLSCR1 also interacts with Proteinase 3 (PR3), a target of autoantibodies in Wegener granulomatosis in the neutrophils [156]. Table 4 provides a summary of all the interaction partners of PLSCR1 along with the localization of interactions.

#### Role of PLSCR1 as a DNA-binding protein and transcription factor:

Nuclear localized PLSCR1 is proposed to participate as a DNA binding and transcription factor [24, 147]. PLSCR1 has a putative DNA binding domain (86-118 aa) through which it binds genomic DNA; specific target genes included IP<sub>3</sub>R (inositol triphosphate receptor class I) [23]. In addition, PLSCR1 interacts with topoisomerase type II enzyme which may implicate PLSCR1 in DNA repair and

replication [148]. Additionally, nuclear PLSCR1 is involved in the production of mature neutrophils from myeloid progenitors following exposure to granulocyte colony stimulating factor (G-CSF) [157] although the underlying mechanism is unclear. Collectively, these reports implicate nuclear PLSCR1 as a potential player in transcriptional regulation as well as in DNA replication and repair pathways. With respect to other PLSCR family members, PLSCR2 was predominantly nuclear localized when stably expressed in Chinese hamster ovary K1 cell line [158]; the function of nuclear localized PLSCR2 has yet to be investigated.

### **Functions of PLSCR1: Innate Immune Recognition, Cell Death Pathways, and Cancer**

#### Antiviral functions of PLSCR1 and viral entry:

Interferons (IFNs) are cytokines that elicit antiviral functions [159-162]. Since PLSCR1 is one of the most highly inducible IFN responsive genes, studies have focused on whether it mediates the antiviral functions of IFN. Knockdown of PLSCR1 via siRNA and fibroblasts isolated from PLSCR1<sup>-/-</sup> knockout mice revealed increased viral titers of vesicular stomatitis (VSV) and encephalomyocarditis (EMCV) viruses upon treatment with IFN implicating PLSCR1 in IFN-mediated antiviral responses [4]. Further, overexpression of PLSCR1 led to an antiviral effect similar to IFN treatment in which increased expression of various IFN stimulated genes (ISGs) results in reduced viral titers. These results implicate PLSCR1 in IFN signaling [4]. Furthermore, PLSCR1 mediates protective function by inhibiting the effects of Staphylococcal  $\alpha$  toxin [163]. PLSCR1 also antagonizes hepatitis B viral (HBV) replication and propagation [8]. Overexpression of PLSCR1 significantly inhibited HBV synthesis both *in vivo* and *in vitro*; this appears to be partly mediated by activation of JAK-STAT pathway [8]. Hepatitis C virus (HCV) infection results in liver damage and can promote development of hepatocellular carcinomas [164-166]. Using RNAi based approach, PLSCR1 was identified as one of the major mediators of IFN-dependent inhibition of HCV replication [7]. Interestingly, PLSCR1 also aids in Hepatitis C viral entry suggesting potential dual role (promoting and suppressing) of PLSCR1 in HCV propagation [167]. Yeast-2-hybrid screens and co-immunoprecipitation studies revealed PLSCR1 as an interacting partner of HCV

viral coat proteins E1 and E2; furthermore, reduction of PLSCR1 expression in hepatoma cells significantly reduces HCV entry into cells suggesting a potential dual role in HCV responses [167]. PLSCR1 directly interacts with viral components through which it inhibits the viral propagation in host cells [5, 6]. For instance, PLSCR1 binds directly to the human T-cell leukemia virus type-1 (HTLV-1)

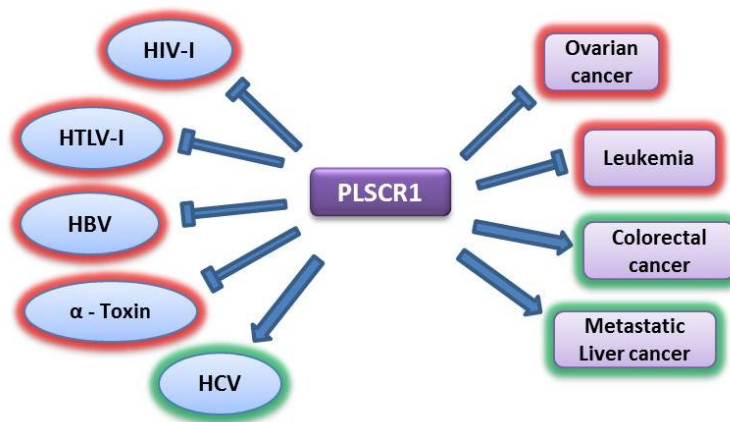


**Figure 6: Role of PLSCR1 in viral/bacterial responses and in cancer development**

PLSCR1 inhibits the replication and propagation of HIV-1, HTLV-1 and HBV viruses and also mediates the protection against Staphylococcal  $\alpha$ -toxin while it facilitates the replication of HCV [4-8]. PLSCR1 overexpression has as a tumor suppressive effects in ovarian carcinomas (*in vivo*) [15] and leukemia [16, 17] while in colorectal cancer and metastatic liver cancer, it functions as a tumor promoter [20-22]. (\*Figure created by Madhav Karthik Kodigepalli)

encoded viral protein Tax, which aids in the activation of provirus, and inhibit its subcellular distribution and function, thereby inhibiting the activation of virus [5]. Similarly, PLSCR1 binds to Tat protein encoded by human immunodeficiency virus type-1 (HIV-1) both *in vivo* and *in vitro* inhibiting transcriptional activation of HIV long term repeat by Tat [6]. Furthermore, the interaction is mediated by amino acid 160 to 250 in PLSCR1 [6]. PLSCR1 as well as PLSCR4 interact with CD4 receptor on T-cells; this process is important in HIV-1 infection of T cells suggesting a pro-viral function of these proteins [149]. Collectively, these studies implicate an interesting role of PLSCR1 in viral responses in host cells where it can both assist in the viral infection and inhibit viral replication and propagation.

### Role of PLSCR1 in autoimmune diseases (systemic lupus erythematosus):

Recent evidence suggests that PLSCR1 may regulate autoimmune disorders such as systemic lupus erythematosus (SLE). SLE is characterized by the immune system attacking the cells and tissues of the host, thereby leading to inflammation in various organs of the body. Additionally, ~10% of SLE patients exhibit an unusual increase in blood coagulation (hyper-coagulation). Interestingly, Suzuki and colleagues identified three splice variants of PLSCR1 (in addition to the full-length form) which were overexpressed in monocytes of SLE patients [132]. Interestingly, these cells also had increased PS externalization which led to the increased coagulation [132]. Therefore, PLSCR1 may play a role in regulating the pathophysiology of SLE. However, the extent to which PLSCR1 mediates this process remains unclear. Among the three splice variants identified, splice variant 1 (905 bp) has a deletion in exon 4, thereby missing a part of the N-terminal proline-rich region of PLSCR1 [132]. Variant 2 (750 bp) contains a deletion in exon 6 and variant 3 (551 bp) contains a deletion in both exon 6 and 7 [132]. As shown in Figure 4 (Upper panel), exon 6 of PLSCR1 codes for the region containing the palmitoylation region. The significance of these PLSCR1 splice forms in the SLE patient monocytes remains to be investigated. It is interesting to note that all these three splice variants had an intact EF (calcium binding) domain which is known to play a major role in scramblase activity of PLSCR1 [132].

### PLSCR1 in innate immune responses: TLR signaling:

Toll like receptors (TLRs) are a major component of the innate immune system cellular responses by functioning as receptors recognizing the foreign and pathogenic nucleic acids or proteins that enter the cells [168-170]. Following cellular recognition, TLRs are activated via proteolysis leading to activation of downstream signaling cascades including activation of IRF3/7 or NF $\kappa$ B transcription factors in which lead to induction of antiviral cytokines including IFNs and interleukins (ILs) [168, 171, 172]. Recent studies in plasmacytoid dendritic cells (pDCs), a group of antigen presenting cells, revealed a role for PLSCR1 in regulating TLR9 signaling in response to treatment with viral particles and synthetic CpG DNAs [42]. These studies indicate that TLR9-mediated IFN production in these cells requires expression of PLSCR1 [42]. However, the complete mechanism by which PLSCR1 modulates the TLR signaling and

innate immune responses require further investigation. Collectively these observations provide a link between PLSCR1 regulation and innate immune responses.

#### Role of PLSCR1 in Apoptosis and Autophagy:

As described earlier, externalization of PS is an event associated with apoptotic cell membranes important for clearance by macrophages [111, 112]. Although PLSCR family members appear to be involved in the process of PS externalization during apoptosis, PLSCR1 deficient mice did not demonstrate any defect in PS externalization [37, 116]. Interestingly, Scrm1, a *C. elegans* ortholog of human PLSCR1, mediates PS scrambling in apoptotic cells [135, 173]. WAH-1, *C. elegans* homolog of apoptosis inducing factor (AIF) promotes the PS externalization in apoptotic cells via its association with Scrm1, an event that helps in clearance of apoptotic cells by the macrophages [135, 173]. Other PLSCR family members also appear to be involved in both the intrinsic and extrinsic apoptotic signaling pathways. For instance, PLSCR3 appears to play a role in apoptosis induced by UV and tBid [174]; other studies implicate PLSCR3 in apoptotic cell death via the activity of PKC $\delta$  [151]. Similarly, PLSCR3 overexpression markedly increases TRAIL (TNF related apoptosis inducing ligand) induced mitochondrial apoptotic pathway and activation of caspases suggesting that PLSCR3 plays a role in the intrinsic apoptotic pathway [175]. Similarly, PLSCR1 increases UV-induced apoptotic process by mediating the intrinsic apoptotic signaling [176]. Although studies demonstrate that reduction or blocking of PLSCR1 via siRNA or N-terminal antibodies, respectively, results in increased apoptosis in colorectal cancer [20] and ovarian cancer cells treated with chemotherapeutics [177], it has yet to be shown that PLSCR1 is directly involved in altering the process of apoptosis in these cases. In addition to apoptosis, PLSCR3 plays a role in autophagy, another type of cell death pathway, in which it is involved in externalizing cardiolipin which is important in targeting the damaged mitochondria to autophagosomes/lysosomes during mitophagy (a type of autophagy that specifically targets the damaged mitochondria for degradation) [178]. Additionally, recent studies on hybrid mapping of yeast and human interaction networks identified PLSCR1 as one of the interaction partners of ATG12, an ubiquitin like



protein that helps in the elongation step of autophagosome formation [179]. These findings suggest a potentially important role of PLSCR1 in the process of autophagy which still remains to be investigated.

#### Role of PLSCR1 in blood and solid cancers:

PLSCR1 mRNA expression was markedly induced upon treatment with all-trans retinoic acid (ATRA), a chemotherapeutic used in treatment of APL [17]. Further, reduced PLSCR1 expression in these cells significantly suppressed the differentiation of APL cells indicating role of PLSCR1 as an anti-leukemic molecule [17]. Studies in acute myelogenous leukemia (AML) patients revealed that elevated PLSCR1 mRNA expression correlated with the increased survival rate in AML patients [41] implicating a role for PLSCR1 as a tumor suppressor. Future reports support the role of PLSCR1 in leukemic cell differentiation; further, PLSCR1 induction upon treatment of APL cells with differentiation-inducing agents such as ATRA and phorbol myristate acetate (PMA) was mediated by activation of PKC $\delta$  [40]. Similarly, PLSCR1 expression and localization were also altered when AML cells were treated with wogonoside, a Chinese herbal medicine used to treat the blood-related malignancies [180, 181]. In addition to cell differentiation, PLSCR1 expression inhibited U937 myeloid leukemia cell proliferation by modulating the expression of pro-survival and anti-apoptotic proteins [16]. Collectively, all the above observations implicate PLSCR1 as mechanism tumor suppressor in leukemia development. A similar function is attributed to PLSCR1 in ovarian cancer cells [15]. Murine xenografts containing overexpressed PLSCR1 (in HEY1B ovarian carcinoma cells) was found to be growth suppressed compared to control xenografts [15]. However, overexpression of PLSCR1 did not result in any functional effect in *in vitro* [15]. In contrast, evidence is accumulating in support of PLSCR1 as an oncogenic molecule in ovarian, colorectal, and metastatic liver cancers [20-22]. PLSCR1 was highly elevated in various colorectal cancer (CRC) patient tissues and was consequently identified as a biomarker in CRC [22]. Furthermore, antibody or siRNA mediated downregulation of PLSCR1 in colorectal and liver cancers dramatically reduced tumorigenesis [21, 36].

## Hypotheses and Objectives

As stated earlier, we have previously shown that As<sub>2</sub>O<sub>3</sub> treatment leads to cytoprotective autophagy in ovarian cancer cells mediated by induced SnoN expression. However, the exact mechanisms regulating SnoN expression in ovarian cancers treated with As<sub>2</sub>O<sub>3</sub> are unclear. In this regard, we hypothesized that SnoN expression in ovarian cancers is regulated by molecular pathways involving other genes amplified at the 3q26 region as a mechanism of cooperative oncogenicity. Despite numerous reports suggesting involvement of PLSCR1 in pathogenesis of ovarian and colorectal cancers, the exact role and regulation of PLSCR1 in ovarian cancers remains unknown. It also remains to be investigated whether PLSCR1 can also alter the chemotherapeutic sensitivity of ovarian cancers. Therefore, we hypothesized that PLSCR1, located at 3q23, is regulated via crosstalk by SnoN, located at 3q26 in ovarian cancer. As mentioned above, PLSCR1 is an IFN-stimulated gene and is also implicated in regulation of antiviral and autoimmune responses. However, it remains unknown whether PLSCR1 can also regulate innate immune responses of which IFN is a downstream product. We hypothesized that PLSCR1, an IFN stimulated gene is also regulated by the innate immune TLR signaling.

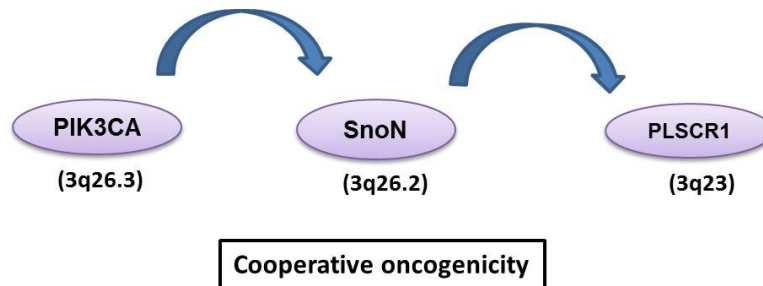


**Figure 7: Model of proposed hypotheses for Aims 1 and 2**

Mechanisms regulating the expression of SnoN/SkiL (located at 3q26.2) in ovarian cancer cells treated with As<sub>2</sub>O<sub>3</sub> remain unclear. Similarly, the exact role and regulation of PLSCR1 in ovarian cancers remains unknown. We propose that PIK3CA (located at 3q26.3) regulates SnoN expression and SnoN regulates PLSCR1 (located at 3q23) expression via cooperative oncogenicity in ovarian cancer [9, 11]. (\*Model created by Madhav Karthik Kodigepalli)

One of the major objectives of our studies is to understand the mechanisms of regulation of SnoN (3q26.2) and PLSCR1 (3q23) located near the highly amplified 3q26 locus in ovarian and other epithelial carcinomas. We also aimed to determine the role of PLSCR1 in ovarian cancer chemotherapeutic responses. We addressed the above hypotheses by performing the studies presented under the following specific aims.

Specific Aim1 (presented in Chapter 3): Identification of molecular mechanisms leading to altered SnoN expression in ovarian cancers upon treatment with chemotherapeutics.

*Aim 1.1:* To identify the signaling pathways activated upon arsenic trioxide treatment in ovarian cancer cells.

*Aim 1.2:* To validate the signaling pathways involved utilizing specific inhibitors and siRNAs.

Specific Aim2 (presented in Chapter 4): Identification of crosstalk of SnoN with other genes located near the 3q26 amplicon in ovarian cancers.

*Aim 2.1:* Determine the correlation between SnoN and PLSCR1 alterations in ovarian cancers.

*Aim 2.2:* Investigate the transcriptional regulation of PLSCR1 by SnoN.

*Aim 2.3:* Determine the role of PLSCR1 in ovarian cancer chemotherapeutic responses by utilizing siRNAs.

Specific Aim3 (presented in Chapter 5): To determine the role of TLR-IRF3 pathway in regulating the PLSCR1 expression in normal ovarian and ovarian cancer cells treated with dsDNA.

*Aim 3.1:* To determine the effects of TLR signaling on PLSCR1 expression by utilizing dsDNA.

*Aim 3.2:* To identify the transcriptional regulation of PLSCR1 by TLR-IRF3 pathway.

### **Overall Impact and Significance**

SnoN, located at the 3q26 amplicon, is known to be amplified and overexpressed in ovarian cancers and its expression correlates with the aggressiveness of the cancers [9]. Further, SnoN overexpression is also known to result in chemoresistance in ovarian cancer patients [9]. Understanding the mechanisms leading to dysregulated expression of SnoN in ovarian cancer is very important to

developing improved treatment strategies. PLSCR1 is located centromeric to the 3q26 amplicon which harbors genes that are dysregulated in ovarian cancer. PLSCR1 is also known to be overexpressed in solid cancers and was identified as an anti-leukemic molecule. Thus, understanding the role of PLSCR1 and its crosstalk with SnoN in ovarian cancer would aid in the development of combinatorial treatment strategies targeting both molecules.

## Chapter 2

### Materials and Methods

#### Culture and Propagation of Cell Lines

**Table 5: List of all cell lines utilized for dissertation**

Name of Cell Line	Cell Type	Culture Medium	Passage Number	Obtained/Purchased
HEY	Ovarian serous epithelial carcinoma	RPMI	p=n+5 – p=n+35	Dr. Gordon B Mills, MD Anderson Cancer Center
T80	Large T antigen/hTERT Immortalized normal ovarian surface epithelial cells	RPMI	p=n+9 – p=n+27	Dr. Gordon B Mills, MD Anderson Cancer Center
HMEC	Primary mammary epithelial cells	Mammary epithelial cell basal medium	p=6	ATCC
TOV112D	Endometrioid ovarian carcinoma	Medium199 +MCDB131 (1:1)	p=4	ATCC
TOV21G	Clear cell ovarian carcinoma	Medium199 +MCDB131 (1:1)	p=n+4	Dr. Jonathan Lancaster, Moffitt Cancer Center
HeLa	Cervical adenocarcinoma	EMEM	p=n+1 – p=n+18	ATCC
HEK293T	Human embryonic kidney epithelial cells	RPMI	p=n+5 – p=n+22	Dr. Gordon B Mills, MD Anderson Cancer Center
PANC-1	Pancreatic ductal adenocarcinoma	DMEM	p=n+7 – p=n+22	ATCC
AsPC-1	Pancreatic adenocarcinoma	DMEM	p=n+2 – p=n+7	ATCC
MIA PaCa-2	Pancreatic epithelial carcinoma	RPMI	p=n+5 – p=n+23	Dr. Said Sebti, Moffitt Cancer Center
BxPC-3	Pancreatic adenocarcinoma	RPMI	p=n+6 – p=n+20	ATCC
A431	Human epidermoid carcinoma	DMEM	p=2 – p=11	ATCC

All the cell lines used for the studies presented throughout this thesis are listed in Table 5 along with the information regarding the respective culture media used, source, and passage numbers. All the cell lines were cultured in an incubator at 37°C in the presence of 5% CO<sub>2</sub> in the appropriate media. The media used for the culture of all cell lines, with the exception of the primary human mammary epithelial cells (HMEC), were supplemented with 8% fetal bovine serum (FBS) and 5% penicillin/streptomycin. The complete growth medium for the culture of HMECs was prepared by combining the components of the Mammary Epithelial Growth Kit (PCS-600-040) with the Mammary Epithelial Cell Basal Medium (PCS-600-030) obtained from ATCC (Manassas, VA). For subculturing, all the cells were first trypsinized with 0.25% Trypsin-EDTA at room temperature with the exception of A431 cells and TOV21G cells which were trypsinized at 37°C and HMEC cells which were trypsinized using 0.05% Trypsin-EDTA at 37°C. Once detached, cells were collected in appropriate complete growth media and were pelleted at 1,000 rpm for 5 minutes before re-plating the cells at 1:5 dilution in appropriate growth media. Detached HMEC cells were collected in trypsin neutralization solution (5% FBS in PBS) and were pelleted at 1,000 rpm for 3 minutes before replating. All cell lines used for the cell lines reported in this thesis were tested negative for mycoplasma and were authenticated by STR profiling.

### **Genomic DNA Isolation and STR Profiling**

Cells grown to confluence in a T25 flask were trypsinized and collected into FBS-containing culture media. These cells were spun down at 1,000 rpm for 5 minutes; the resultant pellet was resuspended in 200 µl phosphate buffered saline (PBS). Genomic DNA isolation was performed using the DNeasy blood and tissue kit from Qiagen (Valencia, CA) following the manufacturer's protocol. The isolated genomic DNA was quantified using a Nanodrop and the samples were then submitted for STR (short tandem repeats) profiling to Genetica DNA Laboratories (Burlington, NC). The STR profiling data was analyzed against a reference cell profile in available public databases.

## **Cellular Treatments with Growth Factors, Chemotherapeutic Agents, and Signaling Pathway Inhibitors**

Cells were plated, as appropriate for experimental purpose, into 35mm dishes or 6, 24, or 96-well plates or at densities of 250,000, 52,000, and 5,000 cells per well, respectively, except for MIA PaCa-2, PANC-1 and AsPC-1 cells which were plated at a density of 500,000 in 6-well plates. Epidermal growth factor (EGF) (Calbiochem, Rockland, MA) was prepared in 10 mM Acetic acid containing 0.1% BSA (100 µg/ml) and was used at a concentration of 100 ng/ml. Transforming Growth Factor-β (TGF-β) (Calbiochem, Rockland, MA) (80 nM) was prepared in 500 µl of 4 mM HCl and 0.1% BSA and utilized at a concentration of 50 pM. Arsenic trioxide (As<sub>2</sub>O<sub>3</sub>) (Sigma Aldrich, St. Louis, MO) was dissolved in 10 N NaOH, then diluted with nanopure water, and adjusted to a pH of 7; the As<sub>2</sub>O<sub>3</sub> was utilized at a concentration between 5-25 µM. Interferon-2α (IFN) (MBL international) was dissolved in nanopure water (2X10<sup>8</sup> IU/ml) and was utilized at a concentration between 3,000–10,000 IU/ml. Src family kinase inhibitor PP2 (10 mM stock) (Calbiochem) and SU6656 (10 mM stock) (Calbiochem), PI3K kinase inhibitors LY294004 (10 mM stock) (Cell Signaling, Danvers, MA) and GDC0941 (1.95 mM stock) (Selleckchem, Houston, TX), MAP kinase inhibitor U0126 (10 mM stock) (Cell Signaling technology, Danvers, MA), and EGF receptor kinase inhibitor PD153035 (2.5 mM stock) (A.G. Scientific, San Diego, CA) were all dissolved in dimethyl sulfoxide (DMSO) and were utilized at concentrations ranging from 100 nM to 10 µM. Transcriptional inhibitor Actinomycin D (ActD) (100 µg/ml) prepared in complete growth media, was used at a concentration of 100 ng/ml. Translational inhibitor Cycloheximide (CHX) (2 mg/ml stock), and proteasomal inhibitor MG132 (10 mM stock) were all dissolved in DMSO and were utilized at concentrations of 2 µg/ml, and 5 µM, respectively. The anti-oxidant, N-Acetyl-L-Cysteine (NAC) (50 mM stock), was dissolved in serum free media and was used at a concentration between 100 – 1,000 µM. Dilutions of the above growth factors and inhibitors were diluted into serum free media prior to use. Cells were pre-treated with PP2, U0126, PD153035 and SU6656 inhibitors for minimum of 2 hours prior to treating them with EGF or As<sub>2</sub>O<sub>3</sub> whereas all other inhibitors were used to co-treat the cells along with EGF or As<sub>2</sub>O<sub>3</sub>.

## Plasmids, MicroRNAs and Cloning of PLSCR1 into pBABE-puro

pcDNA3, pcDNA3 containing wild type-PLSCR1 cDNA, pcDNA3 containing C/A-PLSCR1 cDNA (mutated palmitoylation site; <sup>184</sup>CCCPC<sup>189</sup>-<sup>184</sup>AAAPAA<sup>189</sup>), pGL3-basic, and pGL3-basic vector containing human PLSCR1 genomic construct (5' 1 – 4177 nucleotides)[39], were kindly provided by Dr. Peter J. Sims (University of Rochester)[24, 39]. pGFP-V-RS retroviral vector containing shRNA targeting PLSCR1 was kindly provided by Dr. Igor Prudovsky (Maine Medical Center Research Institute)[182]. Retroviral vector pBABE-puro and retroviral vectors pCGP and pVSVG containing sequences coding for the viral components *gag*, *pol*, and *env*, were obtained from Dr. Gordon Mills (MD Anderson Cancer Center). Retroviral vectors pGFP-V-RS and pQCXIN, and pEGFP-C1 vectors were obtained from Clontech (Mountain View, CA). pEGFP-LC3 vector containing GFP-tagged LC3 were obtained from Addgene (Cambridge, MA) (Deposited by Dr. Toren Finkel). Mimics of hsa-miR-216b (ID: MC12302), hsa-miR-410 (ID: MC11119), hsa-miR-494 (ID: MC12409), hsa-miR-495 (ID: MC11526), and miRNA negative control (#4464058) were purchased from Ambion (Grand Island, NY).

Wild type (WT)-PLSCR1 and C/A-PLSCR1 (palmitoylation mutant, see above) were cloned into pBABE-puro retroviral vector using the constructs from Dr. Sims as template (pcDNA3 vectors, see above) using the following strategy. Briefly, WT-PLSCR1 and C/A-PLSCR1 were excised from pcDNA3 vector by incubating these vectors (10 µg of each vector) with EcoRI and BamHI enzymes. The reaction mixtures were then run on a 1% agarose gel to gel-purify the insert (QIAquick Gel Extraction Kit, Qiagen, #28706) which was eluted from the column into 30 µl of EB buffer. The gel purified insert was used for the ligation reaction along with dephosphorylated pBABE-puro vector (1 µg) that was digested with BamHI and EcoRI. Ligation reaction was performed by incubating the mixture of 8 µl gel purified insert, 1 µl dephosphorylated pBABE-puro vector along with 10 µl ligase buffer and 1 µl of DNA ligase enzyme at 37°C for 5 minutes at room temperature and then at 4°C for 3 hours. The ligated products were then transformed into Top10F<sup>2</sup> bacteria and next day successful colonies were selected and analyzed to identify positive transformants by performing double digestion with BamHI and EcoRI. The correct



orientation and sequence of the insert was validated by sequencing at the Molecular Genomics Core (Moffitt Cancer Center, Tampa, Florida) using pBABE-5' and pBABE-3' primers.

### **Generation and Cloning of PLSCR1 Mutants**

Below PLSCR1 mutants with a C-terminal HA tag were generated via PCR-based mutagenesis for the studies described in Chapter 6.

1. Wild type PLSCR1-HA
2. C/A-PLSCR1-HA (Palmitoylation mutant, see above)
3.  $\Delta$ N-PLSCR1-HA (N-terminal amino acids 1-97 deleted from wild type PLSCR1)
4.  $\Delta$ TM-PLSCR1-HA (amino acids 287-318 harboring transmembrane domain deleted from wild type PLSCR1)

The following primers with EcoRI restriction sites (underlined) and sequences for HA-tag (bolded) were designed and used together with the pcDNA3 vectors harboring WT-PLSCR1 or C/A-PLSCR1 as templates to generate the above PLSCR1 variants.

#### WT-PLSCR1-HA and C/A-PLSCR1-HA:

*Forward:*

5' GGCGGAATTCTCCACCATGGACAAACAAAAC 3'

*Reverse:*

5' GCGCGAATTCCTAAGCGTAGTCTGGGACGTCGTATGGGTACCACACTCC 3'

#### $\Delta$ N-PLSCR1-HA:

*Forward:*

5' GGCGGAATTCTCCACCATGGGATTAGAATATTTA 3'

*Reverse:*

5' GCGCGAATTCCTAAGCGTAGTCTGGGACGTCGTATGGGTACCACACTCC 3'

ΔTM-PLSCR1-HA:

*Forward:*

5' GGCGGAATTCCTCCACCATGGACAAACAAAAC 3'

*Reverse:*

5'GCGCGAATTCCTAAGCGTAGTCTGGGACGTCGTATGGGTATTTAACATCAAGGTC 3'

pcDNA3 containing wild type PLSCR1 cDNA was used as template for generation of wild type, ΔN, and ΔTM PLSCR1 variants, while pcDNA3 containing C/A-PLSCR1 was used for generating the C/A-PLSCR1-HA variant. PCR was performed using appropriate primers (forward and reverse), template and Platinum PCR super mix (#12532-016, Invitrogen, Grand Island, NY ) at the following reaction conditions: 95°C for 4 minutes, 95°C for 5 minutes (melting), 35 cycles of 50°C for 30 seconds (annealing), 68°C for 1 minute (extension) and 68°C for 15 minutes (final extension). The amplified product was then cloned into pCR2.1-TOPO vector (#450641, Invitrogen) by performing TOPO-TA cloning (2 μl of PCR product, 0.5 μl of salt solution and 0.5 μl pCR2.1-TOPO vector incubated at room temperature for 30 minutes). This reaction mixture was then transformed into TOP10 (for WT and C/A-PLSCR1) or TOP10F' (for ΔN and ΔTM-PLSCR1) bacteria which were then plated on LB agar media containing kanamycin and X-gal or kanamycin, X-gal and IPTG respectively to identify the positive clones next day (white colored colonies). Positive clones were then validated for the presence of respective PLSCR1 variants by performing restriction digestion with EcoRI and by sequencing using M13 Forward and M13 Reverse primers. Respective HA-tagged PLSCR1 variants were then subcloned from pCR2.1-TOPO vector into retroviral vector pQCXIN using following strategy. Briefly, all the HA-tagged PLSCR1 variants were excised from their respective pCR2.1-TOPO vectors (50 μg for WT, CA,

and  $\Delta$ TM-PLSCR1 and 25  $\mu$ g for  $\Delta$ N-PLSCR1) by incubating them with EcoRI restriction enzyme. Then the reaction mixture was run on a 1% agarose gel to gel purify the insert as described above. The gel purified product was then ligated with the dephosphorylated pQCXIN vector (1-2  $\mu$ g) that was digested with EcoRI. Ligation reaction was performed as described above using DNA ligase with the exception of  $\Delta$ N PLSCR1 and  $\Delta$ TM PLSCR1 for which the ligation reaction was performed by incubating 3.5  $\mu$ l of insert, 1  $\mu$ l of dephosphorylated vector, 5  $\mu$ l of ligase buffer, and 0.5  $\mu$ l of DNA ligase at room temperature for 5 minutes and then at 4°C for 3 hours. The ligated products were transformed into TOP10F' bacteria and successful colonies were analyzed for successful cloning and correct orientation by performing double digestion with EcoRI and NaeI with the exception of HA- $\Delta$ N PLSCR1 which was verified by double digestion with EcoRI and XbaI. The positive clones were further validated by sequencing at Molecular Genomics Core (Moffitt Cancer Center, Tampa, Florida).

### **Plasmid and MicroRNA (miRNA) Transfection**

Cells were plated into 6 well plates or 35 mm dishes at a density of 250,000 cells in 2 mls of complete growth media or in a 24 well plate at 52,000 cells 400  $\mu$ l of complete growth media respectively. Twenty-four hours post adherence, cells were maintained in serum free conditions for the transfection procedure. Plasmid transfection was performed using Fugene HD (Promega). Briefly, 1  $\mu$ g of the appropriate plasmid DNA or 200 pmoles of appropriate miRNA mimic was added to 100  $\mu$ l of serum free media followed by the addition of 3  $\mu$ l of Fugene HD in cryovials. This mixture was then incubated at room temperature for 15 minutes which was followed by adding this mixture to the cells in a drop-wise manner. The cells were then incubated at 37°C for 6 hours at which time 2 mls of complete growth media was overlaid onto the 2 ml existent serum free media covering the transfected cells. Twenty-four hours post-transfection, the media on top of the cells was replaced with 2 mls of complete growth media; 48 hours post-transfection, cells were then harvested for RNA/protein as needed. Negative controls, mock transfection control containing only transfection reagent and an empty vector transfection were routinely performed for overexpression studies.

### siRNA Mediated Knockdown

ON-TARGETplus siRNAs targeting c-Src (L-003175-00), PIK3CA (L-003018-00), MAPK1 (L-003555-00), STAT3 (L-003544-00), EGFR (L-003114-00), PLSCR1 (L-003729-00), TLR4 (L-008088-01), TLR9 (L-004066-00), IRF3 (L-006875-00), and non-targeting control siRNA (D-001810-10) were obtained from Dharmacon. Cells were plated into 6-well plates at a density of 325,000 cells per well in complete growth media. Post-adherence, media was changed to serum free conditions followed by siRNA transfection using Dharmafect I transfection reagent (Dharmacon, Lafayette, CO). Five  $\mu$ l of Dharmafect was initially incubated in 100  $\mu$ l of serum free media for 10 minutes at room temperature (in eppendorf tubes). Then 5  $\mu$ l of the appropriate siRNA (at 50 nM) concentration was added followed by a further incubation for 20 minutes at room temperature. This mixture was then added drop-wise to the cells followed by an overlay with 2 mls complete media 3 hours post-transfection. Twenty-four hours post-transfection, the media was replaced with complete growth media for at least 3 hours if additional treatments were performed.

### Establishment of Retroviral Stable Cell lines

Below listed stable cell lines were generated as part of the studies:

**Table 6: List of developed retroviral stable cell lines**

Cell Line	Aim	Plasmid	Insert
HEY	PLSCR1 overexpression	pBABE-puro	Wild type PLSCR1
HEY	PLSCR1 stable knockdown	pGFP-V-RS	shRNA-PLSCR1
HeLa	PLSCR1 stable knockdown	pGFP-V-RS	shRNA-PLSCR1
PANC-1	PLSCR1 stable knockdown	pGFP-V-RS	shRNA-PLSCR1
MIA PaCa-2	PLSCR1 stable knockdown	pGFP-V-RS	shRNA-PLSCR1
BxPC-3	PLSCR1 stable knockdown	pGFP-V-RS	shRNA-PLSCR1

The above six retroviral stable cells lines were developed as follows. HEK293T cell line was used as the packaging cell line for generation of retroviral particles. HEK293T cells, seeded at 1.5 million cells per

well in a 6-well plate and were transfected with the retroviral vector, pBABE-puro containing Wild type-PLSCR1 or empty pBABE-puro vector together with the pCGP and pVSVG vectors (that code for viral components *gag* and *pol* as well as *env*, respectively) in a 1:1:1 ratio. Media from HEK293T cells containing the viral particles was collected at 48 hours and 72 hours post-transfection, filtered through a 0.45  $\mu\text{m}$  filter, diluted with complete RPMI media containing 8  $\mu\text{g/ml}$  of polybrene (1:1 ratio) and added to HEY cells (seeded in a 6-well plate at 250,000 cells per well). Forty eight hours after the second infection, the media was changed to complete growth media containing 2  $\mu\text{g/ml}$  of puromycin for selection. Wild type-PLSCR1 expression was validated by collecting total lysates and performing western analysis for PLSCR1. Additionally, empty pGFP-V-RS retroviral vector or pGFP-V-RS containing shRNA-PLSCR1 was used to obtain stable knockdown of PLSCR1 (with the control) in all the above mentioned cell lines. Reduction in PLSCR1 protein in all of these cells was validated by performing western analysis for PLSCR1.

### **Protein Isolation, SDS-PAGE, and Western Blotting**

Cells plated in 6-well or 24-well plates (following treatments described above) were washed once with PBS. Total cell lysates were then prepared by adding 75  $\mu\text{l}$  – 100  $\mu\text{l}$  or 50  $\mu\text{l}$  of RPPA lysis buffer respectively (1% Triton X-100, 50 mM HEPES, 150 mM NaCl, 1 mM  $\text{MgCl}_2$ , 1 mM EGTA, 10% glycerol, and protease inhibitor cocktail (Roche, Indianapolis, IN)) for 1 hour at 4 $^{\circ}\text{C}$ ; this was followed by scraping, collection of the lysed cells, and centrifugation at 14,000 rpm for 10 minutes. The supernatant was retained as the total protein lysates and 2  $\mu\text{l}$  of all the protein samples were added to a transparent 96-well plate in duplicates together with the BSA (bovine serum albumin) standards ranging from 25  $\mu\text{g/ml}$  to 2,000  $\mu\text{g/ml}$ . BCA (bicinchoninic acid, Fisher Scientific) assay was performed by adding 200  $\mu\text{l}$  of BCA reagent (98% Reagent A+ 2% Reagent B) to each well; the plate was next incubated at 37 $^{\circ}\text{C}$  for 30 minutes. Absorbance readings were measured at 570 nm and protein concentrations were determined by using the standard curve equation. All the protein samples were then normalized to the lowest concentration sample followed by the addition of 10  $\mu\text{l}$  of 6X SDS loading dye buffer. Loading samples

were resolved on an 8%, 10%, or 12% SDS-PAGE gel (as appropriate) at 100V for ~2 hours. Gels were then transferred to polyvinylidene fluoride (PVDF) membranes using a semi-dry transfer apparatus for 2 hours at 0.11 A (one membrane) or 0.15 A (two membranes). Transferred membranes were then washed with 1X TBST (1X Tris-Buffered Saline (TBS) containing 0.1% Tween-20 (Biorad)) followed by blocking in 5% milk /1X TBST solution for 1 hour before incubating the membranes in primary antibody at 4°C on an orbital shaker overnight. A complete list of all primary antibodies utilized for the western analyses presented in this thesis is given in Table 7 (with antibody dilutions and company sources). The next day, the membranes were washed with 1X TBST four times for 15 minutes each on an orbital shaker at room temperature. Secondary goat anti-rabbit (#107-5046, Immun-Star, Biorad) or goat anti-mouse antibodies (#107-5047, Immun-Star, Biorad) diluted in 5% milk in TBST were applied to the membranes at concentrations ranging from 0.26 µg/ml to 1 µg/ml and were incubated for a further 1 hour at room temperature on the same shaker. This was followed by six washes with 1X TBST for 15 minutes each prior to the application of the enhanced chemi-luminescence reagent (ECL or Clarity ECL, Bio-Rad, Hercules, CA or LumiGLO, Cell Signaling) followed by detection of the bound antibodies by exposing the membranes to X-ray film in a dark room. All the antibodies listed in Table 7 were detected by application of ECL or LumiGLO substrate with the exception of phospho-JNK which was detected using Clarity ECL substrate.

### **Subcellular Fractionation**

Isolation of cytoplasmic and nuclear fractions was performed using the NE-PER nuclear and cytoplasmic extraction kit (#78833, Thermo Scientific). Briefly, cells plated into T25 flask at a density of 1 million, were treated appropriately post-adherence and were then washed once with PBS. Cells were then collected by scraping with 100 µl of PBS, pelleted at 500 g for 3 minutes and were resuspended into 200 µl of CER-I reagent by vortex mixing followed by incubation on ice for 10 minutes. This suspension was pelleted at 16,000 g for 5 minutes and 200 µl of supernatant was centrifuged again for 5 minutes at 16,000 g. Top 100 µl of the resultant supernatant was collected as cytoplasmic fraction. The pellet was

**Table 7: List of primary antibodies utilized for western analyses**

Antibody	Type	Dilution	Source	Catalog Number.
Bcl-XL	Rabbit monoclonal	1:1000	Cell Signaling	#2764
c-Src	Mouse monoclonal	1:1000	Cell Signaling	#2110
EGFR	Rabbit polyclonal	1:1000	Santa Cruz	SC-03
GAPDH	Rabbit polyclonal	1:5000	Cell Signaling	#2118
GFP	Mouse monoclonal	1:1000	Santa Cruz	SC-9996
Grb2	Mouse monoclonal	1:2000	BD Biosciences	#610111
HA-11	Mouse monoclonal	1:1000	Covance	#14921901
IRF3	Rabbit monoclonal	1:1000	Cell Signaling	#11904
Lamin A/C	Mouse monoclonal	1:1000	Cell Signaling	#4777
LC3B	Rabbit polyclonal	1:1000	Cell Signaling	#2775
MAPK	Rabbit polyclonal	1:1000	Cell Signaling	#4695
MBP	Mouse monoclonal	1:10000	NEB	#E80325
PAI-1	Mouse monoclonal	1:1000	BD Biosciences	#612024
Pan-Actin	Rabbit polyclonal	1:1000	Cell Signaling	#4968
PARP	Rabbit polyclonal	1:1000	Cell Signaling	#9542
Phospho-IRF3	Rabbit monoclonal	1:500	Cell Signaling	#4947
Phospho-AKT	Rabbit polyclonal	1:1000	Cell Signaling	#4060
Phospho-EGFR (PY99)	HRP-conjugated	1:1000	Santa Cruz	SC-7020
Phospho-ERK	Rabbit polyclonal	1:1000	Cell Signaling	#9101
Phospho-JNK	Mouse monoclonal	1:500	Cell Signaling	#9255
Phospho-Src (416)	Rabbit monoclonal	1:1000	Cell Signaling	#2113
Phospho-STAT3	Rabbit polyclonal	1:1000	Cell Signaling	#6145
PIK3CA	Rabbit polyclonal	1:1000	Cell Signaling	#4249
PLSCR1	Mouse monoclonal	1:500	Santa Cruz	SC-59645
pSer-p66-ShcA	Mouse monoclonal	1:1000	Calbiochem	#566807
ShcA	Rabbit polyclonal	1:1000	Millipore	#06-203
SnoN	Rabbit polyclonal	1:1000	Santa Cruz	SC-9141
STAT3	Rabbit polyclonal	1:1000	Cell Signaling	#4904
Total AKT	Rabbit polyclonal	1:1000	Cell Signaling	#4685
Total JNK	Rabbit monoclonal	1:1000	Cell Signaling	#9258
XIAP	Rabbit monoclonal	1:1000	Cell Signaling	#2045

washed once with PBS and was resuspended in 100  $\mu$ l of NER reagent by vortex mixing every 10 minutes for 4 times. This suspension was centrifuged at 16,000 g for 10 minutes and the top 50  $\mu$ l of the supernatant was collected as nuclear fraction. Gel loading samples prepared by adding 10  $\mu$ l of 6X SDS to each of the collected fractions, were analyzed by western blotting using the antibodies against the proteins of interest.

## **Immunoprecipitation**

Cells were seeded in 6-well plates at a density of 250,000 cells/well. After the respective treatment, protein lysates were collected using RPPA lysis buffer. To these lysates, 5  $\mu$ l of antibody (targeting the protein of interest) was added at concentrations between 200–250  $\mu$ g/ml; lysates were incubated on an orbital shaker at 4°C for 3 hours. Following this incubation, 40  $\mu$ l of Protein G Sepharose 4 Fast Flow beads (Amersham Biosciences, Piscataway, NJ) were then added and incubated with shaking for 1 hour at 4°C. The beads were then pelleted at 3,000 rpm for 3 minutes, washed with lysis buffer once and with PBS three times. The immunoprecipitated proteins were eluted by adding 30  $\mu$ l of 5% SDS buffer. The immunoprecipitates were then run on appropriate SDS-PAGE gels together with the total lysate (as “input” fractions), supernatants (to ensure antigen depletion from lysates) and antibody negative controls (antibodies incubated in the RPPA lysis buffer only). Western analysis was performed for the proteins of interest using corresponding antibodies.

## **Total RNA Isolation and Real-Time PCR**

Cells seeded into 6-well plates were washed with PBS. Total RNA was isolated using the RNeasy mini kit (Qiagen) following the protocol provided with the kit. RNA was quantified using Nanodrop and 20 ng/ $\mu$ l dilutions were prepared for use in real-time PCR. Quantitative PCR was performed using the One-step PCR Taqman master mix (4309169), FAM-labeled probes/primers, and the One-Step-Plus detection system (Applied Biosystems, Bedford, MA). FAM-labeled probes/primers specific for SnoN (Hs00180524\_m1), PLSCR1 (Hs00275514\_m1), IFN- $\alpha$  (Hs00855471\_g1), IFN- $\beta$  (Hs01077958\_s1), TLR-4 (Hs00152939\_m1), and TLR9 (Hs00370913\_s1) were obtained from Assays-on-Demand (Applied Biosystems).  $\beta$ -actin (#401846, Applied Biosystems) was used as the endogenous control. All Ct (cycle threshold) values were normalized to that of  $\beta$ -actin ( $\Delta$ Ct) first and then to the untreated control reference sample ( $\Delta\Delta$ Ct). Relative mRNA fold changes were calculated by using the formula  $2^{-(\Delta\Delta Ct)}$ . The RNA-fold changes were then represented as bar graphs with error bars representing the standard deviations.



## **Luciferase Promoter Activity Assays**

T80 cells were plated in 6-well plates at a density of 250,000 cells per well; they were then transfected with the pGL3-basic empty vector or that containing the human PLSCR1 genomic construct as described above. One day post-transfection, the cells were recovered with complete growth media for a minimum of 3 hours and were treated with 50 pM TGF- $\beta$ . Protein lysates were collected and 20  $\mu$ l of normalized lysates were added in duplicate to an opaque 96-well plate. Hundred  $\mu$ l of luciferase assay substrate (Luciferase assay substrate, #E151A, Promega) was added to each well in the dark and luminescence readings were measured using a Biotek plate reader. As a negative control, 100  $\mu$ l of substrate was added to wells containing 20  $\mu$ l of RPPA lysis buffer only. Luminescence readings from these wells were considered as background and were subtracted from the readings obtained from samples. For experiments investigating the effect of knockdown of EVI1 and SnoN on PLSCR1 promoter activity, cells were first transfected with siRNAs targeting EVI1 or SnoN; this was then followed 24 hours later by transfection with pGL3-basic or pGL3-basic containing the human PLSCR1 genomic construct.

## **Immunocytochemistry**

### Direct Immunofluorescence:

Cells were plated on coverslips in a 6-well plate, 24-well plate, 35mm dishes at a density of 250,000, 52,000 and 250,000 per well respectively. Post-adherence, cells were transfected with pEGFP-C1 or pEGFP-LC3 plasmids as appropriate. Forty eight hours post-transfection, cells were washed with PBS and fixed with 4% paraformaldehyde for 30 min at room temperature. All staining/incubation steps were performed in the dark. Cells were then washed in PBS twice for 5 minutes each and then blocked for 1 hour at room temperature with blocking buffer (PBS containing 0.1% Triton-X-100 and 5% goat serum (#PI-31872, Fischer Scientific)). After three washes with PBS, coverslips were mounted on glass slides with DAPI nuclear stain (#H-1200, Vector Laboratories, Burlingame, CA). The edges of the coverslips were sealed with nail polish and imaging was performed using a PerkinElmer UltraVIEW ERS spinning

disk confocal microscope (Department of CMMB, University of South Florida) or Zeiss inverted fluorescence microscope (Microscopy core, Moffitt Cancer Center). For all the immunofluorescence data presented in Chapters 3 and 4 of this thesis, imaging was performed at Moffitt Cancer Center whereas the imaging for all the data presented in Chapters 5 and 6 was performed at Department of CMMB. For the EGFP-LC3 autophagy study, the number of cells positive for GFP-LC3 punctae were counted and their percentage using total number of cells was calculated. For the EGFP-C1 based assay to determine the transfection efficiency, number of cells positive for GFP expression were counted and their percentage using total cells was calculated.

Indirect Immunofluorescence:

**Table 8: List of primary antibodies utilized for indirect immunofluorescence**

Primary Antibody	Dilution	Source	Catalog Number	Secondary antibody
PLSCR1	1:500	Santa Cruz	SC-59645	Alexafluor-488 (Anti-Mouse)
HA-11	1:1000	Covance	#14921901	Alexafluor-488 (Anti-Mouse)
RCAS-1	1:50	Cell Signaling	#12290	Alexafluor-546 (Anti-Rabbit)
Calnexin	1:50	Cell Signaling	#2679	Alexafluor-546 (Anti-Rabbit)

Cells plated on coverslips in 6-well plates or 35mm dishes at a density of 250,000 to 325,000 cells per well, were treated IFN-2 $\alpha$  or transfected with indicated plasmids for appropriate lengths of time. Cells were first washed with PBS once and then fixed with 4% paraformaldehyde for 30 minutes. After 2 washes with PBS, the cells were blocked for 1 hour in blocking buffer (PBS containing 0.1% Triton-X100 and 5% goat serum) and incubated overnight at 4°C with the indicated primary antibody diluted in PBS containing 0.1% Triton-X 100 and 1% goat serum. Next day, the cells were washed with PBS and were incubated in Alexafluor-488 or Alexafluor-546 conjugated goat anti-mouse or anti-rabbit secondary

antibody (1:500, Invitrogen), respectively, for 1 hour at room temperature in the dark. After three PBS washes, coverslips were mounted onto glass slides with DAPI nuclear stain; this was followed by imaging using a confocal microscope. A complete list of all primary antibodies utilized for the indirect immunofluorescence studies presented in this thesis is summarized in Table 8 (with antibody dilutions and corresponding secondary antibodies).

### **Annexin V/PI Assay**

Supernatant media was collected upon experimental completion. To this media, trypsinized adherent cell population was added (by adding 500  $\mu$ l of Trypsin-EDTA for cells in 6-well plates). Cells (floating and adherent cell populations) were then pelleted by spinning them at 1000 rpm for 5 minutes. Cells were resuspended in 500  $\mu$ l PBS; rapid staining procedure was adapted using the Annexin V/PI staining kit (Calbiochem, Rockland, MA). Briefly, cells were incubated with 1.25  $\mu$ l of Annexin V stain followed by 10 $\mu$ l of media binding reagent for 15 minutes at room temperature in the dark. Then the cells were pelleted at 1000 rpm for 5 minutes followed by resuspension in 500  $\mu$ l of ice-cold binding buffer. This was then incubated in 10  $\mu$ l of Propidium Iodide (PI) for 30 min at 4°C in the dark. These stained cells were then analyzed by flow cytometry by detecting signals at 518 nm for FL1 and 620 nm for FL2 using the Flow Cytometry Core, (College of Medicine, University of South Florida).

### **Caspase Activity Assay**

Cells plated in 6-well plates were trypsinized using 500  $\mu$ l of Trypsin-EDTA per well. Cells from each well were counted and were re-seeded into an opaque 96-well plate at a density of 50,000 cells in 100  $\mu$ l of complete growth media per well. One day post-seeding, caspase activity assay was performed using the Caspase Glo-3/7 assay kit (Promega, Madison, WI). Briefly, 100  $\mu$ l of caspase glo-3/7 substrate was added to each well and then the plate was shaken for 2 minutes in the Biotek plate reader; incubation was then performed in the dark at room temperature for 30 minutes before taking luminescence measurements every 30 minutes. A mixture of growth media and caspase glo-3/7 substrate at a 1:1 ratio

was used as a negative control. All the luminescence readings were presented as bar graphs containing error bars representing the standard deviation values.

### **Phosphatase Assay**

Protein lysates were isolated from cells plated in 6-well plates (treated as indicated) using RPPA lysis buffer. Protein lysate concentrations were then normalized to the sample (determined by BCA assay) with the lowest concentration. Normalized protein lysates were then added to a 96-well plate and phosphatase activity was measured using the 1-Step PNPP ( $p$ -nitrophenyl phosphate disodium salt) substrate (Fisher Scientific). Briefly, 100  $\mu$ l of 1-Step PNPP substrate was added to each well followed by shaking in a Biotek plate reader before incubating at room temperature for 30 minutes after which time 50  $\mu$ l of 2 N NaOH was added to terminate the reaction; absorbance readings were measured at a wavelength of 405 nm.

### **ATP Viability Assays**

Cells were plated into opaque 96-well plates at a density of 5000 cells in 100  $\mu$ l of complete growth media per well. Cells were treated and then washed once with 200  $\mu$ l PBS prior to assessing cell viability using the ATP viability kit (Promega, Madison, WI). Briefly, 100  $\mu$ l of PBS was added to each well along with 100  $\mu$ l of Cell Titer Glo substrate; the plate was shaken for 2 minutes using the Biotek plate reader followed by incubation in the dark at room temperature for 10 minutes. Luminescence readings were obtained using the Biotek plate reader.

### **Cell Growth Assays**

Cells were plated into transparent 96-well plates at a seeding density of 5000 per well in 200  $\mu$ l media. After the indicated treatments, media was discarded from the plates and 100  $\mu$ l of crystal violet stain (0.5% crystal violet (Fischer Scientific) in 20% methanol) was added to each well for 15 minutes at room temperature. The stain was washed away using Nanopure water and plates were left at room

temperature for 24 hours to dry followed by the addition of 200  $\mu$ l of Sorenson's buffer (0.1 M Sodium Citrate, pH 4.2 in 50% Ethanol) to each well; the plate was shaken at room temperature for 2 hours. Absorbance readings were then measured using a Biotek plate reader at 570 nm.

### **Statistical Analyses**

All the data presented in the studies presented in this thesis is representative of more than one independent experimental replicate; details of numbers of replicates are indicated in the respective figure legends. All the bar graphs presented in this thesis represent the averages of all independent experiments (replicates) with error bars representing standard deviation. Statistical significance of the data is presented as p-values as generated using the Graphpad Prism software (standard student's t-test). P values are represented as follows:  $P < 0.001$  (\*\*\*) ,  $P < 0.01$  (\*\*),  $P < 0.05$  (\*) and  $p > 0.05$  (NS).

## Chapter 3

### **SnoN/SkiL Expression is Modulated via As<sub>2</sub>O<sub>3</sub>-Induced Activation of PI3K/AKT Pathway in Ovarian Cancer Cells**

#### **Introduction**

Platinum-based chemotherapeutics such as paclitaxel, cisplatin, and carboplatin proceeding surgical resection is the most common strategy for treatment of ovarian cancers [46, 47, 58]. Despite the recent improvements in treatment, the 5-year survival rate of ovarian cancer patients remains less than 50% (National Cancer Institute, <http://seer.cancer.gov/statfacts/html/ovary.html>) [49]. The chromosomal region 3q26 is commonly amplified in a subset of epithelial cancers including ovarian cancers [9-12, 28-30]. Previous studies including those from our research group demonstrate that this region contains various oncogenes including MECOM (MDS1-EV11 complex) [10], SnoN/SkiL [9], and PKC $\iota$  [30] at 3q26.2; and PIK3CA at 3q26.3 [11]. As mentioned in Chapter 1, SnoN (Ski related novel protein N) belongs to the ski family of oncogenes and is an important transcriptional regulator involved in the TGF $\beta$  signaling pathway [28, 76-79]. It binds to the SMAD2/3 and SMAD4 complex thereby preventing them from recruiting transcriptional co-activators (i.e. c-Jun, CBP, p300 and FAST-1/2) [183-185], thereby leading to repression of transcription of TGF $\beta$  target genes and their downstream effects [77-79]. Previous array comparative genomic hybridization (aCGH) data obtained from 235 epithelial ovarian cancer patients demonstrated SnoN/SkiL to be amplified at 3q26.2 as well as overexpressed (at RNA level) in ~80% of serous ovarian carcinomas in comparison to normal ovarian cells [9]. In addition, we determined that arsenic trioxide (As<sub>2</sub>O<sub>3</sub>) induces SnoN expression which mediates cytoprotective autophagic response that antagonizes the cytotoxic effects of As<sub>2</sub>O<sub>3</sub> [1]. However, the mechanisms and signaling pathways mediating these responses remain to be identified.

Upon stimulation with extracellular ligands, epidermal growth factor receptor (EGFR) activates downstream signaling cascades involving Src, Ras-MAPK, and PI3K/AKT pathways which promote cell growth, survival, and proliferation [186, 187]. EGFR and its downstream adaptor and signaling molecules, notably ShcA [188, 189], Grb2 [190-192], PI3K [11, 53, 66, 165, 193, 194], and Src [195-197] pathways are highly altered or dysregulated in cancers [11, 53, 66, 165, 188-190, 198-201]. Additionally, EGFR is also associated with drug resistance and poor clinical outcome of cancer patients [202]. In addition to growth factors (such as EGF and TGF $\alpha$ ), chemotherapeutic agents including cisplatin [203, 204] and As<sub>2</sub>O<sub>3</sub> [205-207] activate EGFR. As<sub>2</sub>O<sub>3</sub> promotes EGFR phosphorylation followed by activation of downstream Src and AKT pathways [205, 206]. In human epidermoid carcinoma (A431) cells, activation of Src and EGFR/ERK pathway mediates As<sub>2</sub>O<sub>3</sub>-induced expression of p21 and cell cycle arrest [206]. Interestingly, TGIF (TGF $\beta$ -interacting factor), a transcriptional co-repressor in the TGF $\beta$  signaling pathway also contributes to this process [208]. Similarly, in human keratinocytes, EGFR is activated in a Src-dependent manner in response to As<sub>2</sub>O<sub>3</sub> [209]. In addition, EGFR is activated by ligand-independent methods including activation by stimuli such as oxidative stress [209, 210], UV [211], and  $\gamma$ -irradiation [212].

As described in Chapter 1, As<sub>2</sub>O<sub>3</sub> is an FDA approved drug used in the treatment of acute promyelocytic leukemia (APL) [90, 91]. As<sub>2</sub>O<sub>3</sub> binds directly to the PML-RAR fusion oncoprotein (characteristic of APL) thus promoting its degradation via SUMOylation [91]. Additionally, it increases cellular cytotoxicity of epithelial cancer cells including those derived from the ovarian tissue by inducing apoptosis [1, 75, 213]. Interestingly, As<sub>2</sub>O<sub>3</sub> activates EGFR and its downstream signaling mediators including Src, PI3K, and ERK [205, 207, 209]. Our recent studies demonstrate that As<sub>2</sub>O<sub>3</sub> also modulates the expression of various TGF $\beta$  signaling mediators [1]. Treatment of ovarian cancer cells with As<sub>2</sub>O<sub>3</sub> markedly reduced the expression of EVI1, TAK1, SMAD2/3, and TGF $\beta$ RII in both a proteasome-dependent and independent manner [1]. In contrast, As<sub>2</sub>O<sub>3</sub> markedly induces SnoN protein and mediates a beclin-1 independent cytoprotective autophagic response that antagonizes the cell death response in these

cells [1]. However, the detailed mechanisms that underlie SnoN induction and the resultant cellular responses remain unclear. Previous studies suggest an important role for EGFR and its downstream signaling pathways in regulating cancer cell responses [186, 199, 203-205, 209]; furthermore, As<sub>2</sub>O<sub>3</sub> activates these pathways [137, 205, 209]. Therefore, we hypothesized that As<sub>2</sub>O<sub>3</sub>-induced SnoN expression and cell responses are mediated by activation of EGFR and its downstream signaling pathways. Herein, our studies indicate that As<sub>2</sub>O<sub>3</sub> treatment activates EGFR and alters its ability to interact with its downstream adaptor proteins (i.e. ShcA/Grb2) at a slower rate compared to cells treated with EGF. Utilizing inhibitor and siRNA knockdown studies, we further demonstrate that inhibition of Src family kinases (SFK) and the PI3K/AKT signaling abrogates the As<sub>2</sub>O<sub>3</sub>-induced changes in SnoN levels. Inhibition of the PI3K pathway increased the sensitivity of ovarian cancer cells to As<sub>2</sub>O<sub>3</sub>. Similarly, reduction of EGFR and MAPK1 altered the As<sub>2</sub>O<sub>3</sub>-mediated cell death responses independent of SnoN expression. Collectively, our studies identify the PI3K/AKT pathway to facilitate the changes in SnoN expression and the subsequent cytoprotective responses upon As<sub>2</sub>O<sub>3</sub> treatment in HEY ovarian carcinoma cells.

## **Results**

### As<sub>2</sub>O<sub>3</sub> activates EGFR and promotes its interaction with downstream adaptor protein Grb2:

In order to determine whether As<sub>2</sub>O<sub>3</sub> activates EGFR and its downstream signaling mediators, we treated HEY cells with As<sub>2</sub>O<sub>3</sub> (5, 10, or 25 μM) or EGF (100 ng/ml) from 1 to 30 hours and analyzed their effects. As shown in Figure 8A, EGF treatment dramatically increased the phosphorylation of EGFR (p-EGF) and AKT by 1 hour post-treatment which decreased gradually until 30 hours. Additionally, we observed slightly slower mobility of p66 isoform of ShcA adaptor protein at 1 hour. Interestingly, EGFR protein levels rapidly decreased by 1 hour when compared to untreated cells which could be attributed to the antibody having high affinity for the unphosphorylated form relative to the phosphorylated form. In contrast, Grb2 and ShcA protein levels reduced from 6 hours onwards whereas there were no



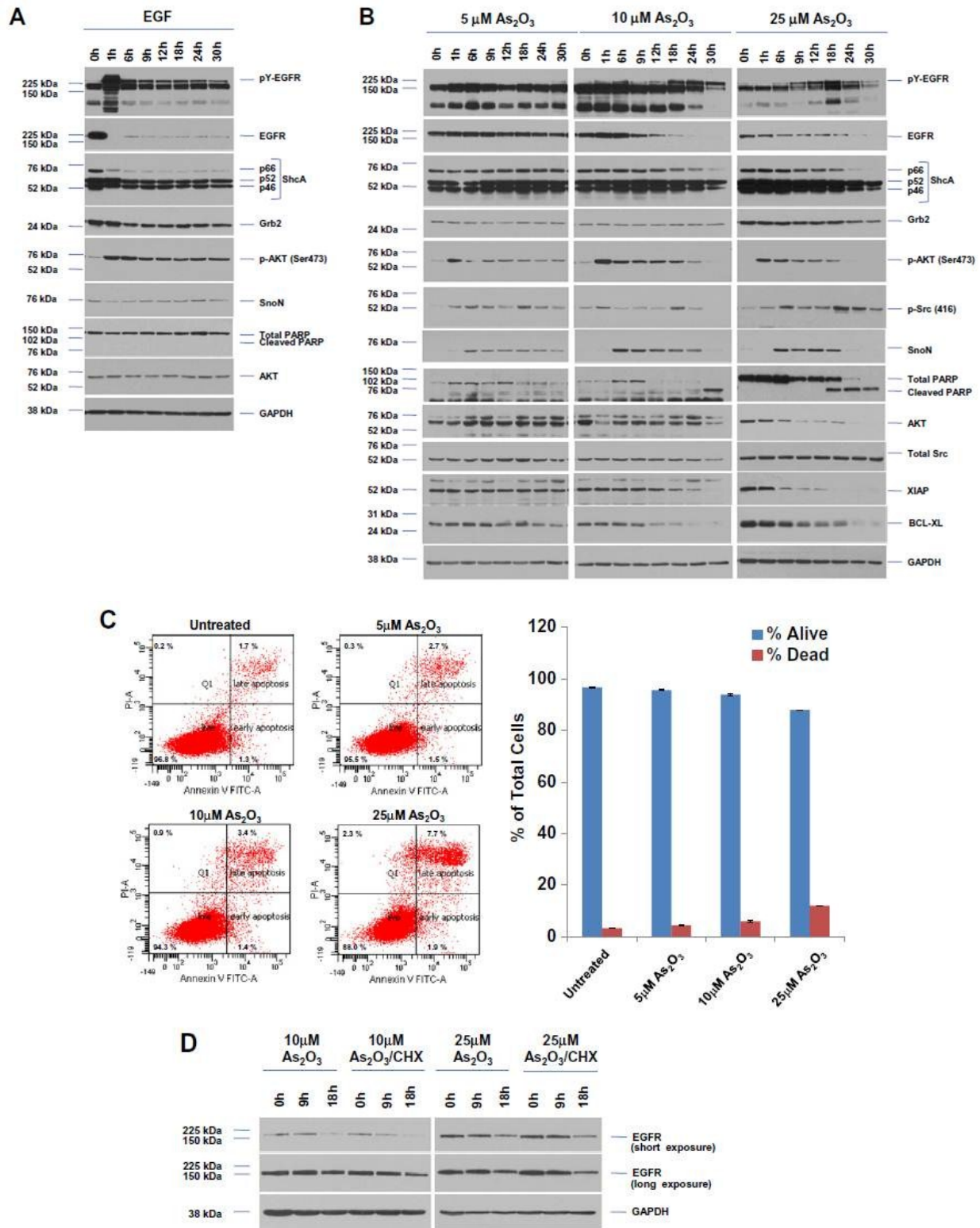


**Figure 8.  $\text{As}_2\text{O}_3$  leads to activation of EGFR, Src, and AKT and modulates EGFR interaction with Grb2 (\*Continued on next page)**

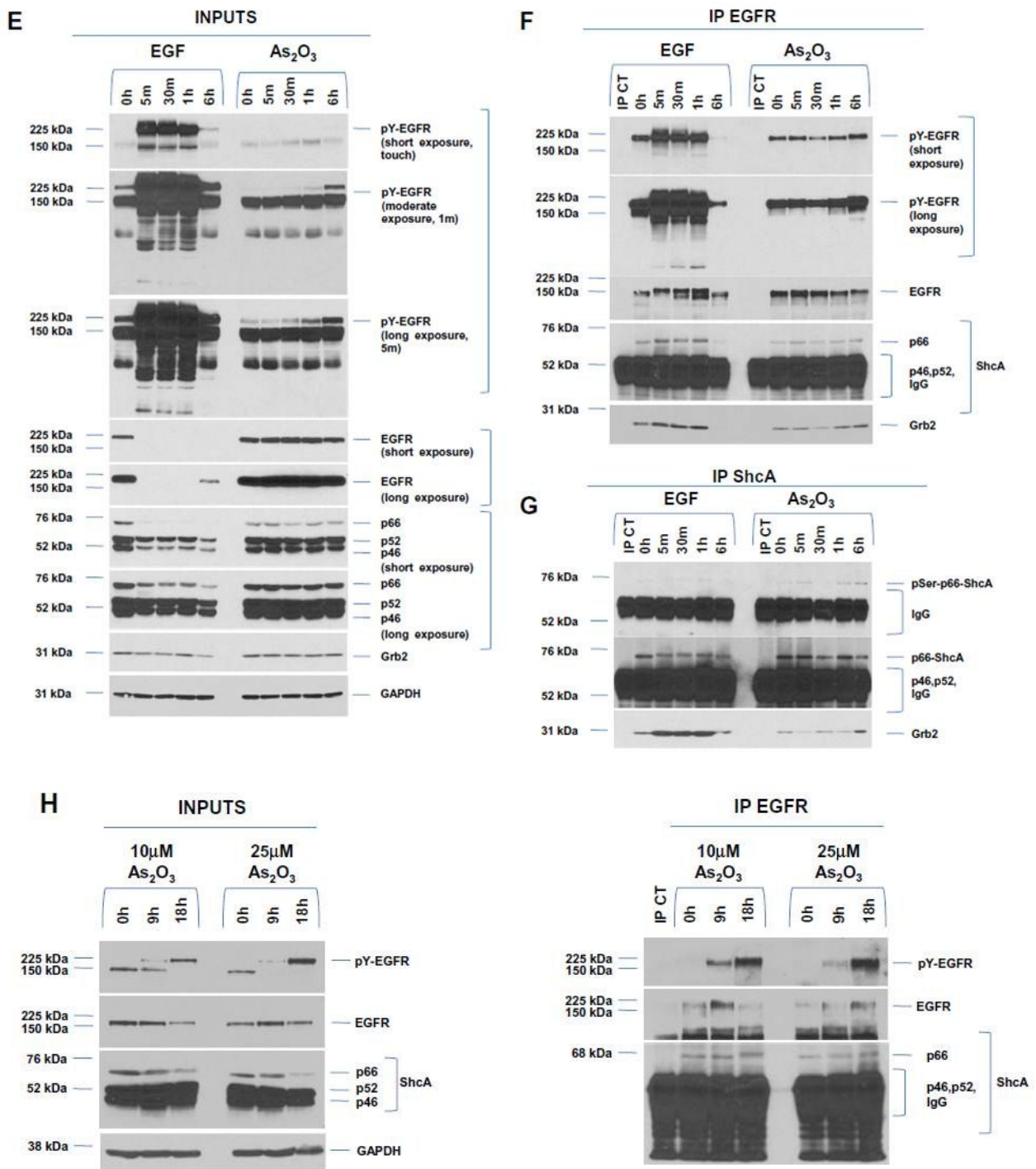


**Figure 8.** As<sub>2</sub>O<sub>3</sub> leads to activation of EGFR, Src, and AKT and modulates EGFR interaction with Grb2 (\*Continued on next page)

**Figure 8. As<sub>2</sub>O<sub>3</sub> leads to activation of EGFR, Src, and AKT and modulates EGFR interaction with Grb2**

(A) HEY ovarian cancer cells were treated with 100 ng/ml EGF from 1 to 30 hours. Total cell lysates were harvested as described in Chapter 2 and western analyses were performed for the indicated antibodies. (B) HEY cells were treated with As<sub>2</sub>O<sub>3</sub> (5 or 10 or 25 μM) from 1 to 30 hours and lysates collected were analyzed by western blotting for the indicated antibodies. (C) Cells were treated with 5 or 10 or 25 μM As<sub>2</sub>O<sub>3</sub> for 18 hours and were stained with Annexin V and propidium iodide (PI) as described in chapter 2. Flow cytometry was performed to obtain the raw plots (Left panel) and to analyze the percentage of dead and viable cells (Right panel) (D) Cells were treated with 10 or 25 μM As<sub>2</sub>O<sub>3</sub> for 9 and 18 hours both in presence and absence of 2 μg/ml CHX. Lysates collected were analyzed via western blotting for the indicated antibodies. (E) Cells were treated with EGF and As<sub>2</sub>O<sub>3</sub> from 5 minutes to 6 hours as described above. Total cell lysates were isolated and western analyses was performed for the indicated antibodies. (F) Cell lysates obtained from (E) were used for immunoprecipitation analyses of EGFR as described in Chapter 2 followed by western analyses. (G) Cell lysates obtained from (E) were used for immunoprecipitation analyses of ShcA followed by western blotting. (H) Cells were treated with 10 or 25 μM As<sub>2</sub>O<sub>3</sub> for 9 and 18 hours and total cell lysates collected were analyzed by western blotting (Left panel). Lysates collected were also utilized for immunoprecipitation analyses of EGFR (Right panel). Data presented in (A), (E) and (F) is representative of four independent experiments while (B), (C), (D), (G), and (H) represent two independent experiments

significant changes in the SnoN and PARP levels (Figure 8A). On the other hand, treatment with 10 and 25 μM As<sub>2</sub>O<sub>3</sub> resulted in a much slower activation of EGFR which peaked at 18 hours post-treatment compared to 1 hour EGF treatment (Figure 8B). The reduction in EGFR, ShcA, and Grb2 protein levels was also slower than that of EGF treatment starting from 18 hours onwards. Interestingly, AKT was phosphorylated by 1 hour gradually decreasing until 30 hours in a manner that was very similar to the EGF treatment. In contrast, Src activation was biphasic with p-Src levels peaking at 6 and 18 hours. As reported by earlier studies, As<sub>2</sub>O<sub>3</sub> treatment resulted in increased levels of SnoN by 6 hours and cleaved PARP from 18 to 30 hours suggestive of increased apoptosis. We validated the apoptotic response via Annexin V/PI staining which indicated increased apoptosis when HEY cells were treated with increasing concentrations of As<sub>2</sub>O<sub>3</sub> (Figure 8C). Consistently, there was a dramatic reduction in the levels of anti-apoptotic proteins XIAP and BCL-XL (Figure 8B). The changes observed upon As<sub>2</sub>O<sub>3</sub> treatment were

observed at all three concentrations (5, 10, and 25  $\mu\text{M}$ ) although there was increased intensity of changes with increasing concentration. Collectively, these results indicate that  $\text{As}_2\text{O}_3$  activates EGFR, Src and AKT and alters the expression of downstream adaptor proteins ShcA and Grb2 with slower kinetics compared to EGF stimulation suggesting that different mechanisms of activation are involved following cellular stimulation with EGF and  $\text{As}_2\text{O}_3$ . We next treated HEY cells with  $\text{As}_2\text{O}_3$  both in the presence and absence of cycloheximide (CHX), a translational inhibitor. Indeed, there was no significant difference in decreased EGFR levels mediated by  $\text{As}_2\text{O}_3$  in the presence of CHX suggesting that EGFR is degraded upon  $\text{As}_2\text{O}_3$  treatment (Figure 8D).

Since  $\text{As}_2\text{O}_3$  alters EGFR activation and expression, we next determined whether  $\text{As}_2\text{O}_3$  modulates the interaction of EGFR with its downstream adaptor proteins ShcA and Grb2. Co-immunoprecipitation against EGFR in HEY cells treated with EGF and  $\text{As}_2\text{O}_3$  indicated that activated EGFR interacted with p66 ShcA in both the untreated and  $\text{As}_2\text{O}_3$  or EGF treated cells (Figure 8F). Interestingly, there was a marked increase in interaction of EGFR with Grb2 upon treatment with both EGF and  $\text{As}_2\text{O}_3$  (Figure 8F).  $\text{As}_2\text{O}_3$  treatment also resulted in increased phosphorylation of p66 ShcA from 6 hours onwards (Figures 8F and 8H) which was further validated by detection of phospho-Ser36 form of p66 ShcA in the co-immunoprecipitate fractions of ShcA (Figure 8G). Together, these results indicate that  $\text{As}_2\text{O}_3$  stimulation induces phosphorylation of p66ShcA and increases the interaction of Grb2 with EGFR-ShcA complex.

#### Inhibition of Src family kinase activity alters the $\text{As}_2\text{O}_3$ -mediated EGFR activation and SnoN induction:

In order to identify the signaling pathways mediating the  $\text{As}_2\text{O}_3$ -induced changes in SnoN expression, we first utilized inhibitors targeting mediators of different pathways: (1) PP2, a general Src family kinase (SFK) inhibitor; (2) U0126, MAP Kinase inhibitor; and (3) PD153035, an EGFR and HER2/neu kinase inhibitor. We treated the HEY cells with  $\text{As}_2\text{O}_3$  both in the presence and absence of these inhibitors at the following doses: PP2, 10 $\mu\text{M}$ ; U0126, 10 $\mu\text{M}$ ; and PD153035, 100 nM. Interestingly,

in the presence of PP2 (and not U0126 and PD153035), we observed a significant reduction in the  $\text{As}_2\text{O}_3$ -induced EGFR activation and SnoN protein levels (Figures 9A-C, 9H, and 10F).

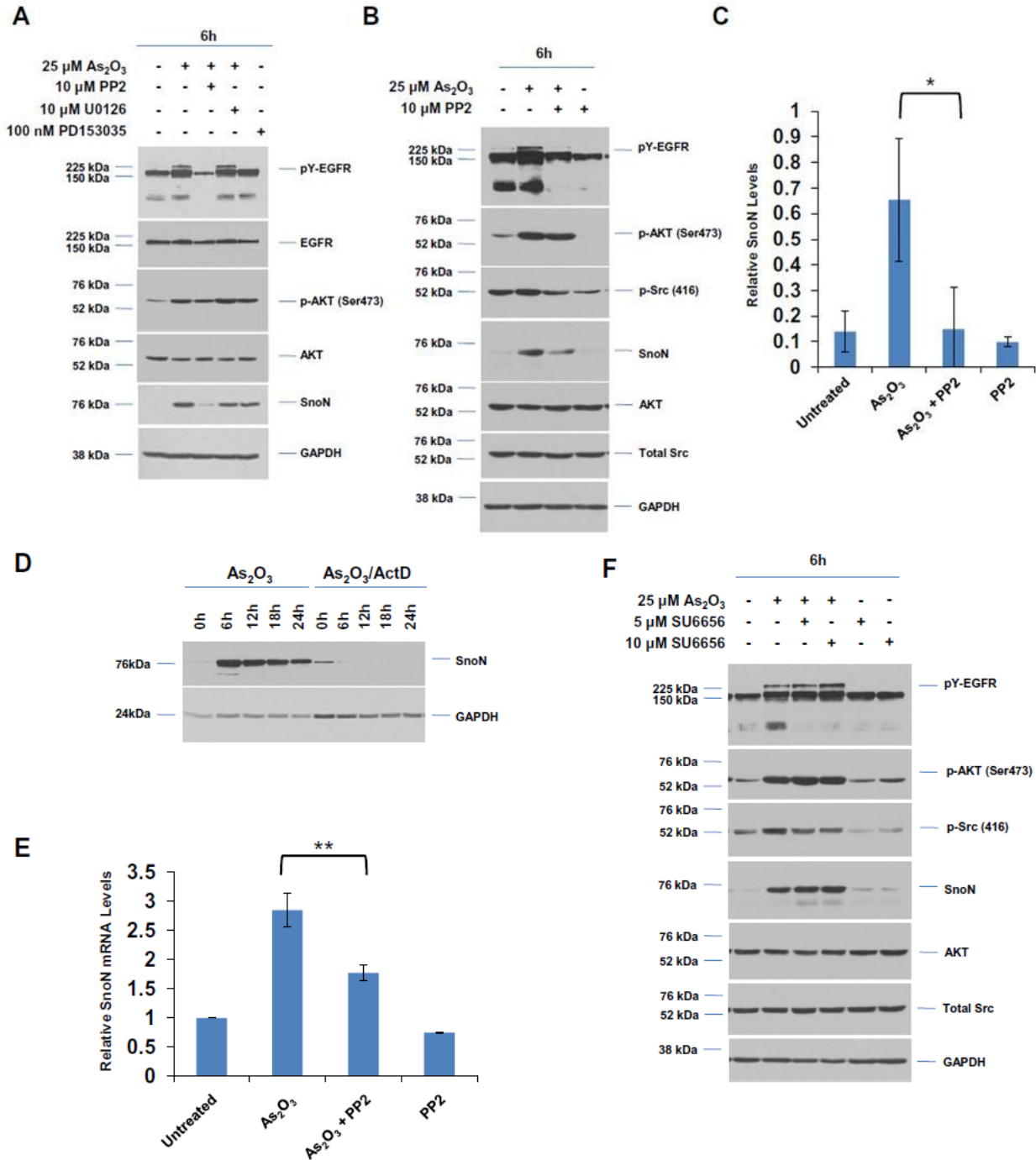


**Figure 9. Inhibition of Src family kinase activity modulates the  $\text{As}_2\text{O}_3$ -mediated EGFR activation and SnoN induction (\*Continued on next page)**

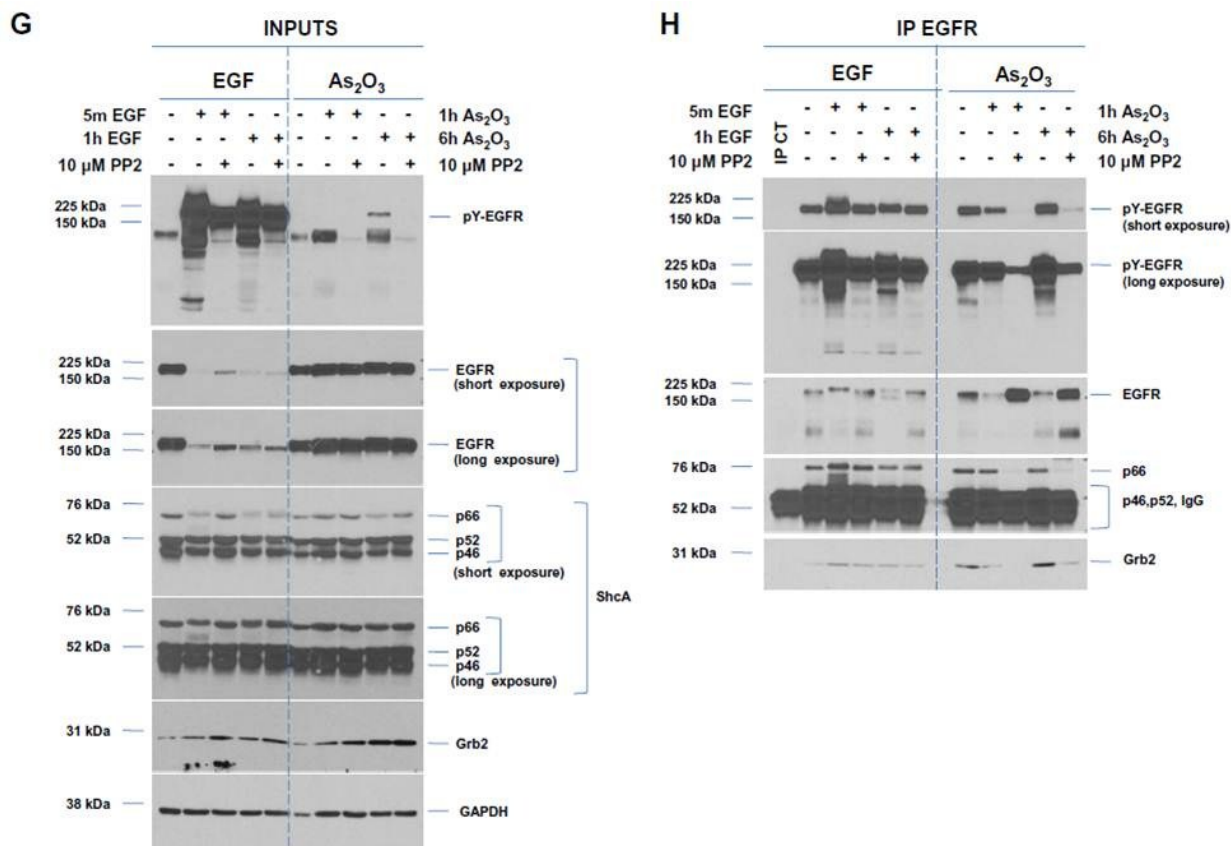


**Figure 9. Inhibition of Src family kinase activity modulates the As<sub>2</sub>O<sub>3</sub>-mediated EGFR activation and SnoN induction**

(A) Cells were treated with 25 μM As<sub>2</sub>O<sub>3</sub> for 6 hours after pretreatment with 10 μM PP2 or 10 μM U0126 and 100 nM PD153035 or DMSO. Total cell lysates collected were analyzed via western blotting for indicated antibodies. (B) Cells were treated with 25 μM As<sub>2</sub>O<sub>3</sub> or 10 μM PP2 or both as described in (A) for 6 hours and lysates collected were analyzed by western blotting for the indicated antibodies. (C) Densitometric analyses were performed to determine the relative SnoN level changes from (B). (D) Cells were treated with 25 μM As<sub>2</sub>O<sub>3</sub> for 6 to 24 hours both in presence and absence of 100 ng/ml ActD. Lysates collected were analyzed via western blotting for the indicated antibodies. (E) Cells were treated with 25 μM As<sub>2</sub>O<sub>3</sub> for 6 hours both in presence and absence of 10 μM PP2 as in (A). Total RNA was isolated and qPCR was performed to determine the relative mRNA levels of SnoN as described in Chapter 2. (F) Cells were pretreated with 5 or 10 μM SU6656 for 2 hours followed by 25 μM As<sub>2</sub>O<sub>3</sub> for 6 hours. Cell lysates obtained were analyzed via western blotting for the indicated antibodies. (G) Following pretreatment with 10 μM PP2 for 2 hours, cells were treated with 100 ng/ml EGF or 25 μM As<sub>2</sub>O<sub>3</sub> for indicated durations and total cell lysates collected were analyzed by western blotting. (H) Lysates collected in (G) were utilized for immunoprecipitation analyses of EGFR as described earlier. Data presented in (A) and (E) are representative of four and three independent experiments respectively while (B), (D), (F), and (G) represent two independent experiments

We next attempted to determine whether As<sub>2</sub>O<sub>3</sub>-induced changes in SnoN expression occurs via transcriptional regulation. In this regard, we treated cells with As<sub>2</sub>O<sub>3</sub> both in the presence and absence of the transcriptional inhibitor Actinomycin D (ActD). Indeed, ActD dramatically reduced SnoN protein levels in As<sub>2</sub>O<sub>3</sub>-treated HEY cells suggesting that As<sub>2</sub>O<sub>3</sub> induction of SnoN occurs via transcriptional regulation of SnoN (Figure 9D). To determine whether PP2 can also modulate the SnoN mRNA levels upon As<sub>2</sub>O<sub>3</sub> treatment, we performed qPCR analyses in HEY cells co-treated with As<sub>2</sub>O<sub>3</sub> and PP2. Consistent with the protein level changes, As<sub>2</sub>O<sub>3</sub> treatment led to a marked increase in SnoN mRNA levels (~2.8 fold, Figure 9E) which reduced significantly (~40%) in presence of PP2 although treatment with PP2 alone did not alter the SnoN mRNA levels. These results clearly suggest that Src family of kinases might contribute to As<sub>2</sub>O<sub>3</sub>-induced transcriptional induction of SnoN. In order to further validate the role of Src kinase activity, we next utilized another specific Src kinase inhibitor, SU6656. However, as shown in Figure 9F, treatment of HEY cells with SU6656 did not inhibit the As<sub>2</sub>O<sub>3</sub>-induced expression of SnoN protein levels. This difference between the effects of these two Src kinase inhibitors could be attributed to the difference in their specificities. PP2 is a general Src family kinase inhibitor whereas SU6656 inhibits only specific Src family members in comparison and different Src family kinases might be targeted by these two inhibitors leading to discrepancy in responses. Since PP2 treatment altered the As<sub>2</sub>O<sub>3</sub>-induced EGFR activation, we then investigated whether PP2 could also inhibit the interaction of EGFR with its downstream adaptor proteins ShcA and Grb2. Indeed, co-IP of EGFR (Figure 9H) in HEY cells treated with As<sub>2</sub>O<sub>3</sub> or EGF performed in the presence or absence PP2 showed a marked reduction in As<sub>2</sub>O<sub>3</sub>-induced association of EGFR with p66 ShcA and Grb2. In contrast, EGF-induced association of EGFR with Grb2 and ShcA was only subtly reduced (Figure 9H). Collectively, these results suggest that Src kinase activity contributes to As<sub>2</sub>O<sub>3</sub>-mediated EGFR activation and downstream interactions concurrently with SnoN induction.



Inhibition of PI3K signaling modulates the As<sub>2</sub>O<sub>3</sub>-induced SnoN expression and cellular sensitivity:

As shown in Figure 8B, we observed that As<sub>2</sub>O<sub>3</sub> activates AKT at 1 hour post-treatment, prior to SnoN induction at 6 hours. In order to determine whether AKT activation is an upstream event contributing to As<sub>2</sub>O<sub>3</sub>-induced SnoN expression, we utilized inhibitors LY294002 and GDC0941, to target and inhibit the PI3K kinase activity. Co-treatment of HEY cells with 25 μM As<sub>2</sub>O<sub>3</sub> for 18 hours in

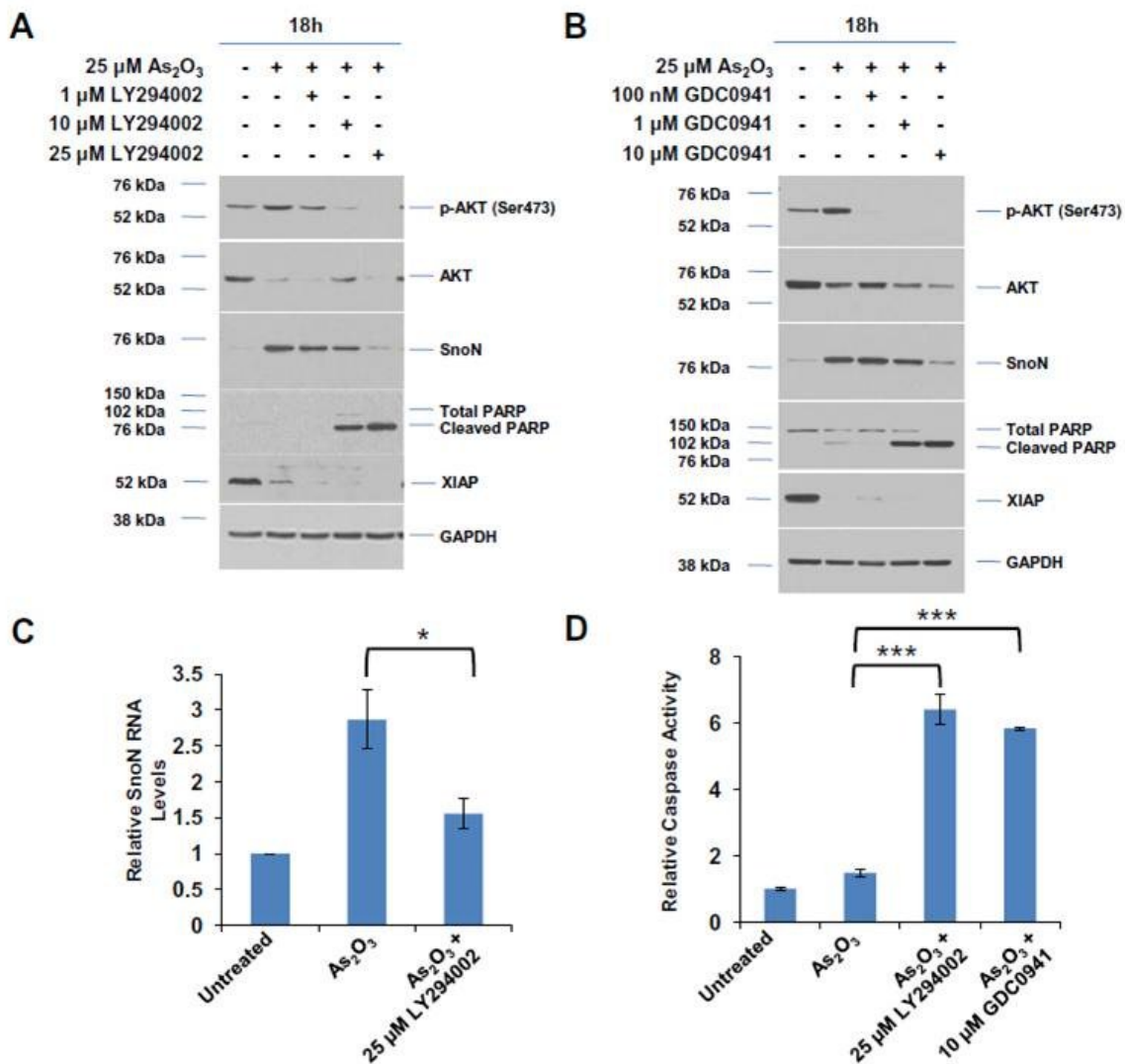


**Figure 10. Inhibition of PI3K-AKT signaling modulates the As<sub>2</sub>O<sub>3</sub>-mediated SnoN induction and cell responses (\*Continued on next page)**



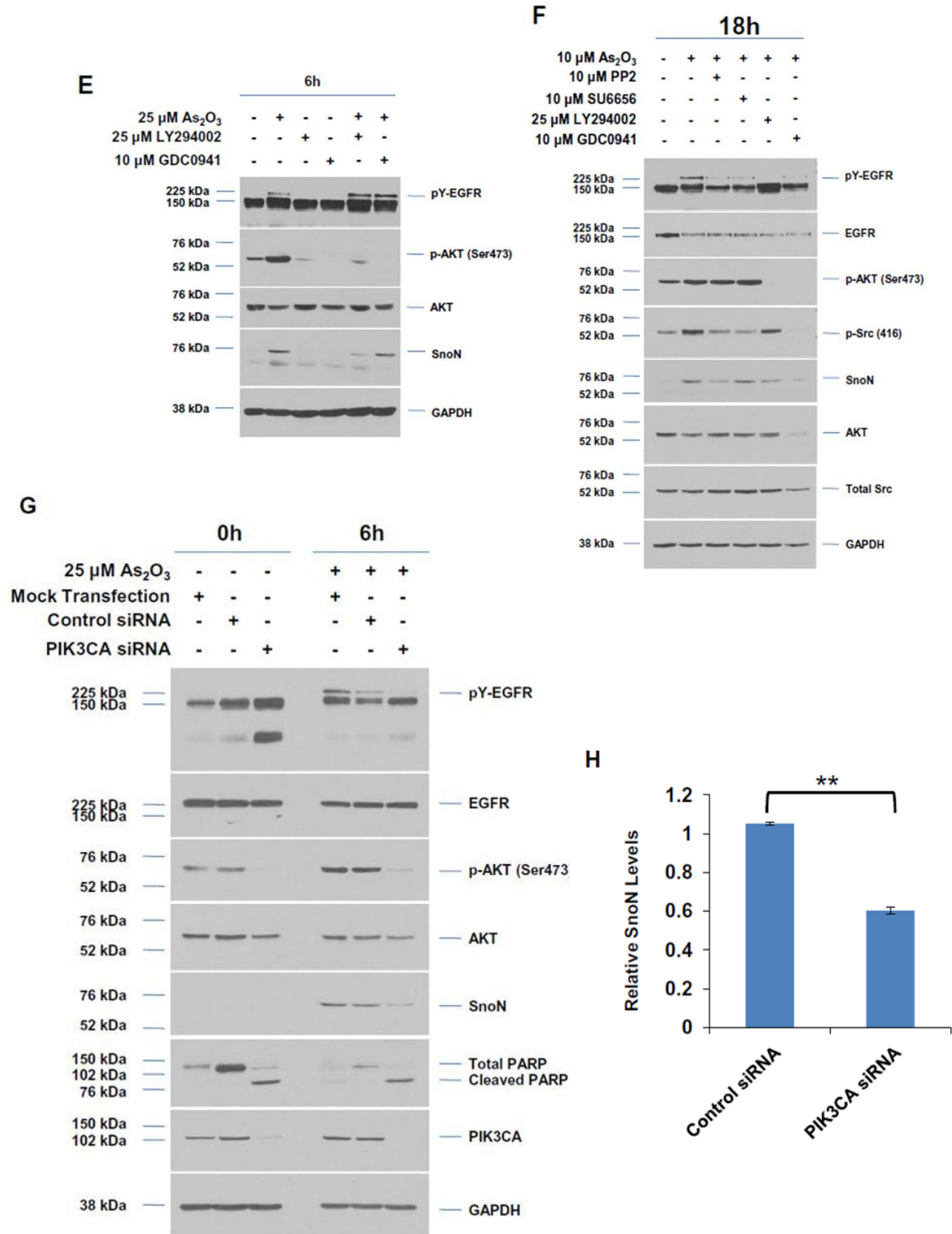


**Figure 10. Inhibition of PI3K-AKT signaling modulates the  $As_2O_3$ -mediated SnoN induction and cell responses (\*Continued on next page)**

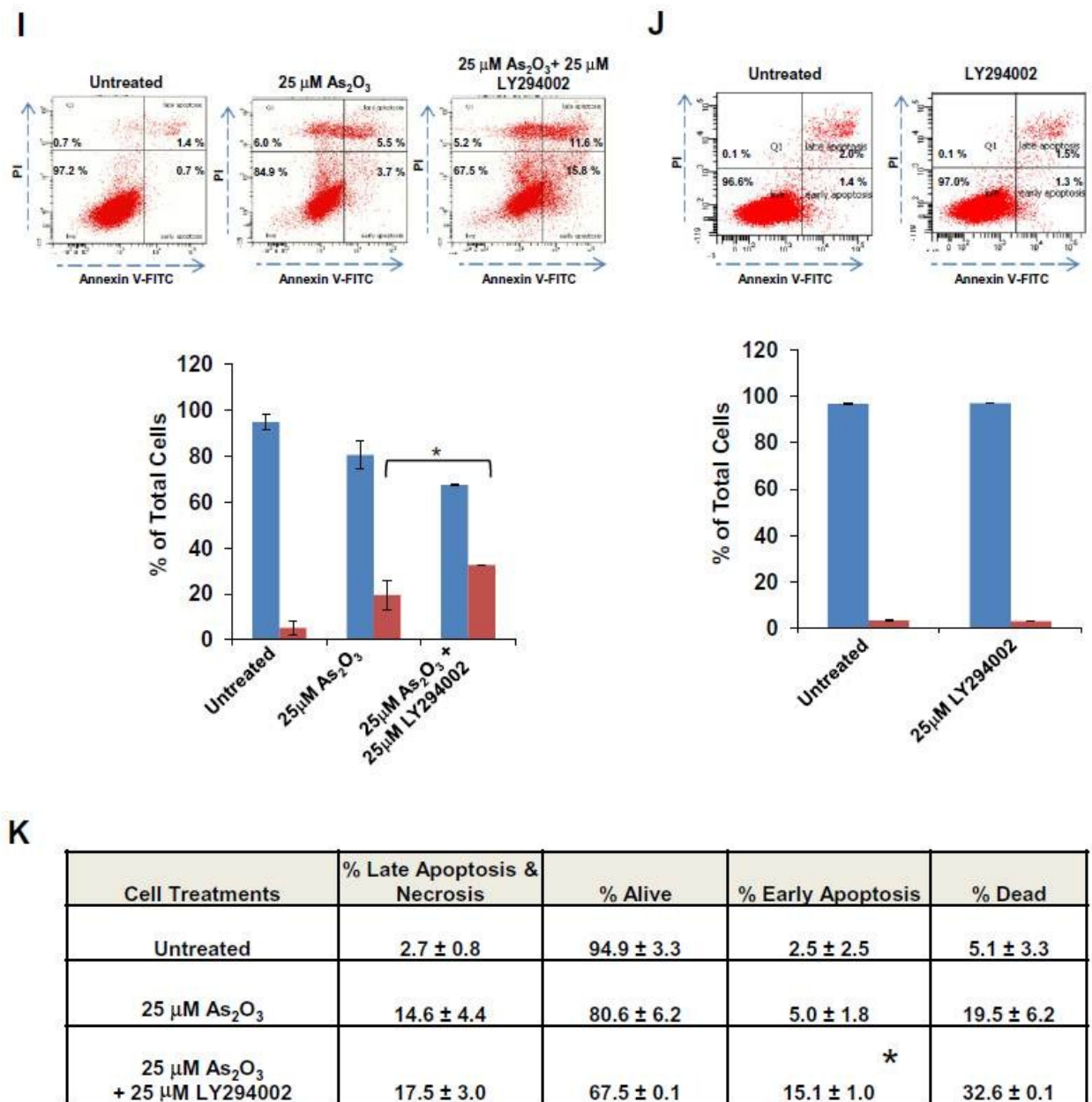


Figure 10. Inhibition of PI3K-AKT signaling modulates the  $\text{As}_2\text{O}_3$ -mediated SnoN induction and cell responses (\*Continued on next page)

**Figure 10. Inhibition of PI3K-AKT signaling modulates the As<sub>2</sub>O<sub>3</sub>-mediated SnoN induction and cell responses**

(A) Cells were treated with 25 μM As<sub>2</sub>O<sub>3</sub> for 18 hours with or without 1 or 10 or 25 μM LY294002. Total cell lysates collected were analyzed via western blotting for indicated antibodies. (B) Cells were treated with 25 μM As<sub>2</sub>O<sub>3</sub> with or without 100 nM or 1 μM or 10 μM GDC0941 for 18 hours and lysates collected were analyzed by western blotting for the indicated antibodies. (C) Cells were treated with 25 μM As<sub>2</sub>O<sub>3</sub> for 18 hours with or without 25 μM LY294002 and total RNA isolated was utilized to perform qPCR analyses to determine SnoN relative mRNA levels. (D) Cells were treated with 25 μM As<sub>2</sub>O<sub>3</sub> for 18 hours both in presence and absence of 25 μM LY294002 or 10 μM GDC0941. Caspase activity levels were measured as described in Chapter 2. (E) Cells were treated with 25 μM As<sub>2</sub>O<sub>3</sub> for 6 hours both in presence and absence of 25 μM LY294002 or 10 μM GDC0941 and lysates collected were analyzed by western blotting. (F) Cells were treated with 10 μM As<sub>2</sub>O<sub>3</sub> with or without 10 μM PP2 or 10 μM SU6656 or 25 μM LY294002 or 10 μM GDC0941 for 18 hours as described above and western analyses were performed on the lysates collected. (G) HEY cells were either mock transfected or transfected with control or PIK3CA siRNA as described in Chapter 2 followed by treatment with 25 μM As<sub>2</sub>O<sub>3</sub> for 6 hours. Lysates collected were analyzed via western blotting for the indicated antibodies. (F) Densitometric analysis was performed on the SnoN protein level changes from (G). (I - J) Apoptosis assay was performed on HEY cells treated with 25 μM As<sub>2</sub>O<sub>3</sub> (I) or 25 μM LY294002 (J) or both (I). (K) Tabular representation of data presented in (I). Data presented in (A), (C), (D) and (F) are representative of three independent experiments while all others represent two independent experiments.

combination with increasing concentrations of LY294002 (1 – 25 μM, Figure 10A) or GDC0941 (1 - 10 μM, Figure 10B) dramatically abolished the As<sub>2</sub>O<sub>3</sub>-mediated induction of SnoN protein concurrently with AKT activation. Similar changes in the SnoN protein in the presence of these inhibitors were observed even with shorter treatment (6 hours, Figure 10E) and lower doses (10 μM, Figure 10F) of As<sub>2</sub>O<sub>3</sub>. To determine whether PI3K inhibitors transcriptionally modulate SnoN mRNA, we performed qPCR analysis after treating HEY cells with As<sub>2</sub>O<sub>3</sub> (18 hours) both in the presence and absence of LY294002; we noted a significant decrease (~50%) in the SnoN transcript levels induced by As<sub>2</sub>O<sub>3</sub> (Figure 10C). Collectively these results indicate that PI3K signaling contributes to transcriptional regulation of As<sub>2</sub>O<sub>3</sub>-mediated induction of SnoN. Additionally, we observed a marked increase in cleaved PARP levels consistent with reduced expression of the anti-apoptotic protein XIAP (Figures 10A and 10B) with increasing concentrations of LY292002 and GDC0941, thus indicating increased apoptosis. In order to validate the increased apoptotic responses, we performed caspase activity assay (Figure 10D) and

Annexin V/PI apoptosis assay (Figure 10I). Indeed, we noted a significant increase in the activity of caspases upon treatment with As<sub>2</sub>O<sub>3</sub> in the presence of both LY294002 and GDC0941 (Figure 10D). Consistently, treatment with As<sub>2</sub>O<sub>3</sub> in the presence of LY294002 resulted in a significant increase in the total apoptotic cell numbers (Figures 10I and 10K) while only LY294002 failed to increase apoptosis (Figure 10J). These results suggest that activation of the PI3K signaling cascade upon As<sub>2</sub>O<sub>3</sub> treatment alters cell survival responses in HEY cells. Since chemical inhibitors might have various non-specific effects, we next reduced the expression of PIK3CA, the catalytic subunit of PI3K by utilizing siRNA followed by 6 hours As<sub>2</sub>O<sub>3</sub> treatment. Similar to the inhibitors, PIK3CA knockdown resulted in a marked reduction in As<sub>2</sub>O<sub>3</sub>-induced SnoN protein with a concurrent increase in cleaved PARP levels (Figure 10G). Furthermore, qPCR analysis demonstrated a significant reduction (~50%) in SnoN mRNA levels in cells transfected with PIK3CA siRNA relative to control siRNA. Together, these results indicate that activation of the PI3K/AKT signaling pathway modulates SnoN expression and cell survival in HEY cells in response to As<sub>2</sub>O<sub>3</sub>.

#### Reduction of EGFR, pp60 c-Src, and MAPK1 alters As<sub>2</sub>O<sub>3</sub>-induced cellular responses:

Since inhibition of Src family kinases results in altered As<sub>2</sub>O<sub>3</sub>-mediated responses, we next attempted to identify the specific Src family member mediating this process. In this regard, we obtained siRNA against pp60c-Src, one of the most studied Src family member to assess its effect on the As<sub>2</sub>O<sub>3</sub>-mediated cellular responses. Mediators of Ras-MAPK signaling play a major role in cancer cell survival and proliferation [214-217]. MAPK1 (p42 ERK1) modulates cancer cell survival and viability upon knockdown. On the other hand, EGFR (as shown in Figure 8B) becomes phosphorylated at tyrosine residues upon stimulation with As<sub>2</sub>O<sub>3</sub>. Therefore, in addition to pp60c-Src siRNA, to determine whether MAPK1 and EGFR reduction would alter the As<sub>2</sub>O<sub>3</sub>-mediated responses in HEY cells we investigated the effect of siRNAs targeting MAPK1 and EGFR. As<sub>2</sub>O<sub>3</sub> treatment (6 and 18 hours) upon transfection with MAPK1 or EGFR siRNA resulted in a dramatic reduction in As<sub>2</sub>O<sub>3</sub>-mediated phosphorylation of EGFR (Figure 11A) although there was no change in SnoN protein. Additionally, we noted markedly decreased

cleaved PARP levels with increased expression of anti-apoptotic XIAP relative to cells transfected with control siRNA; these results suggest that MAPK1 and EGFR knockdown modulates the cellular sensitivity to As<sub>2</sub>O<sub>3</sub>. However in contrast, pp60c-Src knockdown led to an increase in cleaved PARP and reduction in XIAP levels (Figure 11A). Although PP2 treatment resulted in inhibition of As<sub>2</sub>O<sub>3</sub>-mediated EGFR phosphorylation and SnoN levels (Figure 9a and 9b), pp60c-Src knockdown did not alter the EGFR phosphorylation and SnoN induction. This validated the effects of SU6656, a specific Src kinase

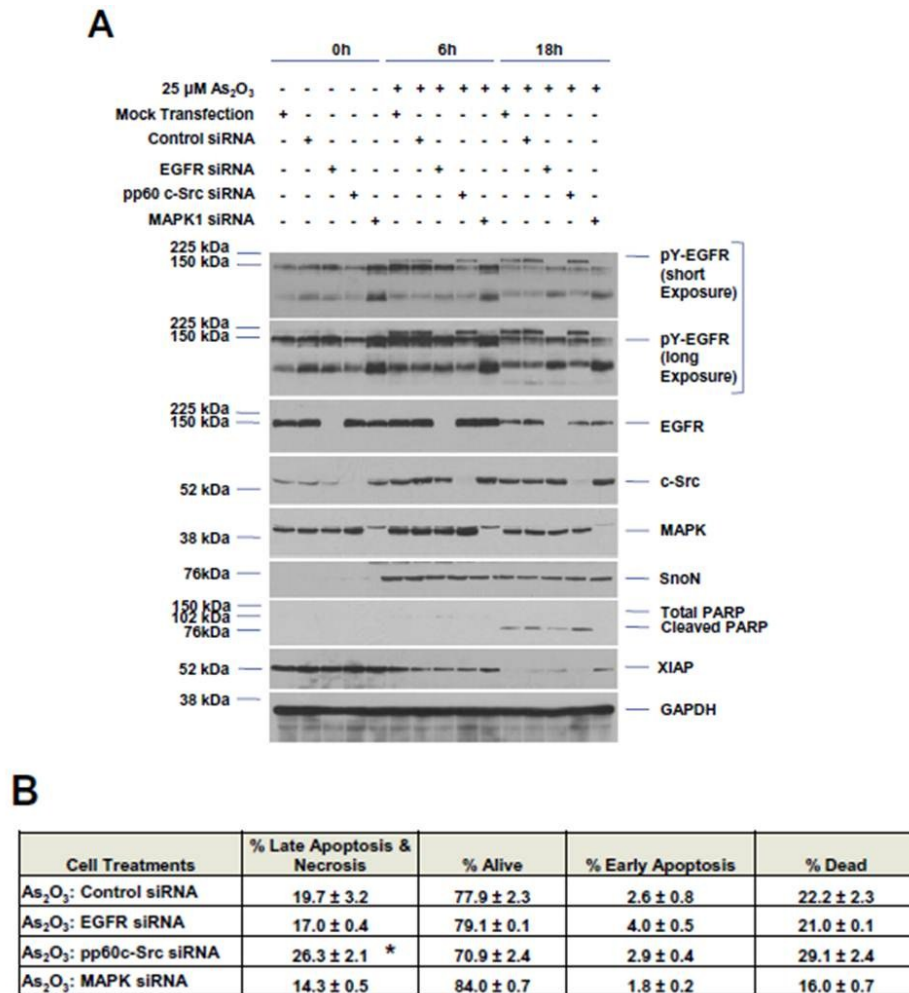
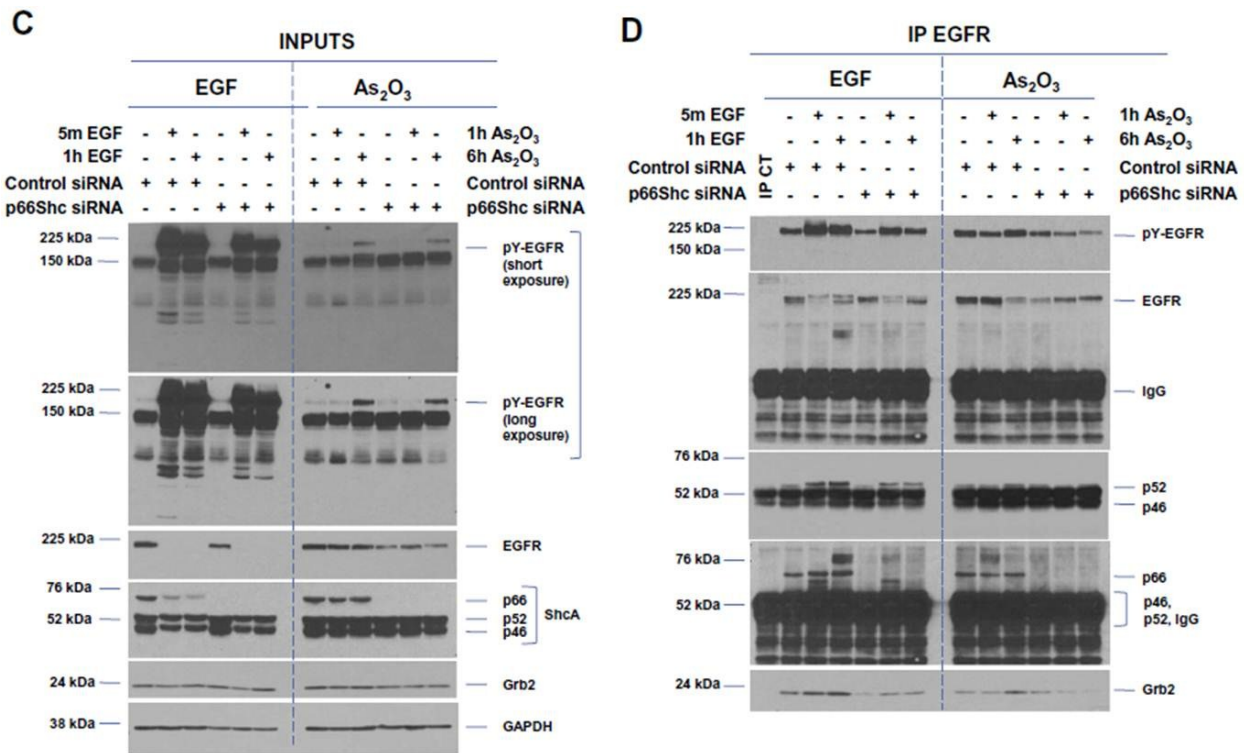


Figure 11. siRNA mediated reduction of EGFR, pp60 c-Src, and MAPK1 modulates the As<sub>2</sub>O<sub>3</sub>-induced cellular responses (\*Continued on next page)



**Figure 11 (Continued). siRNA mediated reduction of EGFR, pp60 c-Src, and MAPK1 modulates the As<sub>2</sub>O<sub>3</sub>-induced cellular responses**

(A) HEY cells were either mock transfected or transfected with control siRNA or EGFR or pp60c-Src or MAPK1 siRNA as described in Chapter 2 followed by treatment with 25  $\mu$ M As<sub>2</sub>O<sub>3</sub> for 6 and 18 hours. Lysates collected were analyzed via western blotting for the indicated antibodies. (B) Cells were transfected with control or EGFR or pp60c-Src or MAPK1 siRNA followed by treatment with 25  $\mu$ M As<sub>2</sub>O<sub>3</sub> for 18 hours apoptosis assay was performed and data is presented in tabular form. (C) Cells transfected with control or p66ShcA siRNA were treated with 100 ng/ml EGF or 25  $\mu$ M As<sub>2</sub>O<sub>3</sub> for indicated durations and total cell lysates collected were analyzed via western analyses. (D) Lysates collected in (C) were utilized to perform immunoprecipitation of EGFR as described earlier. Data presented in (A), (B), (C) and (D) are representative of two independent experiments.

inhibitor and indicates that As<sub>2</sub>O<sub>3</sub>-induced changes in SnoN expression and EGFR activation may not be mediated by pp60c-Src but possibly other members of the Src family of kinases; further investigation is required to identify the specific members of Src family involved in this process. We next validated the effects of these siRNAs on As<sub>2</sub>O<sub>3</sub>-mediated cell death responses by performing apoptosis assays (Figure 11B). Collectively, these results indicate that knockdown of EGFR, MAPK1, and pp60c-Src expression

modulates cell viability of HEY cells via regulation of the anti-apoptotic protein XIAP upon As<sub>2</sub>O<sub>3</sub> stimulation; this process appeared to be independent of SnoN levels. As shown in Figures 8F and 8G, As<sub>2</sub>O<sub>3</sub> stimulation results in phosphorylation of p66 ShcA and increases the association between EGFR and Grb2. Previous studies implicate the p66 isoform of ShcA in cell death while p46 and p52 are associated with cell survival [218-220]. In this regard, we next tried to determine whether p66 ShcA is involved in mediating the As<sub>2</sub>O<sub>3</sub>-induced increase in EGFR-Grb2 interaction. We transfected HEY cells with siRNA that specifically targets the CH2 domain of p66 ShcA (a domain that is absent in the p46 and p52 isoforms) and treated them with As<sub>2</sub>O<sub>3</sub> for 1 and 6 hours. Interestingly, co-immunoprecipitation of EGFR performed in cells with p66 ShcA knockdown (with As<sub>2</sub>O<sub>3</sub>) showed that the association of EGFR with Grb2 was markedly abrogated when compared to control siRNA treatment. Together these results suggest that EGFR and Grb2 interaction stimulated by As<sub>2</sub>O<sub>3</sub> requires p66 ShcA.

## **Discussion**

As described in Chapter 1, SnoN/SkiL a negative transcriptional regulator of TGF- $\beta$  signaling, is amplified at 3q26.2 locus and plays a very important role in ovarian cancer development and pathogenesis [9]. Our previous studies show that As<sub>2</sub>O<sub>3</sub> treatment in HEY (serous epithelial ovarian carcinoma) cells results in a marked induction of SnoN which mediates a beclin-1 independent cytoprotective autophagy that counters the cytotoxic effects of As<sub>2</sub>O<sub>3</sub> [1]. However, the mechanism by which As<sub>2</sub>O<sub>3</sub> induces SnoN expression and its cellular responses was unclear. Herein, our studies presented in this Chapter demonstrate that the As<sub>2</sub>O<sub>3</sub>-induced SnoN expression and cellular response in ovarian cancer cells is mediated by activation of the PI3K/AKT signaling pathway.

Previous studies show that the EGF receptor and its downstream signaling pathways including those involving PI3K/AKT, MAPK, and Src are highly altered in specific cancers including ovarian cancers; they play prominent roles in cancer cell survival and proliferation [9, 70, 189, 190, 198-201, 221, 222].



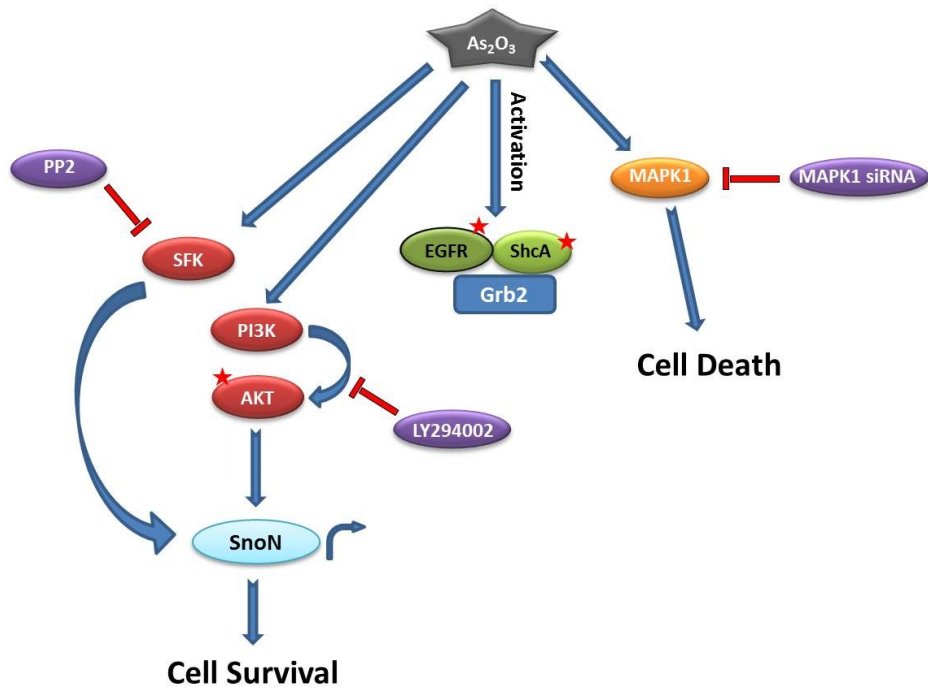


**Figure 12. Schematic representation of the mechanism of SnoN modulation by  $As_2O_3$**

$As_2O_3$  activates EGFR and modulates its interactions with ShcA and Grb2. It also activates PI3K/AKT pathway that mediates the  $As_2O_3$ -mediated SnoN induction and cell survival responses that are blocked by LY294002. MAPK1 and EGFR knockdown lead to decreased sensitivity to  $As_2O_3$  in a SnoN independent manner. (\*Model created by Madhav Karthik Kodigepalli)

Interestingly, these pathways mediate  $As_2O_3$ -induced cellular responses [205, 206, 209]. We demonstrate in this Chapter that  $As_2O_3$  treatment, similar to EGF stimulation, leads to tyrosine phosphorylation of EGFR and further modulates its interaction with ShcA and Grb2 (Figure 8). In addition,  $As_2O_3$  leads to a marked increase in SnoN levels (similar to previous studies [1]) and increases apoptotic responses as evidenced by increased cleaved PARP, reduced BCL-XL, and reduced XIAP levels. Interestingly, the kinetics of  $As_2O_3$ -induced activation of EGFR was slower in comparison to EGF stimulation implicating different mechanisms involved in activation of EGFR upon treatment with EGF and  $As_2O_3$ .  $As_2O_3$  also rapidly activates AKT (by 1 hour) and Src (by 6 hours) prior to the activation of



EGFR (peaking at 18 hours) potentially implicating the PI3K/AKT and Src pathways in As<sub>2</sub>O<sub>3</sub>-induced EGFR activation and cellular responses.

Src activation upon As<sub>2</sub>O<sub>3</sub> treatment appeared to be biphasic, peaking first at 6 hours and then again at 18 hours suggesting a dual function in mediating the As<sub>2</sub>O<sub>3</sub> response. Since Src mediates both cytoprotective and cytotoxic responses [223] depending on the specific Src family member involved [224], we hypothesize that Src activation at the early stages of As<sub>2</sub>O<sub>3</sub> treatment (1 to 6 hours) might mediate the cell survival response while promoting the cell death response at later time points (18 to 30 hours). Indeed, inhibition of Src family kinase activity via PP2 (a general Src family kinase inhibitor) dramatically reduces As<sub>2</sub>O<sub>3</sub>-mediated EGFR activation and induction of SnoN mRNA and protein supporting the role of Src signaling in this process. This observation is consistent with previous studies showing the role of Src in mediating the As<sub>2</sub>O<sub>3</sub>-induced activation of EGFR [209]. However, we did not observe the same effect upon treatment with SU6656, a specific Src kinase inhibitor. This difference in responses could potentially be due to the possibility of PP2 and SU6656 targeting different members of the Src family. Although reduction of pp60c-Src altered the cellular sensitivity to As<sub>2</sub>O<sub>3</sub>, it did not affect SnoN expression suggesting that further studies are needed to identify the specific Src family member involved in this process. Similarly, although treatment with U0126, a drug inhibiting MAP kinase activity did not have any effect on the As<sub>2</sub>O<sub>3</sub> responses, MAPK1, and EGFR siRNAs altered the cell sensitivity to As<sub>2</sub>O<sub>3</sub>. These results implicate EGFR/MAPK pathway to mediate the cellular responses of As<sub>2</sub>O<sub>3</sub> in a SnoN-independent mechanism.

Although EGFR is activated upon As<sub>2</sub>O<sub>3</sub> treatment, the exact mechanism by which As<sub>2</sub>O<sub>3</sub> leads to EGFR activation is unknown and needs to be investigated further. We performed phosphatase activity assays (data not shown) to determine whether reduced phosphatase activity upon As<sub>2</sub>O<sub>3</sub> treatment resulted in increased phosphorylation of EGFR. However, phosphatase activity levels were not altered in presence of As<sub>2</sub>O<sub>3</sub>. Slower kinetics of As<sub>2</sub>O<sub>3</sub>-induced EGFR activation and its interaction with ShcA and Grb2 compared to those with EGF stimulation suggests an indirect mechanism of activation that might involve

other signaling mediators. We propose that the EGFR activation upon As<sub>2</sub>O<sub>3</sub> treatment could be mediated by Src kinase activity. Indeed, previous studies report that As<sub>2</sub>O<sub>3</sub> stimulation leads to EGFR phosphorylation at tyrosines 845 and 1173 which are known targets of Src kinase activity [209]. Few studies also report the role of reactive oxygen species (ROS) in regulating the Src kinase activity [225] and our previous study suggests that As<sub>2</sub>O<sub>3</sub>-induced responses including changes in SnoN expression are also mediated by increased production of ROS [1]. Collectively, these results might suggest a role for Src kinase activity in activating EGFR upon As<sub>2</sub>O<sub>3</sub> treatment in a ROS-dependent manner.

Studies indicate that the genes localized to the 3q26 region may cross-regulate each other as evidenced by EVI1 (3q26.2) regulating the expression of SnoN (3q26.2) [33], PI3K (PIK3CA, 3q26.3) [226, 227], and claudin-1 (3q28) [32]; and PI3K regulating SnoN expression [9]. Interestingly, as shown in Figure 8B, we noted a rapid activation of AKT (at 1 hour) prior to SnoN induction (6 hours) in response to As<sub>2</sub>O<sub>3</sub> suggesting a role of PI3K/AKT pathway activation in mediating the SnoN changes. In this regard, we tried to determine whether SnoN expression is regulated by the PI3K pathway. Indeed, inhibition of the PI3K/AKT pathway via LY294002 and GDC0941 also resulted in reduction of As<sub>2</sub>O<sub>3</sub>-induced SnoN expression. Additionally, PI3K inhibition altered the cellular responses of HEY cells to As<sub>2</sub>O<sub>3</sub> as evidenced by increased percentage of apoptotic cells and decreased levels of anti-apoptotic markers. We further validated these results via siRNA mediated knockdown of PIK3CA which had similar effect on the cell death responses. These results collectively demonstrate that the PI3K signaling regulates SnoN expression and facilitates a cytoprotective pathway which in turn antagonizes the cytotoxic effect of As<sub>2</sub>O<sub>3</sub> in HEY cells. As stated above, PIK3CA gene (at 3q26.3) is amplified in ovarian cancers and is localized at a close proximity to SnoN/SkiL (3q26.2). Therefore, our findings may also suggest a co-operative oncogenicity between SnoN and PIK3CA [9] leading to increased cell survival in ovarian cancer cells upon treatment with chemotherapeutics. Collectively, our studies indicate that PI3K/AKT and Src pathways modulate the As<sub>2</sub>O<sub>3</sub>-induced SnoN expression and cell survival responses in

HEY ovarian carcinoma cells. These findings may aid in the development of novel combinatorial strategies targeting SnoN and PI3K (or Src) pathways in the treatment of ovarian cancer.

### **Acknowledgements**

All the studies presented in this chapter were performed with equal contribution of Punashi S. Dutta as a primary co-author. Experiments for the data presented in Figure 8D and Figure 9D and phosphatase activity assay were performed by Dr. Meera Nanjundan. Flow cytometry for Annexin V/PI apoptosis assay was carried out with assistance of Dr. Karoly Szekeres at the College of Medicine, University of South Florida.

## Chapter 4

### **Phospholipid Scramblase 1, an IFN-Regulated Gene Located at 3q23, is Regulated by SnoN/SkiL in Ovarian Cancer Cells**

#### **Introduction**

Amplification of the chromosomal 3q26 region is a commonly observed genomic aberration in various epithelial cancers including ovarian cancers [9-12, 28-30]. As shown in Figure 1 (Chapter 1, page 3), this region harbors various oncogenes including MECOM [10], SnoN [9, 28], PKC $\iota$  [31] (at 3q26.2), and PIK3CA [11] (at 3q26.3) that are highly amplified at the DNA copy number level in ovarian cancers. Previous studies including ours suggest that the genes located at the 3q26 locus can cross regulate each other [32, 33, 177]. EVI1 (ecotropic viral integration site 1), located at 3q26.2, binds to the SnoN promoter region and regulates SnoN expression [33]. Furthermore, our laboratory has shown that EVI1 regulates claudin-1 mRNA and protein levels; CLDN-1 is located at 3q28 [32]. Our recent studies (presented in Chapter 3) also show that PIK3CA, the catalytic subunit of PI3K located at 3q26.3, regulates SnoN expression in ovarian cancer cells treated with arsenic trioxide (As $_2$ O $_3$ ) [9, 177].

SnoN/SkiL is a negative transcriptional regulator of TGF $\beta$  signaling which binds to SMAD2/3 and SMAD4 complex to repress the transcription of TGF $\beta$  target genes [75-77, 85, 86]. SnoN is amplified and overexpressed in various cancers including ovarian [9], lung [80], breast [79], esophageal [76], and colorectal cancers [82]. Previous aCGH (array comparative genomic hybridization) studies performed in 235 ovarian cancer patient samples indicated that DNA copy number levels of SnoN and mRNA expression are elevated in ovarian cancers [9]. Our research group demonstrated that treatment of HEY ovarian carcinoma cells with As $_2$ O $_3$  results in a dramatic induction in expression of SnoN [1]. Further, SnoN was found to modulate chemotherapeutic responses in HEY cells by mediating cytoprotective

autophagy in response to As<sub>2</sub>O<sub>3</sub> [1]. As presented in Chapter 3, we identified that SnoN expression is modulated in response to As<sub>2</sub>O<sub>3</sub> is via activation of the PI3K/AKT signaling pathway [177].

As described in Chapter 1, PLSCR1 (phospholipid scramblase 1, 318 aa), a type-II transmembrane protein located at chromosome 3q23 belongs to the family of phospholipid scramblases. PLSCR1 was previously implicated in externalization of phosphatidylserine (PS) [34], a phenomenon aiding in disruption of membrane phospholipid asymmetry during cellular events such as blood coagulation and apoptosis. However, recent evidence indicates that TMEM16F and Xkr8 to be responsible for the PS externalization during blood coagulation and apoptosis, respectively [121, 123, 125, 132]. As described in Chapter 1, PLSCR1 is involved in various signaling pathways [19, 42, 133, 144, 153, 228]. PLSCR1 is activated by c-Src upon EGF stimulation [144]. It is also phosphorylated by c-Abl upon treatment with cisplatin [18]. Additionally it also interacts with various proteins of significant signaling functions suggesting a potential role of PLSCR1 in signaling pathways. PLSCR1 interacts with EGF receptor and Shc-A upon stimulation with EGF [19]. Furthermore, PLSCR1 interacts with RELT (receptors expressed in lymphoid tissues) family members [228], c-Abl [18], extracellular matrix protein 1 (ECM1) [155], c-Myc target Onzin [154], and the  $\beta$ -secretase cleaving enzyme (BACE) [133]. Collectively, all these findings indicate a diverse role of PLSCR1 in various signaling processes. As shown in Table 3 (Chapter 1), PLSCR1 expression is upregulated by various stimuli including cytokines, growth factors, and differentiation inducing agents. For instance, treatment with epidermal growth factor (EGF) [19], all-trans retinoic acid (ATRA) [17, 40], granulocyte colony stimulation factor (G-CSF) [157], stem cell factor (SCF) [157] results in induction of PLSCR1 in specific cell types. Additionally, treatment with IFNs, cytokines with antiviral function, dramatically induces the expression of PLSCR1 in specific cell types [38, 39]. In fact, PLSCR1 is one of the most induced interferon stimulated genes (ISG) [38]. Later studies demonstrated that IFN transcriptionally regulates PLSCR1 expression which requires the ISRE element present in the untranslated exon 1 of PLSCR1 [39]. IFN-mediated induction of PLSCR1 occurs by activation of PKC $\delta$ , JNK, and STAT1 [145]. Interestingly, IFN treatment leads to nuclear localization of PLSCR1 in specific cell lines [24]. Although, PLSCR1 expression is induced by various

factors, the exact mechanisms by which it is transcriptionally regulated remains unclear. Recent studies identify the Snail EMT regulator as a direct transcriptional regulator of PLSCR1 mRNA which is the only published evidence of direct transcriptional regulation of PLSCR1 [146].

Recent reports suggest that PLSCR1 plays an important role in cancer development. In colorectal cancer patient specimens, PLSCR1 expression was highly elevated [22] relative to normal colorectal mucosa and its inhibition via siRNA or N-terminal targeted antibodies markedly reduced cancer cell proliferation and tumorigenicity implicating PLSCR1 in a tumor promoting function [20, 21]. On the other hand, mouse xenograft studies by Silverman and colleagues using PLSCR1 overexpressing HEY1B ovarian cancer cells suggests a tumor suppressive role for PLSCR1 *in vivo* [15] which was absent when studied under *in vitro* conditions [15]. Collectively, these studies implicate potential role of PLSCR1 in cancer development and progression. However, the role of PLSCR1 in ovarian cancer development and in chemotherapeutic responses remains uninvestigated. In addition, the mechanisms and mediators involved in transcriptional regulation of PLSCR1 are unclear. As described above, evidence suggests that the oncogenes located at/in proximity of 3q26 locus (EVII, SnoN, PIK3CA, etc.) can cross regulate each other via cooperative oncogenicity. Since PLSCR1 is located at 3q23, proximal to 3q26 locus, we hypothesize that SnoN/SkiL, located at 3q26.2 can regulate the expression of PLSCR1 in ovarian cancers. Furthermore, we hypothesize that PLSCR1 DNA copy number and expression is altered in ovarian cancers relative to normal ovarian cells. In this regard, our goal was to determine whether PLSCR1 DNA copy number and RNA/protein expression is altered in ovarian cancers with a pattern similar to SnoN; and to identify whether PLSCR1 is transcriptionally regulated by SnoN/SkiL in ovarian cancer cells. Herein, indeed our bioinformatic analyses studies indicate that PLSCR1 DNA copy numbers and mRNA levels are elevated in ovarian cancer patient samples and highly correlate with those of SnoN/SkiL. Furthermore, via qPCR and luciferase promoter based assays, we demonstrate that SnoN transcriptionally regulates PLSCR1 expression. Finally, our studies indicate that PLSCR1 knockdown, similar to SnoN knockdown results as previously reported, sensitizes the ovarian cancer cells to treatment with As<sub>2</sub>O<sub>3</sub>.

Collectively, our studies show that PLSCR1, transcriptionally regulated by SnoN, might potentially plays an important role in ovarian cancer development and chemotherapeutic responses.

## Results

Elevated PLSCR1 DNA copy number and mRNA expression in ovarian cancer:

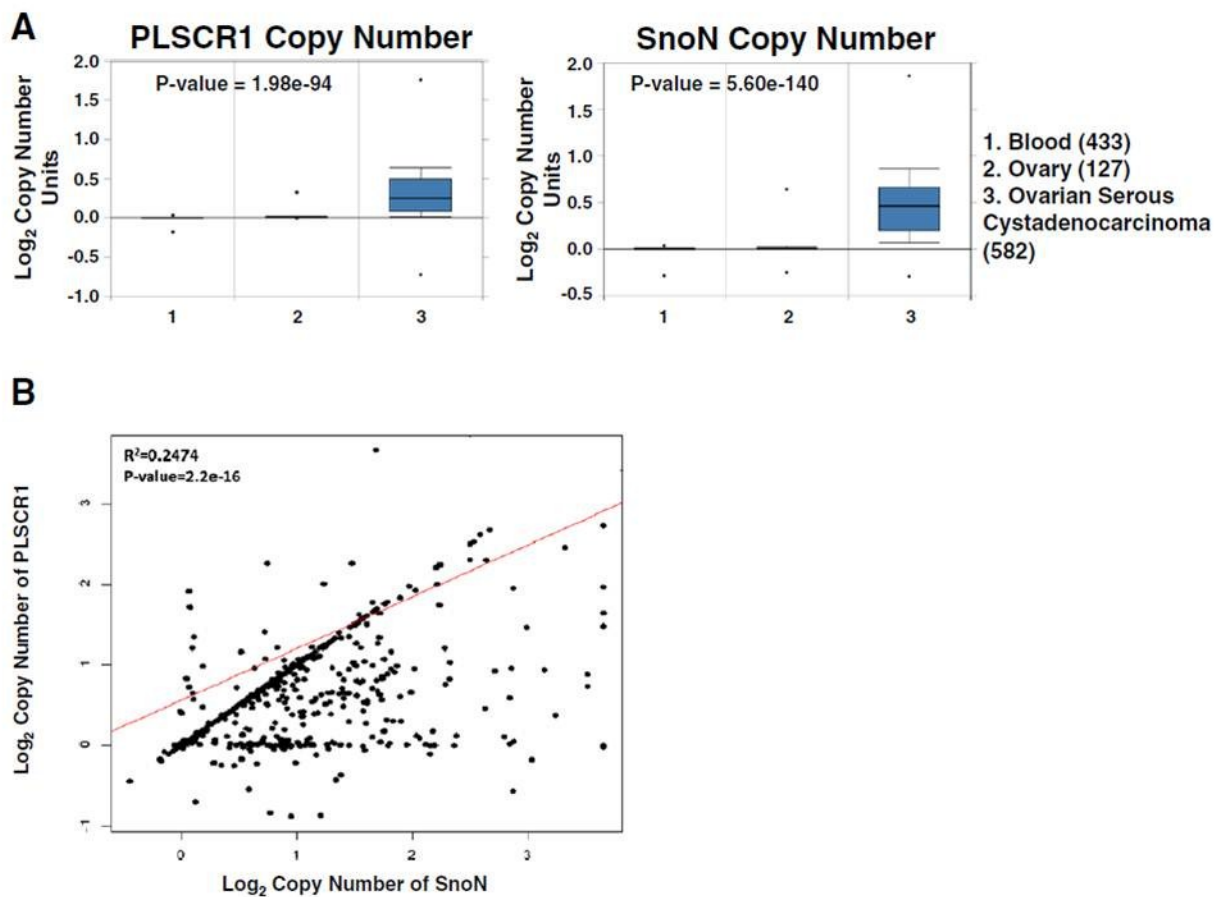
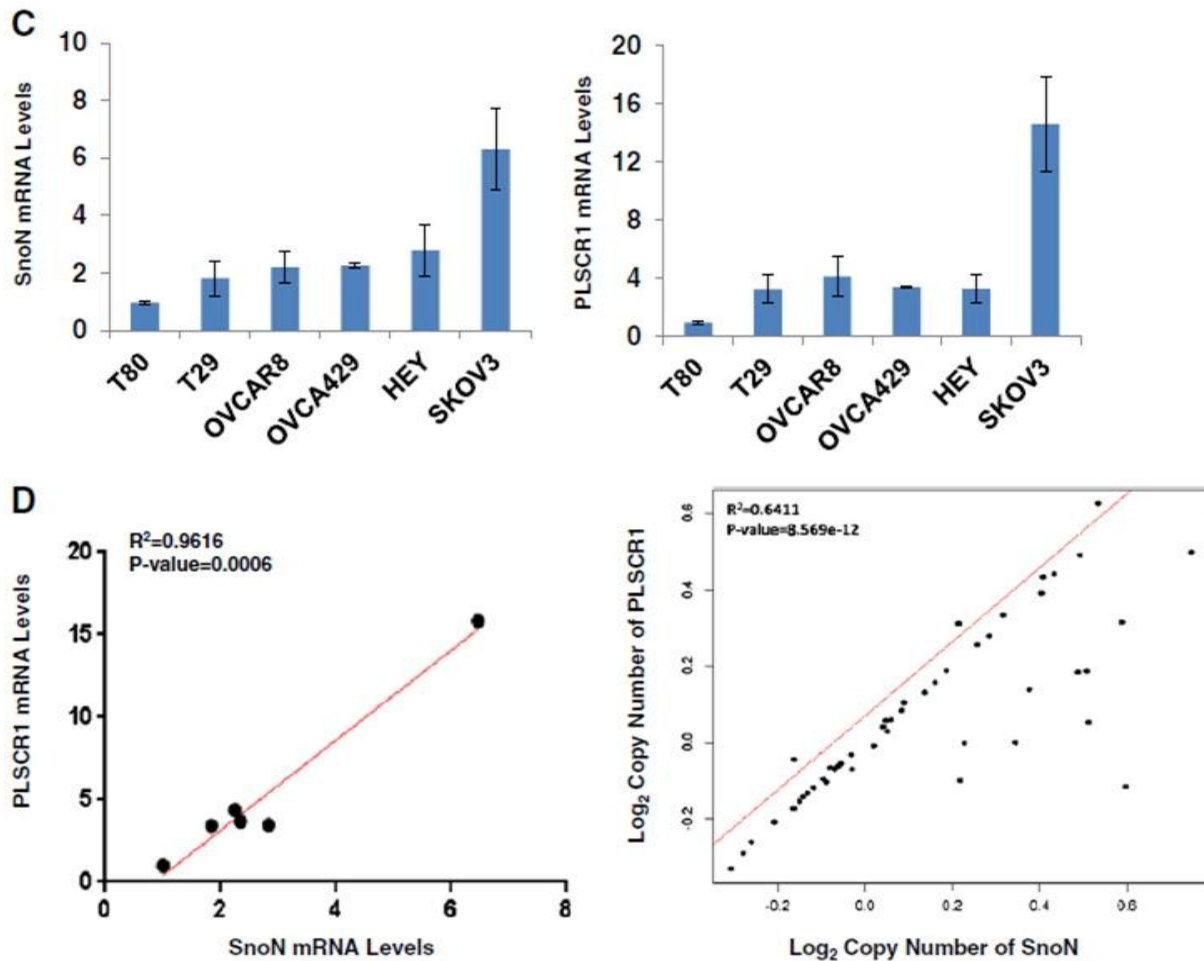


**Figure 13. Correlation between DNA copy number and mRNA alterations of PLSCR1 and SnoN in ovarian cancers (\*Continued on next page)**

Since PLSCR1 is located at 3q23, near the 3q26 region is well known to be amplified in ovarian cancers, we assessed whether its DNA copy number and mRNA/protein expression was also altered in ovarian cancers. In this regard, we utilized bioinformatic programs to analyze the TCGA (The Cancer Genome Atlas) ovarian cancer dataset (<https://tcga-data.nci.nih.gov/tcga/>). As shown in Figure 13A, using Oncomine (<http://www.oncomine.org/>) [229], we demonstrated that the PLSCR1 DNA copy number



levels, similar to SnoN, were elevated in ovarian cancer patients (607/1168). Using cBioPortal

**Figure 13. Correlation between DNA copy number and mRNA alterations of PLSCR1 and SnoN in ovarian cancers (\*Continued on next page)**



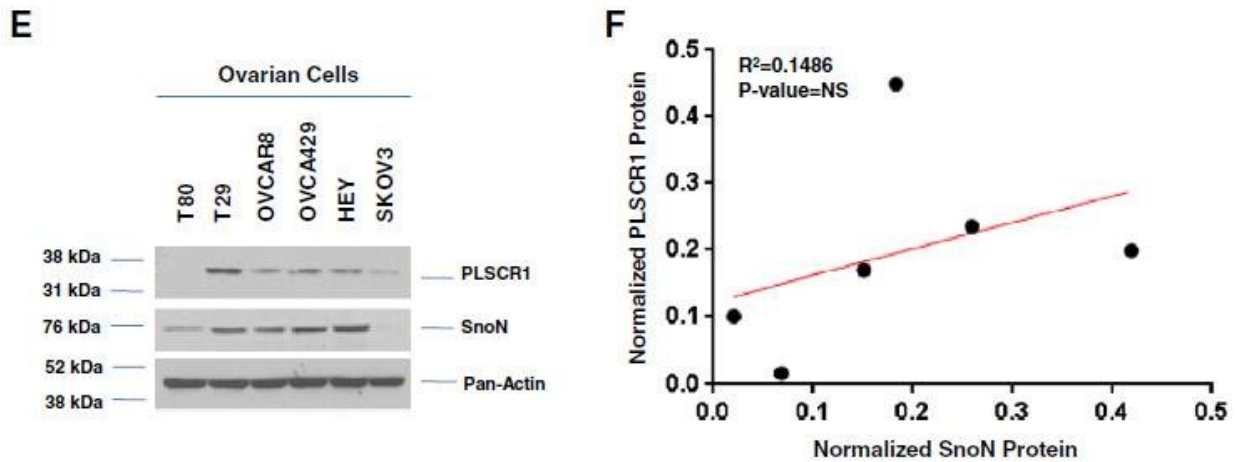


**Figure 13 (Continued). Correlation between DNA copy number and mRNA alterations of PLSCR1 and SnoN in ovarian cancers**

(A) SnoN and PLSCR1 DNA copy number levels were determined in TCGA ovarian serous cystadenocarcinoma dataset via OncoPrint bioinformatic analyses. (B) Correlation of SnoN and PLSCR1 DNA copy number alterations in ovarian cancer patients was analyzed by performing linear regression analyses via R (R-Project). (C) Total RNA was isolated from the normal ovarian (T80 and T29) and ovarian cancer (OVCAR8, OVCA429, HEY and SKOV3) cell lines; relative PLSCR1 (Left panel) and SnoN mRNA levels (Right panel) were determined via quantitative real time PCR as described in chapter 2. (D) Linear regression analyses were performed on the PLSCR1 and SnoN mRNA (Left panel) and DNA copy number levels (Right panel) in the ovarian cancer cell lines. (E) Total lysates were harvested from the cell lines mentioned in (C) and western blotting was performed for the indicated antibodies as described in chapter 2. (F) Linear regression analyses performed on PLSCR1 and SnoN protein levels as mentioned above. Data presented in (C) and (E) is representative of two independent experiments.

(<http://www.cbioportal.org/public-portal/>) [230, 231] and we determined that PLSCR1 and SnoN were amplified in ~13% and ~31% of the patients, respectively. We next determined whether PLSCR1 and SnoN are co-amplified and noted that 70 of the 570 patients (~12%) had amplifications in both the genes. Since SnoN mRNA transcripts are overexpressed in ovarian cancers [9], we next tried to identify whether PLSCR1 mRNA expression also is altered in ovarian cancers. qPCR analyses in normal ovarian and ovarian cancer cell lines indicated that PLSCR1 mRNA levels were elevated in ovarian cancer cells compared to normal immortalized (LTA<sub>g</sub>/hTERT) ovarian surface epithelial (T80) cells (Figure 13C).

### Altered PLSCR1 DNA copy number and mRNA expression correlate with SnoN in ovarian cancers:

Linear regression analyses using R program (<http://www.R-project.org/>) of copy number alterations for PLSCR1 and SnoN demonstrated that most patients with PLSCR1 amplification also had amplified SnoN while only 33% of patients with SnoN amplification had amplification of the PLSCR1 gene ( $R^2 = 0.2474$ ) (Figure 13B). Similarly, DNA copy number variations of both the genes were also correlated in ovarian cancer cell lines (Figure 13D, Right panel). Furthermore, similar to DNA copy number changes, linear regression analyses also indicated that the changes in PLSCR1 mRNA levels are highly correlated with the SnoN mRNA changes (Figure 13D, Left panel). In contrast, western analyses did not show significant correlation between SnoN and PLSCR1 protein level expression in these cell lines (Figure 13E and 13F). Together, these results indicate that the PLSCR1 DNA copy number and mRNA levels are elevated in ovarian cancer and these alterations highly correlate with that of SnoN suggesting a potential synergistic function of these two genes in ovarian cancer development and responses to chemotherapeutics. Furthermore, the discordance in the SnoN and PLSCR1 protein expression suggests differential mechanisms of protein level regulation involved for SnoN and PLSCR1.

### SnoN and TGF $\beta$ transcriptionally regulate the expression of PLSCR1:

Since SnoN and PLSCR1 are located in close proximity to each other (at 3q26.2 and 3q23 respectively) and their DNA copy number level changes are highly correlated in ovarian cancers, we next hypothesized that SnoN regulates the expression of PLSCR1. To address this question, we reduced the expression of SnoN using siRNA in HEY ovarian carcinoma cells (~95% at protein level) and quantified PLSCR1 mRNA levels. Indeed SnoN knockdown significantly reduced (~35%) PLSCR1 mRNA levels (Figure 14A) suggesting that SnoN regulates PLSCR1 transcriptionally. To provide additional evidence of the transcriptional regulation of PLSCR1 by SnoN, we performed luciferase-based PLSCR1 promoter activity assays in T80 cells using pGL3 vector containing genomic PLSCR1 (details described in Chapter 2). SnoN knockdown resulted in a significant reduction of promoter activity of PLSCR1 providing

supporting evidence that SnoN transcriptionally regulates PLSCR1 mRNA levels (Figure 14B). Since SnoN is a negative regulator of TGF $\beta$  signaling [76, 77], we measured the PLSCR1 promoter activity in T80 cells which were treated with TGF $\beta$  (50 pM) and noted that similar to SnoN knockdown, TGF $\beta$  stimulation also resulted in significant reduction of PLSCR1 promoter activity (Figure 14C).

Furthermore, TGF $\beta$  stimulation also significantly reduced PLSCR1 mRNA levels by 18 hours post-treatment after an initial increase at 3 hours, while SnoN mRNA levels increased by 3 hours (as previously reported [9]) and 18 hours (Figure 14D). These results suggest divergent mechanism of regulation of PLSCR1 and SnoN by TGF $\beta$  stimulation. Since TGF $\beta$  stimulation reduced the expression of

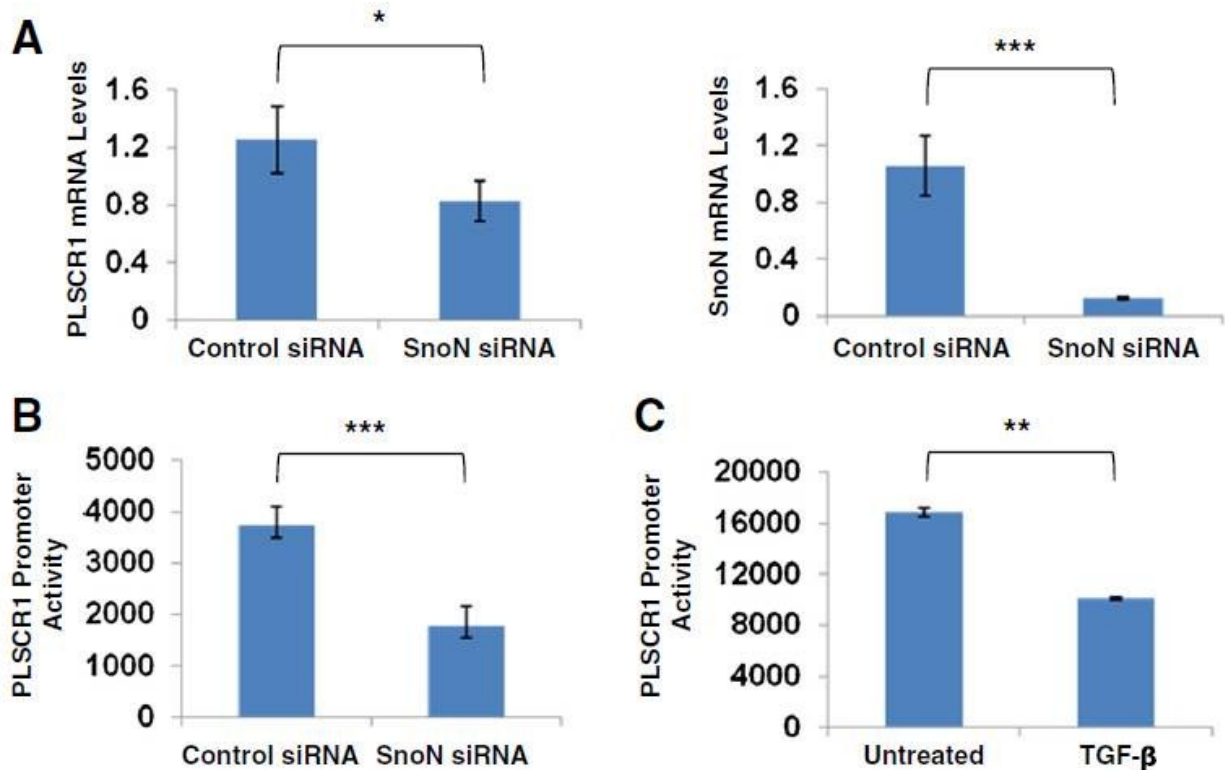
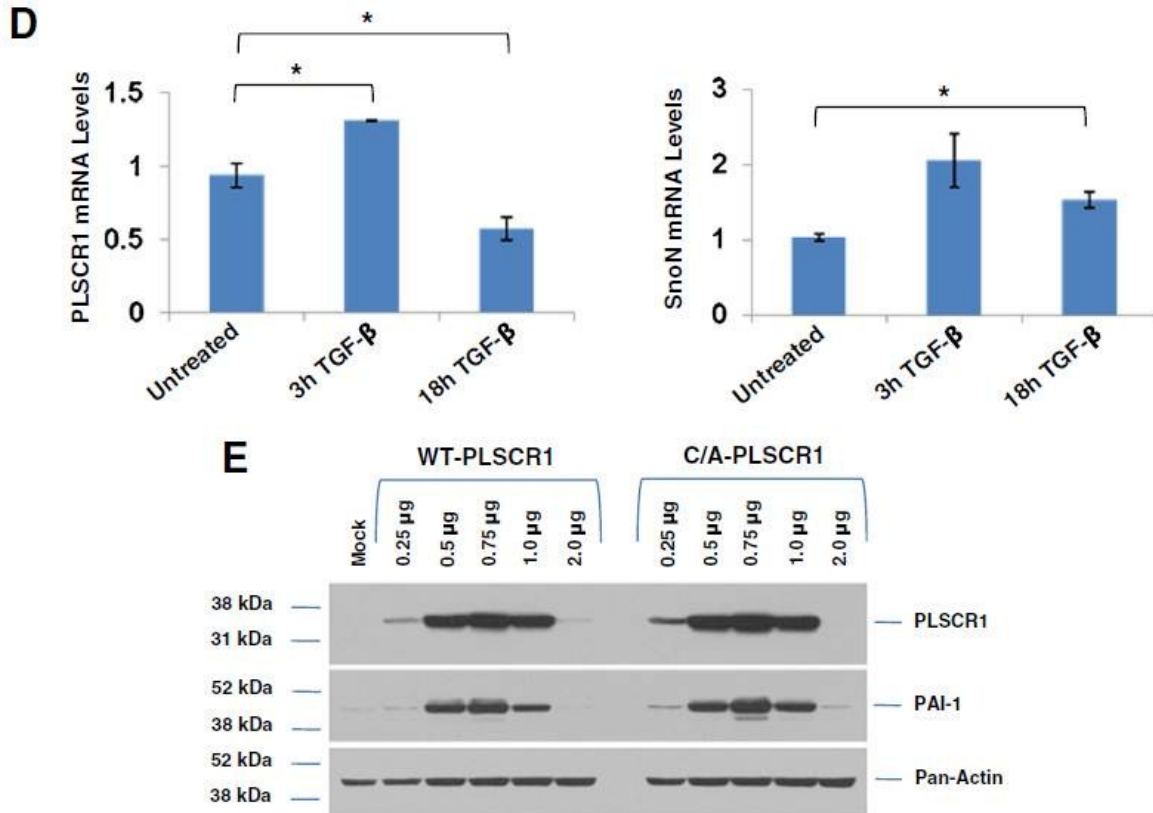


Figure 14. SnoN and TGF $\beta$  transcriptionally regulate PLSCR1 (\*Continued on next page)



**Figure 14. SnoN and TGF $\beta$  transcriptionally regulate PLSCR1**

(A) HEY cells were transfected with control or SnoN siRNA as described in chapter 2 and total RNA was isolated 48 hours post siRNA treatment; relative mRNA levels of PLSCR1 (Left panel) and SnoN (Right panel) were measured as described earlier. (B and C) T80 cells were transfected with pGL3-basic vector containing PLSCR1 genomic construct followed by treatment with control or SnoN siRNA (B) or 50 pM TGF $\beta$  for 24 hours (C); PLSCR1 promoter activity was determined by performing luciferase assay as described in chapter 2. (D) T80 cells were treated with 50 pM TGF $\beta$  for 3 and 18 hours and relative mRNA levels of PLSCR1 (Left panel) and SnoN (Right panel) were determined from total RNA as described earlier. (E) T80 cells were mock transfected or transfected with pcDNA3 plasmid containing WT-PLSCR1 or C-A PLSCR1 at concentrations ranging from 0.25 to 2.0  $\mu$ g/ml; cell lysates were harvested 48 hours post-transfection and western analysis was performed for the indicated antibodies. All the data presented is representative of two independent experiments.

PLSCR1, we next assessed whether PLSCR1 modulates the TGF $\beta$  signaling pathway, we exogenously expressed wild type (WT) PLSCR1 and the palmitoylation mutant (C/A) PLSCR1, which harbors a mutation in palmitoylation site and localizes to the nucleus, in T80 cells and looked at the expression of TGF $\beta$  target molecules. Interestingly, overexpression of both of these PLSCR1 forms resulted in a

dramatic induction of plasminogen activator inhibitor 1 (PAI-1) (Figure 14E), a known target of TGF $\beta$  pathway [232, 233]. PAI-1 expression is known to regulate the TGF $\beta$  induced migratory and invasive potential in breast and gynecological cancers [13]. Collectively, these results indicate that PLSCR1 is transcriptionally regulated by SnoN and TGF $\beta$  stimulation; and similar to SnoN, PLSCR1 expression can also modulate the TGF $\beta$  signaling pathway. However, how PLSCR1 modulates the TGF $\beta$  signaling and its significance remains to be investigated.

#### SnoN regulates the IFN-mediated induction of PLSCR1:

Previous studies report that interferons (IFN) stimulation results in a significant induction of PLSCR1 in various cell lines as shown in Chapter 1 (Table 3) [38, 39]. Since SnoN knockdown resulted in reduced expression of PLSCR1, we next tried to determine whether SnoN could modulate IFN-mediated induction of PLSCR1. Similar to the previous reports [38, 39], we noted a dramatic induction of PLSCR1 protein levels in HEY ovarian carcinoma cells upon treatment with 3,000 IU/ml IFN-2 $\alpha$  (Figure 15A) starting from 6 hours up to 24 hours. We further validated this by performing qPCR which showed a significant increase in PLSCR1 mRNA levels (~3-fold) at 3 hours post-treatment with IFN-2 $\alpha$  (Figure 15B, Left panel). Interestingly, we also detected SnoN protein levels to be elevated upon IFN-2 $\alpha$  treatment starting at 3 hours prior to PLSCR1 induction (at 6 hours) (Figure 15A). These results suggested a potential role of SnoN in transcriptional activation of PLSCR1 upon IFN-2 $\alpha$  stimulation. However, we did not note any significant changes in the SnoN mRNA levels upon IFN-2 $\alpha$  treatment (Figure 15B Right panel). Our previous studies demonstrate that As<sub>2</sub>O<sub>3</sub>-induced SnoN expression and apoptosis in ovarian cancer cells is mediated by increased production of reactive oxygen species (ROS) [1]; and treatment with N-acetyl cysteine (NAC), an anti-oxidant and free radical scavenger [213] markedly reduced these effects.

In order to determine whether IFN-mediated PLSCR1 and SnoN induction also is mediated by production of ROS, we treated HEY cells with IFN both in the presence and absence NAC. However, western analyses indicated no change in the induction of PLSCR1 or SnoN protein levels upon IFN-2 $\alpha$

treatment in the presence of NAC suggesting that their induction is independent of ROS production (Figure 15H). Previous studies have identified IFN-induced PLSCR1 to be localized to plasma membrane and/or nuclear compartment in specific cell types [24]. In this regard, we performed immunostaining for PLSCR1 in HEY cells treated with IFN-2 $\alpha$ . As shown in Figure 15C, PLSCR1, dramatically induced following 18 hour IFN stimulation, was localized predominantly to the plasma membrane and perinuclear regions. Similarly, subcellular fractionation studies revealed that although a minor fraction of PLSCR1 was detected in the nuclear fraction, PLSCR1 was largely detected in the cytoplasmic fraction (Figure 15D).

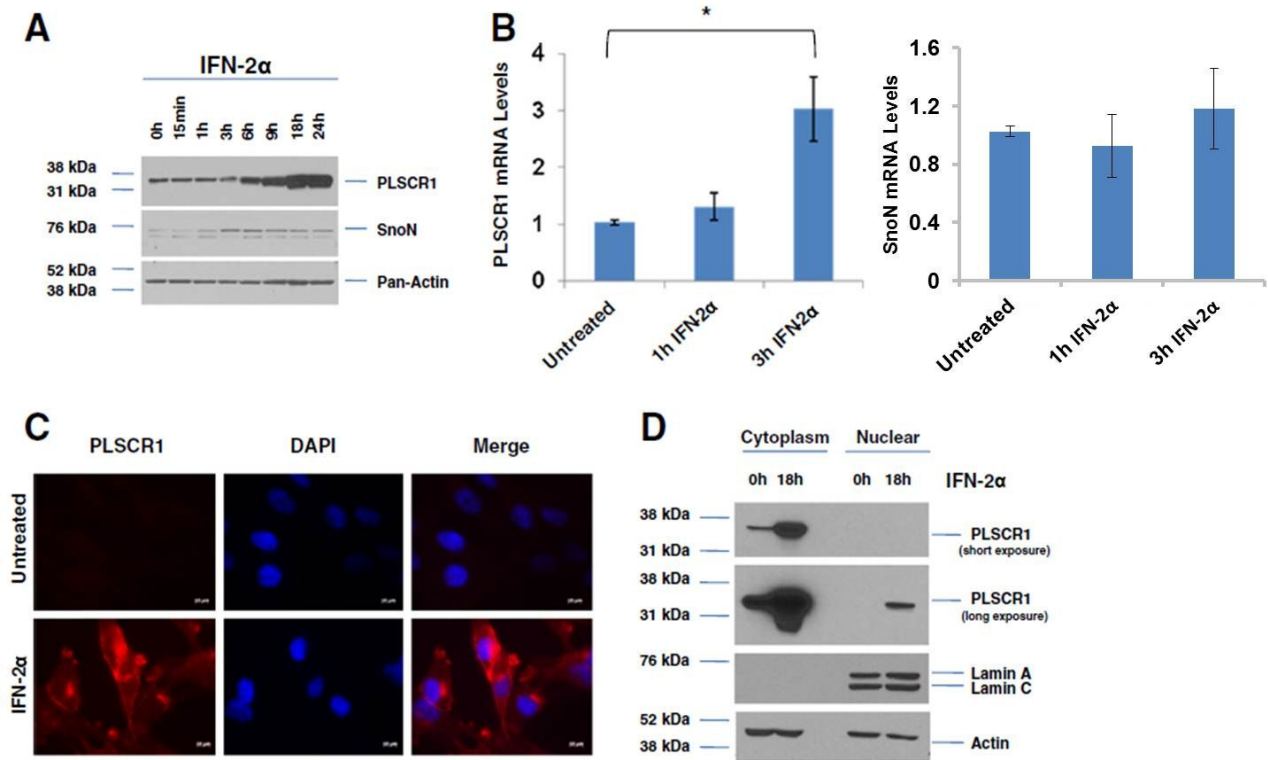


**Figure 15. Interferon-induced PLSCR1 mRNA expression is regulated by SnoN (\*Continued on next page)**

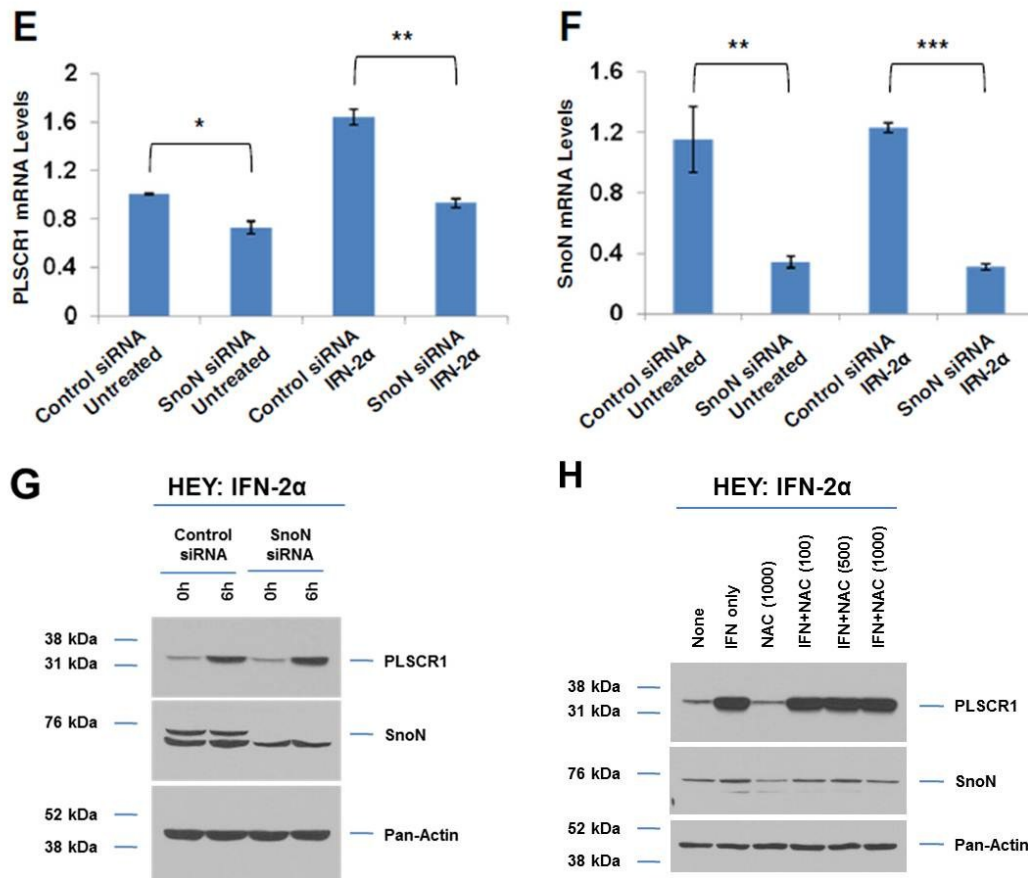


**Figure 15. Interferon-induced PLSCR1 mRNA expression is regulated by SnoN**

(A) HEY cells were treated with 3,000 IU/ml of IFN-2α from 15 minutes up to 24 hours. Cell lysates were harvested and analyzed by western blotting for the indicated antibodies. (B) HEY cells were treated with 3,000 IU/ml IFN-2α for 1 and 3 hours and total RNA was isolated. Relative PLSCR1 (Left panel) and SnoN (Right panel) mRNA levels were determined via qPCR. (C) HEY cells were treated with 3,000 IU/ml IFN-2α for 24 hours followed by immunostaining against PLSCR1 as (described in chapter 2). (D) HEY cells treated with IFN-2α as in (C) followed by subcellular fractionation (described in chapter 2). Fractions were analyzed via western blotting for indicated antibodies. (E and F) HEY cells were transfected with control or SnoN siRNA followed by treatment with IFN-2α for 3 hours. Total RNA isolated was isolated and qPCR was performed to determine the relative PLSCR1 (E) and SnoN (F) mRNA levels. (G) HEY were treated with IFN-2α for 6 hours and cell lysates harvested followed by western analysis for the indicated antibodies. (H) HEY cells were treated with IFN-2α in presence or absence of 100 – 1000 μM NAC for 9 hours. Cell lysates were harvested and analyzed via western blotting for the indicated antibodies. Data presented in (A) is representative of three independent experiments while (B), (C), (D) and (E) represent two independent experiments.

In order to determine whether SnoN modulates the IFN-mediated PLSCR1 induction, we next treated the HEY cells with IFN-2 $\alpha$  after knockdown of SnoN via siRNA. Indeed, we noticed significant reduction in IFN-induced PLSCR1 mRNA levels (~1.8 fold, Figure 15E) upon SnoN knockdown (Figure 15F); however, SnoN knockdown did not alter the IFN-induced PLSCR1 protein levels (Figure 15G) implicating involvement of other mechanisms in the process of PLSCR1 induction. The lack of changes in PLSCR1 protein upon SnoN knockdown could also potentially be attributed to the long half-life of PLSCR1 protein (which has yet to be formally assessed). Our studies in HEY cells treated with cycloheximide (CHX), an inhibitor of translation did not show significant reduction in PLSCR1 levels even 24 hours after CHX treatment (Data not shown). Further studies are needed to investigate the mechanisms involved in this process. Collectively, these results indicate that SnoN plays a part in regulating the IFN-induced PLSCR1 expression.

#### PLSCR1 knockdown modulates the ovarian cancer cell responses to As<sub>2</sub>O<sub>3</sub>:

As mentioned earlier, our previous studies indicate that As<sub>2</sub>O<sub>3</sub> treatment results in induction of SnoN levels which mediates a cytoprotective autophagy that antagonizes the ROS-mediated cell death responses in HEY ovarian carcinoma cells [1]. In order to determine whether PLSCR1, similar to SnoN could mediate this process, we first tried to identify whether As<sub>2</sub>O<sub>3</sub> could alter the PLSCR1 expression in HEY cells. Interestingly, PLSCR1 protein levels significantly decreased upon treatment with 25  $\mu$ M As<sub>2</sub>O<sub>3</sub> from 1 to 24 hours (Figure 16A and B). Previous studies report As<sub>2</sub>O<sub>3</sub> to be involved in proteasomal degradation of proteins including EVI1 in HEY cells [1]. In this regard, we next tried to determine whether the reduction of PLSCR1 protein levels upon As<sub>2</sub>O<sub>3</sub> treatment is due to its degradation via the proteasomal pathway. However, 25  $\mu$ M As<sub>2</sub>O<sub>3</sub> in combination with 5  $\mu$ M MG132 (a proteasomal inhibitor) did not recover the PLSCR1 levels reduced by As<sub>2</sub>O<sub>3</sub> treatment (Figure 16C) indicating that reduction in PLSCR1 levels is independent of the proteasomal degradation pathway. In order to determine



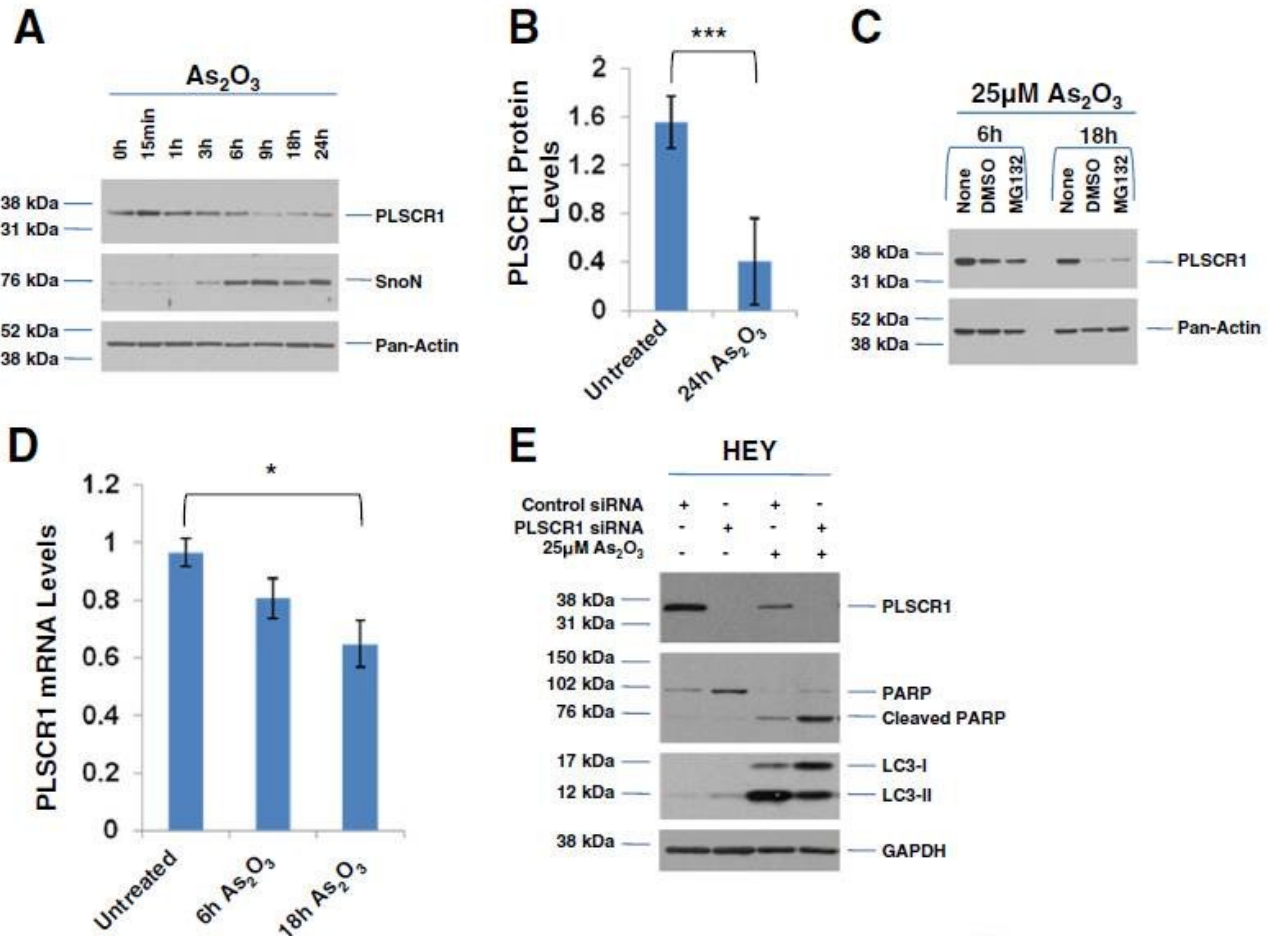


**Figure 16. PLSCR1 knockdown alters the sensitivity of ovarian cancer cells to  $As_2O_3$  (\*Continued on next page)**

whether  $As_2O_3$  treatment transcriptionally reduced the PLSCR1 expression, we performed qPCR analyses to quantify the PLSCR1 mRNA levels in  $As_2O_3$  treated HEY cells. Consistent with the protein levels, PLSCR1 mRNA levels were also reduced significantly upon  $As_2O_3$  treatment (Figure 16D) indicating that  $As_2O_3$ -induced transcriptional regulation of PLSCR1.

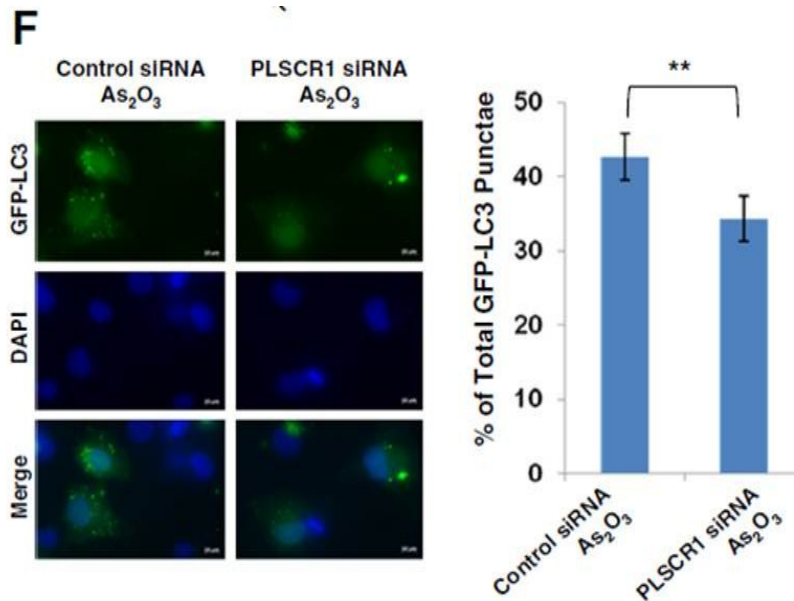


**Figure 16. PLSCR1 knockdown alters the sensitivity of ovarian cancer cells to As<sub>2</sub>O<sub>3</sub>**

(A) HEY cells were treated with 25  $\mu$ M of As<sub>2</sub>O<sub>3</sub> from 15 minutes up to 24 hours. Cell lysates were harvested and analyzed by western blotting for the indicated antibodies. (B) Densitometric analyses were performed on PLSCR1 protein changes observed in (A). (C) HEY cells were treated with 25  $\mu$ M of As<sub>2</sub>O<sub>3</sub> in presence and absence of 5  $\mu$ M MG132 for 6 and 18 hours. Cell lysates harvested were analyzed via western blotting for the indicated antibodies. (D) HEY cells treated with As<sub>2</sub>O<sub>3</sub> as in (A) for 6 and 18 hours followed by total RNA isolation; qPCR was performed to determine the relative PLSCR1 mRNA levels. (E) HEY cells were transfected with control or PLSCR1 siRNA followed by treatment with 25  $\mu$ M As<sub>2</sub>O<sub>3</sub> 18 hours; Cell lysates were harvested followed by western analysis for the indicated antibodies. (F) HEY cells were transfected with pEGFP-LC3 vector followed by treatment with control or PLSCR1 siRNA. As<sub>2</sub>O<sub>3</sub> treatment was performed (10  $\mu$ M, 18 hours) EGFP-LC3 assay (Left panel) was performed as described in chapter 2. Percentage of cells positive for LC3 punctae was represented in bar graphs (Right panel). Data presented in (A) and (E) is representative of three independent experiments while (B), (C), (D) and (F) represent two independent experiments.

SnoN knockdown alters the sensitivity of HEY ovarian cancer cells to As<sub>2</sub>O<sub>3</sub> by increasing apoptosis and reducing cytoprotective autophagic flux [1]. Since PLSCR1 is regulated by SnoN and their expression is altered similarly in ovarian cancers, we hypothesized that PLSCR1 knockdown would also alter the chemotherapeutic responses in ovarian cancer cells. In this regard, we treated HEY cells with As<sub>2</sub>O<sub>3</sub> after treatment with non-targeting siRNA and PLSCR1 siRNA. Indeed, as shown in Figure 16E, we

noticed a marked increase in cleaved PARP levels, a marker of apoptosis in the As<sub>2</sub>O<sub>3</sub> treated cells upon PLSCR1 knockdown. This suggests that PLSCR1 modulates the chemo-sensitivity in these cells. Additionally, we also noticed a dramatic reduction in the conversion of LC3-I to LC3-II (an important step in the formation of autophagosomes during the process of autophagy [2]) in the presence of As<sub>2</sub>O<sub>3</sub> in PLSCR1 reduced cells (Figure 16F). These results were further validated via EGFP-LC3 autophagy assay showing a significant reduction in number of EGFP-LC3 punctae (Figure 16F) formed upon As<sub>2</sub>O<sub>3</sub> treatment in the PLSCR1 knockdown cells. Collectively, these results clearly indicate that PLSCR1, similar to SnoN, alters the ovarian cancer cell responses to As<sub>2</sub>O<sub>3</sub> by altering the autophagic and apoptotic processes. The complete mechanism by which PLSCR1 increases the sensitivity of ovarian cancer cells to chemotherapeutic agents needs to be investigated.

## **Discussion**

PLSCR1 is located at chromosome 3q23, adjacent to the 3q26 locus that is amplified in various cancers including ovarian cancer [9, 10, 12, 28-30]. Previous reports suggest that the genes amplified at 3q26 might cross-regulate other genes that are located in close proximity [32, 33, 234]. Although presumed to regulate translocation of phospholipids between the inner and outer leaflets of plasma membrane, recent studies have indicated elevated expression and a potential tumor promoting function of PLSCR1 in colorectal and metastatic cancers [15, 20-22]. Recent immunohistochemistry (IHC) studies show PLSCR1 expression to be elevated in colorectal cancers specimens [22]. Moreover, inhibition of PLSCR1 (via siRNAs and specific antibodies) delays colorectal cancer and metastatic liver cancer development implicating PLSCR1 as a tumor promoter [20, 21]. Although mouse xenograft studies performed utilizing HEY1B ovarian carcinoma cells implicated a potential role for PLSCR1 in tumor suppression in ovarian cancer, these observations were not detected *in vitro* [15].

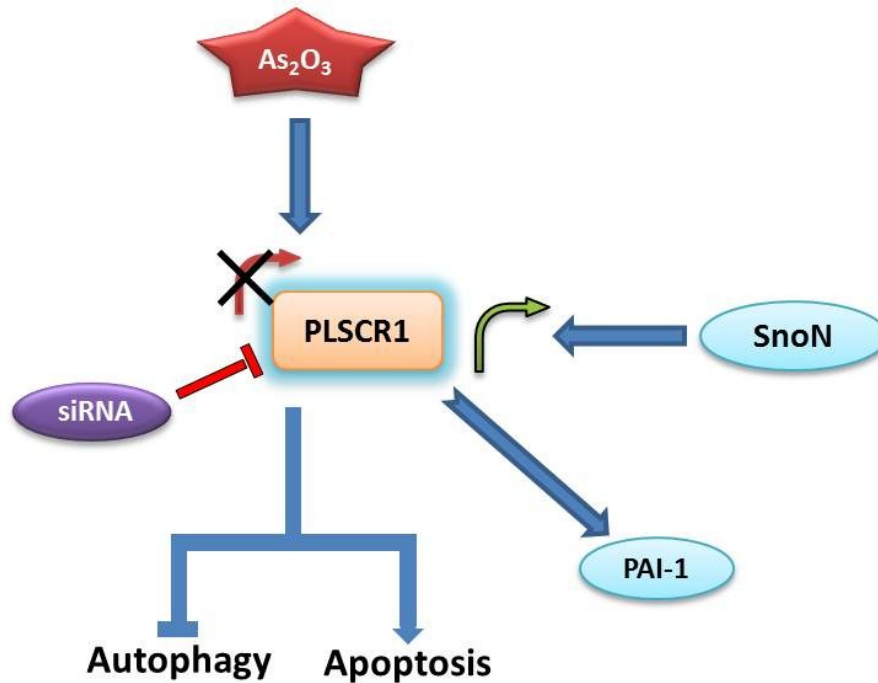


**Figure 17: Model of the regulation of PLSCR1 by SnoN and modulation of As<sub>2</sub>O<sub>3</sub>-induced cell death response by PLSCR1**

SnoN transcriptionally upregulates PLSCR1 expression while As<sub>2</sub>O<sub>3</sub> leads to its downregulation. Upregulated PLSCR1 results in increased expression of PAI-1, a target of TGFβ signaling [13]. siRNA-mediated reduction of PLSCR1 increases the sensitivity of ovarian cancer cells to treatment with As<sub>2</sub>O<sub>3</sub> via increased apoptosis and decreased autophagy. (\*Model created by Madhav Karthik Kodigepalli)

Herein, we demonstrate, using OncoPrint and cBioPortal bioinformatic analyses of the TCGA cancer genomic dataset that the DNA copy number levels of PLSCR1 are elevated in ovarian cancer patient samples and cell lines. Via qPCR analyses, we also identified that mRNA expression levels of PLSCR1 are also elevated in ovarian cancer cell lines compared to immortalized normal ovarian cells (Figure 13C). More importantly, alterations in PLSCR1 DNA copy number and mRNA expression levels highly correlate with that of SnoN, which is amplified at 3q26.2 and plays a prominent role in ovarian cancer pathogenesis and chemotherapeutic responses [1, 9]. These observations suggest that PLSCR1 might play a similar function as SnoN in ovarian cancer development. Interestingly, we did not find any

correlation between SnoN and PLSCR1 at the protein level and we propose that this discordance might be due to different translational and post-translational mechanisms between SnoN and PLSCR1 which needs further investigation. We also demonstrate that PLSCR1 mRNA level expression is regulated by SnoN and TGF $\beta$  stimulation in ovarian cancer. SnoN knockdown resulted in significant reduction of both endogenous and IFN-2 $\alpha$  induced PLSCR1 mRNA levels. Interestingly, in addition to SnoN reduction, TGF $\beta$  treatment also resulted in a significant reduction in promoter activity of PLSCR1 validating the role of SnoN and TGF $\beta$  in transcriptional regulation of PLSCR1. On the other hand, overexpression of PLSCR1 (both wild type (WT) and C/A mutant, that localizes to nuclear compartment) led to dramatic increase in protein expression of PAI-1, an important TGF $\beta$  target gene [233] which is known to inhibit the migratory and invasive capabilities of breast and gynecological cancers [13]. This suggests a potential role for PLSCR1 in modulating TGF $\beta$ -stimulated migration and invasion in cancer cells. However, the exact mechanisms involved in the regulation of PLSCR1 by SnoN or TGF $\beta$  and the regulation of TGF $\beta$  signaling by PLSCR1 remain to be investigated. Recent reports of Snail, an important transcription factor associated with EMT, binding directly to PLSCR1 promoter region to down-regulate its expression is the only evidence thus far of direct transcriptional regulation of PLSCR1 [146]. It is currently unknown whether SnoN, similar to Snail, could also bind to the promoter region of PLSCR1 to alter its transcription. Interestingly, SnoN knockdown did not result in significant changes in PLSCR1 protein levels (Figure 15G) which suggest involvement of other mediators and/or mechanisms involved in the regulation of PLSCR1 expression. Additionally, the longer half-life of PLSCR1 (as determined by CHX time course experiment; data not presented) could potentially contribute to the lack of PLSCR1 protein level reduction upon SnoN knockdown. Collectively, our studies suggest that SnoN contributes in part to regulation of both endogenous and IFN-2 $\alpha$  induced expression of PLSCR1. Together, PLSCR1 and SnoN co-amplified and co-overexpressed in ovarian cancers could potentially exhibit cooperative oncogenicity.

We have previously shown that As<sub>2</sub>O<sub>3</sub>-treatment leads to dramatic induction of SnoN in ovarian cancer cells which mediates a cytoprotective autophagy antagonizing the pro-apoptotic effects of As<sub>2</sub>O<sub>3</sub>

[1]. In contrast, our current study shows that As<sub>2</sub>O<sub>3</sub> results in a significant reduction in PLSCR1 mRNA and protein expression in a process-independent of proteasomal degradation pathway that is known to mediate degradation of EVI1-induced by As<sub>2</sub>O<sub>3</sub>. Importantly, siRNA mediated reduction of PLSCR1 increased the sensitivity of HEY cells to As<sub>2</sub>O<sub>3</sub> as evidenced by increased cleaved PARP levels. Additionally, PLSCR1 knockdown in As<sub>2</sub>O<sub>3</sub> treated cells also resulted in reduction in levels of LC3-II, an important mediator in the process of autophagy. However, the exact mechanism by which PLSCR1 modulates As<sub>2</sub>O<sub>3</sub>-induced processes of apoptosis and autophagy is currently unknown. Collectively, these results implicate PLSCR1, similar to SnoN, as a key player in ovarian cancer development and chemotherapeutic responses (Figure 17). Further studies are necessary to completely understand its exact role that would aid in the development of novel and better therapeutic strategies in treatment of ovarian cancers.

PLSCR1 is one of the most induced IFN-regulated genes [38] and consistent with previous reports, our studies also demonstrated a dramatic induction in PLSCR1 protein and mRNA levels upon IFN-2 $\alpha$  stimulation (Figures 15A and 15B). Although predominantly localized to the plasma membrane, PLSCR1 is also present at other subcellular locations such as nucleus, endosomes, Golgi, and ER under different conditions [19, 24, 133, 180]. Importantly, defective palmitoylation and IFN stimulation result in its nuclear localization in specific cell types as mentioned in Chapter 1. Our studies show PLSCR1 to be predominantly localized at the plasma membrane (Figures 15C and 15D) although a small percentage was found in the nuclear fractions (Figure 15D). At the plasma membrane, PLSCR1 is implicated in various signaling functions via its interaction with various signaling mediators; on the other hand, nuclear functions of PLSCR1 include transcriptional regulation of genes (such as IP<sub>3</sub>R) and interactions with DNA topoisomerase II significance of which still remains uninvestigated. Collectively, these reports suggest that subcellular localization of PLSCR1 plays a decisive role in determining its function. Although, IHC studies in colorectal cancer patient specimens have shown increased PLSCR1 expression [22], the subcellular localization of PLSCR1 in these specimens remains to be determined. Altered

localization of PLSCR1 in these cancers could lead to its altered functions which can in turn potentially modulate the development and cellular responses in these cancers. Together, further studies would aid in understanding the role of PLSCR1 completely which could potentially lead to development of better strategies in ovarian cancer treatment.

### **Acknowledgements**

Determination of PLSCR1 and SnoN DNA copy number alterations using TCGA ovarian cancer genomics data via cBioPortal as well as linear regression analyses via R (R-project) were performed by Dr. Pavana Anur and Dr. Paul Spellman (Department of Molecular and Medical Genetics at Oregon Health and Science University, Portland). OncoPrint bioinformatic analyses of DNA copy number alterations of PLSCR1 and SnoN were performed by Dr. Meera Nanjundan.

## Chapter 5

### Regulation of PLSCR1 by IRF3 Following Vector Transfection in Normal and Malignant Epithelial Cells

#### Introduction

Although plasmid transfection is a commonly utilized method for exogenous expression of specific proteins, few studies suggest that plasmid transfection leads to non-specific and off-target effects. Microarray based gene expression studies by Lobenhofer et al. [235] suggest that plasmid transfection may result in differential induction of various off-target genes including those that are associated with regulating primary immune responses (i.e. IFNs and other inflammatory cytokines such as interleukins (ILs)) in response to viral/foreign DNA entry into the host cells [235].

Toll-like receptors (TLRs) are evolutionarily conserved receptors of the innate immune system that detect the pathogen associated molecular patterns (PAMPs) [236]. The TLR family is composed of 10 members which are type I transmembrane receptors localized either to the plasma membrane and endosomal compartments. Plasma membrane localized TLRs (1, 2, 4, 5, 6, and 10) are involved in recognizing pathogenic protein components such as viral envelope proteins or bacterial wall proteins [168]. On the other hand, the remaining endosome-localized TLR family members (3, 7, 8, and 9) are nucleic acid sensing receptors that are active where they detect pathogenic nucleic acids such as viral and bacterial nucleic acids along with non-pathogenic foreign nucleic acids such as plasmid DNA [237] [238] [169]. Upon recognizing pathogenic components, Toll-like receptors undergo proteolysis to become activated triggering the activation of downstream signaling mediators followed by production of antiviral/inflammatory cytokines such as IFNs and ILs. Activated TLRs recruit adaptor proteins such as



myeloid differentiation factor 88 (Myd88), TRIF (Toll-interleukin-1 receptor (TIR) domain containing adaptor protein inducing IFN), TIRAP (Toll-interleukin-1 receptor (TIR) domain containing adaptor protein), and TRAM (TRIF-related adaptor molecule). This complex between TLR and adaptor proteins leads to activation of various signaling mediators such as IRAK1/4 finally leading to activation of two groups of transcription factors including IRF3/7 on one hand and NF $\kappa$ B on the other [43]. Upon activation IRF3/7 proteins enter the nuclear compartments resulting in induction of various IFN and IFN-dependent genes. On the other hand, activated NF $\kappa$ B induces the transcription of various cytokines such as IL-1/3 and other inflammatory cytokines. In addition to IRF and NF $\kappa$ B pathways, TLR signaling associates with other signaling pathways such as PI3K [171] and MAPK pathways [172, 239] which play a prominent role in cell proliferation and survival. TLR signaling is reported to result in activation of AKT which is required for the activation of downstream NF $\kappa$ B activation. On the other hand, MAP kinase proteins such as ERK1/2, p38MAPK, and JNK are reported to be directly activated by TLR signaling [172]. In addition, various other mediators of MAPK signaling (i.e. TAK1 and ASK1) [240] regulate TLR signaling. These studies indicate an important role for TLR signaling in cell survival and proliferation via crosstalk with PI3K and MAPK signaling pathways.

As described in Chapter 1, PLSCR1, located at 3q23, is a type II transmembrane protein previously implicated in the process of PS externalization leading to disruption of membrane asymmetry during important cellular events such as blood coagulation and apoptosis [34]. PLSCR1 is one of the most highly induced IFN-stimulated genes and mediates the antiviral functions of IFNs [38, 39, 163, 241]. PLSCR1 is transcriptionally regulated by IFN via activation of PKC $\delta$ , JNK, and STAT-1 [145]. Although primarily localized to the plasma membrane, PLSCR1 is also located in the nucleus, endoplasmic reticulum, Golgi, and endosomal compartments [19, 24, 25, 42, 133] under specific conditions. For instance, defective palmitoylation and IFN treatment results in nuclear localization of PLSCR1 in specific cell types [24, 177]. Previous studies including our recent studies have suggested that PLSCR1 plays an important role in regulating cancer development and cancer cell responses to chemotherapeutic agents

[15, 21, 22, 36, 177]. As described earlier in Chapter 1, PLSCR1 is also implicated in viral responses in host cells by antagonizing viral entry, replication, and propagation (i.e. hepatitis B virus (HBV) [8], hepatitis C virus (HCV) [7], vesicular stomatitis (VSV) [4], encephalomyocarditis (ECMV) [4], human immunodeficiency (HIV-1) [6], and human T cell leukemia (HTLV-1) [5] viruses). These findings suggest an important antiviral function of PLSCR1.

Recent studies by Talukder et al. have shown an important role for PLSCR1 in TLR9 signaling in plasmacytoid dendritic cells (pDCs) [42]. These studies report that PLSCR1 interacts with TLR9 in endosomal compartments and its knockdown in human pDC cell line results in ablation of TLR9 mediated induction of IFN in response to stimulation with CpG ODN (oligodeoxynucleotide) [42]. These studies indicate a potential function of PLSCR1 in modulating the innate immune responses. Furthermore, TLR signaling is also activated upon stimulation with dsDNA (plasmid) in human neutrophils leading to IFN production [45]. However, it is unknown whether PLSCR1 mediates immune responses upon entry of dsDNA into host cells [45]. Since PLSCR1 is an IFN-regulated gene and regulates TLR9 signaling, we hypothesize that PLSCR1 alters cellular responses upon dsDNA transfection. Herein, we report that transfection with dsDNA in immortalized normal ovarian surface epithelial (T80) and primary mammary epithelial (HMEC) cells markedly induces PLSCR1 mRNA and protein expression. In addition, dsDNA increases the activation of IRF3, a downstream mediator of TLR signaling, which is well-established to induce expression of type I IFNs ( $\alpha/\beta$ ) [45, 242]. Furthermore, we also detected a significant increase in mRNA levels of nucleic acid sensing TLRs, namely TLR9 and TLR4. Via siRNA and inhibitor studies, we further show that PLSCR1 induction is mediated by IRF3 and partly by ERK1/2 activation. In contrast, dsDNA transfection in ovarian cancer cells did not result in PLSCR1 induction and IRF3 activation. Collectively these studies suggest that activation of IRF3 may mediate PLSCR1 induction in dsDNA stimulated normal epithelial cells. Further investigation is needed to delineate the detailed underlying mechanism and the significance of these altered dsDNA responses in normal epithelial cells relative to ovarian cancer cells.

## Results

### dsDNA plasmid transfection induces PLSCR1 mRNA/protein in T80 ovarian epithelial cells and HMEC mammary epithelial cells:

As mentioned earlier, PLSCR1 is a highly induced IFN-stimulated gene [38, 39], and plasmid DNA transfection leads to induction of IFN-stimulated genes [45]; therefore, we first compared the effects of dsDNA transfection with that of IFN-2 $\alpha$  (3,000 IU/ml) treatment from 15 minutes to 24 hours in T80 cells. As previously noted in HEY ovarian cancer cells [177], IFN increases PLSCR1 protein from 6 hours until 24 hours (Figure 18A). Since IFN stimulated PLSCR1 induction is mediated by activation of PKC $\delta$ , JNK,

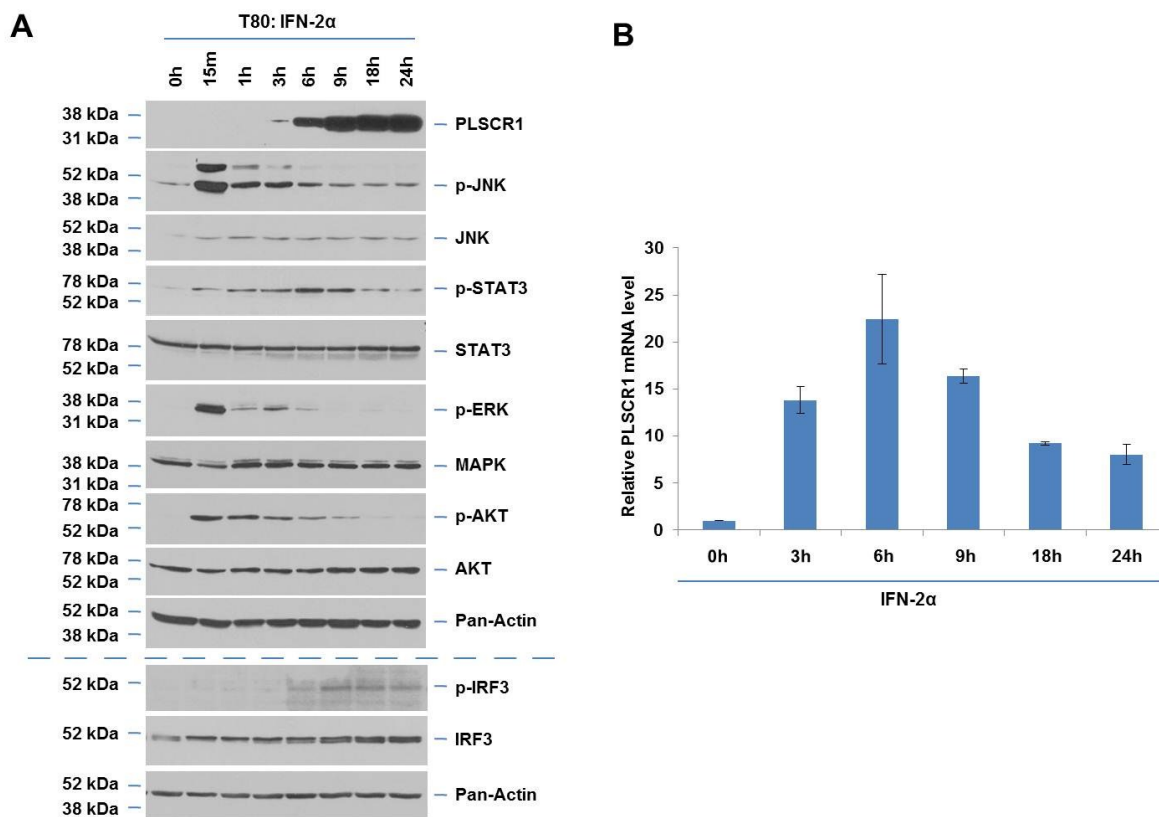


**Figure 18. IFN and empty plasmid transfection induce PLSCR1 mRNA and protein**  
(\*Continued on next page)

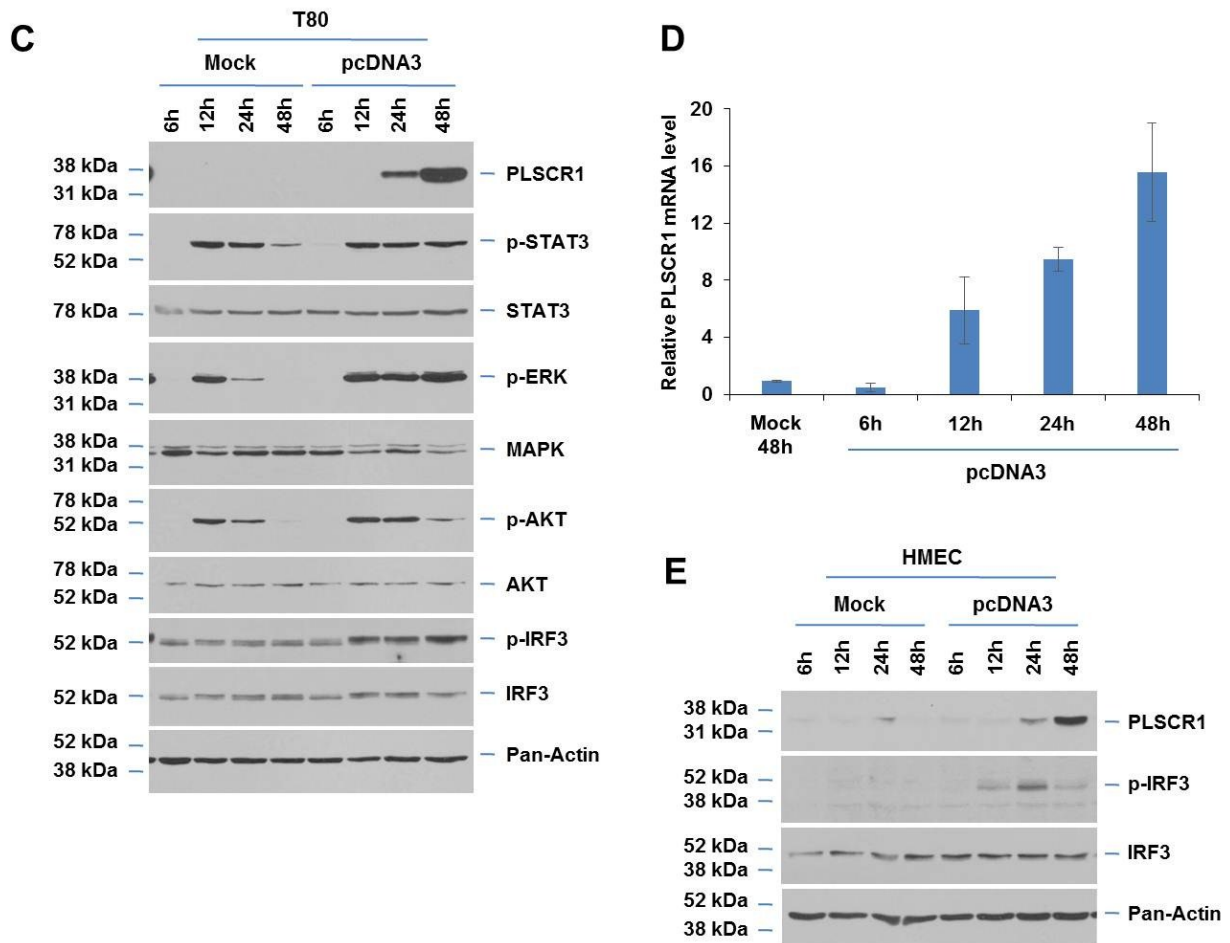


**Figure 18. IFN and empty plasmid transfection induce PLSCR1 mRNA and protein**

(A) T80 cells were treated with 3,000 IU/ml IFN-2 $\alpha$  from 15 minutes up to 24 hours. Cell lysates were analyzed by western blotting with the indicated antibodies. (B) Total RNA was isolated from cells treated as described in (A). PLSCR1 mRNA levels, detected via real-time PCR, are presented. (C) T80 cells were transfected with empty pcDNA3 plasmid (“pcDNA3”) or transfection reagent only (“mock”). Cell lysates were harvested from 6 up to 48 hours post-transfection and analyzed via western blotting with the indicated antibodies. (D) Total RNA was isolated from cells treated as described in (C). PLSCR1 mRNA levels, detected via real-time PCR, are presented. (E) HMEC cells were treated similarly as described for T80 cells (C) and cell lysates were then analyzed by western blotting with the indicated antibodies. Data presented in (A), (B), (C) and (D) is representative of three independent experiments while (E) represent two independent experiments.

and STAT1 [145], we assessed whether these mediators were activated in T80 cells following IFN stimulation. Indeed, we observed IFN-mediated activation of JNK (peaking at 15 minutes) and STAT3 (peaking at 6 hours) (Figure 18A) although activated PKC $\delta$  was undetectable under our conditions. Additionally, we observed increased phosphorylated AKT and MAPK at 15 minutes which rapidly decreased by 1 hour (Figure 18A). These results indicate that multiple signaling pathways are activated in T80 cells upon IFN stimulation including MAPK, AKT, JNK, and STAT3. To assess whether induction of PLSCR1 protein with IFN is a result of its elevated transcription, we performed quantitative PCR utilizing specific PLSCR1 probes/primers with RNA isolated from T80 cells treated with 3,000 IU/ml IFN from 3 to 24 hours. As shown in Figure 18B, similar to the protein level changes, PLSCR1 mRNA significantly increased by 6 hours IFN treatment. Collectively, these results indicate that IFN transcriptionally induces PLSCR1 expression of in T80 cells.

We next determined the effects of dsDNA (pcDNA3 vector) on PLSCR1 expression in T80 cells. As shown in Figure 18C, we noted a dramatic increase in PLSCR1 protein from 24 to 48 hours post-dsDNA transfection. We next assessed whether pcDNA3 transfection activates JNK and PKC $\delta$  (similar to that observed with IFN stimulation). However, phosphorylation of PKC $\delta$  and JNK were undetectable following pcDNA3 transfection. Although we detected activated STAT3 in dsDNA transfected cells, it was also phosphorylated in mock transfected cells suggesting dsDNA transfection did not further activate STAT3 (Figure 18C). Similar to IFN stimulation, dsDNA transfection markedly activates MAPK signaling pathway (relative to mock transfection). On the other hand, although AKT was activated in dsDNA treated cells, there was only a subtle increase in its phosphorylation in comparison to mock transfected cells. As mentioned earlier, TLR signaling is activated in response to cellular presentation of foreign DNA including plasmid DNA [45, 243]. Therefore, we assessed the activation status of IRF3, a downstream target of this pathway. Indeed, there was a marked increase in phosphorylated IRF3 levels upon dsDNA transfection (relative to mock) indicating that the TLR signaling pathway may be activated in response to dsDNA treatment. To determine whether dsDNA transfection leads to increased PLSCR1

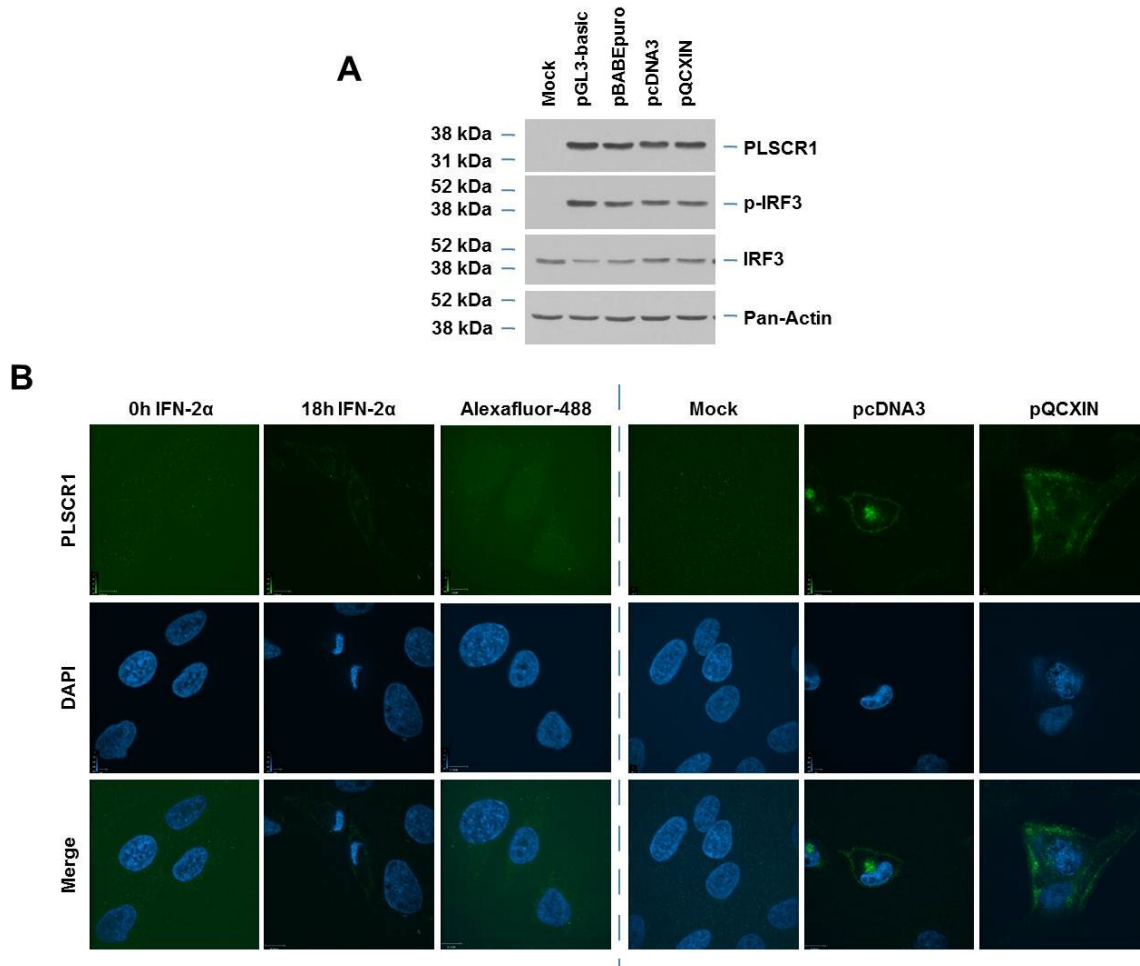


**Figure 19. Subcellular localization of PLSCR1 following IFN treatment and dsDNA transfection**

(A) T80 cells, transfected with empty pGL3-basic, pBABE-puro, pcDNA3 and pQCXIN vectors or transfection reagent only were analyzed by western blotting for the indicated antibodies. (B) T80 cells (grown on coverslips) were treated with 3,000 IU/ml IFN-2 $\alpha$  (Left panel) for 18 hours or transfected with empty pcDNA3, empty pQCXIN, or mock as described in (A) (Right panel). Cells were immunostained for PLSCR1 and DAPI. Images were then captured using a confocal microscope. Data presented (A) and (B) is representative of three and two independent experiments respectively.

mRNA levels, we performed quantitative real-time PCR using mRNA from T80 cells transfected with pcDNA3. As shown in Figure 18D, PLSCR1 mRNA was significantly increased from 12 until 48 hours post-transfection; this may suggest that PLSCR1 is transcriptionally induced by vector transfection. We next determined whether the PLSCR1 induction following dsDNA transfection is specific to T80 cells

only or if it occurs in other normal epithelial cell types also. In this regard, we transfected the primary mammary epithelial cells (HMECs) with pcDNA3 plasmid (Figure 18E) and determined whether PLSCR1 is induced relative to mock transfected cells. Indeed, we observed that similar to T80 cells, PLSCR1 protein was induced in dsDNA transfected cells from 24 to 48 hours post-transfection. Furthermore, we noted that IRF3 was activated upon dsDNA transfection in HMECs. Collectively, these results indicate that dsDNA transfection in epithelial cells results in transcriptional activation of IRF3 (a downstream mediator of the TLR signaling), MAPK, and STAT3 along with induction of PLSCR1.

To determine whether dsDNA-mediated PLSCR1 induction is specific to pcDNA3 vector transfection or whether this observation could be generalized to other vectors, we transfected T80 cells with pGL3-basic luciferase reporter plasmid (4.8 kb), pBABE-puro plasmid (5.2 kb), and pQCXIN plasmid (7.4 kb) in addition to pcDNA3 and assessed whether it would lead to PLSCR1 induction. Indeed, as presented in Figure 19A, similar to pcDNA3, transfection with pGL3-basic, pBABE-puro, and pQCXIN also resulted in a dramatic PLSCR1 induction along with IRF3 activation in T80 cells. This suggests that dsDNA response in T80 cells is not vector specific. Since previous studies indicate that IFN- $2\alpha$  stimulation leads to plasma membrane localization of *de novo* synthesized PLSCR1 [24, 177], we performed immunostaining of PLSCR1 and assessed the localization of PLSCR1 upon dsDNA transfection in the T80 cells. Consistent with the western analysis, there was a dramatic increase in PLSCR1 staining in the vector-transfected T80 cells (Figure 19C, Right panel). Additionally, we observed that PLSCR1 was predominantly localized to the plasma membrane in the ~70% of the cells; however, PLSCR1 was also detected in the perinuclear regions (i.e. endoplasmic reticulum/Golgi). Similar to previous studies including ours in HEY cells, IFN- $2\alpha$  treatment in T80 cells also resulted in plasma membrane localization of PLSCR1. However, the intensity of its expression was markedly lower (Figure 19C, Left panel) relative to vector transfection.

Inhibition of MAP kinase activity and reduction of STAT3 expression does not modulate the dsDNA-induced PLSCR1 mRNA levels:

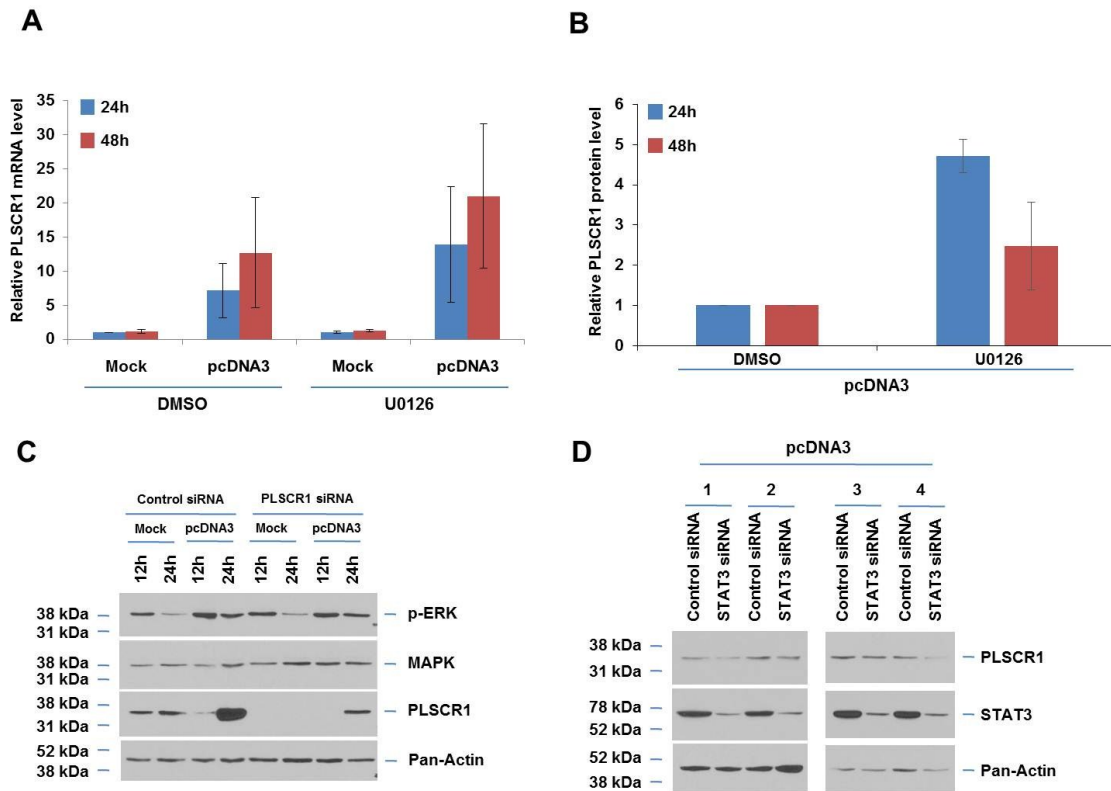


**Figure 20. Inhibition of MAPK activity does not antagonize PLSCR1 induction upon dsDNA transfection**

(A) T80 cells were pre-treated with 10  $\mu$ M U0126 or DMSO for at least 2 hours prior to and 6 hours after transfection with pcDNA3. PLSCR1 mRNA levels were quantified by real-time PCR. (B) Empty plasmid or mock transfection was performed in T80 cells that were treated with PLSCR1 siRNA. Cell lysates were isolated at the indicated time points following transfection and analyzed via western blotting with the indicated antibodies. (C) T80 cells were pre-treated with 10  $\mu$ M U0126 for at least 2 hours prior to and after 6 hours post-transfection with empty plasmid. Lysates were collected at 24 and 48 hours post-transfection and analyzed via western blotting and densitometric analysis of PLSCR1 western was obtained using Image-J software. (D) T80 cells were transfected with siRNA targeting STAT3 followed by empty plasmid pcDNA3 transfection for 24 hours. Cell lysates were then analyzed by western blotting with the indicated antibodies. Data presented in (A) and (C) is representative of three independent experiments while (B) and (D) represent two and four independent experiments respectively.



Since we have observed increased phosphorylation of ERK1/2 upon dsDNA transfection, we next determined whether MAPK signaling activity contributes to the dsDNA stimulated PLSCR1 induction. In this regard, we pretreated the T80 cells with U0126, an inhibitor of MAP Kinase activity followed by transfection with pcDNA3. We then analyzed the RNA and protein levels at 24 and 48 hours post-transfection. However, pretreatment with U0126 only resulted in a subtle increase in PLSCR1 mRNA levels upon 48 hours post vector transfection in comparison to treatment with DMSO (Figure 20A). Furthermore, as shown in Figure 20B, the changes in the PLSCR1 protein levels upon U0126 treatment were also variable and insignificant. We next determined whether PLSCR1 induction is an upstream event to ERK1/2 activation and performed PLSCR1 siRNA mediated knockdown followed by dsDNA transfection for 12 and 24 hours. As shown in Figure 20C, we did not observe any marked changes in ERK activation with PLSCR1 reduction. Together, these results suggest that the MAPK signaling inhibition does not modulate the PLSCR1 mRNA level induction and PLSCR1 does not regulate the MAPK activation upon dsDNA transfection. Since dsDNA transfection resulted in activation of STAT3 (Figure 18C), we next tried to determine whether STAT3 activation is required for the vector mediated PLSCR1 induction. In this regard, we reduced the expression of STAT3 via siRNA and assessed the dsDNA-induced PLSCR1 protein level changes. However, we did not observe any significant changes in PLSCR1 protein levels in the presence of STAT3 siRNA (Figure 20D) suggesting that PLSCR1 upregulation is independent of STAT3 activation.

#### Reduction of IRF3 modulates the dsDNA-mediated PLSCR1 induction:

As described earlier, upon recognition of PAMPs, Toll like receptors (TLRs) stimulate the downstream signaling cascade which activates transcription factors, NF $\kappa$ B and IRF3/7, resulting in induction of inflammatory cytokines including Type I IFNs [168, 236]. Recently, it has been reported that PLSCR1 can regulate TLR9 signaling in plasmacytoid dendritic cells (pDCs) [42]. TLR9, one of the nucleic acid sensing TLRs, functions in the endosomal compartments to recognize foreign/pathogenic nucleic acids that enter endosomes via endocytosis. [169]. On the other hand, although TLR4 is predominantly

localized to the plasma membrane, it is capable of recognizing plasmid DNA following its internalization into endosomal compartments [244]. Since we have observed that IRF3 is phosphorylated following dsDNA treatment (Figure 18C), we assessed whether dsDNA transfection in T80 cells alters TLR9 and TLR4 mRNA. Indeed, as shown in Figure 21A, we observed TLR4 (Upper panel) and TLR9 (Lower panel) mRNA levels to be significantly induced following dsDNA transfection in T80 cells. Similarly, we detected significant induction of IFN- $\alpha$  (Figure 21B Upper panel) and IFN- $\beta$  (Figure 21B Lower panel) mRNA levels (IFN- $\gamma$  was undetectable), downstream transcriptional targets of IRF3 activation [44].

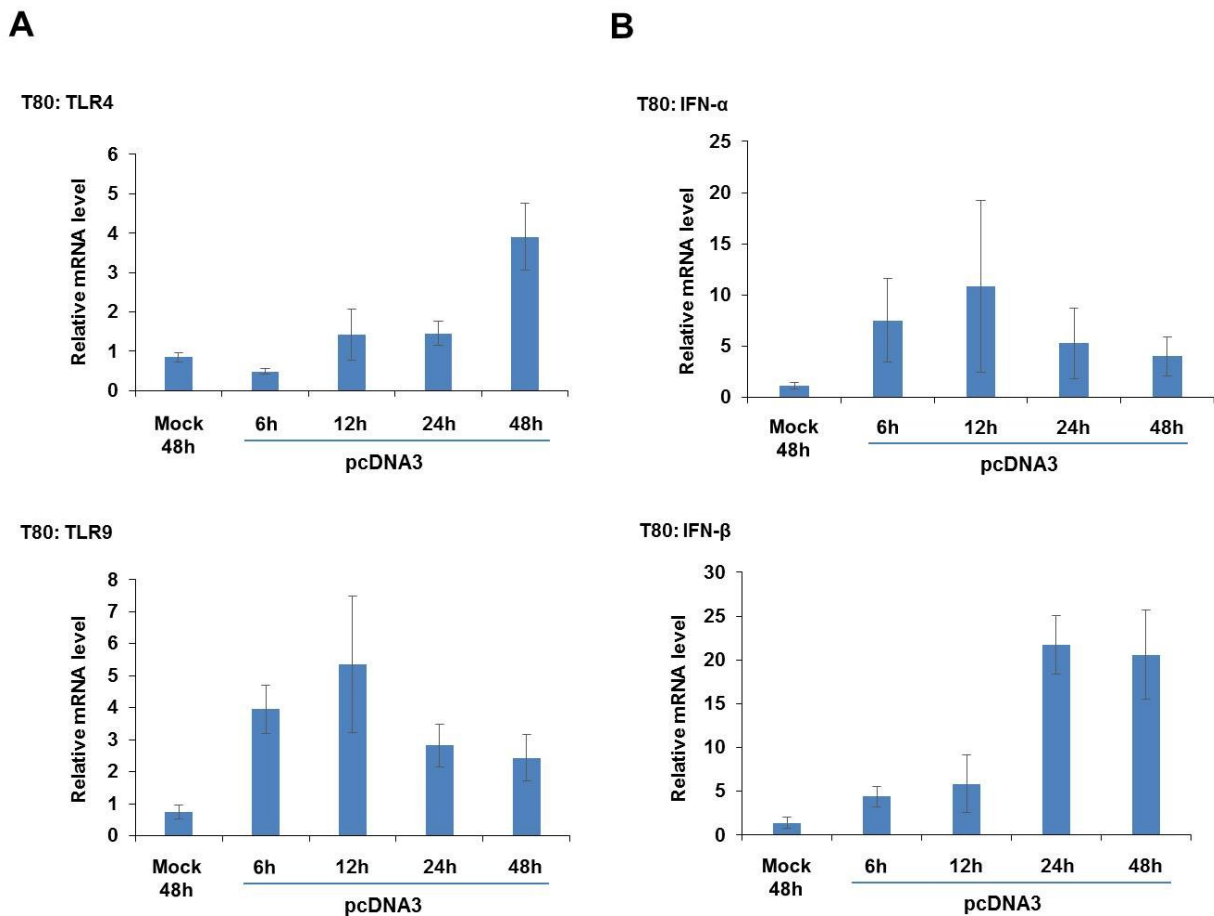


**Figure 21. IRF3 knockdown antagonizes dsDNA-induced PLSCR1 expression (\*Continued on next page)**

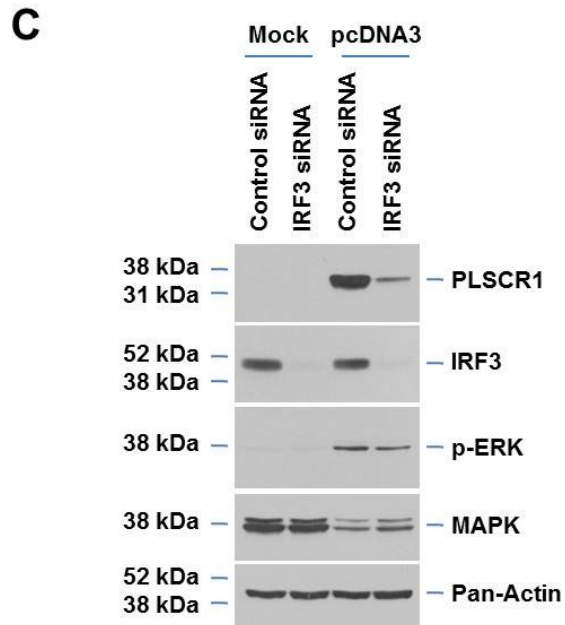


**Figure 21. IRF3 knockdown antagonizes dsDNA-induced PLSCR1 expression**

T80 cells were mock or empty pcDNA3 transfected. RNA was isolated following 6 to 48 hours transfection. TLR4/TLR9 (A) and IFN- $\alpha$ /IFN- $\beta$  (B) mRNA levels were detected by real-time PCR. (C) Empty plasmid or mock transfection was performed in T80 cells that were treated with IRF3 siRNA. Cell lysates were isolated at 48 hours following transfection and analyzed via western blotting with the indicated antibodies. Data presented in (A) and (B) is representative of four independent experiments while (C) represents two independent experiments.

Collectively, these results indicate that dsDNA transfection leads to induction of TLR4 and TLR9 as well as IFN- $\alpha$  and IFN- $\beta$ . In order to assess the contribution of TLR receptor signaling to PLSCR1 induction following dsDNA transfection, we made attempts to reduce TLR4 and TLR9 expression using knockdown strategies. However, protein level changes in TLR4 and TLR9 were not detected with knockdown. Therefore, we obtained siRNA targeting IRF3, a downstream TLR signaling target that is activated upon transfection with dsDNA. Strikingly, IRF3 knockdown (~90% reduction at the protein level) markedly ablates PLSCR1 induction following dsDNA transfection (Figure 21C). Therefore, IRF3 appears indispensable in the regulation of PLSCR1 expression in response to dsDNA.

Plasmid transfection does not lead to PLSCR1 induction in ovarian cancer cells:

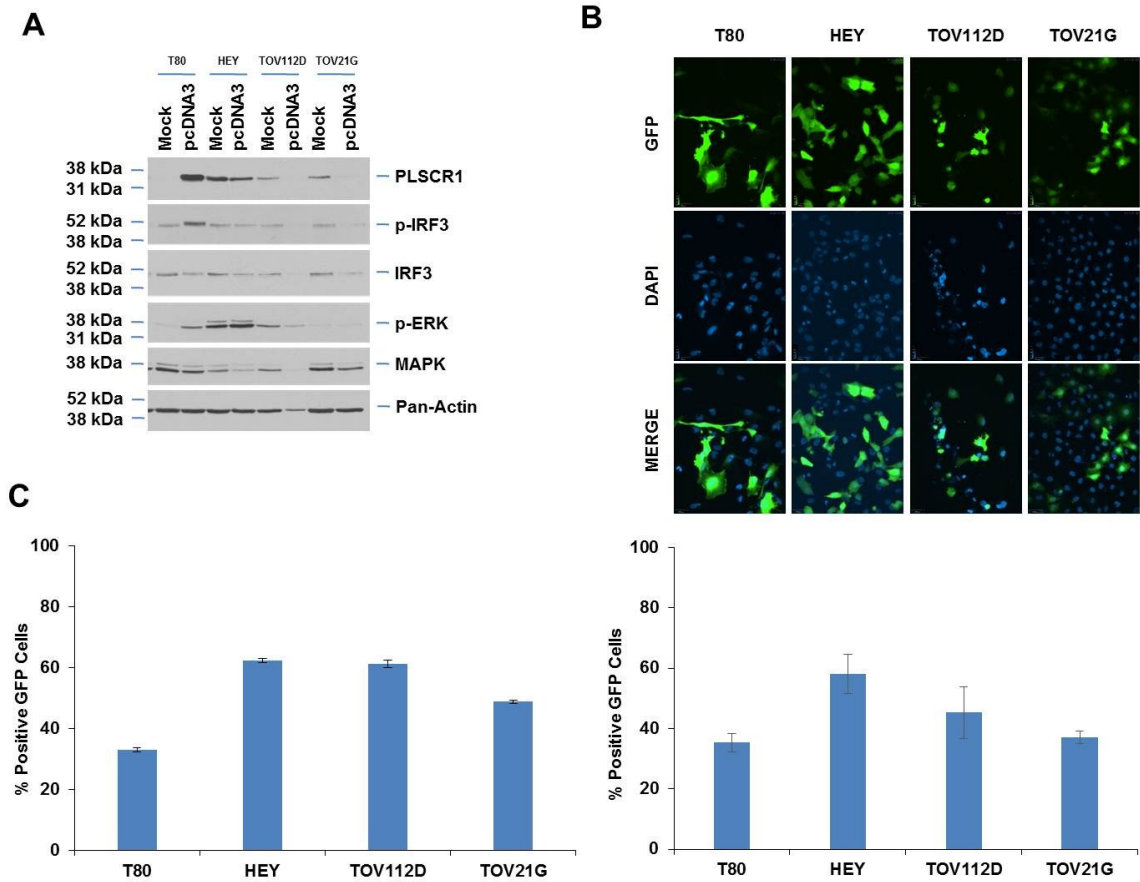


**Figure 22. Lack of PLSCR1 induction upon plasmid transfection in ovarian cancer cells**

(A) T80, HEY, TOV112D, and TOV21G cells were “mock” or empty pcDNA3 transfected. Cell lysates were collected 48 hours post-transfection followed by western analysis with the indicated antibodies. (B) Transfection efficiency was assessed in T80, HEY, TOV112D, and TOV21G cells (grown on coverslips) using pEGFP-C1 vector. Representative images are presented (*Top panel*). Percentages of GFP-positive cells in each of these cell lines is graphically presented (*Lower panel*). (C) T80, HEY, TOV112D, and TOV21G cells, transfected with pEGFP-C1 vector were collected 48 hours post-transfection and percent GFP positive cells were assessed via flow cytometry. Data presented in (A) and (B) is representative of two independent experiments and (C) is representative of three independent experiments.

To determine whether dsDNA transfection responses could be altered in ovarian cancer cell lines (relative to the normal T80 cell lines), we utilized serous (HEY), endometrioid (TOV112D), and clear cell (TOV21G) ovarian carcinoma cell lines and assessed their downstream responses to dsDNA transfection. In contrast to T80 cells, there was no increase in PLSCR1 protein upon vector transfection in the ovarian cancer cell lines. In contrast, as shown in Figure 22A, there was a subtle reduction in PLSCR1 expression in these cancer cell lines. Furthermore, we observed that the pattern of PLSCR1 expression was similar to the pattern of activated IRF3. However, the total IRF3 levels were variable following pcDNA3 transfection particularly in the TOV112D and TOV21G cell lines (Figure 22A); therefore, interpretation

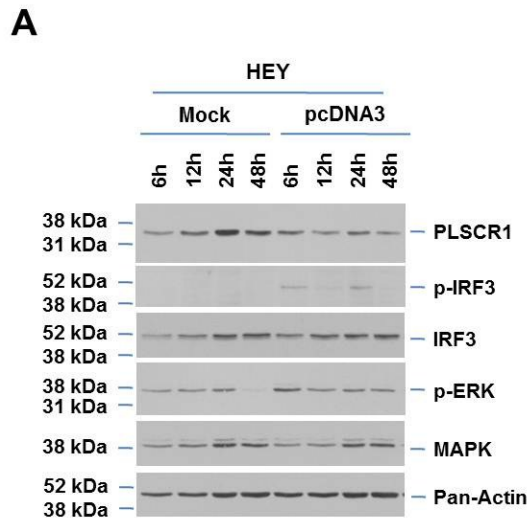


**Figure 23. Induction of TLR9 and IFN- $\alpha$  mRNA with lack of PLSCR1 or TLR4 transcript induction in ovarian cancer cells (\*Continued on next page)**

of the activation status of IRF3 is unclear. To determine whether this differential PLSCR1 induction between the normal and cancer cells may be due to differences in transfection efficiency, we transfected these cell lines with pEGFP-C1 plasmid and assessed the transfection efficiency of these cell lines via microscopy and flow cytometry. However, as shown in Figure 22B and 22C, the transfection efficiency of these cancer cell lines was similar to that in T80 cells suggesting that the activation of the TLR signaling cascade may be dysregulated in the cancer cell lines. In addition, to determine if the kinetics in the cancer

## B

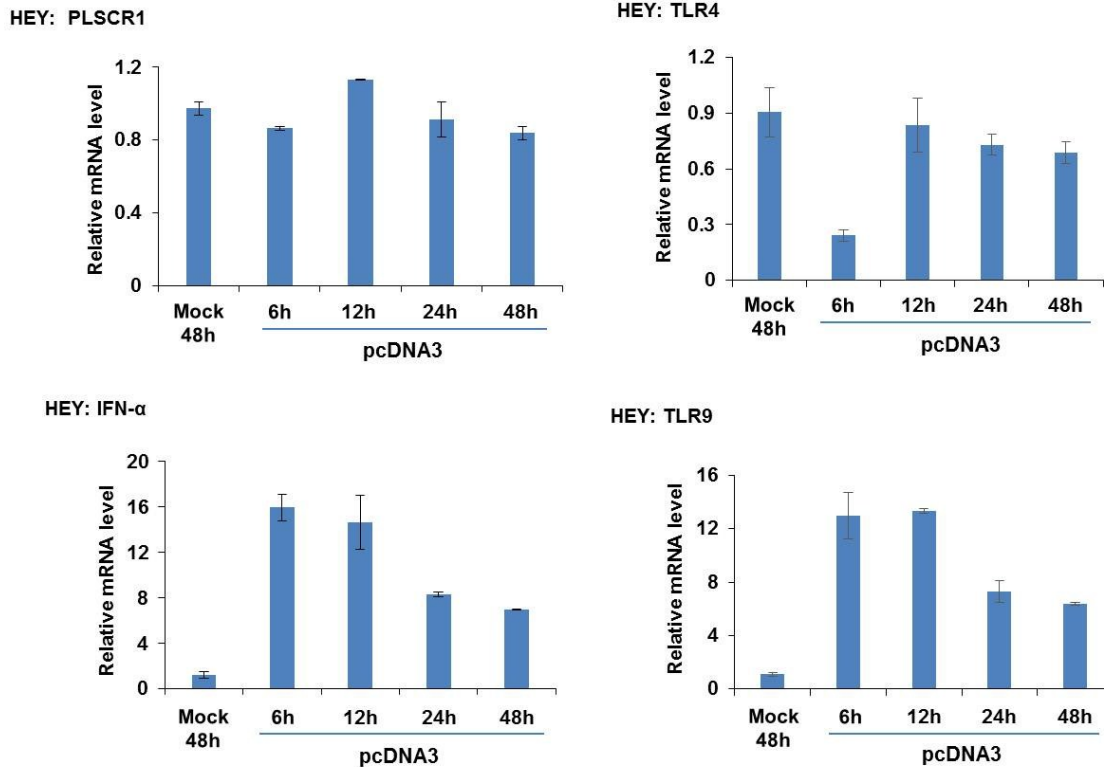


**Figure 23. Induction of TLR9 and IFN- $\alpha$  mRNA with lack of PLSCR1 or TLR4 transcript induction in ovarian cancer cells**

(A) HEY cells were “mock” or pcDNA3 transfected. Cell lysates were collected from 6 up to 48 hours post-transfection and analyzed by western blotting with the indicated antibodies. (B) Total RNA was isolated from HEY cells that were either mock (48 hours) or pcDNA3 transfected (from 6 up to 48 hours post-transfection). PLSCR1, TLR4, TLR9, and IFN- $\alpha$  mRNA levels were quantified by real-time PCR. All the data presented is representative of two independent experiments.

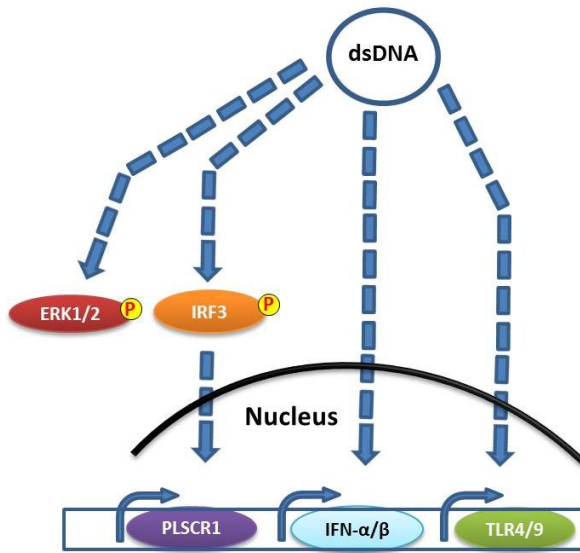
cells may differ to that of T80 cells upon dsDNA entry, we performed dsDNA transfection from 6 to 48 hours in the HEY cell line. As shown in Figure 23A, phosphorylated IRF3 was variable and induction of PLSCR1 was absent at all the time points assessed following dsDNA transfection (relative to mock transfection). Additionally, as shown in Figure 23B, the TLR4 mRNA was not elevated (as we observed for T80 cells (Fig. 17A, Upper panel) although TLR9 mRNA was markedly elevated in HEY cells.

Consistent with the protein level changes, PLSCR1 was also not significantly altered at the mRNA level although IFN- $\alpha$  was elevated at 6 hours post-dsDNA transfection in HEY cells. We did not detect IFN- $\beta$  and IFN- $\gamma$  mRNA in HEY cells transfected with dsDNA. Collectively, these results implicate the presence of an altered TLR signaling pathway in ovarian cancer cells following recognition of dsDNA. Further studies are needed to understand the complete mechanisms and significance of these differential signaling responses in cancer cells.

## **Discussion**

As described in Chapter 1, PLSCR1 expression is upregulated by growth factors including epidermal growth factor (EGF) [19], stem cell factor (SCF) [37], granulocyte colony stimulating factor (G-CSF) [37], cytokines (IFN) [39], and differentiation-inducing agents such as ATRA [40]. Importantly, previous studies including ours (in HEY cells) demonstrate that IFN markedly induces PLSCR1 [39, 177]. This process is mediated via activation of PKC $\delta$ , JNK, and STAT1 [18]. In the current study, we report a novel finding that transfection with dsDNA (plasmid DNA) in normal immortalized ovarian (T80) and mammary (HMEC) epithelial cells also leads to induction of PLSCR1 mRNA and protein levels. We also observed sustained activation of MAPK in the dsDNA transfected cells however, its inhibition by U0126 treatment did not lead to convincing changes in the induced PLSCR1 mRNA levels. Additionally, dsDNA transfection leads to activation of the IRF3, a downstream signaling mediator of TLR signaling [45] (Figure 24). Furthermore, IRF3 knockdown reduces PLSCR1 induction following dsDNA transfection suggesting that IRF3 expression is essential in this process. However, the exact mechanism through which activated IRF3 regulates PLSCR1 expression upon dsDNA transfection remains unknown and needs to be further investigated. As mentioned earlier, PLSCR1 is one of the most induced IFN-stimulated genes and IRF3 activates transcription of IFN along with IFN related genes [45]. Recently studies report that Snail, a transcription factor regulating EMT in cancer cells, binds to the

**Immortalized Normal Ovarian Surface Epithelial Cells (T80)**



**Serous Epithelial Ovarian Cancer Cells (HEY)**

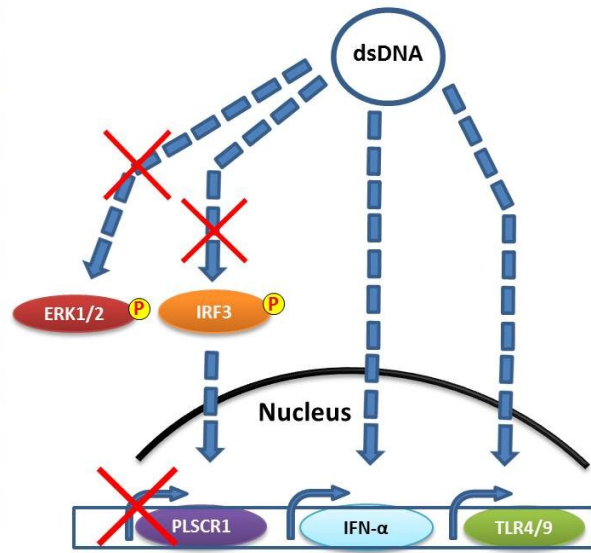


**Figure 24. dsDNA transfection in normal epithelial cells induces PLSCR1 expression mediated by IRF3 activation**

Plasmid dsDNA transfection in normal epithelial cells leads to induction of PLSCR1 via activation of IRF3. dsDNA transfection also results in activation of MAPK (ERK1/2) and induction of TLR4/9 and IFN- $\alpha/\beta$  mRNA. In contrast, in ovarian cancer cells dsDNA transfection does not lead to activation of MAPK or IRF3, thus leading to a lack of PLSCR1 mRNA induction. (\*Model created by Madhav Karthik Kodigepalli)

PLSCR1 promoter to down regulate its expression [146]. In this regard, it would be interesting to identify any potential IRF3 binding sites within the PLSCR1 promoter region to determine whether IRF3 could directly regulate PLSCR1 transcription.

As described earlier, although PLSCR1 is primarily localized to the plasma membrane, it is also localized to various intracellular compartments including the nucleus, endoplasmic reticulum, golgi, and endosomes [19, 24, 42, 133] under specific conditions. For instance, mutation (via site directed mutagenesis [24]) in the palmitoylation site leading to defective palmitoylation or treatment with the



palmitoylation inhibitor 2-bromopalmitate [24], results in nuclear distribution of PLSCR1 in specific cell lines [24]. Previous studies including ours demonstrate that treatment with IFN-2 $\alpha$  not only induces the expression of PLSCR1 but also leads to plasma membrane or nuclear localization of PLSCR1 in specific cells [39, 177]. In the nuclear compartment, PLSCR1 transcriptionally regulates the inositol 1,4,5-triphosphate receptor (IP<sub>3</sub>R) [23] and interaction with components of the DNA replication machinery including topoisomerases [148]. Herein, upon dsDNA transfection in normal ovarian epithelial cells, we noted that the *de novo* synthesized PLSCR1 localizes predominantly to the plasma membrane (~70% of the total cells with PLSCR1 induction) as well as to perinuclear regions (Figure 19B). PLSCR1 localizes to endosomes in plasmacytoid dendritic cells upon stimulation with CpG-ODN [42]. Furthermore, PLSCR1 interacts with TLR9 in the endosomes and regulates TLR9 mediated induction of IFN following CpG-ODN treatment in these cells [42]. Additionally, PLSCR1 knockdown reduces TLR9 levels in the endosomal compartments suggesting that PLSCR1 is important in the translocation of TLR9 from ER to the endosomes. However, our studies indicate that PLSCR1 is localized at the plasma membrane and perinuclear regions upon stimulation with dsDNA in normal ovarian and mammary epithelial cells. The function of *de novo* PLSCR1 at the plasma membrane and endoplasmic reticulum/golgi upon dsDNA transfection requires further investigation.

As described earlier, previous studies suggest a very important role of PLSCR1 in immune cell responses (Figure 6) [4-8]. Recent studies in plasmacytoid dendritic cells implicate PLSCR1 in the regulation of the TLR9 signaling pathway [42]. Additionally, here we show that dsDNA stimulation in normal ovarian and mammary epithelial cells induces PLSCR1 together with activation of IRF3, a downstream TLR signaling mediator. Collectively these results indicate a potential role for PLSCR1 in innate immunity in response to pathogenic/foreign DNA. The exact role of PLSCR1 in the dsDNA responses in T80 cells and whether PLSCR1 is also induced upon activation of TLR signaling by other stimulants such as LPS, CpG-ODN, or viral particles remains to be investigated.

Interestingly, we have noted a striking difference in the effect of dsDNA transfection on PLSCR1, IRF3 and TLRs between normal ovarian epithelial cells and ovarian cancer cells. As shown in Figure 22A, PLSCR1 induction was observed only in normal cells (T80 and PMEC (Figure 18E)) but not in ovarian carcinoma cells (HEY, TOV112D and TOV21G) transfected with dsDNA. Additionally, dsDNA did not lead to increased activation of IRF3 in the cancer cells. Although the basal level of PLSCR1 was elevated in the ovarian cancer cell lines relative to the normal T80 cells, there was no difference in the total IRF3 or phosphorylated IRF3 levels. It remains to be investigated whether other members of the IRF and TLR family are involved in PLSCR1 regulation in these cancer cells. Collectively, these results suggest that the mechanism of PLSCR1 upregulation or IRF3 activation in response to stimulation with dsDNA could be dysregulated in ovarian cancer cells. However, exact role of PLSCR1 in inflammation or innate immunity in ovarian cancer development is currently unknown and needs to be further investigated. Additionally, the detailed signaling pathway events leading to these changes are presently unclear and need to be investigated. Understanding the altered immune responses in ovarian cancer cells could potentially aid in the development of novel immune therapy strategies in the treatment of ovarian cancers.

### **Acknowledgements**

Flow cytometry to determine the transfection efficiency of ovarian cancer cells was carried out with the assistance of Dr. Karoly Szekeres at the College of Medicine, University of South Florida.

## Chapter 6

### Significance of PLSCR1 in Ovarian Cancer and Immunotherapy

#### Overview

Our studies presented herein primarily focus on the role and regulation of SnoN/SkiL (a TGF $\beta$  pathway regulator) and PLSCR1 (an interferon-regulated gene), which are located at 3q26.2 and 3q23, respectively, in epithelial ovarian cancer. In Chapter 3, we delineated a mechanism by which SnoN is modulated upon As<sub>2</sub>O<sub>3</sub> treatment in HEY ovarian cancer cells. As described in Chapter 3, via inhibitor and siRNA mediated knockdown studies, we have now identified that PI3K signaling pathway is responsible for As<sub>2</sub>O<sub>3</sub>-induced change in SnoN expression; we also demonstrate that inhibition of PI3K signaling cascade leads to increased sensitivity of ovarian cancer cells to As<sub>2</sub>O<sub>3</sub> treatment. In Chapter 4, we attempt to identify the role of PLSCR1 in ovarian cancer development and cellular responses to As<sub>2</sub>O<sub>3</sub>. We determined that PLSCR1 is amplified in ovarian cancer patient samples and these DNA copy number changes and mRNA expression changes are correlated. We also identify that SnoN and PLSCR1 mRNA expression in ovarian cancer cell lines is highly correlated in the absence of any significant correlation at the protein level. We also determined that reduced PLSCR1 in ovarian cancer cells leads to increased cellular sensitivity to As<sub>2</sub>O<sub>3</sub> indicating a potential role for PLSCR1 in modulating the chemotherapeutic responses in ovarian cancer cells.

In Chapter 5, we report that dsDNA (empty plasmid) transfection results in upregulation of endogenous PLSCR1 in T80 (normal immortalized ovarian surface epithelial cells) and HMEC (primary mammary epithelial cells), which localizes to the plasma membrane and perinuclear regions. Through siRNA and inhibitor studies, we have identified that IRF3 activation, a downstream event of activated

TLR signaling pathway, is required for PLSCR1 upregulation. Furthermore, dsDNA treatment results in induction of TLR4/9 and IFN $\alpha/\beta$  mRNA in these cells. Strikingly, dsDNA did not result in either induction of PLSCR1 or activation IRF3 in ovarian cancer cells indicating that the TLR signaling cascade may be altered in cancer cells.

### **Regulation of SnoN Expression upon Chemotherapeutic Treatment**

As described in Chapter 1, amplification of chromosome 3q26 region is a common genomic aberration found in various epithelial cancers [10, 12, 29, 30, 245, 246]. Our laboratory and others have identified gene amplifications in specific oncogenes located at the 3q26.2 locus including MECOM (MDS1-EV11 Complex) [10], SnoN (Ski related novel protein N) [9], PKC $\zeta$  (protein kinase C $\zeta$ ) [31], as well as PIK3CA (catalytic subunit of PI3 Kinase) located at 3q26.3 [11] (see Figure 1). In our studies published in 2010 [1], our group has reported that upon As<sub>2</sub>O<sub>3</sub> treatment, SnoN is increased at the RNA and protein levels in contrast to EV11 (at MECOM locus) which is decreased [1, 247]. Furthermore, elevated levels of SnoN appeared to antagonize the As<sub>2</sub>O<sub>3</sub>-induced cell death response by activating a cytoprotective autophagic pathway in ovarian cancer cells [1, 75]. Herein, in Chapter 3, we demonstrate that PI3K (PIK3CA) contributes significantly to the upregulation of SnoN upon As<sub>2</sub>O<sub>3</sub> treatment. SnoN, in contrast to EV11, has a short half-life; indeed, SnoN is regulated by specific E3 ubiquitin ligases such as Smurf2 [85], APC/C [88], and Arkadia [248]. Moreover, our group has recently identified miRNA binding sites in 3'UTR of SnoN which appears to have a role in regulating its expression. This work is currently being pursued by another graduate student from our laboratory (Dutta and Nanjundan, Submitted, 2014). Whether SnoN and the catalytic subunit of PI3K (PIK3CA) are co-amplified or co-regulated in ovarian cancer specimens is currently unknown as well as whether there is a correlation between their expressions with chemotherapeutic responses is also unclear. Further studies need to be advanced in the direction of identifying whether a combinatorial targeting strategy (i.e. SnoN and PIK3CA) in ovarian cancers would result in a synergistic effect to improve patient survival. These studies

could potentially aid in the development of improved strategies for prevention and treatment of ovarian cancers.

### **Phospholipid Scramblase Family Members and Their Impact in Cancer Development**

The role of phospholipid scramblase (PLSCR) family members (PLSCR1, PLSCR2, PLSCR3 and PLSCR4) in cancer initiation and progression is presently unclear. There are only a few reports which implicate PLSCR1 in cancer development. For instance, PLSCR1 is implicated as a tumor suppressor in ovarian cancers; using mouse xenograft studies and a PLSCR1 overexpressing HEY1B ovarian carcinoma cell line, PLSCR1 expression appeared to regress the tumor growth over a period of three weeks [15]. Additionally, recent data in colorectal cancers has implicated PLSCR1 as a potential oncogene [21, 22, 36]; evidence indicates that the intensity of PLSCR1 expression is elevated in colorectal cancer specimens [22]. Furthermore, our work presented in Chapter 4, indicates that PLSCR1 DNA copy number is increased in ovarian cancers. As previously noted, PLSCR1 is located at chromosome 3q23 which lies adjacent to and upstream of the 3q26.2 amplicon which is amplified in epithelial cancers including a subset of breast, head and neck, esophageal, cervical, and ovarian carcinomas [12, 29, 30, 245, 246, 249]. Thus far, there is no evidence implicating other members of the scramblase family (PLSCR2, PLSCR3 and PLSCR4) in cancer development. It is interesting to note that PLSCR2 and PLSCR4 are located adjacent to PLSCR1 at the 3q24 chromosomal locus whereas PLSCR3 is located on chromosome 17p13.1. As shown in Figure 5, there is a high degree of homology amongst the protein sequences of PLSCR2, PLSCR3, PLSCR4 and PLSCR5 (73.63%, 50.00%, 48.14% and 57.36% identity, respectively) when compared to PLSCR1 [131].

Therefore, in order to advance our knowledge of PLSCR1 in cancer development, we proceeded to analyze ‘The Cancer Genome Atlas’ (TCGA) genomics data using the cBioPortal bioinformatic program [230, 231]. As presented in Table 9, we have noted a highly similar level of DNA copy number changes (~14% each) between PLSCR1 (80/569), PLSCR2 (81/569), PLSCR4 (81/569) and PLSCR5 (79/569) (altered at ~20% altogether in 569 ovarian cancers) (Figure 25, Upper panel) while all the four

were co-amplified in 14% (79/569) of the patients. Furthermore, as shown in Figure 26, we noted that there is a strong and significant tendency for these three scramblases to co-occur indicating a potential similarity in function. However, although the PLSCR1, PLSCR2, PLSCR4 and PLSCR5 DNA copy number changes were similar (Figure 25, Upper panel), their mRNA expression in ovarian cancers were vastly different (Figure 25, Lower panel). This difference between the pattern of DNA copy number changes and mRNA expression changes indicates that these phospholipid scramblase family member genes may have very different regulatory mechanisms. In addition, with regards to PLSCR3 (Table 9 and Figure 25), its DNA copy number profile differs markedly from that of the other family members, thus implicating PLSCR3 in an independent function.

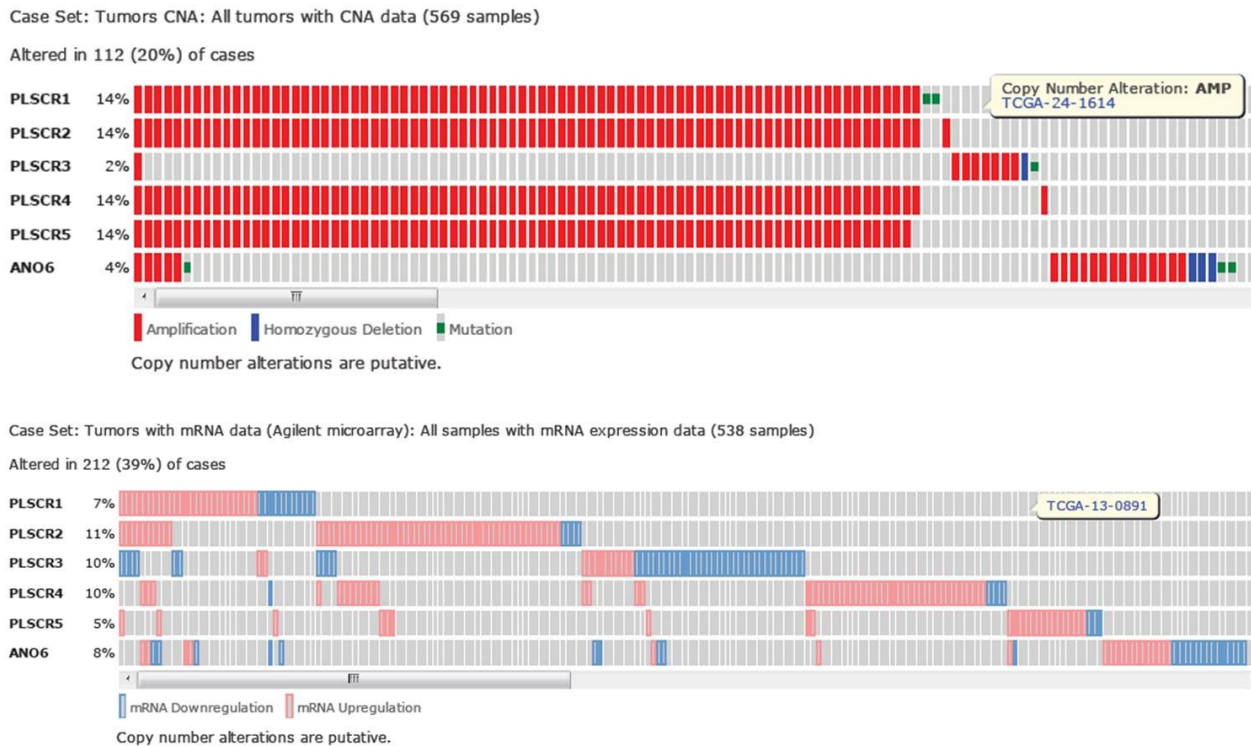


**Figure 25: Altered DNA copy number levels and mRNA expression of PLSCR family members in ovarian cancers**

TCGA (The Cancer genome Atlas) ovarian carcinoma genomic data was analyzed via cBioPortal bioinformatic program (<http://www.cbioportal.org/public-portal/>) to determine the DNA copy number variations (Upper panel) and altered mRNA expression of PLSCR1, PLSCR2, PLSCR3, PLSCR4, PLSCR5 and ANO6 (TMEM16F).

Based on the above described data, we propose that a thorough analysis of additional ovarian cancer specimens should be performed in order to validate the bioinformatically analyzed TCGA data; we propose to assess (1) DNA copy number level changes using a real-time PCR-based approach, (2) mRNA level changes by utilizing specific FAM-labeled qPCR probes/primers, and (3) protein level changes by

Gene	PLSCR4	PLSCR2	PLSCR1	PLSCR5	ANO6	PLSCR3
PLSCR4	---	<0.000001	<0.000001	<0.000001	0.362591	0.265102
PLSCR2		---	<0.000001	<0.000001	0.419211	0.417343
PLSCR1			---	<0.000001	0.149527	0.133332
PLSCR5				---	0.460002	0.282027
ANO6					---	0.08616
PLSCR3						---

p-values <0.05, as derived via Fisher's Exact test are outlined in red. p-values are *not* adjusted for FDR.

Legend
Strong tendency towards mutual exclusivity (0 < Odds Ratio < 0.1)
Some tendency towards mutual exclusivity (0.1 < Odds Ratio < 0.5)
No association (0.5 < Odds Ratio < 2)
Tendency toward co-occurrence (2 < Odds Ratio < 10)
Strong tendency towards co-occurrence (Odds Ratio > 10)
No events recorded for one or both genes

**Figure 26: Mutual exclusivity/co-occurrence of alterations of PLSCR family members in ovarian cancers**

Mutual exclusivity or co-occurrence of DNA copy number and mRNA expression alterations of the PLSCR family members and ANO6 in ovarian carcinomas was determined via cBioPortal bioinformatic program (<http://www.cbioportal.org/public-portal/>).

using validated antibodies for western analysis to assess the protein expression of PLSCR family members. We have made attempts to assess currently available antibodies for PLSCR2, PLSCR3 and PLSCR4 (Table 10A). However, with these antibodies, we could not detect their endogenous protein in any of our cell lines under our experimental conditions. Moreover, in the absence of a positive control (i.e. respective cDNA constructs to allow their overexpression in mammalian cells followed by their

**Table 9: Altered DNA copy number and mRNA expression of PLSCR family members in ovarian cancers (cBioPortal Analysis)**

TCGA (The Cancer genome Atlas) ovarian carcinoma genomic data was analyzed via cBioPortal bioinformatic program (<http://www.cbioportal.org/public-portal/>) to determine the percent of patients with DNA copy number variations, altered mRNA expression, and mutations of PLSCR1, PLSCR2, PLSCR3, PLSCR4, PLSCR5 and ANO6 (TMEM16F).

No.	Protein name	Amplification (DNA:CNA) (569 samples)	Mutations		RNA level expression (538 samples)
			% mutated	Mutations	
1.	PLSCR1	14%	0.6% (2/316)	A88V D301H	7%
2.	PLSCR2	14%	None	-	11%
3.	PLSCR3	2%	None	-	10%
4.	PLSCR4	14%	0.3% (1/316)	T96M	10%
5.	PLSCR5	14%	None	-	5%
5.	ANO6	4%	0.9% (3/316)	E257Q, L601F, R700T	8%



detection by western blotting), we were unable to ascertain with confidence whether or not these antibodies could detect endogenous PLSCR family members. In future studies, we will obtain validated antibodies which recognize these proteins in several assays including western analyses, immunocytochemistry, immunohistochemistry, as well as reverse phase protein array (RPPA) analyses. In the case that such antibodies are commercially unavailable, we plan to formulate these antibodies independently. Table 10B provides the list of some of the currently available antibodies specific for PLSCR2, PLSCR3 and PLSCR4.

**Table 10: List of (A) assessed and (B) commercially available antibodies for PLSCR family members**

**A**

Antibody	Source	Catalog No.	Dilution
PLSCR2	Santacruz	SC-103122	1:500
PLSCR3	Santacruz	SC-68122	1:500
PLSCR4	Santacruz	SC-68124	1:500

**B**

Protein	Source-1	Source-2	Source-3	Source-4
PLSCR2	Life Span Biosciences (LS-C152181)	Aviva Systems Biology (OAAB03222)	Atlas Antibodies (HPA051352)	Abcam (AB135425)
PLSCR3	Novus Biologicals (NBP1-33072)	BioRbyt (ORB101767)	He Y et al. JCB, 2007	Inzuka et al. Bioscience reports, 2013
PLSCR4	Life Span Biosciences (LS-C163801)	Aviva Systems Biology (OAAB10272)	Atlas Antibodies (HPA002276)	Abcam (AB116672)

Although the tissue microarray (TMA) profiling studies reported in colorectal cancers suggested that PLSCR1 was overexpressed in these tissues [22], there was no presented data or discussion regarding the subcellular distribution of PLSCR1; thus, it remains unclear whether the localization of PLSCR1 is altered in the development of cancer. This is an important concept to assess since PLSCR1 can be localized to multiple subcellular sites including plasma membrane, nucleus, endoplasmic reticulum (ER),

**Table 11: Altered DNA copy number, mRNA expression, and mutations of PLSCR1 in cancers (cBioPortal Analysis)**

cBioPortal bioinformatic program (<http://www.cbioportal.org/public-portal/>) was used to analyze the TCGA cancer genomic data to determine the percent of patients with DNA copy number variations, altered mRNA expression, and mutations of PLSCR1 in various cancers including ovarian carcinoma, breast invasive carcinoma, head and neck squamous cell carcinoma, lung carcinoma, cervical carcinoma, pancreatic ductal adenocarcinoma, uterine corpus endometrioid carcinoma and stomach adenocarcinoma.

No.	Cancer Type	PLSCR1 Amplification (DNA:CNA)	MECOM Amplification (DNA:CNA)	Mutations		RNA level expression
				% mutated	Mutations	
1.	Ovarian Serous cystadenocarcinoma	14% (80/569)	37% (212/569)	0.6% (2/316)	A88V D301H	7% (37/538)
2.	Breast Invasive Carcinoma	10% (102/1033)	4% (46/1033)	none	-	8% (90/1062)
3.	Head and Neck Squamous cell carcinoma	16% (49/306)	19% (57/306)	1% (3/306)	F30L P23R 72_78 del	7% (36/497)
4.	Lung Adenocarcinoma	2% (5/230)	4% (10/230)	0.4% (2/229)	R5L G20W	9% (3/32)
5.	Lung Squamous Cell Carcinoma	21% (37/179)	34% (60/179)	1.1% (2/177)	P56L M289I	8% (12/154)
6.	Cervical squamous/endocervical adenocarcinoma	21% (41/192)	20% (30/192)	none	-	16% (33/212)
7.	Pancreatic ductal adenocarcinoma	-	4% (2/50)	none	-	6% (3/50)
8.	Colorectal adenocarcinoma	0% (0/589)	0% (0/589)	1% (2/223)	T218A R151Q	5% (12/222)
9.	Uterine Corpus endometrioid carcinoma	3% (11/363)	8% (28/363)	1.6% (5/248)	Q31R, Q90H, E171*, R5Q, H111N	6% (3/54)
10.	Stomach Adenocarcinoma	2% (5/293)	7% (20/293)	0.9% (2/220)	N5_Splice S315L	3% (1/36)

Golgi, and endosomes [19, 24, 133]. Therefore we propose that a thorough analyses of PLSCR1 expression and its localization should be performed via tissue microarray in available ovarian and pancreatic cancer specimens with one of our collaborators. We propose to assess the localization of PLSCR1 in such TMA samples to determine whether PLSCR1 elicits altered expression and localization which may support a role for PLSCR1 in the development and aggressiveness of these cancers. The functionality of PLSCR1 at these locations has been previously reported; at the plasma membrane,

PLSCR1 appears to regulate growth factor receptor signaling and receptor trafficking [144] whereas in the nucleus, PLSCR1 appears to regulate the transcription of the inositol triphosphate receptor (IP<sub>3</sub>R) [23].

**Table 12: Mutations identified in PLSCR1 in cancers (COSMIC Analysis)**

COSMIC bioinformatic program (<http://cancer.sanger.ac.uk/cancergenome/projects/cosmic/>) was used to analyze the to identify the percent of patients with mutations in PLSCR1 in various cancers including ovarian carcinoma, breast carcinoma, lung carcinoma, cervical carcinoma, pancreatic ductal adenocarcinoma, and stomach adenocarcinoma

No.	Cancer Type	Mutations	
		% mutated	Mutations
1.	Ovarian serous carcinoma	0.6% (3/489)	P23A, A88V, D301H
2.	Breast Carcinoma	0.1% (1/978)	F304I
3.	Lung Adenocarcinoma	0.6% (4/608)	P27L, G35V, G200C, G204V
4.	Lung Squamous Cell Carcinoma	1.1% (2/181)	P56L, M289I
5.	Cervical squamous/endocervical adenocarcinoma	none	-
6.	Pancreatic ductal adenocarcinoma	none	-
8.	Stomach Adenocarcinoma	none	-

In addition to ovarian carcinomas, we also analyzed the PLSCR1 DNA level copy number and RNA expression alterations in various other epithelial cancers. As shown in Table 11, by cBioPortal (<http://www.cbioportal.org/public-portal/>) analyses, we noted that PLSCR1 was markedly amplified in head and neck carcinoma (16%), lung squamous cell carcinoma (21%) and cervical squamous carcinoma (21%). Interestingly, as reported earlier, we also noted amplification of MECOM (MDS1-EVI1 complex, located at 3q26.2) in more cases of ovarian carcinoma (37%), head and neck carcinoma (19%), lung

squamous carcinoma (34%) and cervical carcinoma (20%) relative to PLSCR1 amplification. Additionally, mutational analysis of PLSCR1 on the available TCGA data indicates that about 0.6% of ovarian carcinoma patients harbored a mutation in the PLSCR1 gene (A88V and D301H) (See Table 9 and 11). In addition, we have identified up to three patients with mutations in PLSCR1 using COSMIC (<http://cancer.sanger.ac.uk/cancergenome/projects/cosmic/>) (Table 12) bioinformatic program, respectively. We suggest that mutational analyses of PLSCR1 is important since such amino acid mutations could potentially be associated with altered functionality and subcellular localization in ovarian carcinoma cells. Indeed, investigator-initiated cysteine to alanine mutations in the palmitoylation site (<sup>184</sup>CCCPC<sup>189</sup>) of PLSCR1 alters its localization from the plasma membrane to the nuclear compartment where it binds to genomic DNA and functions as a transcriptional regulator [24, 148, 157]. Therefore, in cancer specimens associated with PLSCR1 mutations, altered PLSCR1 function and altered subcellular localization may be expected. As shown in Tables 11 and 12, PLSCR1 was mutated in 0.6% of the ovarian cancer patients and ranging from 0.4 to 1.1% in other cancers. We further noted that these mutations included predominantly missense mutations along with one deletion mutation. The complete list of mutations in PLSCR1 in different cancer patient samples is summarized in Tables 11 and 12. Interestingly, we noted that many of the mutations (14 out 29 mutations) were in the N-terminal region of PLSCR1 (1-100 amino acids) which is the proline-rich region within PLSCR1 that harbors various interaction sequences allowing it to bind with various proteins of signaling importance [18, 19, 133]. In addition, we noted that 5 patients had mutations in the C-terminal transmembrane region of PLSCR1 (289-304 amino acids). We also assessed the mutational status of the other three members of the scramblase family (PLSCR2, PLSCR3, PLSCR4 and PLSCR5). As shown in Table 9, only one ovarian cancer patient had a missense mutation (T96M) in PLSCR4; no mutations were identified in PLSCR2, PLSCR3 and PLSCR5 in any of the ovarian cancer specimens assessed (TCGA and COSMIC databases).

We have generated different HA-tagged PLSCR1 variants harboring deletions/mutations: (1) deleted N-terminal region and (2) C-terminal regions (as described in Chapter 2 (Page 35)). These constructs include HA-tagged WT PLSCR1 (wild type), HA-tagged C/A-PLSCR1 (palmitoylation

mutant), HA-tagged  $\Delta$ N-PLSCR1 (deletion of the N-terminal 1-97 amino acids), and HA-tagged  $\Delta$ TM-PLSCR1 (deletion of the C-terminal 287-318 amino acids). These have all been successfully cloned into the retroviral vector pQCXIN and expression validated in T80 cells (Appendix A). In the future, these constructs can be utilized to identify the significance of these regions to PLSCR1 localization and function.

We have also generated multiple cancer cell lines that stably knockdown expression of PLSCR1 using a retroviral shRNA-based approach. A comprehensive list of all the PLSCR1 knockdown cell lines that were generated is presented in Table 6 in Chapter 2 (Page 38). Unfortunately, thus far, we have not been able to identify any significant functional changes of PLSCR1 knockdown in these cell lines at this point (note: only cell survival assays were performed (cleaved PARP, changes in LC3, and cell viability assays)). However, knowing that PLSCR2 and PLSCR4 are located adjacent and co-amplified and co-expressed with PLSCR1 (as shown in Table 9 and Figures 25 and 26), it is highly possible that phospholipid scramblase family members may elicit redundant function and therefore may be able to compensate for the loss of PLSCR1 expression. Moreover, knockdown of PLSCR1 may have resulted in an upregulation of the PLSCR2 and/or PLSCR4 proteins (or possibly even PLSCR3). Therefore, to address this issue, one could generate a cell line with a double or triple knockdown of PLSCR1, PLSCR2, and PLSCR4 (and PLSCR3) proteins in order to assess the functional outcome of knocking down the three scramblase family members.

From cBioPortal analyses of PLSCR1 in various cancers, we noted that the in pancreatic ductal adenocarcinomas (PDAC) and colorectal adenocarcinomas, PLSCR1 mRNA levels were in fact increased in 6% and 5% of patients respectively in absence of any DNA copy number changes (Table 11). This variation could indicate that there may be mutations in the PLSCR1 promoter or introns (regulatory regions) or other mechanisms leading to its upregulation including changes in the miRNAs expression pattern. Based on this data, we have performed *in silico* miRNA analyses using commonly used bioinformatic programs including TargetScanHuman, miRDB, miRANDA, and MicroCosm and utilizing

the 3' untranslated region (3'UTR) of PLSCR1 from Switchgear Genomics (S807025, NM\_021105 (NCBI)). Figure 27 shows the Venn-diagram summarizing all the potential “top hits” for miRNAs that

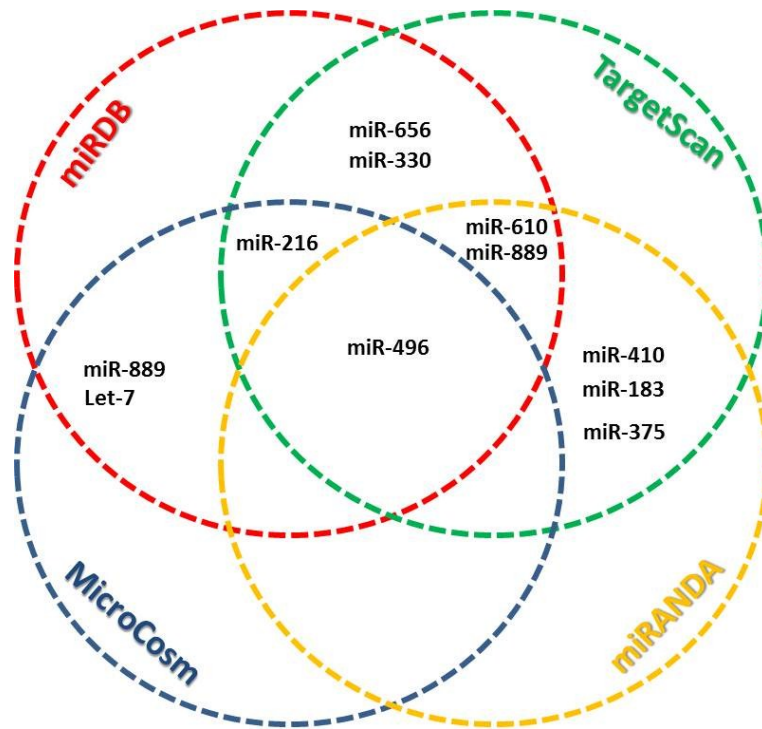
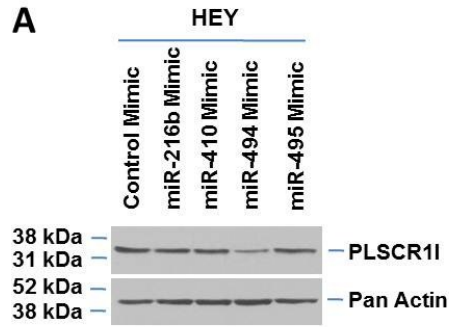


**Figure 27: miRNAs with putative binding sites in the 3'UTR of PLSCR1**

PLSCR1 3' untranslated region (UTR) (Switchgear Genomics (S807025, NM\_021105 (NCBI)) was analyzed via bioinformatic programs including TargetScan, miRDB, MicroCosm, miRANDA for identifying miRNAs with putative binding sites. Venn-diagram was constructed to identify the miRNA “top hits” with binding sites in 3' UTR of PLSCR1. (\*Created by Madhav Karthik Kodigepalli)

may bind to the 3'UTR of PLSCR1. We then assessed the PubMed literature for these “top miRNA hits” to identify any experimental data implicating them in modulating “hallmarks” of cancer. Indeed, we noted that some of these top hits miR-610, miR-216 and miR410 were implicated in different cancers including gastric cancer, hepatocellular carcinoma, glioma, neuroblastoma, and pancreatic cancers [250-254]. In order to identify whether any of these miRNAs that have putative binding sites on PLSCR1 3' UTR could regulate PLSCR1 expression, we transfected HEY ovarian cancer cells with mimics of miR-216b, miR-



**B** (miR-494 binding site: ATGTTTC)

```

AGGAACAAAAATCAGGAGTGTGGTAGTGGATTAGTGAAAGTCTCCTCAGGAAATCTGAAGTCTGTATATTGATTG
AGACTATCTAAACTCATACCTGTATGAATTAAGCTGTAAGGCCTGTAGCTCTGGTTGTATACTTTTGCCTTTTCAAATT
ATAGTTTATCTTCTGTATAACTGATTTATAAAGGTTTTGTACATTTTTTAATACTCATTGTCAATTTGAGAAAAAGG
ACATATGAGTTTTTGCATTTATTAATGAAACTTCCTTTGAAAAACTGCTTTGAATTATGATCTCTGATTCAATGTTCCA
TTTTACTACCAAATATTAAGTAAAGGCCTTATTAATTTTTATATAAAATTATATCTTGTCTTAAATCTAGTTACAATT
TATTTTCATGCATAAGAGCTAATGTTATTTTCAAATGCCATATATTCAAAAAAGCTCAAAGATAATTTCTTTACTAT
TATGTTCAAATAATATCAATATGCATATTATCTTTAAAAAGTTAAATGTTTAAATCTTCAAGAAATCATGCTAC
ACTTAACCTTCTCCTAGAAGCTAATCTATACCATAATTTTTCATATTCACAAGATATTAATTAACCAATTTTCAAATTA
TTGTTAGTAAAGAACAAAATGATTCTCTCCCAAAGAAAGACACATTTTAAATACTCCTTCACTCTAAAACCTCTGGTA
TTATACTTTTGAAGGTAATATTTCTACATGAAATGTTTAGCTCTTACACTCTATCCTTCTAGAAAATGGTAATTG
AGATTACTCAGATATTAATTAACAATATCATATATATTTACAGAGTATAAACCTAAATAATGATCTATTAGA
TTCAAATATTTGAAAATAAAAACCTTGATTTTTTTGTATTTTGTATTTTGTATTTTAAACGAAATGTGTTTCAGATGGTATT
TTGAGCACTCATTGATTAATGATGGTACATTTGAAGCAGGATATTTCCCTGA

```

**Figure 28: miR-494 reduces PLSCR1 protein**

(A) HEY ovarian cancer cells were transfected with control mimic or with mimics of miR-216b, miR-410, miR-494 and miR-495 using Fugene HD transfection reagent. Cell lysates were harvested 96 hours post-transfection and were analyzed via western blotting for the indicated antibodies. (B) 3'UTR sequence of PLSCR1 (Switchgear Genomics (S807025, NM\_021105 (NCBI)) was utilized to identify miR-494 binding site (ATGTTTC). Imperfect miR-494 binding sites (ATGTTT) are highlighted.

410, miR-494 and miR-495. Interestingly, although miR-494 was not identified by any of the bioinformatic programs (Figure 27) to have a putative binding site in the 3'UTR of PLSCR1, as shown in Figure 28A, transfection with miR-494 mimic resulted in a marked reduction in PLSCR1 protein relative to control mimic. This suggests that miR-494 might regulate the expression of PLSCR1 in ovarian cancer cells. Interestingly, as shown in Figure 28B, although PLSCR1 3'UTR did not have perfect miR-494 binding sites, we identified that miR-494 has two imperfect 'ATGTTT' binding sites in the 3' UTR of PLSCR1 (Figure 28B). Further studies are needed to determine whether miR-494 directly binds to the

3'UTR of PLSCR1 through these indirect binding sites and to validate and understand the complete mechanism mediating this process.

### **Scrambling Activity of PLSCR1**

Historically, phospholipid scramblases were associated with the function of phospholipid scrambling [34, 35], maintaining the plasma membrane asymmetry by translocating phospholipids from the inner leaflet to outer leaflet of plasma membrane. Indeed, externalization of phosphatidylserine (PS) to outer leaflet of plasma membrane in apoptotic cells is an event that aids in their recognition and clearance by macrophages which was earlier credited to PLSCR1 function [34, 37]. Additionally, *Scrm1*, the *C. elegans* homolog of PLSCR1, was shown to be required for PS externalization in apoptotic germ cells [135]. However, later studies performed in PLSCR1<sup>-/-</sup> mice did not demonstrate altered scrambling activity and PS exposure and further, the mice also did not exhibit any bleeding disorders suggesting PLSCR1 might not be a major player in this process [37, 116]. Later in 2012, using Scott Syndrome cells that are deficient in PLSCR activity and a screening approach, TMEM16F, a calcium dependent chloride channel, was identified to be responsible for the PS externalization and deficiency of scramblase activity in the Scott Syndrome patients [117, 121, 178]. Furthermore, reconstitution of PLSCR1 in these cells did not alter the scramblase activity indicating that PLSCR1 is not critically responsible for the scrambling of phospholipids. Via cBioPortal analyses (Table 9), we noted that the copy number and mRNA expression alterations of TMEM16F (*Ano6*, located at chromosome 12q12) in ovarian cancers was markedly different to that of the members of the phospholipid scramblase family. Furthermore, we also noted that DNA copy number changes and mRNA expression levels between TMEM16F and PLSCR1 were not correlated (Figure 25 and 26). As shown in Figure 4B in Chapter 1, bulk of PLSCR1 protein is in the cytoplasm with only one c-terminal end transmembrane region. It would be interesting to determine how PLSCR1 can regulate phospholipid scrambling with only one transmembrane domain. In this regard, it could be possible that PLSCR1 could potentially interact with other known scramblases such TMEM16F (with 8 transmembrane regions) and thus regulating the scramblase activity indirectly. In this regard, we



would determine any possible interaction between PLSCR1 and TMEM16F. We would perform REMTH (retrovirus based mammalian two hybrid screen) to identify all the interaction partners of TMEM16F and perform PCA (protein complementation assay) to validate the interaction between TMEM16F and PLSCR1. As mentioned in above, although, PLSCR1<sup>-/-</sup> deficient mice exhibited normal PS externalization, it is important to consider the role of other members of PLSCR family which also have been shown to regulate the scrambling activity [136, 138, 174]. In this regard it would be important to generate multiple knockout mice of PLSCR family members and then examine whether scramblase activity is still unaltered in presence of calcium or in apoptotic cells. In this regard, we have looked at the existing PLSCR members knockout mouse models. PLSCR1<sup>-/-</sup> and PLSCR3<sup>-/-</sup> mice have been generated and utilized for previous studies by Sims et al. [255]. Additionally PLSCR2<sup>-/-</sup> are available at the UC Davis knockout mouse project (KOMP) repository. In order to generate the PLSCR4<sup>-/-</sup> and multiple knockout mice, we would employ the CRISPR (clustered regularly interspaced short palindromic repeats) cas9 genetic deletion system based approach.

### **Role of PLSCR1 in Modulating Autophagic Flux**

Recent studies implicate PLSCR3 in regulating mitophagy [178], a form of autophagy that specifically targets the damaged mitochondria to the autophagosomes for degradation. Using SH-SY5Y human neuroblastoma cells, it was demonstrated that PLSCR3 regulates the externalization of cardiolipin from the inner to the outer mitochondrial membrane; this is an event that aids in the recognition and delivery of the mitochondria to the autophagosomes [178]. Apart from this report, there is no other reported evidence implicating the other phospholipid scramblase members (including PLSCR1) in the process of autophagy.

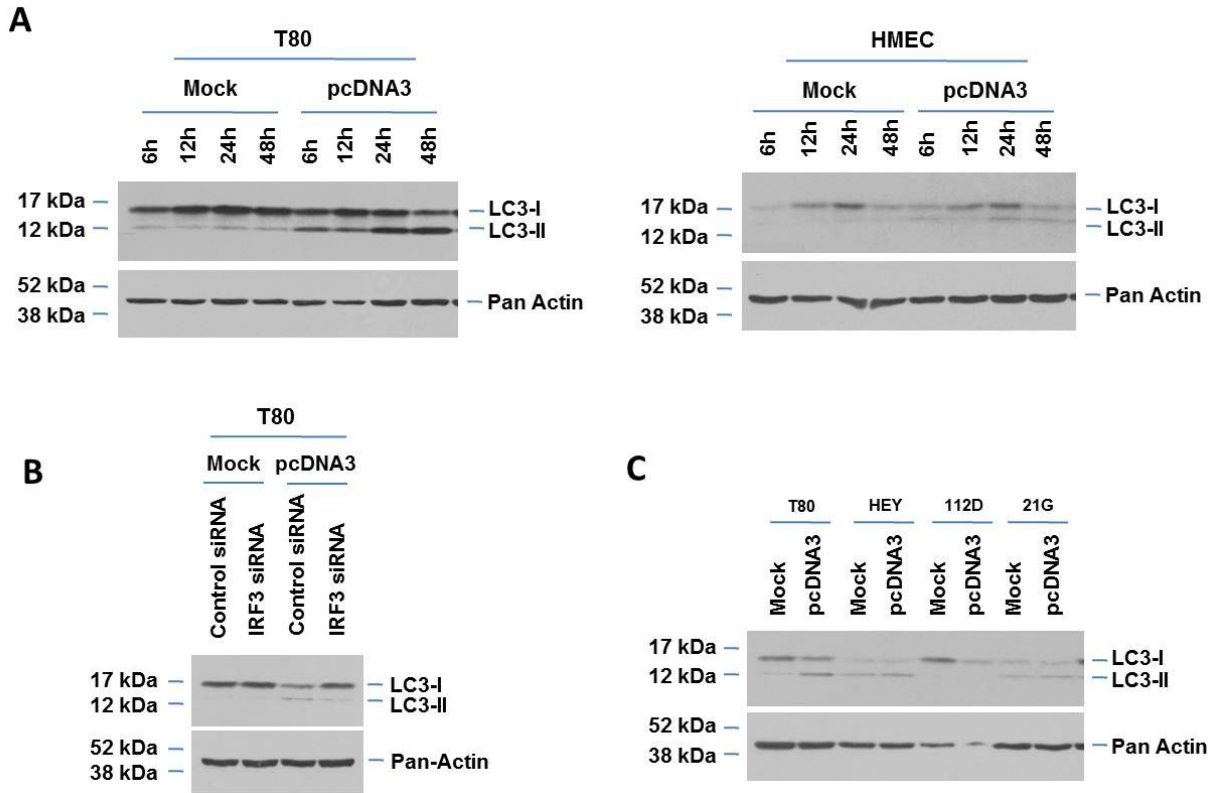


**Figure 29: IRF3 knockdown reduces the dsDNA transfection-induced increase in LC3-II levels in normal epithelial cells**

(A) T80 (Left panel) and HMEC cells were transfected with empty pcDNA3 plasmid or transfection reagent only (“mock”). Cell lysates were harvested from 6 up to 48 hours post-transfection and analyzed via western blotting with the indicated antibodies. (B) Empty plasmid or mock transfection was performed in T80 cells that were treated with IRF3 siRNA. Cell lysates were isolated at 48 hours following transfection and analyzed via western blotting with the indicated antibodies. (C) T80, HEY, TOV112D, and TOV21G cells were “mock” or empty pcDNA3 transfected. Cell lysates were collected 48 hours post-transfection followed by western analysis with the indicated antibodies.

From our studies presented in Chapter 4, we have observed that siRNA-mediated knockdown of PLSCR1 markedly reduced the LC3B levels in HEY ovarian cancer cells treated with  $As_2O_3$ . This observation implicates PLSCR1 in process of autophagy. Furthermore, we have noted that dsDNA transfection in normal ovarian and mammary epithelial cells leads to a marked increase in LC3-II levels (Figure 29A, Right and Left panels). It is currently unclear whether the induction of PLSCR1 and LC3-II

upon dsDNA transfection is linked. Interestingly, we also noted that knockdown of IRF3, which leads to reduction in PLSCR1 induction levels, alters the LC3-I to LC3-II ratio (Figure 29B). It is unknown whether knockdown of IRF3 would modulate other important autophagic mediators such as ATG5, ATG7, ATG9, hVps34, and beclin-1. In addition, knockdown of PLSCR1 using siRNA could provide evidence of altered LC3B levels and punctae formation upon dsDNA transfection in T80 or HMEC cells. If, indeed, we find changes in the autophagic response upon knockdown of IRF3 or PLSCR1, further studies are needed to investigate the mechanism by which PLSCR1 modulates the autophagic responses. Based on the preliminary data, as shown in Figure 30, we propose an important role of PLSCR1 and IRF3 in regulating the process of autophagy in response to treatment with chemotherapeutic agents ( $As_2O_3$ ) (Left panel) and dsDNA (Right panel).

### **PLSCR1 and Cancer Immunotherapy**

Ovarian cancer is one of the most common causes of gynecological cancer related deaths in women. In 2014 alone, it is estimated that there would be 14,270 deaths due to ovarian cancer and incidence of 21,980 new cases (National Cancer Institute, SEER 18 2004-2010). Although we have made considerable progress in understanding ovarian cancer and there have been considerable improvements in treatment strategies, the 5-year survival rate has been a meager 44.6 % (National Cancer Institute, SEER 18 2004-2010). Therefore, there is a dire need for novel treatment strategies for this devastating disease. Based on our work presented in Chapter 5, we propose that PLSCR1 could potentially be a promising target to improve treatment of ovarian cancer using an immunotherapeutic approach. As presented in Chapter 5, when we treated normal and cancer cells with dsDNA molecule, we noted that in T80 (normal ovarian epithelial cells) and HMEC (primary mammary epithelial cells), there was a marked upregulation of PLSCR1, the most highly inducible IFN responsive gene. On the other hand, in ovarian cancer cells, there were no marked changes in the expression of PLSCR1. A similar pattern was also noted for the

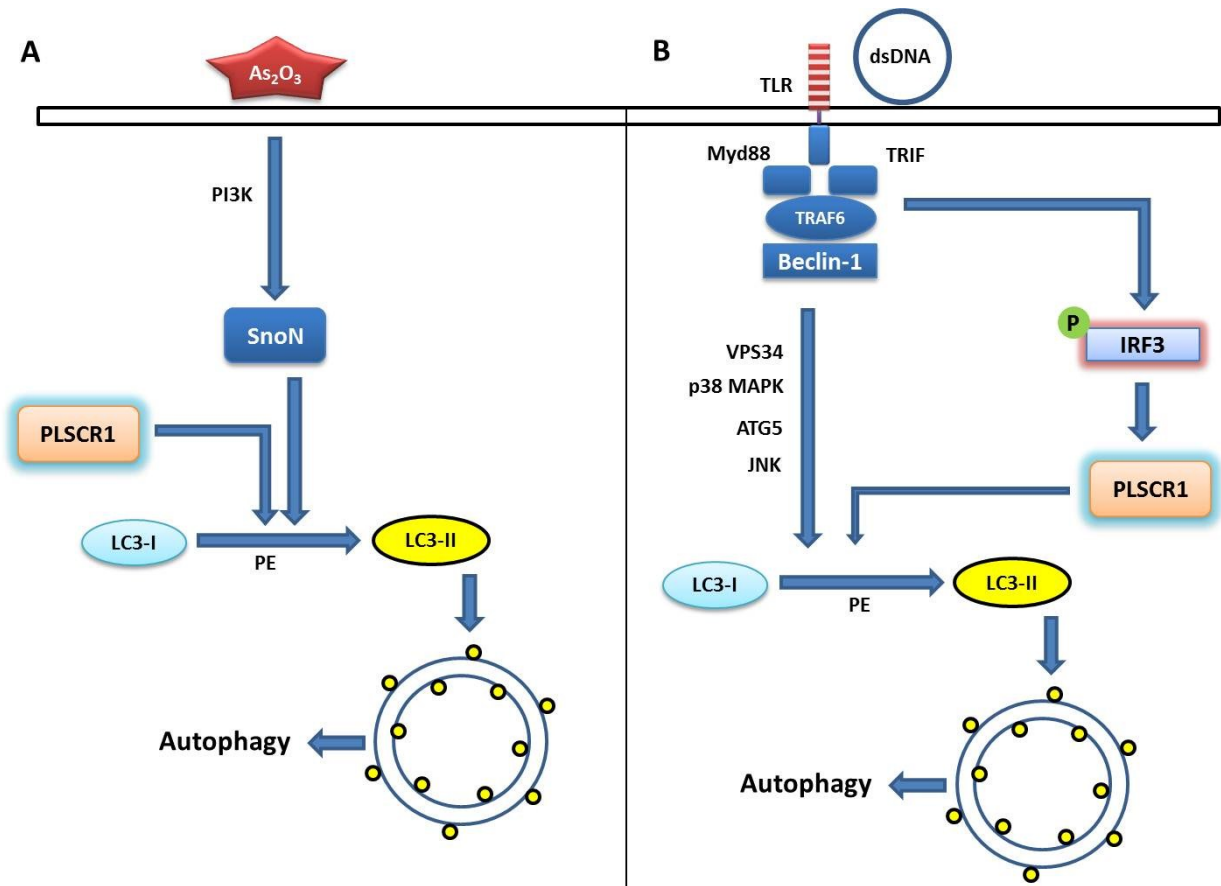


**Figure 30: Schematic of the proposed role of PLSCR1 and IRF3 in autophagic regulation**

(A)  $As_2O_3$  treatment results in induction of cytoprotective autophagy in ovarian cancer cells [1]. Since PLSCR1 reduction via siRNA results in increased apoptosis and decreased conversion of LC3-I to LC3-II (Figure 16E), we propose that PLSCR1 might potentially regulate the process of autophagy in ovarian cancer cells in response to chemotherapeutic treatment. (B) dsDNA transfection leads to activation of IRF3, induction of PLSCR1 consistent with increased levels of LC3-I to LC3-II conversion, which is ablated by siRNA mediated reduction of IRF3. Therefore, we propose that IRF3 activation and PLSCR1 induction might be critical to process of dsDNA-induced autophagy in normal epithelial cells. (\*Model created by Madhav Karthik Kodigepalli)

activation of IRF3 upon dsDNA transfection in these cell lines. These results could suggest that the mechanism of PLSCR1 upregulation or IRF3 activation is dysregulated in ovarian cancer cells. The detailed signaling pathway events leading to these changes are presently unclear and need to be investigated. Mechanisms of interaction between tumor cells and the cells associated with immune system such as dendritic cells (DCs), macrophages, and natural killer T cells, also needs to be investigated further

with respect to the role of PLSCR1. In this regard, an *in vitro* co-culture system based approach may be appropriate for such studies. Mouse models bearing ovarian tumors could be studied for such *in vivo* interactions within an intact tumor microenvironment. Typically, TLRs that are activated upon entry of pathogenic or foreign nucleic acids would stimulate the DCs allowing them to differentiate into antigen specific T cells. Indeed, stimulants of TLR signaling could be classified as ‘vaccine adjuvants’ which would specifically target TLR9 in endosomes; this pathway is well studied in terms of innate immunity and protection against bacterial and viral infections. A similar activation could be used to eliminate the tumor cells. Therefore, the uptake of these foreign DNAs into ‘effector’ cells could promote their anti-tumor characteristics. PLSCR1 overexpression in HEY1B ovarian cancer cells that were subcutaneously administered to athymic nude mice showed a marked reduction in tumor volumes overtime relative to control cells with no PLSCR1 overexpression [15]. Whether the host mouse immune responses played a role in progression of these tumors that overexpressed PLSCR1 is presently unknown. Therefore, it would be interesting to investigate this further by using a different mouse model having intact immune system.

### **Prospective Studies**

Specific Aim 1: To determine localization and function of PLSCR members in the aggressiveness and chemoresistance in ovarian and pancreatic cancers.

- I. We will perform immunohistochemical analyses for PLSCR family members in ovarian and pancreatic cancer tissue specimens. We will determine whether the expression and localization of these proteins is altered in these cancers.
- II. We will generate ovarian and pancreatic cancer cell lines with double or triple knockdown of PLSCR1, PLSCR2 and PLSCR4 to assess their function in these cancers.

Specific Aim 2: To delineate the mechanisms by which IRF3 and PLSCR1 modulate the dsDNA-induced autophagy in normal epithelial cells.

- I. We will perform PLSCR1 siRNA mediated knockdown experiments to determine the role of PLSCR1 in mediating the dsDNA-induced autophagy in T80 and HMEC cells.
- II. We will perform IRF3 knockdown studies to determine its role in dsDNA-induced autophagy in T80 and HMEC cells.
- III. We will further determine the role of PLSCR1 and IRF3 in dsDNA-induced autophagy by identifying whether these proteins interact directly with the autophagy mediators.

Specific Aim 3: To delineate the mechanism leading to altered immune responses in ovarian cancer cells upon dsDNA transfection.

- I. We will perform siRNA or specific inhibitor mediated strategies against mediators of TLR signaling to delineate the complete mechanism of dsDNA-induced immune responses in T80 immortalized normal ovarian surface epithelial cells and ovarian carcinoma cells.

## References

1. Smith, D.M., et al., *Arsenic trioxide induces a beclin-1-independent autophagic pathway via modulation of SnoN/SkiL expression in ovarian carcinoma cells*. Cell Death Differ, 2010. 17(12): p. 1867-81.
2. Levine, B. and D.J. Klionsky, *Development by self-digestion: molecular mechanisms and biological functions of autophagy*. Dev Cell, 2004. 6(4): p. 463-77.
3. Levine, B. and G. Kroemer, *Autophagy in the pathogenesis of disease*. Cell, 2008. 132(1): p. 27-42.
4. Dong, B., et al., *Phospholipid scramblase 1 potentiates the antiviral activity of interferon*. J Virol, 2004. 78(17): p. 8983-93.
5. Kusano, S. and Y. Eizuru, *Human phospholipid scramblase 1 interacts with and regulates transactivation of HTLV-1 Tax*. Virology, 2012. 432(2): p. 343-52.
6. Kusano, S. and Y. Eizuru, *Interaction of the phospholipid scramblase 1 with HIV-1 Tat results in the repression of Tat-dependent transcription*. Biochem Biophys Res Commun, 2013. 433(4): p. 438-44.
7. Metz, P., et al., *Identification of type I and type II interferon-induced effectors controlling hepatitis C virus replication*. Hepatology, 2012. 56(6): p. 2082-93.
8. Yang, J., et al., *Inhibition of Hepatitis B virus replication by phospholipid scramblase 1 in vitro and in vivo*. Antiviral Res, 2012. 94(1): p. 9-17.
9. Nanjundan, M., et al., *Overexpression of SnoN/SkiL, amplified at the 3q26.2 locus, in ovarian cancers: a role in ovarian pathogenesis*. Mol Oncol, 2008. 2(2): p. 164-81.
10. Nanjundan, M., et al., *Amplification of MDS1/EVII and EVII, located in the 3q26.2 amplicon, is associated with favorable patient prognosis in ovarian cancer*. Cancer Res, 2007. 67(7): p. 3074-84.
11. Shayesteh, L., et al., *PIK3CA is implicated as an oncogene in ovarian cancer*. Nat Genet, 1999. 21(1): p. 99-102.
12. Sugita, M., et al., *Molecular definition of a small amplification domain within 3q26 in tumors of cervix, ovary, and lung*. Cancer Genet Cytogenet, 2000. 117(1): p. 9-18.
13. Whitley, B.R., et al., *Expression of active plasminogen activator inhibitor-1 reduces cell migration and invasion in breast and gynecological cancer cells*. Exp Cell Res, 2004. 296(2): p. 151-62.
14. Luo, K., *Ski and SnoN: negative regulators of TGF-beta signaling*. Curr Opin Genet Dev, 2004. 14(1): p. 65-70.
15. Silverman, R.H., et al., *Suppression of ovarian carcinoma cell growth in vivo by the interferon-inducible plasma membrane protein, phospholipid scramblase 1*. Cancer Res, 2002. 62(2): p. 397-402.
16. Huang, Y., et al., *Antileukemic roles of human phospholipid scramblase 1 gene, evidence from inducible PLSCR1-expressing leukemic cells*. Oncogene, 2006. 25(50): p. 6618-27.
17. Nakamaki, T., et al., *Role of MmTRA1b/phospholipid scramblase1 gene expression in the induction of differentiation of human myeloid leukemia cells into granulocytes*. Exp Hematol, 2002. 30(5): p. 421-9.
18. Sun, J., et al., *c-Abl tyrosine kinase binds and phosphorylates phospholipid scramblase 1*. J Biol Chem, 2001. 276(31): p. 28984-90.

19. Sun, J., et al., *Plasma membrane phospholipid scramblase 1 is enriched in lipid rafts and interacts with the epidermal growth factor receptor*. *Biochemistry*, 2002. 41(20): p. 6338-45.
20. Chen, C.Y., et al., *Antibody Against N-terminal Domain of Phospholipid Scramblase 1 Induces Apoptosis in Colorectal Cancer Cells Through the Intrinsic Apoptotic Pathway*. *Chem Biol Drug Des*, 2014. 84(1): p. 36-43.
21. Cui, W., et al., *Silencing phospholipid scramblase 1 expression by RNA interference in colorectal cancer and metastatic liver cancer*. *Hepatobiliary Pancreat Dis Int*, 2012. 11(4): p. 393-400.
22. Kuo, Y.B., et al., *Identification of phospholipid scramblase 1 as a biomarker and determination of its prognostic value for colorectal cancer*. *Mol Med*, 2011. 17(1-2): p. 41-7.
23. Zhou, Q., et al., *Phospholipid scramblase 1 binds to the promoter region of the inositol 1,4,5-triphosphate receptor type 1 gene to enhance its expression*. *J Biol Chem*, 2005. 280(41): p. 35062-8.
24. Wiedmer, T., et al., *Palmitoylation of phospholipid scramblase 1 controls its distribution between nucleus and plasma membrane*. *Biochemistry*, 2003. 42(5): p. 1227-33.
25. Chen, M.H., et al., *Phospholipid scramblase 1 contains a nonclassical nuclear localization signal with unique binding site in importin alpha*. *J Biol Chem*, 2005. 280(11): p. 10599-606.
26. Zhou, Q., P.J. Sims, and T. Wiedmer, *Identity of a conserved motif in phospholipid scramblase that is required for Ca<sup>2+</sup>-accelerated transbilayer movement of membrane phospholipids*. *Biochemistry*, 1998. 37(8): p. 2356-60.
27. Sims, P.J. and T. Wiedmer, *Unraveling the mysteries of phospholipid scrambling*. *Thromb Haemost*, 2001. 86(1): p. 266-75.
28. Imoto, I., et al., *SNO is a probable target for gene amplification at 3q26 in squamous-cell carcinomas of the esophagus*. *Biochem Biophys Res Commun*, 2001. 286(3): p. 559-65.
29. Imoto, I., et al., *Identification of ZASC1 encoding a Kruppel-like zinc finger protein as a novel target for 3q26 amplification in esophageal squamous cell carcinomas*. *Cancer Res*, 2003. 63(18): p. 5691-6.
30. Riazimand, S.H., et al., *Investigations for fine mapping of amplifications in chromosome 3q26.3-28 frequently occurring in squamous cell carcinomas of the head and neck*. *Oncology*, 2002. 63(4): p. 385-92.
31. Eder, A.M., et al., *Atypical PKC $\alpha$  contributes to poor prognosis through loss of apical-basal polarity and cyclin E overexpression in ovarian cancer*. *Proc Natl Acad Sci U S A*, 2005. 102(35): p. 12519-24.
32. Dutta, P., et al., *EVII splice variants modulate functional responses in ovarian cancer cells*. *Mol Oncol*, 2013. 7(3): p. 647-68.
33. Yatsula, B., et al., *Identification of binding sites of EVII in mammalian cells*. *J Biol Chem*, 2005. 280(35): p. 30712-22.
34. Basse, F., et al., *Isolation of an erythrocyte membrane protein that mediates Ca<sup>2+</sup>-dependent transbilayer movement of phospholipid*. *J Biol Chem*, 1996. 271(29): p. 17205-10.
35. Zhou, Q., et al., *Molecular cloning of human plasma membrane phospholipid scramblase. A protein mediating transbilayer movement of plasma membrane phospholipids*. *J Biol Chem*, 1997. 272(29): p. 18240-4.
36. Fan, C.W., et al., *Blockade of phospholipid scramblase 1 with its N-terminal domain antibody reduces tumorigenesis of colorectal carcinomas in vitro and in vivo*. *J Transl Med*, 2012. 10: p. 254.
37. Zhou, Q., et al., *Normal hemostasis but defective hematopoietic response to growth factors in mice deficient in phospholipid scramblase 1*. *Blood*, 2002. 99(11): p. 4030-8.
38. Der, S.D., et al., *Identification of genes differentially regulated by interferon alpha, beta, or gamma using oligonucleotide arrays*. *Proc Natl Acad Sci U S A*, 1998. 95(26): p. 15623-8.
39. Zhou, Q., et al., *Transcriptional control of the human plasma membrane phospholipid scramblase 1 gene is mediated by interferon-alpha*. *Blood*, 2000. 95(8): p. 2593-9.



40. Zhao, K.W., et al., *Protein kinase Cdelta mediates retinoic acid and phorbol myristate acetate-induced phospholipid scramblase 1 gene expression: its role in leukemic cell differentiation*. Blood, 2004. 104(12): p. 3731-8.
41. Yokoyama, A., et al., *MmTRAI1b/phospholipid scramblase 1 gene expression is a new prognostic factor for acute myelogenous leukemia*. Leuk Res, 2004. 28(2): p. 149-57.
42. Talukder, A.H., et al., *Phospholipid scramblase 1 regulates Toll-like receptor 9-mediated type I interferon production in plasmacytoid dendritic cells*. Cell Res, 2012. 22(7): p. 1129-39.
43. Fitzgerald, K.A., et al., *LPS-TLR4 signaling to IRF-3/7 and NF-kappaB involves the toll adapters TRAM and TRIF*. J Exp Med, 2003. 198(7): p. 1043-55.
44. Schafer, S.L., et al., *Regulation of type I interferon gene expression by interferon regulatory factor-3*. J Biol Chem, 1998. 273(5): p. 2714-20.
45. Tamassia, N., et al., *IFN-beta expression is directly activated in human neutrophils transfected with plasmid DNA and is further increased via TLR-4-mediated signaling*. J Immunol, 2012. 189(3): p. 1500-9.
46. Winter-Roach, B.A., H.C. Kitchener, and H.O. Dickinson, *Adjuvant (post-surgery) chemotherapy for early stage epithelial ovarian cancer*. Cochrane Database Syst Rev, 2009(1): p. CD004706.
47. Bookman, M.A., *First-line chemotherapy in epithelial ovarian cancer*. Clin Obstet Gynecol, 2012. 55(1): p. 96-113.
48. Kurman, R.J. and M. Shih Ie, *The origin and pathogenesis of epithelial ovarian cancer: a proposed unifying theory*. Am J Surg Pathol, 2010. 34(3): p. 433-43.
49. Vaughan, S., et al., *Rethinking ovarian cancer: recommendations for improving outcomes*. Nat Rev Cancer, 2011. 11(10): p. 719-25.
50. Zorn, K.K., et al., *Gene expression profiles of serous, endometrioid, and clear cell subtypes of ovarian and endometrial cancer*. Clin Cancer Res, 2005. 11(18): p. 6422-30.
51. Lim, D. and E. Oliva, *Precursors and pathogenesis of ovarian carcinoma*. Pathology, 2013. 45(3): p. 229-42.
52. Koshiyama, M., N. Matsumura, and I. Konishi, *Recent concepts of ovarian carcinogenesis: type I and type II*. Biomed Res Int, 2014. 2014: p. 934261.
53. Kuo, K.T., et al., *Frequent activating mutations of PIK3CA in ovarian clear cell carcinoma*. Am J Pathol, 2009. 174(5): p. 1597-601.
54. Wiegand, K.C., et al., *ARID1A mutations in endometriosis-associated ovarian carcinomas*. N Engl J Med, 2010. 363(16): p. 1532-43.
55. Levanon, K., et al., *Primary ex vivo cultures of human fallopian tube epithelium as a model for serous ovarian carcinogenesis*. Oncogene, 2010. 29(8): p. 1103-13.
56. Piek, J.M., et al., *Dysplastic changes in prophylactically removed Fallopian tubes of women predisposed to developing ovarian cancer*. J Pathol, 2001. 195(4): p. 451-6.
57. Prat, J., *Ovarian carcinomas: five distinct diseases with different origins, genetic alterations, and clinicopathological features*. Virchows Arch, 2012.
58. Kim, A., et al., *Review: Therapeutic strategies in epithelial ovarian cancer*. J Exp Clin Cancer Res, 2012. 31(1): p. 14.
59. Dasari, S. and P. Bernard Tchounwou, *Cisplatin in cancer therapy: Molecular mechanisms of action*. Eur J Pharmacol, 2014. 740C: p. 364-378.
60. Lawrie, T.A., et al., *Pegylated liposomal doxorubicin for first-line treatment of epithelial ovarian cancer*. Cochrane Database Syst Rev, 2013. 10: p. CD010482.
61. Liu, J.F., P.A. Konstantinopoulos, and U.A. Matulonis, *PARP inhibitors in ovarian cancer: current status and future promise*. Gynecol Oncol, 2014. 133(2): p. 362-9.
62. Lopez, J., S. Banerjee, and S.B. Kaye, *New developments in the treatment of ovarian cancer--future perspectives*. Ann Oncol, 2013. 24 Suppl 10: p. x69-x76.
63. Monk, B.J., et al., *Antiangiogenic agents as a maintenance strategy for advanced epithelial ovarian cancer*. Crit Rev Oncol Hematol, 2013. 86(2): p. 161-75.

64. Bonome, T., et al., *Expression profiling of serous low malignant potential, low-grade, and high-grade tumors of the ovary*. *Cancer Res*, 2005. 65(22): p. 10602-12.
65. Catusus, L., et al., *Molecular genetic alterations in endometrioid carcinomas of the ovary: similar frequency of beta-catenin abnormalities but lower rate of microsatellite instability and PTEN alterations than in uterine endometrioid carcinomas*. *Hum Pathol*, 2004. 35(11): p. 1360-8.
66. Campbell, I.G., et al., *Mutation of the PIK3CA gene in ovarian and breast cancer*. *Cancer Res*, 2004. 64(21): p. 7678-81.
67. Cuatrecasas, M., et al., *K-ras mutations in nonmucinous ovarian epithelial tumors: a molecular analysis and clinicopathologic study of 144 patients*. *Cancer*, 1998. 82(6): p. 1088-95.
68. Ichikawa, Y., et al., *Mutation of K-ras protooncogene is associated with histological subtypes in human mucinous ovarian tumors*. *Cancer Res*, 1994. 54(1): p. 33-5.
69. Sunde, J.S., et al., *Expression profiling identifies altered expression of genes that contribute to the inhibition of transforming growth factor-beta signaling in ovarian cancer*. *Cancer Res*, 2006. 66(17): p. 8404-12.
70. Maihle, N.J., et al., *EGF/ErbB receptor family in ovarian cancer*. *Cancer Treat Res*, 2002. 107: p. 247-58.
71. Elliott, R.L. and G.C. Blobe, *Role of transforming growth factor Beta in human cancer*. *J Clin Oncol*, 2005. 23(9): p. 2078-93.
72. Shi, Y. and J. Massague, *Mechanisms of TGF-beta signaling from cell membrane to the nucleus*. *Cell*, 2003. 113(6): p. 685-700.
73. Massague, J., S.W. Blain, and R.S. Lo, *TGFbeta signaling in growth control, cancer, and heritable disorders*. *Cell*, 2000. 103(2): p. 295-309.
74. Chou, J.L., et al., *TGF-beta: friend or foe? The role of TGF-beta/SMAD signaling in epigenetic silencing of ovarian cancer and its implication in epigenetic therapy*. *Expert Opin Ther Targets*, 2010. 14(11): p. 1213-23.
75. Raffoul, F., C. Campla, and M. Nanjundan, *SnoN/SkiL, a TGFbeta signaling mediator: a participant in autophagy induced by arsenic trioxide*. *Autophagy*, 2010. 6(7): p. 955-7.
76. Edmiston, J.S., et al., *Inability of transforming growth factor-beta to cause SnoN degradation leads to resistance to transforming growth factor-beta-induced growth arrest in esophageal cancer cells*. *Cancer Res*, 2005. 65(11): p. 4782-8.
77. Vignais, M.L., [*Ski and SnoN: antagonistic proteins of TGFbeta signaling*]. *Bull Cancer*, 2000. 87(2): p. 135-7.
78. He, J., et al., *The transforming activity of Ski and SnoN is dependent on their ability to repress the activity of Smad proteins*. *J Biol Chem*, 2003. 278(33): p. 30540-7.
79. Zhang, F., et al., *Ski-related novel protein N (SnoN), a negative controller of transforming growth factor-beta signaling, is a prognostic marker in estrogen receptor-positive breast carcinomas*. *Cancer Res*, 2003. 63(16): p. 5005-10.
80. Zhu, Q., et al., *Dual role of SnoN in mammalian tumorigenesis*. *Mol Cell Biol*, 2007. 27(1): p. 324-39.
81. Buess, M., et al., *Amplification of SKI is a prognostic marker in early colorectal cancer*. *Neoplasia*, 2004. 6(3): p. 207-12.
82. Chia, J.A., et al., *SnoN expression is differently regulated in microsatellite unstable compared with microsatellite stable colorectal cancers*. *BMC Cancer*, 2006. 6: p. 252.
83. Jahchan, N.S., G. Ouyang, and K. Luo, *Expression profiles of SnoN in normal and cancerous human tissues support its tumor suppressor role in human cancer*. *PLoS One*, 2013. 8(2): p. e55794.
84. Pan, D., Q. Zhu, and K. Luo, *SnoN functions as a tumour suppressor by inducing premature senescence*. *EMBO J*, 2009. 28(22): p. 3500-13.
85. Bonni, S., et al., *TGF-beta induces assembly of a Smad2-Smurf2 ubiquitin ligase complex that targets SnoN for degradation*. *Nat Cell Biol*, 2001. 3(6): p. 587-95.

86. Kajino, T., et al., *TAK1 MAPK kinase mediates transforming growth factor-beta signaling by targeting SnoN oncoprotein for degradation*. J Biol Chem, 2007. 282(13): p. 9475-81.
87. Levy, L., et al., *Arkadia activates Smad3/Smad4-dependent transcription by triggering signal-induced SnoN degradation*. Mol Cell Biol, 2007. 27(17): p. 6068-83.
88. Stroschein, S.L., et al., *Smad3 recruits the anaphase-promoting complex for ubiquitination and degradation of SnoN*. Genes Dev, 2001. 15(21): p. 2822-36.
89. Huff, J., P. Chan, and A. Nyska, *Is the human carcinogen arsenic carcinogenic to laboratory animals?* Toxicol Sci, 2000. 55(1): p. 17-23.
90. Zhang, T.D., et al., *Arsenic trioxide, a therapeutic agent for APL*. Oncogene, 2001. 20(49): p. 7146-53.
91. Zhang, X.W., et al., *Arsenic trioxide controls the fate of the PML-RARalpha oncoprotein by directly binding PML*. Science, 2010. 328(5975): p. 240-3.
92. Qian, W., et al., *Arsenic trioxide induces not only apoptosis but also autophagic cell death in leukemia cell lines via up-regulation of Beclin-1*. Leuk Res, 2007. 31(3): p. 329-39.
93. Kroemer, G., et al., *Classification of cell death: recommendations of the Nomenclature Committee on Cell Death 2009*. Cell Death Differ, 2009. 16(1): p. 3-11.
94. Mizushima, N. and D.J. Klionsky, *Protein turnover via autophagy: implications for metabolism*. Annu Rev Nutr, 2007. 27: p. 19-40.
95. Coates, J.M., J.M. Galante, and R.J. Bold, *Cancer therapy beyond apoptosis: autophagy and anoikis as mechanisms of cell death*. J Surg Res, 2010. 164(2): p. 301-8.
96. Eskelinen, E.L., *The dual role of autophagy in cancer*. Curr Opin Pharmacol, 2011. 11(4): p. 294-300.
97. Hanahan, D. and R.A. Weinberg, *Hallmarks of cancer: the next generation*. Cell, 2011. 144(5): p. 646-74.
98. Elmore, S., *Apoptosis: a review of programmed cell death*. Toxicol Pathol, 2007. 35(4): p. 495-516.
99. Cory, S. and J.M. Adams, *The Bcl2 family: regulators of the cellular life-or-death switch*. Nat Rev Cancer, 2002. 2(9): p. 647-56.
100. Carswell, E.A., et al., *An endotoxin-induced serum factor that causes necrosis of tumors*. Proc Natl Acad Sci U S A, 1975. 72(9): p. 3666-70.
101. Holler, N., et al., *Fas triggers an alternative, caspase-8-independent cell death pathway using the kinase RIP as effector molecule*. Nat Immunol, 2000. 1(6): p. 489-95.
102. He, S., et al., *Toll-like receptors activate programmed necrosis in macrophages through a receptor-interacting kinase-3-mediated pathway*. Proc Natl Acad Sci U S A, 2011. 108(50): p. 20054-9.
103. Chromik, J., et al., *Smac mimetic primes apoptosis-resistant acute myeloid leukaemia cells for cytarabine-induced cell death by triggering necroptosis*. Cancer Lett, 2014. 344(1): p. 101-9.
104. Micheau, O. and J. Tschopp, *Induction of TNF receptor I-mediated apoptosis via two sequential signaling complexes*. Cell, 2003. 114(2): p. 181-90.
105. Cho, Y.S., et al., *Phosphorylation-driven assembly of the RIP1-RIP3 complex regulates programmed necrosis and virus-induced inflammation*. Cell, 2009. 137(6): p. 1112-23.
106. Vanden Berghe, T., et al., *Necroptosis, necrosis and secondary necrosis converge on similar cellular disintegration features*. Cell Death Differ, 2010. 17(6): p. 922-30.
107. Zwaal, R.F., P. Comfurius, and E.M. Bevers, *Surface exposure of phosphatidylserine in pathological cells*. Cell Mol Life Sci, 2005. 62(9): p. 971-88.
108. Bevers, E.M., et al., *Generation of prothrombin-converting activity and the exposure of phosphatidylserine at the outer surface of platelets*. Eur J Biochem, 1982. 122(2): p. 429-36.
109. Zwaal, R.F., P. Comfurius, and E.M. Bevers, *Lipid-protein interactions in blood coagulation*. Biochim Biophys Acta, 1998. 1376(3): p. 433-53.
110. Bevers, E.M., P. Comfurius, and R.F. Zwaal, *Changes in membrane phospholipid distribution during platelet activation*. Biochim Biophys Acta, 1983. 736(1): p. 57-66.

111. Fadok, V.A., et al., *Exposure of phosphatidylserine on the surface of apoptotic lymphocytes triggers specific recognition and removal by macrophages*. J Immunol, 1992. 148(7): p. 2207-16.
112. Fadok, V.A., et al., *Loss of phospholipid asymmetry and surface exposure of phosphatidylserine is required for phagocytosis of apoptotic cells by macrophages and fibroblasts*. J Biol Chem, 2001. 276(2): p. 1071-7.
113. Bevers, E.M., et al., *Regulatory mechanisms of transmembrane phospholipid distributions and pathophysiological implications of transbilayer lipid scrambling*. Lupus, 1998. 7 Suppl 2: p. S126-31.
114. Bevers, E.M., P. Comfurius, and R.F. Zwaal, *Regulatory mechanisms in maintenance and modulation of transmembrane lipid asymmetry: pathophysiological implications*. Lupus, 1996. 5(5): p. 480-7.
115. Lange, Y., J. Ye, and T.L. Steck, *Scrambling of phospholipids activates red cell membrane cholesterol*. Biochemistry, 2007. 46(8): p. 2233-8.
116. Fadeel, B., et al., *Phosphatidylserine exposure during apoptosis is a cell-type-specific event and does not correlate with plasma membrane phospholipid scramblase expression*. Biochem Biophys Res Commun, 1999. 266(2): p. 504-11.
117. Suzuki, J., et al., *Calcium-dependent phospholipid scrambling by TMEM16F*. Nature, 2010. 468(7325): p. 834-8.
118. Castoldi, E., et al., *Compound heterozygosity for 2 novel TMEM16F mutations in a patient with Scott syndrome*. Blood, 2011. 117(16): p. 4399-400.
119. Duran, C. and H.C. Hartzell, *Physiological roles and diseases of Tmem16/Anoctamin proteins: are they all chloride channels?* Acta Pharmacol Sin, 2011. 32(6): p. 685-92.
120. Lhermusier, T., H. Chap, and B. Payraastre, *Platelet membrane phospholipid asymmetry: from the characterization of a scramblase activity to the identification of an essential protein mutated in Scott syndrome*. J Thromb Haemost, 2011. 9(10): p. 1883-91.
121. Yang, H., et al., *TMEM16F forms a Ca<sup>2+</sup>-activated cation channel required for lipid scrambling in platelets during blood coagulation*. Cell, 2012. 151(1): p. 111-22.
122. Suzuki, J., et al., *Calcium-dependent phospholipid scramblase activity of TMEM16 protein family members*. J Biol Chem, 2013. 288(19): p. 13305-16.
123. Suzuki, J., et al., *Xk-related protein 8 and CED-8 promote phosphatidylserine exposure in apoptotic cells*. Science, 2013. 341(6144): p. 403-6.
124. Suzuki, J. and S. Nagata, *Phospholipid scrambling on the plasma membrane*. Methods Enzymol, 2014. 544: p. 381-93.
125. Marino, G. and G. Kroemer, *Mechanisms of apoptotic phosphatidylserine exposure*. Cell Res, 2013. 23(11): p. 1247-8.
126. Williamson, P., et al., *Ca<sup>2+</sup> induces transbilayer redistribution of all major phospholipids in human erythrocytes*. Biochemistry, 1992. 31(27): p. 6355-60.
127. Smeets, E.F., et al., *Calcium-induced transbilayer scrambling of fluorescent phospholipid analogs in platelets and erythrocytes*. Biochim Biophys Acta, 1994. 1195(2): p. 281-6.
128. Chang, C.P., et al., *Contribution of platelet microparticle formation and granule secretion to the transmembrane migration of phosphatidylserine*. J Biol Chem, 1993. 268(10): p. 7171-8.
129. Basse, F., et al., *Translocation of spin-labeled phospholipids through plasma membrane during thrombin- and ionophore A23187-induced platelet activation*. Biochemistry, 1993. 32(9): p. 2337-44.
130. Zhao, J., et al., *Level of expression of phospholipid scramblase regulates induced movement of phosphatidylserine to the cell surface*. J Biol Chem, 1998. 273(12): p. 6603-6.
131. Wiedmer, T., et al., *Identification of three new members of the phospholipid scramblase gene family*. Biochim Biophys Acta, 2000. 1467(1): p. 244-53.
132. Suzuki, E., et al., *Increased expression of phospholipid scramblase 1 in monocytes from patients with systemic lupus erythematosus*. J Rheumatol, 2010. 37(8): p. 1639-45.

133. Kametaka, S., et al., *Identification of phospholipid scramblase 1 as a novel interacting molecule with beta -secretase (beta -site amyloid precursor protein (APP) cleaving enzyme (BACE))*. J Biol Chem, 2003. 278(17): p. 15239-45.
134. Lott, K., et al., *A minimal nuclear localization signal (NLS) in human phospholipid scramblase 4 that binds only the minor NLS-binding site of importin alpha1*. J Biol Chem, 2011. 286(32): p. 28160-9.
135. Wang, X., et al., *C. elegans mitochondrial factor WAH-1 promotes phosphatidylserine externalization in apoptotic cells through phospholipid scramblase SCRM-1*. Nat Cell Biol, 2007. 9(5): p. 541-9.
136. Francis, V.G. and S.N. Gummadi, *Biochemical and functional characterization of human phospholipid scramblase 4 (hPLSCR4)*. Biol Chem, 2012. 393(10): p. 1173-81.
137. Liu, J., et al., *Role of phospholipid scramblase 3 in the regulation of tumor necrosis factor-alpha-induced apoptosis*. Biochemistry, 2008. 47(15): p. 4518-29.
138. Rayala, S., et al., *N-terminal proline-rich domain is required for scrambling activity of human phospholipid scramblases*. J Biol Chem, 2014. 289(19): p. 13206-18.
139. Zhou, Q., P.J. Sims, and T. Wiedmer, *Expression of proteins controlling transbilayer movement of plasma membrane phospholipids in the B lymphocytes from a patient with Scott syndrome*. Blood, 1998. 92(5): p. 1707-12.
140. Mutch, D.M., et al., *Mobilization of pro-inflammatory lipids in obese Plscr3-deficient mice*. Genome Biol, 2007. 8(3): p. R38.
141. Rosing, J., et al., *Impaired factor X and prothrombin activation associated with decreased phospholipid exposure in platelets from a patient with a bleeding disorder*. Blood, 1985. 65(6): p. 1557-61.
142. Toti, F., et al., *Scott syndrome, characterized by impaired transmembrane migration of procoagulant phosphatidylserine and hemorrhagic complications, is an inherited disorder*. Blood, 1996. 87(4): p. 1409-15.
143. Kunzelmann, K., et al., *Molecular functions of anoctamin 6 (TMEM16F): a chloride channel, cation channel, or phospholipid scramblase?* Pflugers Arch, 2014. 466(3): p. 407-14.
144. Nanjundan, M., et al., *Plasma membrane phospholipid scramblase 1 promotes EGF-dependent activation of c-Src through the epidermal growth factor receptor*. J Biol Chem, 2003. 278(39): p. 37413-8.
145. Zhao, K.W., et al., *Interferon-alpha-induced expression of phospholipid scramblase 1 through STAT1 requires the sequential activation of protein kinase Cdelta and JNK*. J Biol Chem, 2005. 280(52): p. 42707-14.
146. Francis, V.G., P. Padmanabhan, and S.N. Gummadi, *Snail interacts with hPLSCR1 promoter and down regulates its expression in IMR-32*. Biochem Biophys Res Commun, 2014.
147. Ben-Efraim, I., et al., *Phospholipid scramblase 1 is imported into the nucleus by a receptor-mediated pathway and interacts with DNA*. Biochemistry, 2004. 43(12): p. 3518-26.
148. Wyles, J.P., et al., *Nuclear interactions of topoisomerase II alpha and beta with phospholipid scramblase 1*. Nucleic Acids Res, 2007. 35(12): p. 4076-85.
149. Py, B., et al., *The phospholipid scramblases 1 and 4 are cellular receptors for the secretory leukocyte protease inhibitor and interact with CD4 at the plasma membrane*. PLoS One, 2009. 4(3): p. e5006.
150. Kowalczyk, J.E., et al., *Association of protein kinase C delta and phospholipid scramblase 3 in hippocampal mitochondria correlates with neuronal vulnerability to brain ischemia*. Neurochem Int, 2009. 55(1-3): p. 157-63.
151. He, Y., et al., *Phosphorylation of mitochondrial phospholipid scramblase 3 by protein kinase C-delta induces its activation and facilitates mitochondrial targeting of tBid*. J Cell Biochem, 2007. 101(5): p. 1210-21.

152. Merrick, B.A., et al., *Proteomic profiling of S-acylated macrophage proteins identifies a role for palmitoylation in mitochondrial targeting of phospholipid scramblase 3*. Mol Cell Proteomics, 2011. 10(10): p. M110 006007.
153. Pastorelli, C., et al., *IgE receptor type I-dependent tyrosine phosphorylation of phospholipid scramblase*. J Biol Chem, 2001. 276(23): p. 20407-12.
154. Li, Y., et al., *The negative c-Myc target onzin affects proliferation and apoptosis via its obligate interaction with phospholipid scramblase 1*. Mol Cell Biol, 2006. 26(9): p. 3401-13.
155. Merregaert, J., et al., *Phospholipid scramblase 1 is secreted by a lipid raft-dependent pathway and interacts with the extracellular matrix protein 1 in the dermal epidermal junction zone of human skin*. J Biol Chem, 2010. 285(48): p. 37823-37.
156. Kantari, C., et al., *Proteinase 3, the Wegener autoantigen, is externalized during neutrophil apoptosis: evidence for a functional association with phospholipid scramblase 1 and interference with macrophage phagocytosis*. Blood, 2007. 110(12): p. 4086-95.
157. Chen, C.W., et al., *Nuclear phospholipid scramblase 1 prolongs the mitotic expansion of granulocyte precursors during G-CSF-induced granulopoiesis*. J Leukoc Biol, 2011. 90(2): p. 221-33.
158. Yu, A., et al., *Stimulation of phosphatidylserine biosynthesis and facilitation of UV-induced apoptosis in Chinese hamster ovary cells overexpressing phospholipid scramblase 1*. J Biol Chem, 2003. 278(11): p. 9706-14.
159. Clarke, C.J., J.A. Trapani, and R.W. Johnstone, *Mechanisms of interferon mediated anti-viral resistance*. Curr Drug Targets Immune Endocr Metabol Disord, 2001. 1(2): p. 117-30.
160. Hughes, R., G. Towers, and M. Noursadeghi, *Innate immune interferon responses to human immunodeficiency virus-1 infection*. Rev Med Virol, 2012. 22(4): p. 257-66.
161. Borden, E.C., et al., *Interferons at age 50: past, current and future impact on biomedicine*. Nat Rev Drug Discov, 2007. 6(12): p. 975-90.
162. Schoggins, J.W. and C.M. Rice, *Interferon-stimulated genes and their antiviral effector functions*. Curr Opin Virol, 2011. 1(6): p. 519-25.
163. Lizak, M. and T.O. Yarovinsky, *Phospholipid Scramblase 1 Mediates Type I Interferon-Induced Protection against Staphylococcal alpha-Toxin*. Cell Host Microbe, 2012. 11(1): p. 70-80.
164. Aghemo, A. and M. Colombo, *Hepatocellular carcinoma in chronic hepatitis C: from bench to bedside*. Semin Immunopathol, 2013. 35(1): p. 111-20.
165. Tornesello, M.L., et al., *Mutations in TP53, CTNBN1 and PIK3CA genes in hepatocellular carcinoma associated with hepatitis B and hepatitis C virus infections*. Genomics, 2013. 102(2): p. 74-83.
166. Zemel, R., A. Issachar, and R. Tur-Kaspa, *The role of oncogenic viruses in the pathogenesis of hepatocellular carcinoma*. Clin Liver Dis, 2011. 15(2): p. 261-79, vii-x.
167. Gong, Q., et al., *Phospholipid scramblase 1 mediates hepatitis C virus entry into host cells*. FEBS Lett, 2011. 585(17): p. 2647-52.
168. Barton, G.M. and J.C. Kagan, *A cell biological view of Toll-like receptor function: regulation through compartmentalization*. Nat Rev Immunol, 2009. 9(8): p. 535-42.
169. He, X., et al., *Recognition of pathogen-associated nucleic acids by endosomal nucleic acid-sensing toll-like receptors*. Acta Biochim Biophys Sin (Shanghai), 2013. 45(4): p. 241-58.
170. Kaisho, T. and S. Akira, *Toll-like receptors and their signaling mechanism in innate immunity*. Acta Odontol Scand, 2001. 59(3): p. 124-30.
171. Laird, M.H., et al., *TLR4/MyD88/PI3K interactions regulate TLR4 signaling*. J Leukoc Biol, 2009. 85(6): p. 966-77.
172. An, H., et al., *Involvement of ERK, p38 and NF-kappaB signal transduction in regulation of TLR2, TLR4 and TLR9 gene expression induced by lipopolysaccharide in mouse dendritic cells*. Immunology, 2002. 106(1): p. 38-45.
173. Hsu, T.Y. and Y.C. Wu, *Engulfment of apoptotic cells in C. elegans is mediated by integrin alpha/SRC signaling*. Curr Biol, 2010. 20(6): p. 477-86.

174. Liu, J., et al., *Phospholipid scramblase 3 controls mitochondrial structure, function, and apoptotic response*. Mol Cancer Res, 2003. 1(12): p. 892-902.
175. Ndebele, K., et al., *Tumor necrosis factor (TNF)-related apoptosis-inducing ligand (TRAIL) induced mitochondrial pathway to apoptosis and caspase activation is potentiated by phospholipid scramblase-3*. Apoptosis, 2008. 13(7): p. 845-56.
176. Bailey, K., H.W. Cook, and C.R. McMaster, *The phospholipid scramblase PLSCR1 increases UV induced apoptosis primarily through the augmentation of the intrinsic apoptotic pathway and independent of direct phosphorylation by protein kinase C delta*. Biochim Biophys Acta, 2005. 1733(2-3): p. 199-209.
177. Kodigepalli, K.M., et al., *Phospholipid Scramblase 1, an interferon-regulated gene located at 3q23, is regulated by SnoN/SkiL in ovarian cancer cells*. Mol Cancer, 2013. 12: p. 32.
178. Chu, C.T., et al., *Cardiolipin externalization to the outer mitochondrial membrane acts as an elimination signal for mitophagy in neuronal cells*. Nat Cell Biol, 2013. 15(10): p. 1197-205.
179. Huett, A., et al., *A novel hybrid yeast-human network analysis reveals an essential role for FBNPIL in antibacterial autophagy*. J Immunol, 2009. 182(8): p. 4917-30.
180. Chen, Y., et al., *Wogonoside induces cell cycle arrest and differentiation by affecting expression and subcellular localization of PLSCR1 in AML cells*. Blood, 2013. 121(18): p. 3682-91.
181. Zhang, K., et al., *Wogonin induces the granulocytic differentiation of human NB4 promyelocytic leukemia cells and up-regulates phospholipid scramblase 1 gene expression*. Cancer Sci, 2008. 99(4): p. 689-95.
182. Kirov, A., et al., *Phosphatidylserine externalization and membrane blebbing are involved in the nonclassical export of FGF1*. J Cell Biochem, 2012. 113(3): p. 956-66.
183. Feng, X.H., et al., *The tumor suppressor Smad4/DPC4 and transcriptional adaptor CBP/p300 are coactivators for smad3 in TGF-beta-induced transcriptional activation*. Genes Dev, 1998. 12(14): p. 2153-63.
184. Labbe, E., et al., *Smad2 and Smad3 positively and negatively regulate TGF beta-dependent transcription through the forkhead DNA-binding protein FAST2*. Mol Cell, 1998. 2(1): p. 109-20.
185. Liu, F., C. Pouppnot, and J. Massague, *Dual role of the Smad4/DPC4 tumor suppressor in TGFbeta-inducible transcriptional complexes*. Genes Dev, 1997. 11(23): p. 3157-67.
186. Bogdan, S. and C. Klambt, *Epidermal growth factor receptor signaling*. Curr Biol, 2001. 11(8): p. R292-5.
187. Normanno, N., et al., *Epidermal growth factor receptor (EGFR) signaling in cancer*. Gene, 2006. 366(1): p. 2-16.
188. Davol, P.A., et al., *Shc proteins are strong, independent prognostic markers for both node-negative and node-positive primary breast cancer*. Cancer Res, 2003. 63(20): p. 6772-83.
189. Jackson, J.G., et al., *Elevated levels of p66 Shc are found in breast cancer cell lines and primary tumors with high metastatic potential*. Clin Cancer Res, 2000. 6(3): p. 1135-9.
190. Daly, R.J., M.D. Binder, and R.L. Sutherland, *Overexpression of the Grb2 gene in human breast cancer cell lines*. Oncogene, 1994. 9(9): p. 2723-7.
191. Varis, A., et al., *Targets of gene amplification and overexpression at 17q in gastric cancer*. Cancer Res, 2002. 62(9): p. 2625-9.
192. Yu, G.Z., Y. Chen, and J.J. Wang, *Overexpression of Grb2/HER2 signaling in Chinese gastric cancer: their relationship with clinicopathological parameters and prognostic significance*. J Cancer Res Clin Oncol, 2009. 135(10): p. 1331-9.
193. Garcia-Carracedo, D., et al., *Loss of PTEN expression is associated with poor prognosis in patients with intraductal papillary mucinous neoplasms of the pancreas*. Clin Cancer Res, 2013. 19(24): p. 6830-41.
194. Broek, R.V., et al., *The PI3K/Akt/mTOR axis in head and neck cancer: functions, aberrations, crosstalk, and therapies*. Oral Dis, 2013.

195. Kelber, J.A., et al., *KRas induces a Src/PEAK1/ErbB2 kinase amplification loop that drives metastatic growth and therapy resistance in pancreatic cancer*. *Cancer Res*, 2012. 72(10): p. 2554-64.
196. Okamoto, W., et al., *Identification of c-Src as a potential therapeutic target for gastric cancer and of MET activation as a cause of resistance to c-Src inhibition*. *Mol Cancer Ther*, 2010. 9(5): p. 1188-97.
197. Maki, H.E., et al., *Screening of genetic and expression alterations of SRC1 gene in prostate cancer*. *Prostate*, 2006. 66(13): p. 1391-8.
198. Roskoski, R., Jr., *The ErbB/HER receptor protein-tyrosine kinases and cancer*. *Biochem Biophys Res Commun*, 2004. 319(1): p. 1-11.
199. Siwak, D.R., et al., *Targeting the epidermal growth factor receptor in epithelial ovarian cancer: current knowledge and future challenges*. *J Oncol*, 2010. 2010: p. 568938.
200. Wilde, A., et al., *EGF receptor signaling stimulates SRC kinase phosphorylation of clathrin, influencing clathrin redistribution and EGF uptake*. *Cell*, 1999. 96(5): p. 677-87.
201. Donepudi, M. and M.D. Resh, *c-Src trafficking and co-localization with the EGF receptor promotes EGF ligand-independent EGF receptor activation and signaling*. *Cell Signal*, 2008. 20(7): p. 1359-67.
202. Seshacharyulu, P., et al., *Targeting the EGFR signaling pathway in cancer therapy*. *Expert Opin Ther Targets*, 2012. 16(1): p. 15-31.
203. Benhar, M., D. Engelberg, and A. Levitzki, *Cisplatin-induced activation of the EGF receptor*. *Oncogene*, 2002. 21(57): p. 8723-31.
204. Cenni, B., et al., *Epidermal growth factor enhances cisplatin-induced apoptosis by a caspase 3 independent pathway*. *Cancer Chemother Pharmacol*, 2001. 47(5): p. 397-403.
205. Huang, H.S., et al., *Opposite effect of ERK1/2 and JNK on p53-independent p21WAF1/CIP1 activation involved in the arsenic trioxide-induced human epidermoid carcinoma A431 cellular cytotoxicity*. *J Biomed Sci*, 2006. 13(1): p. 113-25.
206. Liu, Z.M. and H.S. Huang, *As2O3-induced c-Src/EGFR/ERK signaling is via Sp1 binding sites to stimulate p21WAF1/CIP1 expression in human epidermoid carcinoma A431 cells*. *Cell Signal*, 2006. 18(2): p. 244-55.
207. Udensi, U.K., et al., *Aberrantly Expressed Genes in HaCaT Keratinocytes Chronically Exposed to Arsenic Trioxide*. *Biomark Insights*, 2011. 6: p. 7-16.
208. Liu, Z.M. and H.S. Huang, *Inhibitory role of TGIF in the As2O3-regulated p21 WAF1/CIP1 expression*. *J Biomed Sci*, 2008. 15(3): p. 333-42.
209. Tseng, H.Y., Z.M. Liu, and H.S. Huang, *NADPH oxidase-produced superoxide mediates EGFR transactivation by c-Src in arsenic trioxide-stimulated human keratinocytes*. *Arch Toxicol*, 2012. 86(6): p. 935-45.
210. Burova, E.B., I.V. Gonchar, and N.N. Nikol'skii, *[STAT1 and STAT3 activation by oxidative stress in A431 cells involves Src-dependent EGF receptor transactivation]*. *Tsitologiya*, 2003. 45(5): p. 466-77.
211. Yamauchi, T., et al., *UVC radiation induces downregulation of EGF receptor via phosphorylation at serine 1046/1047 in human pancreatic cancer cells*. *Radiat Res*, 2011. 176(5): p. 565-74.
212. Sturla, L.M., et al., *Requirement of Tyr-992 and Tyr-1173 in phosphorylation of the epidermal growth factor receptor by ionizing radiation and modulation by SHP2*. *J Biol Chem*, 2005. 280(15): p. 14597-604.
213. Han, Y.H., et al., *Suppression of arsenic trioxide-induced apoptosis in HeLa cells by N-acetylcysteine*. *Mol Cells*, 2008. 26(1): p. 18-25.
214. Hoyle, P.E., et al., *Differential abilities of the Raf family of protein kinases to abrogate cytokine dependency and prevent apoptosis in murine hematopoietic cells by a MEK1-dependent mechanism*. *Leukemia*, 2000. 14(4): p. 642-56.



215. Chang, F., L.S. Steelman, and J.A. McCubrey, *Raf-induced cell cycle progression in human TF-1 hematopoietic cells*. *Cell Cycle*, 2002. 1(3): p. 220-6.
216. McCubrey, J.A., et al., *Roles of the RAF/MEK/ERK and PI3K/PTEN/AKT pathways in malignant transformation and drug resistance*. *Adv Enzyme Regul*, 2006. 46: p. 249-79.
217. Yen, A., et al., *Expression of activated RAF accelerates cell differentiation and RB protein down-regulation but not hypophosphorylation*. *Eur J Cell Biol*, 1994. 65(1): p. 103-13.
218. Migliaccio, E., et al., *Opposite effects of the p52shc/p46shc and p66shc splicing isoforms on the EGF receptor-MAP kinase-fos signalling pathway*. *EMBO J*, 1997. 16(4): p. 706-16.
219. Arany, I., et al., *p66shc inhibits pro-survival epidermal growth factor receptor/ERK signaling during severe oxidative stress in mouse renal proximal tubule cells*. *J Biol Chem*, 2008. 283(10): p. 6110-7.
220. Xi, G., X. Shen, and D.R. Clemmons, *p66shc negatively regulates insulin-like growth factor I signal transduction via inhibition of p52shc binding to Src homology 2 domain-containing protein tyrosine phosphatase substrate-1 leading to impaired growth factor receptor-bound protein-2 membrane recruitment*. *Mol Endocrinol*, 2008. 22(9): p. 2162-75.
221. Friess, H., et al., *Enhanced erbB-3 expression in human pancreatic cancer correlates with tumor progression*. *Clin Cancer Res*, 1995. 1(11): p. 1413-20.
222. Mirzoeva, O.K., et al., *Autophagy suppression promotes apoptotic cell death in response to inhibition of the PI3K-mTOR pathway in pancreatic adenocarcinoma*. *J Mol Med (Berl)*, 2011. 89(9): p. 877-89.
223. Thomas, S.M. and J.S. Brugge, *Cellular functions regulated by Src family kinases*. *Annu Rev Cell Dev Biol*, 1997. 13: p. 513-609.
224. Ingley, E., *Src family kinases: regulation of their activities, levels and identification of new pathways*. *Biochim Biophys Acta*, 2008. 1784(1): p. 56-65.
225. Sun, X., S. Wu, and D. Xing, *The reactive oxygen species-Src-Stat3 pathway provokes negative feedback inhibition of apoptosis induced by high-fluence low-power laser irradiation*. *FEBS J*, 2010. 277(22): p. 4789-802.
226. Liu, Y., et al., *Evi1 is a survival factor which conveys resistance to both TGFbeta- and taxol-mediated cell death via PI3K/AKT*. *Oncogene*, 2006. 25(25): p. 3565-75.
227. Yoshimi, A., et al., *Evi1 represses PTEN expression and activates PI3K/AKT/mTOR via interactions with polycomb proteins*. *Blood*, 2011. 117(13): p. 3617-28.
228. Cusick, J.K., et al., *Identification of PLSCR1 as a protein that interacts with RELT family members*. *Mol Cell Biochem*, 2012. 362(1-2): p. 55-63.
229. Rhodes, D.R., et al., *ONCOMINE: a cancer microarray database and integrated data-mining platform*. *Neoplasia*, 2004. 6(1): p. 1-6.
230. Cerami, E., et al., *The cBio cancer genomics portal: an open platform for exploring multidimensional cancer genomics data*. *Cancer Discov*, 2012. 2(5): p. 401-4.
231. Gao, J., et al., *Integrative analysis of complex cancer genomics and clinical profiles using the cBioPortal*. *Sci Signal*, 2013. 6(269): p. p11.
232. Song, C.Z., T.E. Siok, and T.D. Gelehrter, *Smad4/DPC4 and Smad3 mediate transforming growth factor-beta (TGF-beta) signaling through direct binding to a novel TGF-beta-responsive element in the human plasminogen activator inhibitor-1 promoter*. *J Biol Chem*, 1998. 273(45): p. 29287-90.
233. Wakahara, K., et al., *Transforming growth factor-beta1-dependent activation of Smad2/3 and up-regulation of PAI-1 expression is negatively regulated by Src in SKOV-3 human ovarian cancer cells*. *J Cell Biochem*, 2004. 93(3): p. 437-53.
234. Kodigepalli, K.M., et al., *SnoN/SkiL expression is modulated via arsenic trioxide-induced activation of the PI3K/AKT pathway in ovarian cancer cells*. *FEBS Lett*, 2013. 587(1): p. 5-16.
235. Jacobsen, L., S. Calvin, and E. Lobenhofer, *Transcriptional effects of transfection: the potential for misinterpretation of gene expression data generated from transiently transfected cells*. *Biotechniques*, 2009. 47(1): p. 617-24.

236. Basith, S., et al., *Roles of toll-like receptors in cancer: a double-edged sword for defense and offense*. Arch Pharm Res, 2012. 35(8): p. 1297-316.
237. Leifer, C.A., et al., *TLR9 is localized in the endoplasmic reticulum prior to stimulation*. J Immunol, 2004. 173(2): p. 1179-83.
238. Heil, F., et al., *Species-specific recognition of single-stranded RNA via toll-like receptor 7 and 8*. Science, 2004. 303(5663): p. 1526-9.
239. Huang, Q., et al., *Differential regulation of interleukin 1 receptor and Toll-like receptor signaling by MEKK3*. Nat Immunol, 2004. 5(1): p. 98-103.
240. Matsuzawa, A., et al., *ROS-dependent activation of the TRAF6-ASK1-p38 pathway is selectively required for TLR4-mediated innate immunity*. Nat Immunol, 2005. 6(6): p. 587-92.
241. Yarovinsky, T.O., *Role of phospholipid scramblase 1 in type I interferon-induced protection from staphylococcal alpha-toxin*. Virulence, 2012. 3(5): p. 457-8.
242. Sato, M., et al., *Distinct and essential roles of transcription factors IRF-3 and IRF-7 in response to viruses for IFN-alpha/beta gene induction*. Immunity, 2000. 13(4): p. 539-48.
243. Yoshida, H., et al., *TLR9-dependent systemic interferon-beta production by intravenous injection of plasmid DNA/cationic liposome complex in mice*. J Gene Med, 2009. 11(8): p. 708-17.
244. Husebye, H., et al., *Endocytic pathways regulate Toll-like receptor 4 signaling and link innate and adaptive immunity*. EMBO J, 2006. 25(4): p. 683-92.
245. Sattler, H.P., et al., *Novel amplification unit at chromosome 3q25-q27 in human prostate cancer*. Prostate, 2000. 45(3): p. 207-15.
246. Weber-Mangal, S., et al., *Breast cancer in young women (< or = 35 years): Genomic aberrations detected by comparative genomic hybridization*. Int J Cancer, 2003. 107(4): p. 583-92.
247. Shackelford, D., et al., *Targeted degradation of the AML1/MDS1/EV11 oncoprotein by arsenic trioxide*. Cancer Res, 2006. 66(23): p. 11360-9.
248. Nagano, Y., et al., *Arkadia induces degradation of SnoN and c-Ski to enhance transforming growth factor-beta signaling*. J Biol Chem, 2007. 282(28): p. 20492-501.
249. Or, Y.Y., et al., *Characterization of chromosome 3q and 12q amplicons in nasopharyngeal carcinoma cell lines*. Int J Oncol, 2005. 26(1): p. 49-56.
250. Chen, L., et al., *MiR-410 regulates MET to influence the proliferation and invasion of glioma*. Int J Biochem Cell Biol, 2012. 44(11): p. 1711-7.
251. Gattolliat, C.H., et al., *Expression of miR-487b and miR-410 encoded by 14q32.31 locus is a prognostic marker in neuroblastoma*. Br J Cancer, 2011. 105(9): p. 1352-61.
252. Hou, B., et al., *[Expression of miR-216a in pancreatic cancer and its clinical significance]*. Nan Fang Yi Ke Da Xue Xue Bao, 2012. 32(11): p. 1628-31.
253. Wang, J., et al., *MicroRNA-610 inhibits the migration and invasion of gastric cancer cells by suppressing the expression of vasodilator-stimulated phosphoprotein*. Eur J Cancer, 2012. 48(12): p. 1904-13.
254. Zhan, M.X., et al., *[Expression of serum microRNAs (miR-222, miR-181, miR-216) in human hepatocellular carcinoma and its clinical significance]*. Zhonghua Yi Xue Za Zhi, 2013. 93(23): p. 1830-2.
255. Wiedmer, T., et al., *Adiposity, dyslipidemia, and insulin resistance in mice with targeted deletion of phospholipid scramblase 3 (PLSCR3)*. Proc Natl Acad Sci U S A, 2004. 101(36): p. 13296-301.

## Appendices

### Appendix A: Overexpression and Validation of HA-tagged PLSCR1 Mutants in T80 Cells

As mentioned earlier in Chapter 6 (Page 118), we have generated the following PLSCR1 mutant constructs via a PCR based approach (Please refer to Chapter 2, Page 35).

1. Wild type PLSCR1-HA
2. C/A-PLSCR1-HA (Palmitoylation mutant, see above)
3.  $\Delta$ N-PLSCR1-HA (Deletion of N-terminal amino acids 1-97 from wild type PLSCR1)
4.  $\Delta$ TM-PLSCR1-HA (Deletion of amino acids 287-318 harboring transmembrane domain from wild type PLSCR1)

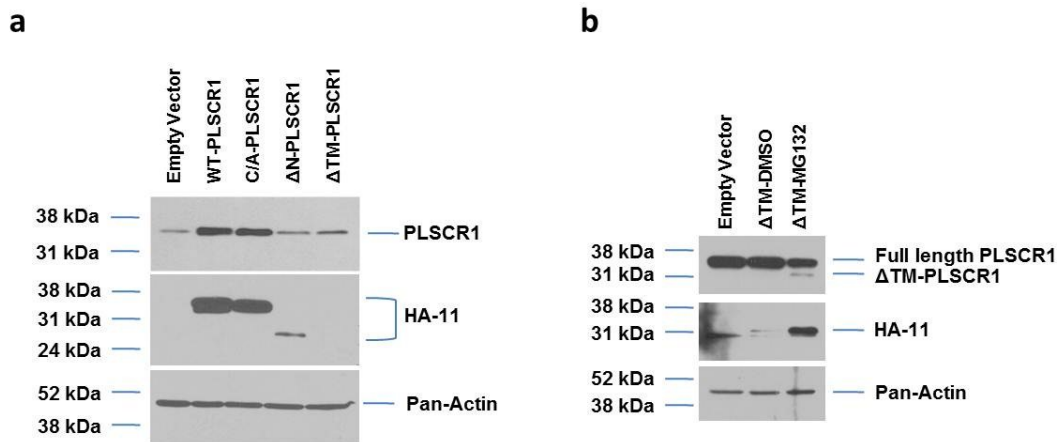


**Figure A1: Overexpression and validation of HA-tagged PLSCR1 mutants**

(a) T80 cells were transfected with empty pQCXIN vector or pQCXIN vector containing WT-PLSCR1, C/A-PLSCR1,  $\Delta$ N-PLSCR1, or  $\Delta$ TM-PLSCR1 as described in Chapter 2. Forty-eight hours post-transfection, cell lysates were harvested and analyzed by western blotting with the indicated antibodies. (b) T80 cells were transfected with empty pQCXIN vector or pQCXIN containing  $\Delta$ TM-PLSCR1 followed by treatment with 5  $\mu$ M MG132 or equal volume of DMSO for 18 hours. Collected cell lysates were analyzed by western blotting with the indicated antibodies.

The above variants were cloned into pQCXIN vector as described in Chapter 2. After validating the desired mutations via sequencing, these variants were transiently overexpressed in T80 cells to validate their expression. As shown in Figure A1a, utilizing anti-HA-11 antibody, we detected WT-PLSCR1 and C/A-PLSCR1 forms at 37 kDa while  $\Delta$ N-PLSCR1 was detected at 26 kDa (due to absence of 98 amino acids compared to WT -PLSCR1). Interestingly,  $\Delta$ TM-PLSCR1 was not detected by both anti-PLSCR1 and anti-HA-11 antibodies. In order to determine whether the  $\Delta$ TM-PLSCR1 protein is degraded after translation via proteasomal degradation pathway, we overexpressed the  $\Delta$ TM-PLSCR1 in presence of 5  $\mu$ M MG132, an inhibitor of proteasomal degradation pathway. Indeed, as shown in Figure A1b, treatment with MG132 and not DMSO (control) recovered  $\Delta$ TM-PLSCR1 expression which was detected both by PLSCR1 and HA-11 antibodies at 33 kDa (due to lack of 29 aa compared to WT-PLSCR1). These results suggest that  $\Delta$ TM-PLSCR1 protein may potentially be degraded via proteasomal pathway when expressed. However, the mechanism involved and significance of degradation of  $\Delta$ TM-PLSCR1 requires further investigation.

## Appendix B

Request for permission to reproduce the work published in FEBS Letters as "**SnoN/SkiL expression is modulated via arsenic trioxide-induced activation of the PI3K/AKT pathway in ovarian cancer cells**"

Anne Rougeaux <anne.rougeaux@bzh.uni-heidelberg.de> Apr 16

Dear Madhav Karthik Kodigepali,

Thank you very much for your message.

You can reproduce the article below entitled,

**"SnoN/SkiL expression is modulated via arsenic trioxide-induced activation of the PI3K/AKT pathway in ovarian cancer cells",**

Karthik M. Kodigepalli, Punashi S. Dutta, Kyle A. Bauckman, Meera Nanjundan, FEBS Letters Vol. 587, Issue 1, Pages 5-16, 4 January 2013, published in FEBS Letters in your thesis, providing the original publication is acknowledged accordingly and the authors' approval is obtained.

Thank you.

With best regards,

Anne Rougeaux

FEBS Letters Editorial Office

On 15/04/2014 18:59, Madhav Karthik Kodigepalli wrote:

Dear Editor,

I am a doctoral candidate from University of South Florida, Tampa FL. USA. I am currently writing my doctoral thesis and would like to rewrite and include data/content from one of the articles that was published in FEBS Letters Journal.

In this regard, I am writing to you to request your permission to rewrite the article entitled '**SnoN/SkiL expression is modulated via arsenic trioxide-induced activation of the PI3K/AKT pathway in ovarian cancer cells**' (Volume 587, Issue 1, 4 January 2013, Pages 5-16). I am a primary co-author on the article and it was accepted for publication in 'FEBS Letters' on November 1, 2012.

I would greatly appreciate your help and thank you in advance for your valuable time.

Sincerely,

Madhav Karthik Kodigepalli

Doctoral candidate, Department of CMMB,

University of South Florida, Tampa. FL. USA

--

Anne Rougeaux

Editorial Assistant

FEBS Letters Editorial Office  
Heidelberg University Biochemistry Center  
Im Neuenheimer Feld 328  
D-69120 Heidelberg  
Germany

tel: [+49 6221 54 4285](tel:+496221544285)

fax: [+49 6221 54 4260](tel:+496221544260)

[febs.letters@bzh.uni-heidelberg.de](mailto:febs.letters@bzh.uni-heidelberg.de)

-----  
Submit your manuscript to FEBS Letters to be considered for the 10,000 Euro Young Scientist Award.

For more details see: <http://www.febsletters.org/content/younggroupleader>

### Appendix C

Request for permission to reproduce the work published in Molecular Cancer as “**Phospholipid Scramblase 1, an interferon regulated gene located at 3q23, is regulated by SnoN/SkiL in ovarian cancer cells'** (2013,12:32 doi: 10.1186/1476-4598-12-32)”

Dear Dr. Kodigepalli,

Thank you for your email.

All of our authors retain copyright of their manuscripts and can therefore use any part of it again as long as the original article is properly cited.

Biomed Central's full copyright policy can be found here: <http://www.biomedcentral.com/authors/license/>

Please let us know if you have any further questions.

Best Wishes,

Limuel

Limuel Garin

Journal Editorial Office

BioMed Central

Web: [biomedcentral.com](http://biomedcentral.com)

From: Madhav Karthik Kodigepalli [mailto:[kkarthik@mail.usf.edu](mailto:kkarthik@mail.usf.edu)]

Sent: Tuesday, April 15, 2014 11:59 PM

To: Molecular Cancer

Subject: Requesting permission to use published content in thesis

Dear Editor,

I am a doctoral candidate from University of South Florida, Tampa FL. USA. I am currently writing my doctoral thesis and would like to rewrite and include data/content from one of the articles that was published in Molecular Cancer Journal.

In this regard, I am writing to you to request your permission to rewrite the article entitled '**Phospholipid Scramblase 1, an interferon regulated gene located at 3q23, is regulated by SnoN/SkiL in ovarian cancer cells**' (2013,12:32 doi: 10.1186/1476-4598-12-32). I am the primary author on the article and it was published in 'Molecular cancer' on April 26, 2013.

I would greatly appreciate your help and thank you in advance for your valuable time.

Sincerely,

Madhav Karthik Kodigepalli

Doctoral candidate, Department of CMMB,

University of South Florida, Tampa. FL. USA